Spray drying of asparagus waste into flavour-rich ingredients

Joanne Siccama

Propositions

1. The skin formed during spray drying acts as a membrane that hinders the release of flavour compounds. (this thesis)

2. Only by removal or hydrolysis of fibres, one can produce sensorial acceptable asparagus powders. (this thesis)

3. Sustainability evaluation of a unit operation is not useful without considering the entire food production chain.

4. Continuous optimisation of the food production chain is not the solution to feed the growing world population.

5. Opposing Dutch wildlife control by shooting is hypocritical if you are a regular meat consumer.

6. The Netherlands' drastic drop in the World Press Freedom Index is caused by political polarisation.

Propositions belonging to the thesis entitled:

"Spray drying of asparagus waste into flavour-rich ingredients"

Joanne Siccama

Wageningen, 11 November 2022

Spray drying of asparagus waste into flavour-rich ingredients

Joanne Siccama

Thesis committee

Promotor

Dr Maarten A.I. Schutyser

Associate professor, Laboratory of Food Process Engineering

Wageningen University & Research

Co-promotor

Dr Lu Zhang

Assistant professor, Laboratory of Food Process Engineering

Wageningen University & Research

Other members

Prof. Dr Vincenzo Fogliano, Wageningen University & Research

Prof. Dr Kees van der Voort Maarschalk, University of Groningen

Prof. Dr Barbara Sturm, Leibniz Institute for Agricultural Engineering and Bioeconomy, Germany

Dr Joris Salari, Corbion, Gorinchem

This research was conducted under the auspices of the Graduate School VLAG

(Advanced studies in Food Technology, Agrobiotechnology, Nutrition and Health

Sciences)

Spray drying of asparagus waste into flavour-rich ingredients

Joanne Siccama

Thesis

submitted in fulfilment of the requirements for the degree of doctor

at Wageningen University

by the authority of the Rector Magnificus,

Prof. Dr A.P.J. Mol,

in the presence of the

Thesis Committee appointed by the Academic Board

to be defended in public

on Friday 11 November 2022

at 1:30 p.m. in the Omnia Auditorium.

Joanne Siccama

Spray drying of asparagus waste into flavour-rich ingredients

212 pages

PhD thesis, Wageningen University, Wageningen, The Netherlands (2022)

With references, with summary in English

ISBN: 978-94-6447-396-4

DOI: https://doi.org/10.18174/576667

Contents

Chapter 1

Introduction and thesis outline

1.1. From vegetable waste to food ingredients

The global food security challenge is to sustainably feed a projected 9.8 billion people by 2050 (Searchinger et al., 2014). If consumption trends continue as projected, the world will need to increase food production by more than 50 % to feed nearly 10 billion people adequately in 2050, besides lowering the environmental footprint in terms of carbon emission and energy use (Searchinger et al., 2014). Reducing food waste and loss is considered one of the key contributors to this balancing act as one-third of the edible parts of food produced for human consumption (~1.3 billion tons) ends up as waste in the food supply chain (Gustavsson et al., 2011). For fruits and vegetables, these food losses can even exceed 50 % in some cases (Gustavsson et al., 2011). Globally, food waste causes ~$940 billion per year in economic losses (€143 billion for Europe) and represent a waste of resources used in production such as land, water and energy, and contributes to unnecessary CO_2 emissions. Effective valorisation of food waste streams will promote full crop use and close the cycle of our food production chain. Worldwide, over 40 % of fruit and vegetables produced end up as waste along the supply chain (FAO, 2014; Too Good To Go, 2022). Vegetable waste includes vegetables that do not meet the quality standards for retail of fresh products or are wasted because of over-production. It is noted that also part of the vegetable waste is inedible and therefore referred to as unavoidable waste (De Laurentiis, Corrado, & Sala, 2018). Much of the vegetable waste produced occurs at or between farm and factory. Hence, this collectable material represents a potentially valuable source of food ingredients.

Consumers have a growing demand for high quality foods that are produced more sustainably. Furthermore, consumers prefer more natural products and the food industry is re-directing its sourcing policy towards clean-labelling and using only minimally-processed food additives. Important food ingredients at the forefront of these pivotal changes relate to vegetable products such as onion, carrot, tomato, pepper, and asparagus, which are used in a variety of foodstuffs such as soups, sauces and ready-to-eat meals. Conventional food ingredients no longer meet the newly devised criteria for both sustainability and quality. It is therefore proposed to produce high quality and fully natural food ingredients, in the form of dried products, from high-value vegetable waste. Dried vegetable products have the advantage of extended shelf life and enable easy application in instant food products. To obtain these high-quality dried products, an innovative processing strategy is designed. White asparagus has been identified as the ideal model crop in this project as the asparagus

production generates sizable, unutilized loss and currently marketed dry asparagus products are lacking the quality and naturalness consumers ask for. The processing strategy could be adopted for other vegetables as well.

1.2. White asparagus as model crop

The genus *Asparagus,* a member of the *Asparagaceae* family, has many species that are widely cultivated for commercial use (Kubota, Konno, & Kanno, 2012). The most economically important and popular species with increasing interest in the food industry is the garden asparagus, *Asparagus officinalis,* which ranks 10th in the list of top-14 healthiest vegetables (Kubota et al., 2012; Pegiou, Mumm, Acharya, de Vos, & Hall, 2019). The garden asparagus is classified into two main types, i.e. green (and green-purple) and white; the latter being harvested underground before being exposed to light (Pegiou et al., 2019). Most asparagus are being sold as fresh, canned and frozen (Chitrakar, Zhang, & Adhikari, 2019; Fuentes-Alventosa et al., 2009). Besides the edible quality of the crop, asparagus is appreciated for its bioactive activities, including antitumor, antifungal, antioxidant and antimutagenic activities (W. Zhang, Wu, Wang, Chen, & Yue, 2014).

The green asparagus variety traditionally has a much larger global market share to the extent that some countries only see the green variety and consumers may not even be aware of the existence of the white asparagus. However, consumers from some countries including the Netherlands, Belgium and Peru, are more familiar with the white varieties compared to green (Pegiou et al., 2019). In the Netherlands, 18 kton asparagus (mostly white) is harvested annually (Eurostat, 2022). The amount of white asparagus waste is extensive and growing. Removal of the lower part of the stem (ca 4 cm = 'cut-offs') after harvest, represents ca 15 % (w/w) loss. Furthermore, an increasing volume of fresh asparagus is sold as peeled spears – asparagus peels represent approximately 20 %. Both the lower part of the stem and peels are considered inedible, therefore contribute to unavoidable loss. Another ca 15 % of asparagus spears are discarded for failing to meet stringent quality criteria (colour, shape, length, damage). Consequently, the overall wastage in the industry can exceed 30 % of the total harvested product. In the European market, more than 95 % of the asparagus produced comes from 8 countries in 2019. Among which, Germany and the Netherlands produced 46 % of the total amount (Eurostat, 2022). The most concentrated asparagus harvest in Europe occurs within a 50-60 km radius between Germany and the Netherlands, centred around Noord-Limburg. It is estimated that ~3000 tons of collectable waste (~7 % dry matter) is

produced in the Netherlands alone. Therefore, this waste stream represents a huge potential source of a high-quality food ingredient.

Currently, dried asparagus powders available to the food industry are often applied in instant products such as instant vegetable soups. The quality of the asparagus powder is inferior as the retention of key asparagus volatile flavour components during drying is poor and these components are generally at low concentrations in the powders. The harsh drying process also leads to early formation of heat-induced flavour compounds, while ideally, we aim to form these heat-induced flavour compounds during the preparation of the product by the consumer. For example, for instant asparagus soup this will be once the asparagus powder is dissolved in hot water. To provide consumers with tasty and natural foods that use dried vegetable ingredients, it is interesting to prepare a high-quality vegetable powder, which has retained maximum levels of key flavour and fragrance components of the freshly cooked vegetable and meets clean-labelling and sustainability requirements without any need for 'artificial' flavourings. Therefore, the drying process of asparagus, as well as other vegetables, needs to be reconsidered.

1.3. Conventional vegetable drying techniques

Vegetable drying is common practice for preservation purposes and enhances more efficient transportation. Conventionally, vegetables are sun-dried or hot air-dried. Traditional solar drying is a cheap method, but often a slow process impeded by weather conditions and the food is exposed to potential contamination sources (insects, birds and other animals) (Guiné, 2018; Karam, Petit, Zimmer, Baudelaire Djantou, & Scher, 2016). The poor quality (in terms of colour, nutritional composition, and hygiene) of the obtained sun-dried product has led to the development of alternative drying technologies. Convective hot air drying (HAD) is the most common drying technique for producing vegetable powder in food industry due to its simplicity and low cost (Karam et al., 2016). HAD is carried out on vegetable pieces, which are consequently milled into powder. Another method for drying vegetable pieces is freeze drying. Freeze drying is a gentle dehydration technique and is often used for high-value heat sensitive products. However, it is expensive and makes it therefore less economically viable for large scale production. Lastly, another promising method is spray drying of concentrated vegetable juices. Spray drying is a well-established technology in the food industry, mainly to produce milk powder, but is relatively new for vegetable drying. Solar drying, HAD, freeze drying and spray drying all could yield a vegetable powder (Fig. 1.1).

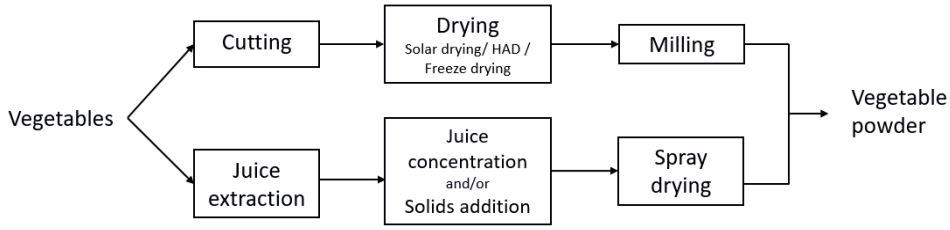

Figure 1.1 Different processing methods to produce vegetable powder from vegetables. HAD: hot air drying.

The HAD process can be either performed batch-wise in the form of a tray dryer or as a continuous process with a belt dryer for example. HAD usually involves high temperatures and long drying times, consequently, the quality of the final products is rather poor. The physical quality is often decreased by phenomena such as shrinkage, crystallization, puffing, colour changes and reduced rehydration capacity (Karam et al., 2016). Furthermore, long exposure to high temperatures results in significantly lower nutritional quality and flavour intensity (taste and aroma) in hot air dried vegetables compared to fresh ones (Nijhuis et al., 1998; Sablani, 2007). Freeze drying, on the other hand, results in high-quality dried products because of the low processing temperatures and absence of oxygen during processing (Karam et al., 2016). For freeze drying, the product is first frozen and then a controlled amount of heat under vacuum is applied to remove water via sublimation. Despite the minimal damage to the structure and preserved flavour quality, freeze drying is much less used for vegetable drying than HAD as the process is far more expensive. Reducing its costs by increasing process efficiency is difficult as freeze drying is a batch process and reducing the freeze drying time could compromise product quality (Nijhuis et al., 1998).

Similar to freeze drying, spray drying is suitable for drying thermally sensitive materials. Spray drying of vegetable juices is a relatively new approach and only a few key players in the spray-dried vegetable powder market are identified (Fortune Business Insights, 2021). Spray drying is, however, economically interesting and requires only a single-step procedure, in which liquid feeds are converted directly into powder (Shishir & Chen, 2017). In the case of vegetables, the juice needs to be extracted first from the crop by using a juicer (Fig. 1.1). The juice extraction could be followed by mild concentration of the juice, e.g. reverse osmosis, and/or addition of solids (e.g. maltodextrin) to reduce the amount of water that needs to be evaporated during spray drying. During spray drying, the vegetable juice is first

atomized into small droplets before entering the drying chamber where the droplets meet the hot drying air and moisture rapidly evaporates from the droplet. During evaporation, the droplets remain at relatively low temperatures despite the high inlet air temperatures applied making spray drying a relative mild method for drying heat sensitive products (Verma & Vir Singh, 2015). Furthermore, spray drying is specifically suitable for the encapsulation of volatile compounds due to the formation of a semi-permeable skin during the drying process (Coumans et al., 1994).

Since spray drying of vegetables requires extraction of the juice, a solid fraction remains. This fraction, which usually consists of fibre-rich material, can also be further processed for example by using conventional HAD. We can refer to this as 'split-stream processing' as we split the vegetable juice from the vegetable fibrous fraction and process both streams separately and then add the streams together again. Split-stream processing allows complete usage of the vegetable and spray drying of vegetable juice is a promising approach to produce flavour-rich vegetable powders. In the next section, the mechanism of flavour encapsulation during spray drying will be further explained.

1.4. Split-stream spray drying of vegetables

Spray drying is a frequently used technique to encapsulate flavours and other bioactive compounds (Madene, Jacquot, Scher, & Desobry, 2006). The flavour retention can be related to drying kinetics during spray drying. Spray drying kinetics can be described by different drying regimes as illustrated in Fig. 1.2.

At the start of drying, the droplets will heat up to the wet-bulb temperature (1). This is followed by the constant rate period (2) during which moisture is removed at a constant rate. The droplet remains at the wet-bulb temperature due to the evaporative cooling effect and the drying rate is dominated by the diffusion rate of water from the surface of the droplet to the drying air (Verma & Vir Singh, 2015). The constant rate period is followed up by the falling rate period (3), which commences once the surface of the droplet reaches a critical moisture concentration and the internal diffusion rate of water from the bulk to the surface of the droplet becomes the limiting factor (Srikiatden & Roberts, 2007). During the falling rate period the moisture evaporation rate decreases, and the product temperature increases. For flavour encapsulation, the start of the falling rate period is of particular importance since a semi-permeable "skin" is formed on the droplet surface, which allows further removal of

water but hinders the release of larger volatile aroma compounds (Coumans, Kerkhof, & Ruin, 1994). When the almost dried particle temperature closely approaches the outlet temperature of the spray dryer, the drying process is practically completed (4) and near-equilibrium is reached between the relative humidity of the outlet air and the (surface) moisture content of the particle.

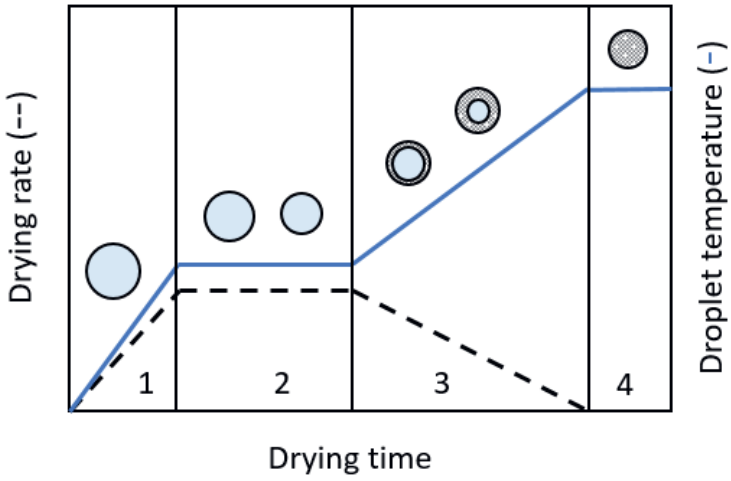

Figure 1.2 Schematic illustration of the drying rate, droplet temperature and morphological changes during spray drying of a droplet containing solids. The drying trajectory can be divided into four periods: (1) initial droplet heating after atomization, (2) constant-rate period, (3) falling rate period and (4) approximating near-equilibrium at the exit of the spray dryer.

Preparation of vegetable powders via spray drying starts with extraction and concentration of the juice. A concentration step is preferred to make the spray drying more efficient since the solid concentration in the juice is low (~ 4 %). Drawback is that vegetable juices are rich in small sugars which have low glass transition temperatures which cause stickiness of the powder in the spray dryer. To prevent stickiness, an additive or so-called carrier agent is usually added to increase the glass transition temperature of the concentrate. These carrier agents can thus ease the spray drying process (Madene et al., 2006). A frequently used group of carrier agents is hydrolysed starch (i.e. maltodextrins). Maltodextrins also promote the retention of aroma compounds by faster skin formation which strongly reduces diffusivity and thus loss of the aroma compounds (Madene et al., 2006; Zuidam & Heinrich, 2010). In general, carriers with low viscosity at high solids content such as maltodextrin are desired,

because it allows for relative higher concentrations and thus more efficient spray drying processes (Reineccius, 2004).

1.5. Scientific challenges

Different analytical techniques are available for the analysis of flavour compounds in foods. An emerging technique for the characterization of volatile profiles in food is mass spectrometry-based metabolomics (Diez-Simon, Mumm, & Hall, 2019). Metabolomics is defined as the comprehensive characterization of all small molecules (<1500 Da) or "metabolites" present in a biological sample (Wishart, 2008; A. Zhang, Sun, Wang, Han, & Wang, 2012). Metabolites are important indicators of food quality as they are often the coloured, fragrant or bioactive compounds contributing directly to nutritional value and both positive sensory attributes as well as negative ones such as off-flavours (Diez-Simon et al., 2019). By following an untargeted metabolomics approach, the overall metabolite profile of a food product can be identified. A few studies have used metabolomics to describe the effects of drying on the volatile aroma profile of tea (Xia, Guo, Fang, Gu, & Liang, 2021), onion and garlic (Farag et al., 2017) and hazelnuts (Cialiè Rosso et al., 2018). To the best of our knowledge, the effect of spray drying on the overall volatile profile of spray-dried food powders using mass spectrometry-based metabolomics has not been reported before. Therefore, performing a systematic study on the influence of spray drying conditions on the overall volatile profile is of interest. As mentioned before, maltodextrin is a commonly used carrier agent for spray drying. Formulating vegetable juice with different concentrations of maltodextrin could provide detailed information on the role of maltodextrin in flavour encapsulation.

Despite the good properties of maltodextrin as carrier agent, a disadvantage of maltodextrin is that it has high caloric content. Additionally, consumers nowadays prefer foods with preferably no additives at all, i.e. so-called "clean-label" foods (Asioli et al., 2017; Ingredion, 2014). The replacement of maltodextrin by for example asparagus fibre for making asparagus powder is therefore of great interest. However, vegetable fibres are insoluble and will increase the viscosity of the feed rapidly. Consequently, treatment, e.g. enzymatic hydrolysis, of the vegetable fibres might be necessary to improve their functionality.

Mass spectrometry-based metabolomics may provide valuable information on the volatile profile of the spray-dried asparagus powder and the profile can be compared to that of the

feed solution to assess the influence of the spray drying process. However, information on the volatile release during drying is more difficult to obtain using this technique. To monitor volatile flavour release during drying, an in-line detection of volatile compounds is needed. It is proposed to employ a thin film dryer equipped with a photo-ionisation detector (i.e. the "electronic nose"). This set-up would allow monitoring volatile compound release and drying kinetics (e.g. mass decrease) simultaneously.

Finally, the flavour profile as perceived by the consumer is of major importance in the production of foods. Sensory analysis can provide valuable information on the aroma and taste of food products. Combining metabolomics with sensory analysis helps to understand which compounds are sensory relevant and how the drying process contributes to the (off-) flavour of the final food products.

1.6. Objective and outline of the thesis

The objective of the work described in this thesis is to develop a novel processing route using spray drying for conversion of asparagus waste streams into flavour-rich powder ingredients. To do this, a split-stream process is proposed which separates the asparagus juice and fibre, after which asparagus juice is spray-dried and the fibre is processed using different methods. We address the role of carrier formulations on the volatile flavour retention after spray drying and the in-line volatile compound release during thin film drying. We explore strategies to improve the functionality of asparagus fibre as carrier agent. Finally, we investigate the obtained products of the split-stream process by metabolomics and sensory evaluation to address their potential as flavour-rich food ingredients. In the following paragraphs, the content of the chapters of this thesis is summarized (Fig 1.3).

Chapter 2 presents a systematic study of spray drying concentrated asparagus juice with maltodextrin. The physical properties and volatile profile of the spray-dried powders are evaluated. The Gordon-Taylor equation is used to describe the glass transition temperatures of the spray-dried powders as function of moisture, maltodextrin and asparagus content.

To maximize the usage of the waste stream, it is of interest to explore the function of vegetable asparagus fibre as the carrier agent for spray drying asparagus juice concentrate. This is explored in **chapter 3** by replacement of the conventional carrier agent maltodextrin with vegetable fibres (i.e. asparagus fibre, citrus fibre and microcrystalline cellulose) during spray drying. The maltodextrin is partially replaced by vegetable fibres and the effects on the

physical properties and volatile profile in spray-dried asparagus powders are analysed. Furthermore, the effect of initial solids content in the spray drying feed is investigated.

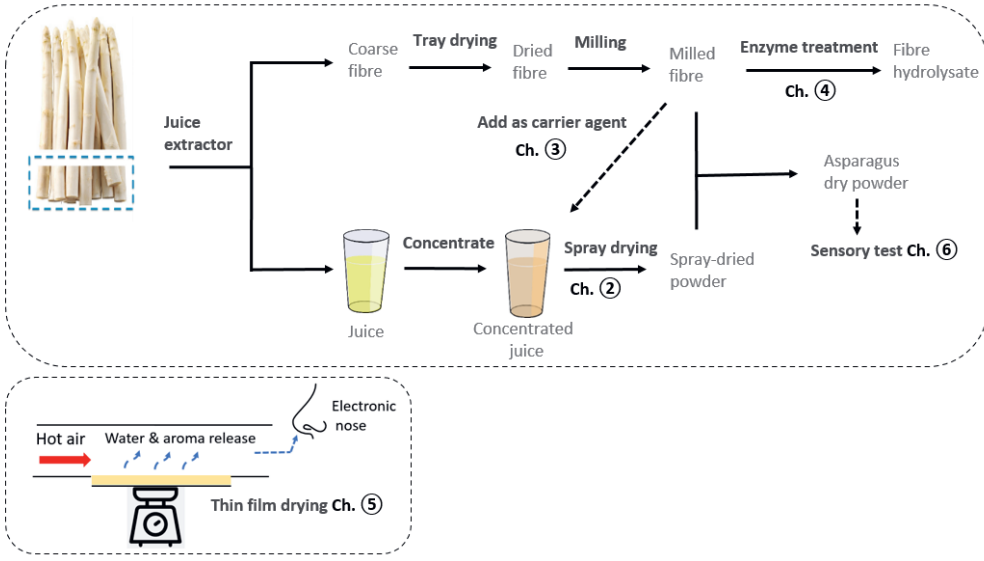

Figure 1.3 Overview of the processing scheme proposed in this thesis with corresponding chapter numbers.

The functionality of asparagus fibre as carrier agent is expected to be improved by modification. Therefore, **chapter 4** presents a study into the effect of an enzymatic treatment of the asparagus fibres to convert the asparagus fibres into soluble cello-oligosaccharides. The potential of these cello-oligosaccharides as carrier agent for spray drying is evaluated.

Chapter 5 describes the aroma release of acetone during thin film drying by using experimental data and a mechanistic heat and mass transfer model. Drying experiments are performed in a thin film dryer set-up and the aroma release is measured in-situ during drying by using a photo-ionisation detector. The mechanistic model is a one-dimensional heat and mass transfer model describing film drying of a mixture consisting of water and acetone in a solid matrix of maltodextrin.

The sensory study presented in **chapter 6** is done to evaluate the asparagus products developed during the previous thesis chapters. The asparagus products are prepared in a soup formulation and compared to a commercial reference asparagus powder. The relevant sensory attributes are linked to metabolomics and analysis of the physical properties of the asparagus soups.

Chapter 7 concludes the thesis with a general discussion. Based on the main findings in this thesis, the split-stream process is tested for another vegetable, i.e. bell pepper. Subsequently, the use of hydrolysed asparagus fibre as carrier agent is further discussed, followed by an outlook for future research.

Chapter 2

Maltodextrin improves physical properties and volatile compound retention of spray-dried asparagus concentrate

This chapter has been published as Siccama, J.W., Pegiou, E., Zhang, L., Mumm, R., Hall, R.D., Schutyser, Boom, R.M., M.A.I. Maltodextrin improves physical properties and volatile compound retention of spray-dried asparagus concentrate. *LWT.* **2021**, *142*. https://doi.org/10.1016/j.lwt.2021.111058.

2.1. Introduction

Asparagus (*Asparagus officinalis*) is a popular vegetable consumed all over the world. The production of asparagus comprised 9.1 million tons globally in 2018 (Knoema, 2021). While the green form is most common, the white form is appreciated by its consumers because of its structure and flavour profile. White asparagus flavour has been the topic of several studies in the past (Tressl, Bahri, Holzer, & Kossa, 1977; Tressl, Holzer, & Apetz, 1977; Ulrich, Hoberg, Bittner, Engewald, & Meilchen, 2001), which has led to the identification of some key aroma components in cooked asparagus (Pegiou et al.,2019).

After harvesting, approximately one-third of the lower part of the white asparagus spear is cut off because of its woody texture and to standardize the length of the spears for the market (W. Zhang et al., 2014). A significant waste stream is thus generated, which could potentially be utilised as a food ingredient, for example in the form of asparagus powder for instant soups. Conventionally, commercial asparagus powder is made by air-drying (i.e. tray drying) small pieces of asparagus spear followed by milling (Karam et al., 2016; Nindo, Sun, Wang, Tang, & Powers, 2003). However, the drying process alters the volatile profile of asparagus powder. Some aroma compounds of asparagus are lost during drying, whereas some other asparagus key odorants can be formed upon drying, including sulfur-containing compounds such as dimethyl sulphide (Nijhuis et al., 1998; Ulrich et al., 2001). Ideally, the formation of those key odorants should be suppressed during drying of asparagus powder to prevent aroma loss upon storage. To ensure flavour stability, artificial flavouring agents are added to the asparagus powders. These flavouring agents may not fit in a formulation targeted to be perceived as natural and healthy by consumers (Bearth, Cousin, & Siegrist, 2014; Eiser, Coulson, & Eiser, 2002; Shim et al., 2011). Therefore, to obtain asparagus powders with better aroma profile, new drying strategies need to be developed. These strategies include the selection of a drying method as well as the optimisation of this drying method.

Spray drying has been widely used to encapsulate flavour compounds in vegetable powders (Verma & Vir Singh, 2015). Thus, asparagus powder with improved flavour profile may be obtained by using spray drying (Siccama, Zhang, & Schutyser, 2019). More specifically, asparagus juice can be pressed and concentrated from the side stream and then spray-dried to produce asparagus powder. However, direct spray drying of this concentrate is problematic due to stickiness issues leading to fouling in the drying chamber. This is because asparagus concentrate is rich in small sugars that have a low glass transition temperature (T_g). Hence,

the addition of carrier agents with a high T_g, e.g. maltodextrins with a low dextrose equivalent (DE), to the concentrate can be used to avoid fouling and to improve powder quality (Verma & Vir Singh, 2015).

During spray drying, the liquid feed is atomized into small droplets and exposed to hot air. Initially, the drying is externally limited, but an internal moisture gradient evolves when the surface of the droplet reaches a critical moisture concentration. After this, a semi-permeable "skin" is formed on the droplet surface, which allows further removal of water but hinders the release of larger volatile aroma compounds (Coumans et al., 1994). Loss of volatile compounds mainly occurs before this "skin" is formed, i.e. during the constant drying rate period (Thijssen, 1971). Hence, a shorter constant rate period is favourable for aroma retention during spray drying. Specifically, addition of hydrolysed starches (i.e. maltodextrins) can encapsulate flavours by faster skin formation and increase the T_g of the mixture (Madene et al., 2006; Zuidam & Heinrich, 2010). Besides, adding high molecular weight carrier agents could reduce the diffusion of flavour compounds from within the drying matrix to the droplet surface until the semi-permeable skin is formed (Anandharamakrishnan & Padma Ishwarya, 2015). In general, carriers with low viscosity at high solids content such as maltodextrin are desired, because it allows for relative higher concentrations (Reineccius, 2004).

Furthermore, the drying conditions (e.g. inlet temperature) influence volatile retention during spray drying. For example, a higher inlet temperature may improve aroma retention because it shortens the constant rate period (Coumans et al., 1994; Reineccius, 2004). Nevertheless, a too high inlet temperature can lead to worse aroma retention by inducing excessive bubble formation and surface cracks (King, 1995).

Thus, both carrier choice and drying conditions affect the volatile profile of spray-dried powders. In this study we employ mass spectrometry-based metabolomics, being an emerging technique for the characterization of volatile profiles in foods (Diez-Simon et al., 2019). To the best of our knowledge, the combination of spray drying experiments and gas chromatography-mass spectrometry (GC-MS) analysis of the overall volatile profile of spray-dried powders following a metabolomics approach has not been reported before. Therefore, we here aim to assess the volatile profile and the retention of key volatiles in spray-dried asparagus concentrate as influenced by the addition of maltodextrin DE12 and

drying conditions. Maltodextrin DE12 was selected since Bangs and Reineccius (1982) found that the overall retention of twelve volatile compounds was maximised for maltodextrins with DE 10-15. In brief, asparagus juice was extracted from a white asparagus waste stream (i.e. bottom of the spears), concentrated with reverse osmosis and mixed with maltodextrin DE12 at different solids ratios. Subsequently, the solutions were spray-dried at different inlet and outlet temperature combinations. The powders were evaluated in terms of physical properties (i.e. moisture content, T_g, particle size distribution and particle morphology) and their volatile profile. The volatile profiles were analysed by headspace solid-phase microextraction (HS-SPME), followed by gas chromatography-mass spectrometry (GC–MS).

2.2. Materials & Methods

2.2.1. Sample preparation

Raw fresh asparagus cut-offs (*Asparagus officinalis*) were kindly provided by Teboza BV (Helden, the Netherlands). Concentrated asparagus juice was prepared from these asparagus cut-offs by Wageningen Food Biobased Research (Wageningen, the Netherlands). Specifically, asparagus juice was pressed and centrifuged to remove any fibres. The juice was concentrated to a factor of 5.6 with reverse osmosis into a final dry matter content of 21.7 % w/w. The sugar composition of the asparagus concentrate consists of 78 mg/ml fructose, 72 mg/ml glucose and 8 mg/ml sucrose, which was determined with high-performance liquid chromatography (HPLC) using a Shodex KS-802 8.0 × 300 (mm) column. The column was operated at 50°C and connected to a refractive index detector (Shodex RI-501). Milli-Q water was used as eluent with a flow rate of 1 ml/min. The concentrate was aliquoted into test tubes and stored at -20 °C before the experiments. For every experiment, a new tube was taken from the freezer and the concentrate was defrosted in the fridge at 4 °C for 18-20 hours.

Maltodextrin DE12 (MD12, Roquette, France) was added to the concentrated asparagus juice to formulate the mixtures for the spray drying experiments shown in Table 2.1. The mass ratios between asparagus solids and maltodextrin in the mixtures were adjusted to 2:1, 1:1 and 1:2, respectively. In addition, one sample with a 1:2 ratio was diluted to obtain the same total solids content as the 1:1 ratio sample. This sample will be referred to as 1:2*. Pure concentrated asparagus juice was used as a reference sample (i.e., 1:0). All the samples were stirred at room temperature at 400 rpm for 1 hour before each spray drying experiment.

Table 2.1 Overview of the experimental design for spray drying of asparagus juice concentrate and maltodextrin mixtures

	Sample composition			Drying condition	
Sample	Asparagus solids (w/w)	Maltodextrin (w/w)	Total solids (w/w)	Inlet (°C)	Outlet (°C)
1:0	22	0	22	160	90-95
2:1	20	10	29	160	90-95
1:1	18	18	36	160	90-95
1:2	15	30	45	160	90-95
1:2*	12	24	36	160	90-95
1:1	18	18	36	180	105
1:1	18	18	36	180	90

2.2.2. Spray drying experiment

The maltodextrin-asparagus concentrate mixtures were spray-dried with a Model B-290 mini spray dryer (BÜCHI Labortechnik AG, Flawil, Switzerland). The aspirator rate was 90 % which corresponded to an airflow of 35 m^3/h. To investigate the effect of the maltodextrin concentration on the properties of spray-dried powders, samples (1:0, 2:1, 1:1 and 1:2) were dried under the same conditions, i.e., the inlet air temperature (T_{in}) was 160 °C and the outlet air temperature (T_{out}) was 90-95 °C. The speed of the peristaltic pump was adjusted to 3 – 10.5 ml feed/min to ensure the desired outlet air temperature. In addition, the sample with a ratio of 1:1 was dried in two inlet/outlet combination experiments (i.e., T_{in}/T_{out}=180 °C/90 °C and 180 °C/105 °C), to investigate the effect of drying conditions. For both combinations, the feed rate was adjusted to reach the desired T_{out}. For every condition (i.e. ratio and drying condition), three independent spray drying experiments were performed and the asparagus powders were collected at the outlet of the spray dryer for further analysis.

2.2.3. Moisture content

Spray-dried powder (~ 0.5 g) was placed in a hot air oven (Binder, Tuttlingen, Germany) to determine its moisture content. The powder was weighed before and after drying at 105 °C overnight, and the moisture content of the powder was calculated on total basis. Measurements were carried out in triplicate.

2.2.4. Glass transition temperature (T_g)

The T_g of the spray-dried powders was determined using differential scanning calorimetry (DSC) (DSC-250, TA Instruments, New Castle, England). In addition, the T_g of asparagus

concentrate was determined after pre-drying the concentrate in a climate chamber (Memmert, Germany) at 25 ºC and relative humidity of 10 % for 24 hours. Samples of about 5 mg were weighed in aluminium Tzero pans which were then hermetically sealed. Temperature ramp measurements were carried out at a rate of 10 ºC/min, and the temperature range was set between -60 ºC and 140 ºC depending on the moisture content of the sample. The DSC thermograms were analysed using Trios software (TA Instruments, New Castle, England). The T_g was determined from the midpoint, which was based on the inflection of the endothermic shift due to glass transition, i.e. the peak of the derivative. After the temperature ramp measurements, a hole was punched in the lid of the pans and the moisture content of the sample was determined by drying the samples overnight at 105 °C. All measurements were in duplicate and the mean values of the measured results were reported.

2.2.5. Particle size distribution and morphology

The particle size distribution of the spray-dried powders was measured using a Mastersizer 3000 analyser (Malvern Inc, Worcestershire, UK) with the dry powder disperser Aero S. The particle size distribution was determined with the Mastersizer 3000 software and presented on a volume basis. Dried particles were visualised using scanning electron microscopy (SEM). The powders were attached to SEM stubs using carbon adhesive tabs, sputter-coated with gold under vacuum, and examined using a Neoscope JCM-7000 (JEOL, USA). SEM was carried out at 10 kV with a magnification of x1600.

2.2.6. Preparation of liquid samples

Before headspace analysis of the spray-dried powders, the influence of maltodextrin on the gas/liquid-equilibrium in liquid samples was evaluated. Samples were prepared by dissolving maltodextrin DE12 in water at different concentrations, followed by mixing of the maltodextrin solutions with concentrated asparagus juice. The resulting mixtures contained maltodextrin concentrations of 0, 15, 25, 34 and 44 %. The pH of all mixtures was measured. The pH-values obtained were the same for all mixtures, thus pH could not influence the gas/liquid partition coefficient in this study. All samples contained the same amount of asparagus solids, i.e. 30 mg, and had similar total weight. The samples were stored at -80 °C before analysis of volatile compounds. The volatile compounds were measured according to the method described in section 2.2.7.

2.2.7. Headspace analysis of volatile compounds

Volatile compounds in the defrosted asparagus concentrate, maltodextrin-asparagus concentrate mixtures and spray-dried asparagus powders were analysed by GC-MS. Samples were weighed (mass in mg) based on equation 2.1, i.e. all the samples contained 30 mg dry weight of asparagus solids.

$$mass = \frac{30}{X_S\, X_{a(db)}} \tag{2.1}$$

Where X_s (kg solids/kg total) is the total solids content of the sample determined via moisture content analysis. $X_{a(db)}$ (kg asparagus solids/kg solids) is the fraction of asparagus solids in the solids content of the sample, which can be derived from the mass ratio between asparagus solids and maltodextrin. For example, X_a of 2:1 ratio equals 0.67. For a 2:1 ratio dry sample with a moisture content of 10 % w/w (i.e., X_s = 0.90), the sample weight for GC-MS analysis was 50 mg.

In addition, quality controls (QCs) were prepared from a mix of the spray-dried powders, except for the 1:0 ratio since there was too little sample. All samples were transferred to 10 ml glass vials which were subsequently stored at -80 °C until experimentation. Before analysis, EDTA and $CaCl_2$ were added to the samples giving a final concentration of 50 mM and 5 M, respectively. In the case of liquid samples (asparagus concentrate, mix) solid $CaCl_2$ was added first and subsequently the EDTA solution to a final volume of 1 ml. In the case of the dry samples (spray-dried powders), a saturated solution of 50 mM EDTA – 5M $CaCl_2$ was added to a final volume of 1 ml.

Volatile compounds were extracted from the headspace using solid-phase microextraction (SPME). A PDMS/DVB/CAR (Polydimethylsiloxane / Divinylbenzene / Carboxen) 50/30 µm diameter, 1 cm length (Supelco, PA, USA) fibre was used. The samples were incubated at 50 °C for 15 min with agitation. Subsequently, volatiles were trapped by exposing the fibre to the headspace of the vial for 15 min at 50 °C without agitation. The fibre was then thermally desorbed in the injector containing an empty glass liner (1 mm ID) (CIS4, Gerstel, Germany) at 250 °C for 2 min with a helium flow of 1 ml/min onto the GC column, in splitless mode. Sample handling was fully automated using a Gerstel MPS-2 autosampler using Gerstel MAESTRO software version 3.2. Analysis of the trapped volatiles was carried out on an Agilent GC7890A coupled to a 5975C quadrupole mass spectrometer. The column used was a Zebron ZB-5MSplus with dimensions 30m x 0.25mm x 1.00µm (Phenomenex).

The GC oven temperature was programmed starting at 45 °C for 2 min, then increased at a rate of 8 °C/min to 250 °C and then at a rate of 15 °C/min to 280 °C and maintained at 280 °C for 3 min. The carrier gas was helium, at a constant flow rate of 1 ml/min. The column effluent was ionised by electron impact at 70 eV, in the scan range m/z 33–330. The interface temperature was set to 280 °C. The retention indices (RIs) were calculated based on a series of n-alkanes (C6-C21) injected at the same conditions as the samples.

GC-MS raw data were processed using an untargeted metabolomics workflow. MetAlign software was used for baseline correction and alignment of the mass signals (S/N>3) (Lommen, 2009). Mass spectra were reconstructed to potential clusters using MSClust (Tikunov, Laptenok, Hall, Bovy, & de Vos, 2012). Metabolites were putatively identified by matching the obtained mass spectra and RIs with those in commercial and in-house libraries (e.g. NIST17). The level of identification given to the detected compounds follows the guidelines of the Metabolomics Standards Initiative (Sumner et al., 2007). Compounds with level 4 of identification are characterised as 'unknowns' and further investigation is required for their identification. Before the statistical analysis, zero values in the processed data were randomised around the limit of detection as determined by MetAlign. Subsequently, SIMCA 15.0.2. (Umetrics, Sartorius Stedim Data Analytics AB, Umeå, Sweden) was used to perform principal component analysis (PCA) after log10 transformation and Pareto scaling.

2.2.8. Volatile retention

All mixes and respective spray-dried powder were analysed with SPME-GCMS. The volatile retention of each independent sample was calculated based on the ratio of the spray-dried powder with the corresponding mix in equation 2.2. The retention was reported as the average retention of the triplicates with standard deviations.

$$retention\ (\%) = \frac{Peak\ intensity_{(spray-dried)}}{Peak\ intensity_{(mix)}} \cdot 100 \tag{2.2}$$

The spray-dried powders were reconstituted to the same maltodextrin concentration as the mix for the headspace analysis, therefore we could safely assume the partition coefficients for the volatiles were similar.

2.2.9. Statistical analysis

All experiments were conducted at least in duplicate and results were presented as mean ± standard deviations. One-way analysis of variance (ANOVA) and Tukey's HSD post hoc test

were performed, and $p \leq 0.05$ meant the difference between groups was statistically significant. In the case of unequal variances, the Games-Howell post hoc test was used. All statistical analyses were performed with SPSS Statistics (SPSS 25; IBM, USA).

2.3. Results and discussion

2.3.1. Moisture content

Moisture contents were measured for the different spray-dried powders (Table 2.2). The moisture content of powder dried from a 2:1 asparagus solids to maltodextrin ratio was found to be higher than that of the 1:2 ratio sample. By increasing the amount of maltodextrin before drying, the total solids content is necessarily increased. Both the maltodextrin concentration and the total solid content of the feed solution were expected to affect the properties of the spray-dried asparagus powder. To separate these effects, the 1:2* sample was also analysed, which was diluted with water to give a similar total solids content as the 1:1 ratio sample.

Diluting the sample from 45 to 36 % w/w initial dry matter, i.e. 1:2 and 1:2*, did not significantly affect the residual moisture content of the obtained powders (see Table 2.2). It can be argued that the 1:2 and 1:2* samples should follow a similar drying curve, in which mostly the constant rate period will be longer for the diluted concentrate. Nevertheless, the equilibrium moisture constant is the same for these powders.

Spray drying of the 1:1 and the 1:2* samples with the same initial dry matter (i.e. 36 %w/w) however resulted in a significant difference in residual moisture content. When maltodextrin is added, the hygroscopicity of the solids is affected, which influences the residual moisture content. These observations are in line with the study of Grabowski, Truong and Daubert (2006), who investigated the influence of varying maltodextrin-matrix ratios in spray drying of sweet potato puree. An increased maltodextrin concentration in their feed resulted in lower residual moisture contents, even at low maltodextrin concentrations (0, 10 and 20 % on dry basis). Furthermore, the drying conditions influence the residual moisture content in the powder. Higher inlet air temperatures and smaller temperature differences between the inlet and outlet air ΔT (T_{in}-T_{out}) generally result in powders with lower moisture content (Reineccius, 2004). The residual moisture content of the powders spray-dried at 180/105 (T_{in}/T_{out}) seems somewhat lower compared to 180/90 (Table 2), however, this difference was not statistically significant.

Table 2.2 Effects of asparagus solids to maltodextrin ratio and spray drying conditions on the moisture content and the glass transition temperature of the asparagus powder.

Solids ratio Asparagus : MD12	T_{in}/T_{out} (°C/°C)	Residual moisture content (% w/w)	Glass transition temperature (°C)
1:0	160/90-95	20.00**	-
2:1	160/90-95	15.03 ± 0.15 [a]	4.18 ± 0.76 [a]
1:1	160/90-95	8.91 ± 0.24 [b]	28.07 ± 0.24 [b]
1:2	160/90-95	5.24 ± 0.17 [c]	44.47 ± 14.14 [abc]
1:2*	160/90-95	5.49 ± 0.51 [c]	55.01 ± 0.11 [c]
1:1	180/105	8.84 ± 0.18 [b]	28.61 ± 0.73 [b]
1:1	180/90	9.33 ± 0.22 [b]	24.10 ± 1.17 [b]

Note: The values followed by different lowercase letters (a–c) within a column are significantly different at $p \leq 0.05$. * The 1:2* samples were diluted to obtain a similar total solids content before spray drying as the 1:1 ratio. ** The sample quantity was too low to analyse the moisture content; therefore, an estimated value is reported.

2.3.2. Glass transition temperature

The formation of glassy powder particles is necessary to effectively encapsulate volatile compounds, to avoid fouling in the equipment and to obtain a free-flowing powder (Y. H. Roos, 2010). Therefore, the glass transition temperatures of the different spray-dried powders were measured (Table 2.2). The T_g of a powder is influenced by both its solids composition and its moisture content, and it is difficult to decouple those. With larger moisture content or less maltodextrin, lower T_g values are found. The T_g values of the 1:1 ratio powders spray-dried at different conditions were not significantly different. This was expected because the composition of those samples was the same and the residual moisture content in the powders was similar.

The effects of solid composition and residual moisture content on the T_g were evaluated with the Couchman-Karasz equation for multicomponent mixtures (equation 2.3), previously described by (Bhandari & Howes, 1999).

$$T_g = \frac{x_w \Delta C_{p,w}\, T_{g,w} + x_m \Delta C_{p,m} T_{g,m} + x_a \Delta C_{p,a} T_{g,a}}{x_w \Delta C_{p,w} + x_m \Delta C_{p,m} + x_a \Delta C_{p,a}} \quad (2.3)$$

Where x_w, x_m and x_a are the weight fractions of water, maltodextrin and asparagus solids on wet basis. $\Delta c_{p,w}$, $\Delta c_{p,m}$ and $\Delta c_{p,a}$ represent the heat capacity change at glass transition of water, maltodextrin and asparagus solids, respectively. $T_{g,w}$, $T_{g,m}$ and $T_{g,a}$ are the glass transition temperatures of water (138 K), maltodextrin DE12 and the asparagus solids, respectively.

Equation 2.3 can be rewritten to 2.4 with k_1 equals $\Delta c_{p,m}/\Delta c_{p,w}$ and k_2 equals $\Delta c_{p,a}/\Delta c_{p,w}$, which is often referred to as the Gordon-Taylor equation:

$$T_g = \frac{x_w T_{g,w} + k_1 x_m T_{g,m} + k_2 x_a T_{g,a}}{x_w + k_1 x_m + k_2 x_a} \quad (2.4)$$

Two coefficients k_2 and $T_{g,a}$ were estimated based on Gordon-Taylor equation (2.4) using experimental data, whereas other parameter values were obtained from literature. Specifically, for water a $\Delta c_{p,w}$ value of 1.91 $kJ \cdot kg^{-1} \cdot K^{-1}$ was used and for maltodextrin a $\Delta c_{p,m}$ value of 0.425 $kJ \cdot kg^{-1} \cdot K^{-1}$ (Siemons, Politiek, Boom, van der Sman, & Schutyser, 2020). The anhydrous T_g of maltodextrin DE12 ($T_{g,m}$) was 426 K (153 ºC) (Siemons et al., 2020).

We obtained a good fit (R^2=0.95) and estimated a $T_{g,a}$ of 32 ºC and a k_2 of 0.48 (Fig. 2.1). The $T_{g,a}$ can be roughly related to its composition as described in section 2.2.1, i.e. fructose (10 ºC), glucose (36 ºC) and sucrose (67 ºC) (Y. Roos, 1993). The $\Delta c_{p,a}$ of 0.91 $kJ \cdot kg^{-1} \cdot K^{-1}$ was derived from the k_2 value and is slightly higher than reported values for mono- and disaccharides, e.g. fructose (0.75-0.84 $kJ \cdot kg^{-1} \cdot K^{-1}$), glucose (0.63-0.88 $kJ \cdot kg^{-1} \cdot K^{-1}$) and sucrose (0.60-0.77 $kJ \cdot kg^{-1} \cdot K^{-1}$) (Y. Roos, 1993).

Concerning storage, it is desired to obtain a powder in the glassy state at ambient temperatures (Y. H. Roos, 2010). When the powder shifts from a glassy to a rubbery state, undesired effects may occur, such as sticking, agglomeration and volatile loss (Bonazzi & Dumoulin, 2011). Based on our findings, only the samples prepared with asparagus solids to maltodextrin ratios of 1:2 or asparagus weight fraction ≤ 0.33 (Fig. 2.1) reached a sufficiently high T_g to be stored at ambient conditions. This model could potentially be used to estimate the T_g of asparagus powder in future when other carrier agents are used.

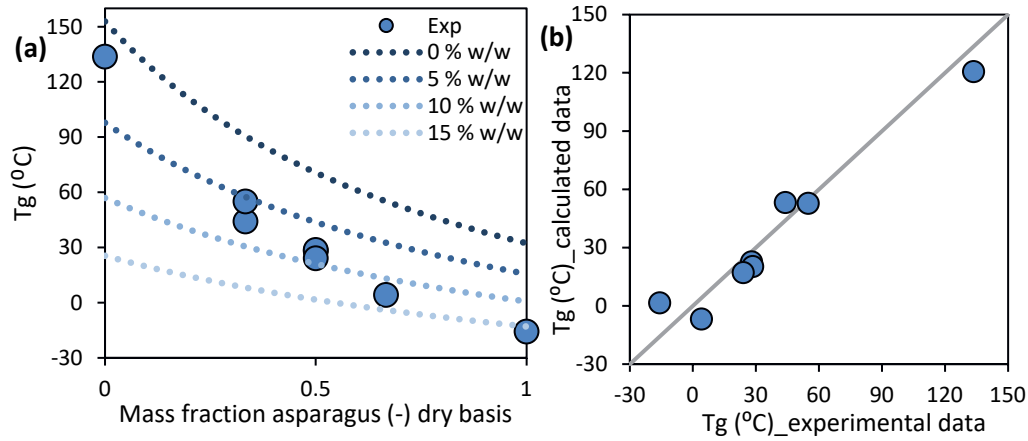

Figure 2.1 (A) The glass transition temperature of spray-dried asparagus concentrate as a function of the mass fraction of asparagus (dry basis). The experimental data is fitted with the Couchman-Karasz equation for multicomponent mixtures (dotted lines) for different residual moisture contents (0. 5, 10, 15 % w/w). Residual moisture contents of the experimental data can be found in Table 2.1. For the data point with asparagus weight fraction of 0, T_g value of a spray-dried maltodextrin solution (30 % w/w) without asparagus concentrate was reported. For the data point with asparagus weight fraction of 1, T_g value of liquid asparagus concentrate that was pre-dried in a climate chamber at 10 % RH was reported. (B) The parity plot of the experimental and the calculated values of T_g based on the model.

2.3.3. Particle size distribution

The particle size distribution of all powders was analysed (Fig. 2.2). Larger powder particle sizes (100-2000 µm) can be explained by undesired agglomeration. Specifically, agglomeration was observed for the 2:1 ratio of asparagus solids to maltodextrin powder. This sample also had the highest residual moisture content (15.0 % w/w), which stimulated agglomeration of the powder particles. A slight shift towards larger particle sizes can be observed with an increase in maltodextrin content. The highest peaks of the 2:1 ratio, 1:1 ratio and 1:2 ratio samples were found to correspond to a particle size of ca. 8 µm, 10 µm and 15 µm, respectively. This increase in average particle size may be explained by the generation of larger droplets during atomization due to the increase of the feed viscosity with the addition of maltodextrin (Bangs & Reineccius, 1982; Reineccius, 2004).

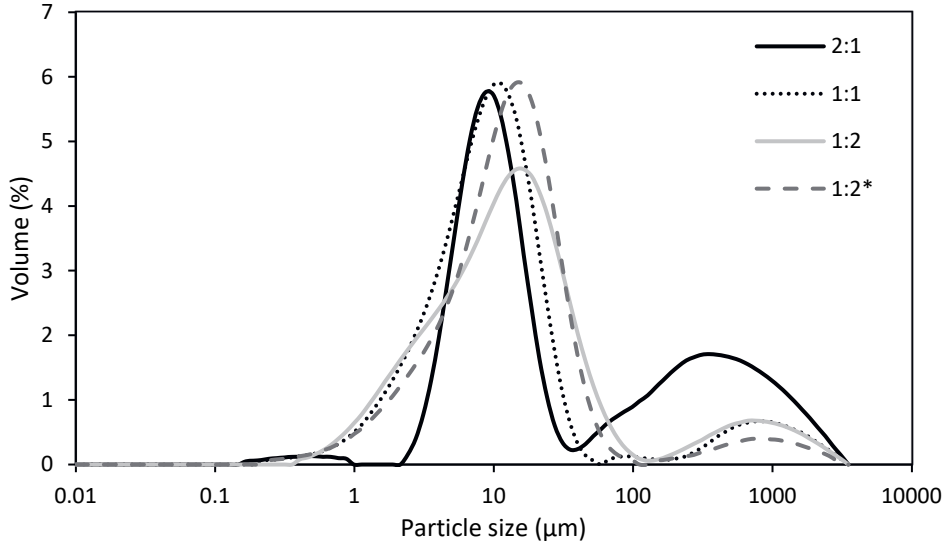

Figure 2.2 Particle size distribution of spray-dried asparagus powders with different asparagus solids to maltodextrin ratios dried at T_{in}/T_{out} of 160/90. The 1:2* samples were diluted to obtain a similar total solids content before spray drying as the 1:1 ratio.

The results of the 1:1 ratio dried at different inlet and outlet temperature combinations were found to be similar (data not shown), indicating no significant effect of drying conditions on particle size distribution in this study.

2.3.4. Morphology

Different particle morphologies such as smooth round and dented particles were observed for the spray-dried powders (Fig. 2.3). Similar dented structures for MD12 were previously observed by Both et al. (2018) and Siemons et al. (2020). For the 2:1 ratio of asparagus solids to maltodextrin (Fig. 2.3A), only small spherical particles with a smooth surface were present in the powder. It is suggested that the high concentration of small sugars from the asparagus concentrate allows more shrinkage of the droplets which results in smoother and more spherical particles. This is also in agreement with Paramita et al., (2010) who observed that replacement of maltodextrin DE 11 by trehalose also provided smoother particles.

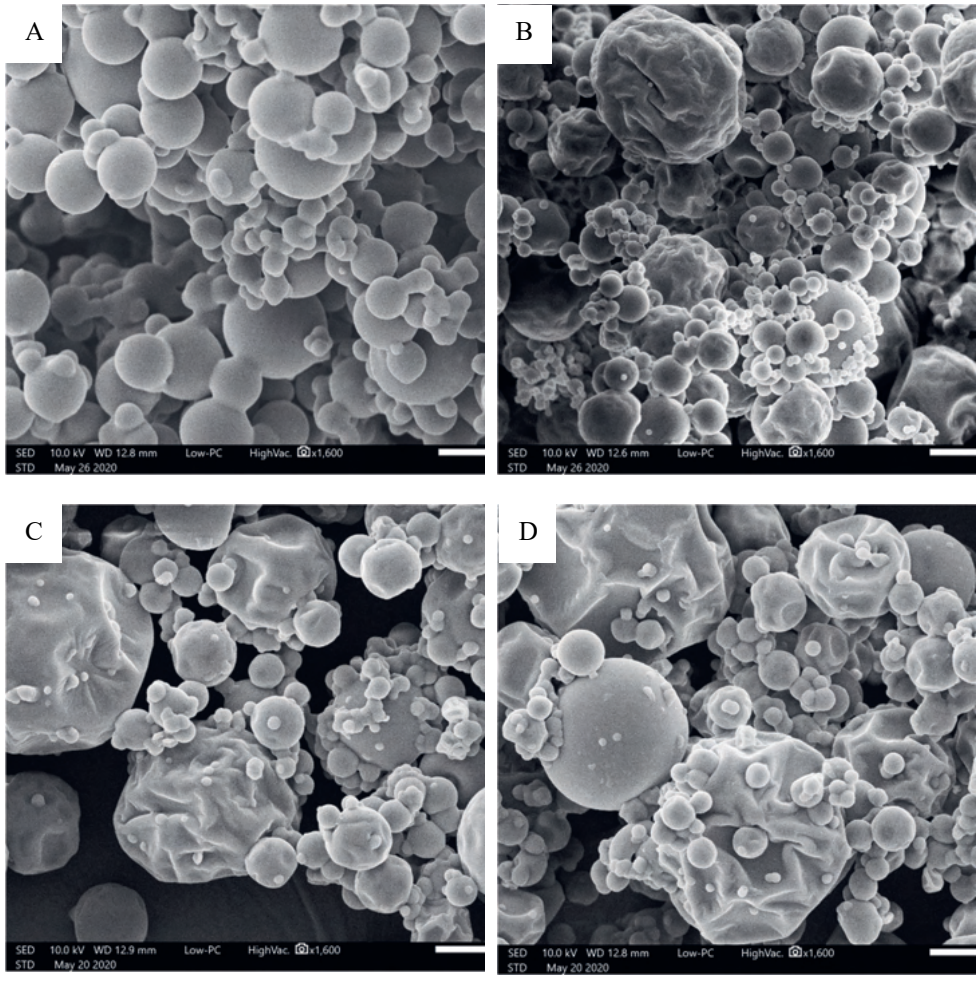

Figure 2.3 Powder morphology of spray-dried asparagus powders with asparagus solids to maltodextrin ratios 2:1 (A), 1:1 (B), 1:2 (C), and 1:2* (D). The 1:2* samples were diluted to obtain a similar total solids content before spray drying as the 1:1 ratio. All powders were spray-dried at 160/90 (T_{in}/T_{out}). Bar = 10 μm.

The influence of the different spray drying conditions on the morphology appeared to be minor (data not shown). All powders had both smooth and dented particles and the particle sizes appear similar based on the SEM images.

2.3.5. Principal component analysis of asparagus aroma compounds

To study the influence of maltodextrin on the volatile compounds after spray drying, first the overall volatile profiles of asparagus concentrate samples before and after spray drying were

compared. Processing of the GC-MS raw data and manual filtering of system artefacts resulted in a list of 70 compounds that were further analysed. Identification was focused on the known key asparagus volatiles from literature (Pegiou et al., 2019).

Principal components analysis (PCA) was performed to obtain a general overview of the samples and how their volatiles composition differ. PCA on all the samples showed that PC1 separates the spray-dried powder and the concentrate/mix before drying, indicating a clear difference in the volatile profiles (Fig. A.2.1A). The QCs consisting of a mix of spray-dried powders were analysed to determine technical variability. The QCs group together in the PCA plot, indicating a low technical variation of the measurements. To get a better view of the difference between the powders, PCA was performed on all the spray-dried powder samples with and without maltodextrin (Fig. A.2.1B). The first two PCs explain 48 % and 19.6 % of the total variation, respectively. The variation on PC1 can be attributed to the different ratios of maltodextrin used. This is more obvious from Fig. 2.4A, where the PCA was performed on the spray-dried powders containing the different concentrations of maltodextrin. Here the first PC explains 38.4 % of the variation between powder samples. The black arrow indicates that spray-dried powders with higher maltodextrin concentrations move towards the negative x-axis.

The loading plot (Fig. 2.4B) shows that the influence of maltodextrin concentration on the retention of aromas is dependent on their molecular properties. Focusing on the PC1, we can see that mainly alcohols and aldehydes were higher present with higher concentrations of maltodextrin. Sulfur-containing volatile compounds (S-compounds) were higher present with lower maltodextrin concentrations, while carboxylic acids, ethers and furans were not significantly affected by the maltodextrin concentration.

Among these 70 compounds, some compounds were previously identified as asparagus aromas including 3-methylthio-propanal, 1-octen-3-ol, 1-pentanol, octanal and dimethyl sulphide (Tressl, Bahri, et al., 1977; Ulrich et al., 2001). Some of these compounds, such as 1-octen-3-ol and octanal, are present in the asparagus concentrate and we aim to retain those during spray drying

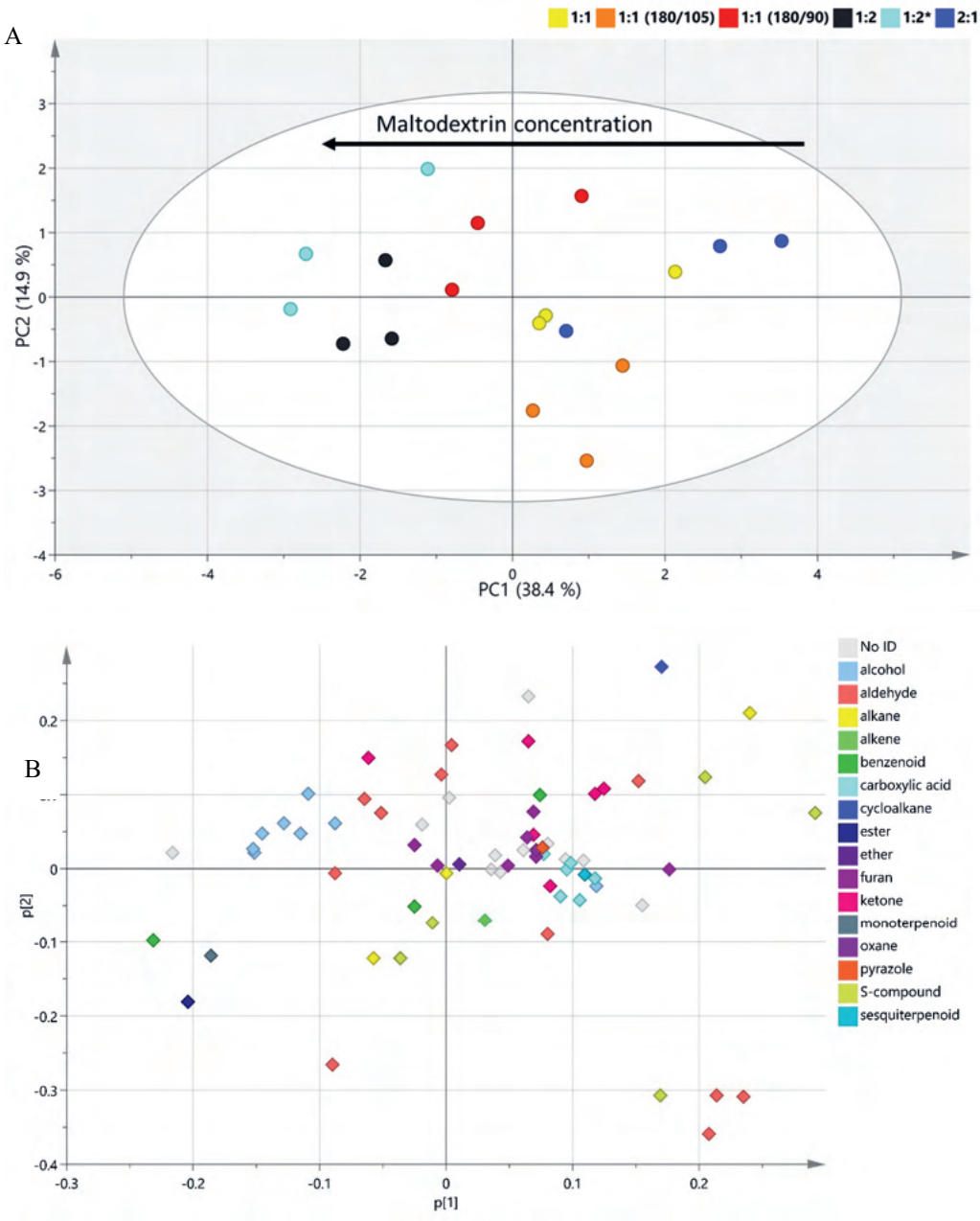

Figure 2.4 (A) Score plot of the volatile profiles of the spray-dried samples prepared with maltodextrin. The score plot is based on 70 volatiles. The colours indicate the ratio of asparagus solids to maltodextrin. The samples were spray-dried at T_{in}/T_{out} of 160/90, unless stated otherwise. (B) The loading plot corresponding to the PCA score plot.

Other compounds, e.g. dimethyl sulphide and 3-methylthio-propanal, are formed upon drying. For the latter category, higher peak intensity values were found with less or no maltodextrin. Most of the compounds in the spray-dried samples are positively correlated with the increasing concentration of maltodextrin (data not shown), which suggests that maltodextrin is effective as a carrier agent. The aromas already present in asparagus as well as the aromas that are generated during asparagus processing can be of great importance to the final aroma and taste of the powder (Pegiou et al., 2019).

2.3.6. Effect of maltodextrin on 1-octen-3-ol in mixtures

One volatile compound was selected for an in-depth analysis, 1-octen-3-ol. This alcohol is a key aroma in cooked asparagus conferring an earthy and mushroom-like aroma and is present in the raw asparagus as well (Pegiou et al., 2019). 1-Octen-3-ol is formed via oxidative degradation of linoleic acid, which involves the transformation of hydroperoxides into the volatile 1-octen-3-ol facilitated by cleaving enzymes (Assaf, Hadar, & Dosoretz, 1997; Tressl, Bahri, et al., 1977). 1-Octen-3-ol was present in the asparagus concentrate at relatively high concentration, indicating that the oxidative degradation might have been initiated during the pressing and concentration of the concentrate.

The influence of maltodextrin solutions on the partitioning of volatile compounds between the gas/liquid phases has been investigated before. Chung and Villota (1990) found that the concentration of butanol in the gas phase decreased when the maltodextrin content was increased. They suggested that maltodextrin forms aggregates with hydrophobic portions on the inside and these hydrophobic portions interact with butanol and other hydrophobic compounds. Jouquand, Ducruet and Giampaoli (2004) also stated that the retention of aroma compounds by maltodextrin is linked to the hydrophobicity of aroma compounds. In our study, we evaluated the effect of maltodextrin on the partition coefficient of 1-octen-3-ol by analysing the headspace of mixtures with equal amounts of 1-octen-3-ol and different maltodextrin concentrations. The results (Fig. 2.5) indicate an inverse correlation between the measured 1-octen-3-ol in the headspace and the concentration of maltodextrin in the liquid phase. This inverse correlation is explained by the relative hydrophobicity of 1-octen-3-ol, i.e. log P = 2.5, and therefore enabled its complexation by maltodextrin.

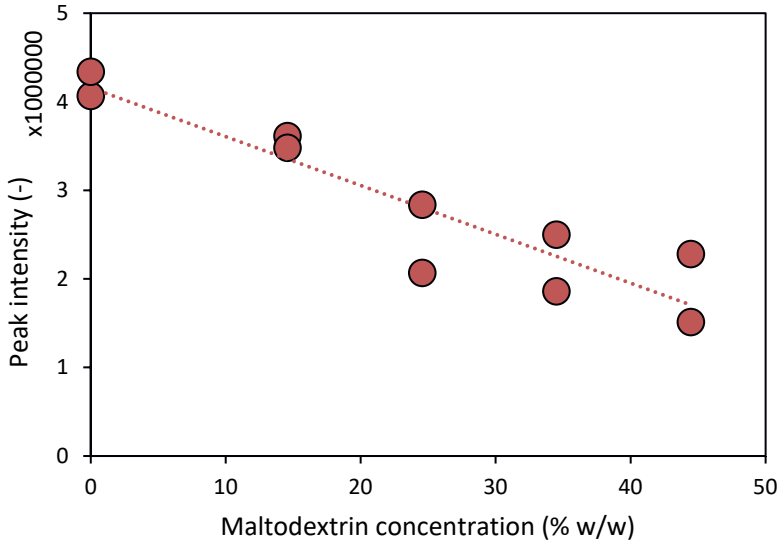

Figure 2.5 The peak intensity of 1-octen-3-ol measured by SPME in asparagus concentrate prepared with different maltodextrin concentrations (results from two independent experiments were shown).

2.3.7. Effect of maltodextrin on retention of 1-octen-3-ol in spray-dried powder

The detected peak intensities of 1-octen-3-ol in the mixes before drying and in the spray-dried powders are shown in Fig. 2.6. The peak intensities in the mix were found to decrease for the higher ratios of maltodextrin, this could be explained by the effect of maltodextrin on the gas-liquid partition coefficient as discussed previously.

The peak intensities of 1-octen-3-ol were lower after spray drying, indicating that 1-octen-3-ol was partially lost during drying. Without maltodextrin (1:0) only a small amount of 1-octen-3-ol could still be detected after drying. Higher concentrations of maltodextrin increased the detection of 1-octen-3-ol. This suggests that maltodextrin DE12 retains part of the 1-octen-3-ol during spray drying, which may be explained by the reduction of the constant rate period. For the samples that were prepared with 1:2 ratios, the diluted samples (triangles) have slightly lower peak intensity after drying. The encapsulation of 1-octen-3-ol may have been decreased by the lower initial solids content.

To discuss the role of maltodextrin on aroma retention, we calculated the retention of 1-octen-3-ol based on the ratio of the peak intensities of the mix and the corresponding spray-dried powder. The retention of 1-octen-3-ol increases with higher concentrations of maltodextrin

(Fig. 2.7). This is in line with the results by Bangs and Reineccius (1982), who evaluated the retention of twelve organic flavour compounds, including 1-octen-3-ol, in a model system with maltodextrin DE10. The overall retention increased from 23 to 80 % when the maltodextrin concentration was increased from 32 % w/w to 50 % w/w. We observe similar trends (Fig. 2.7) for two other major alcohols in white asparagus, namely 1-pentanol and 1-hexanol (Tressl, Bahri, et al., 1977). To a smaller extent the retention of heptanal, an aldehyde previously detected in green asparagus juice (X. Chen et al., 2015), benefitted from an increase in maltodextrin.

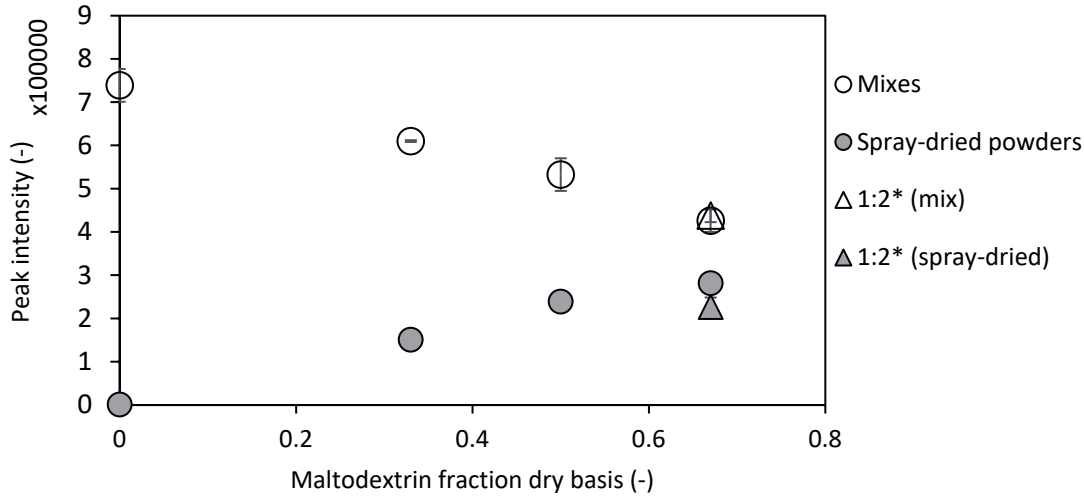

Figure 2.6 The peak intensity profiles of 1-octen-3-ol before (white circles) and after spray drying (grey circles) for asparagus concentrate prepared with different asparagus solids to maltodextrin ratios. The triangles indicate the samples 1:2*, which were diluted with water to give a similar initial solids content as the 1:1 ratio sample. All samples were spray-dried at T_{in}/T_{out} of 160/90. The error bars represent the standard deviation of the experimental data (n = 3).

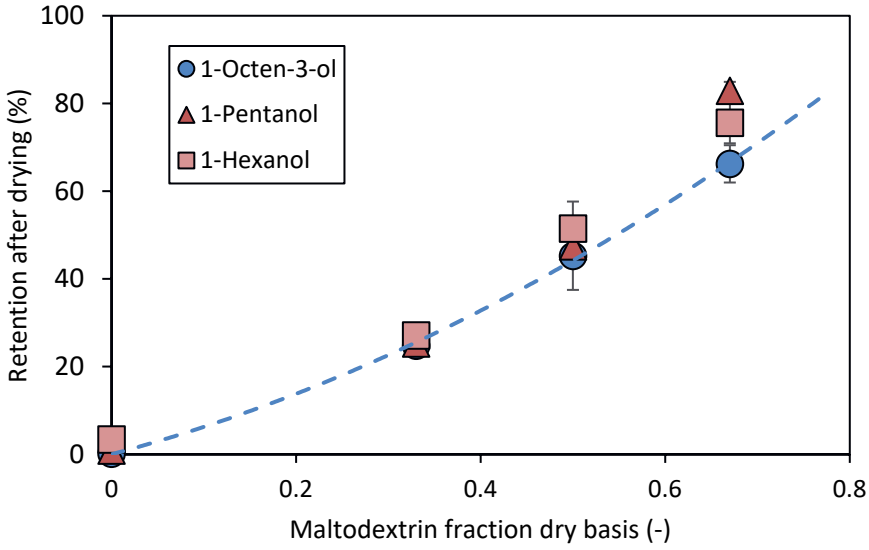

Figure 2.7 The retention after drying of 1-octen-3-ol, 1-pentanol and 1-hexanol. The dashed line is drawn to guide the eye for 1-octen-3-ol. The samples were prepared with different asparagus solids to maltodextrin ratios and spray-dried at T_{in}/T_{out} of 160/90. The retention of the volatile compounds was calculated based on the peak intensities of the mix before drying and the spray-dried powder. The error bars represent the standard deviation of the experimental data (n = 3).

2.3.8. Effect of drying conditions

Three combinations of inlet and outlet temperatures were applied during spray drying of 1:1 ratio mixtures. In Fig. 2.8 the abundance profiles of several compounds have been plotted. Some of the compounds in the asparagus concentrate we would like to retain during drying (e.g. 1-octen-3-ol). Other compounds were not present in the concentrate and were only formed upon drying (e.g. dimethyl sulphide, 2-methylpropanal, 3-methylbutanal and 3-methylthio-propanal).

For 1-octen-3-ol, the influence of the drying conditions tested in this study had a minor influence on the measured abundance profiles. For dimethyl sulphide, there was no significant influence of inlet/outlet temperature combinations on the abundance. For 2-methylpropanal, 3-methylbutanal and 3-methylthio-propanal, however, the temperature combination of 180/105 resulted in larger headspace concentration compared to 160/90 and 180/90. These high values after drying at 180/105 can be related to the high outlet temperature inducing formation of these components. Ideally, we aim to minimise the

formation of volatile compounds during drying. Volatiles that are formed during drying might get lost during storage due to package permeability, consequently, flavour stability will be reduced. Instead, these volatiles should be formed while the consumer prepares the food product.

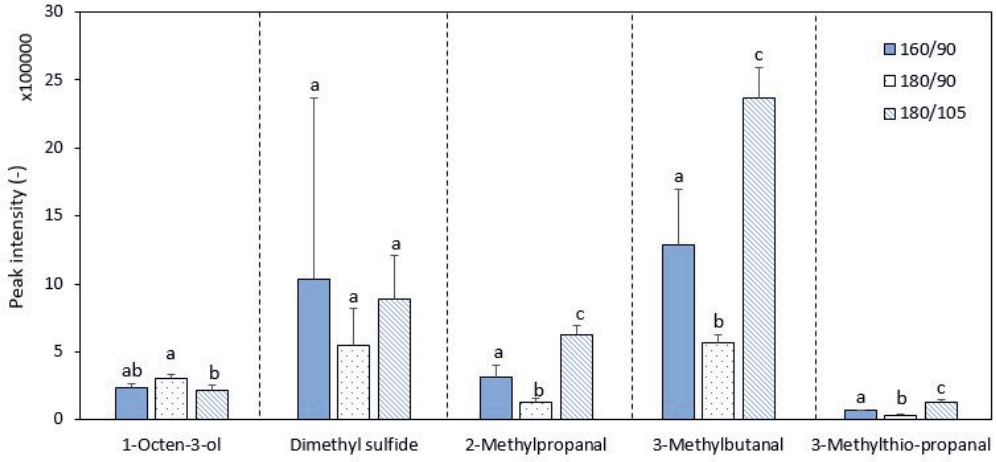

Figure 2.8 Abundance of 1-octen-3-ol, dimethyl sulphide, 2-methylpropanal, 3-methylbutanal and 3-methylthio-propanal in spray-dried asparagus powder dried at different inlet and outlet temperatures (T_{in}/T_{out}). All powders were prepared with 1:1 ratio asparagus solids to maltodextrin. The error bars represent the standard deviation of the experimental data (n = 3). The same letters represent no significant difference ($p \leq 0.05$).

2.4. Conclusions

The influence of maltodextrin concentration and drying conditions on the physical properties and aroma retention of spray-dried asparagus was studied. Increasing maltodextrin concentration resulted in spray-dried powders with a lower moisture content, higher T_g and less undesired agglomeration. A ternary Gordon-Taylor equation reasonably described the effects of the composition of multicomponent mixtures and residual moisture content on the T_g of asparagus powder. The drying conditions tested in this study had a minor effect on the physical properties of asparagus powder. Moreover, maltodextrin concentration in carrier formulations influenced the retention of a key flavour compound 1-octen-3-ol. Increasing maltodextrin concentration increased the retention of 1-octen-3-ol, as well as other alcohols and an aldehyde. Nevertheless, the drying conditions studied did not have a significant

influence on volatile retention. Interestingly, higher outlet air temperature resulted in a higher amount of several asparagus volatiles that were formed during drying. To minimise the formation of these compounds, but also to still have enough drying capacity and avoid fouling issues, the outlet temperature should not be too high, preferably not above 90 °C.

In conclusion, this study showed that maltodextrin can be used to yield maximum volatile retention after spray drying of asparagus concentrate. This is because firstly aroma compounds can form a complex with maltodextrin, and secondly, a shorter constant rate period and fast skin formation during drying could hinder evaporation of aromas when increasing maltodextrin concentration.

2.5. *Appendix*

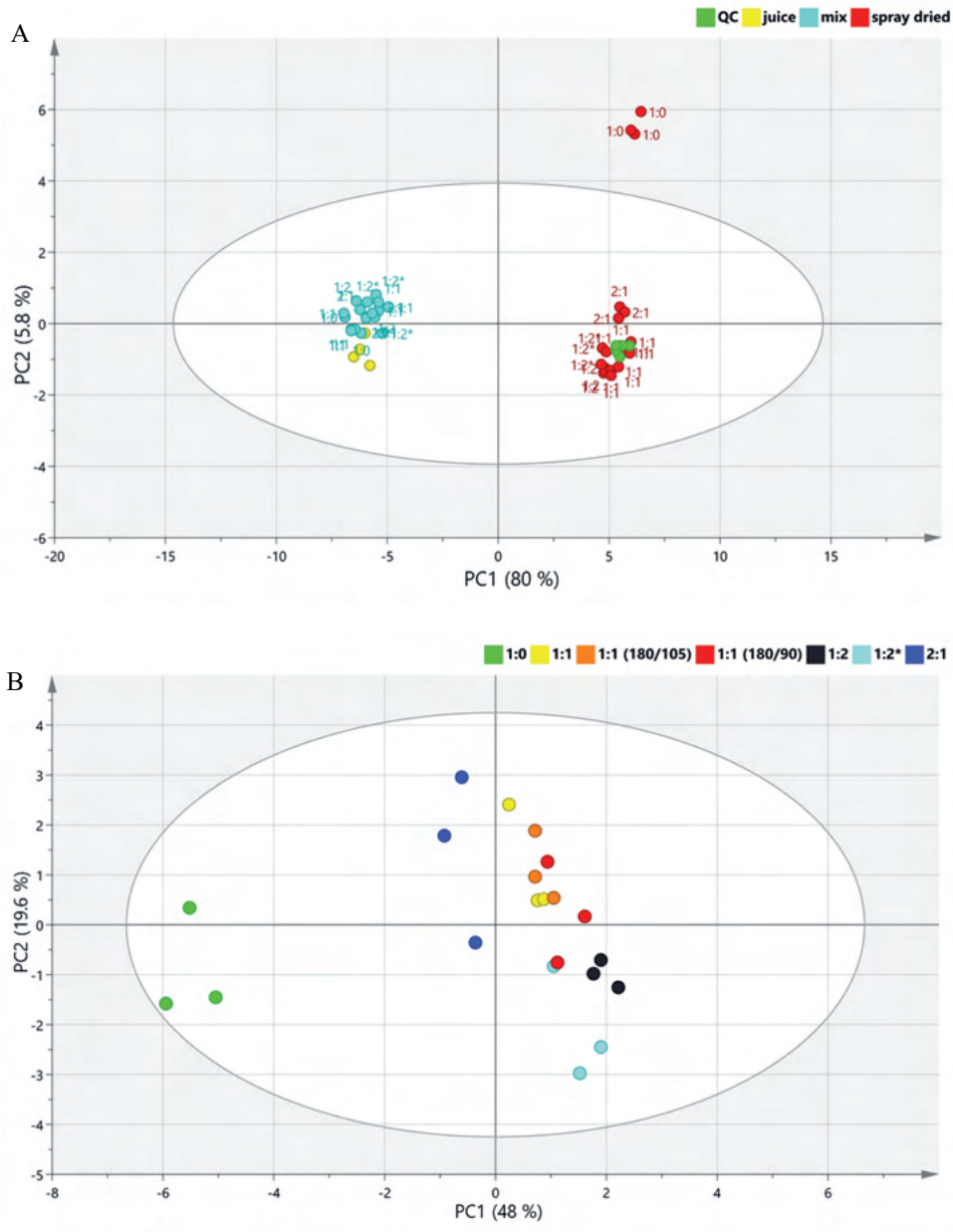

Figure A.2.1 Score plots of the volatile profiles of (A) juice, mix, spray-dried samples and quality controls (QC) and (B) spray-dried powders only. The score plots are based on 70 volatiles. The colours indicate the ratio of asparagus solids to maltodextrin. The samples were spray-dried at T_{in}/T_{out} of 160/90, unless stated otherwise.

Chapter 3

The effect of partial replacement of maltodextrin with vegetable fibres in spray-dried white asparagus powder on its physical and aroma properties

This chapter has been published as Siccama, J.W. [1], Pegiou, E. [1], Eijkelboom, N.M., Zhang, L., Mumm, R., Hall, R.D., Schutyser, M.A.I. The effect of partial replacement of maltodextrin with vegetable fibres in spray-dried white asparagus powder on its physical and aroma properties. *Food Chemistry.* **2021**, *356*. https://doi.org/10.1016/j.foodchem.2021.129567.

3.1. Introduction

White asparagus (*Asparagus officinalis*) is a popular vegetable consumed worldwide (Pegiou et al., 2019). When directly consumed, the cooked spears are considered a speciality / luxury vegetable and are appreciated for their distinct flavour profile which is perceived as being more subtle (slightly more bitter and less sweet) than its green counterpart. Flavour perception of food is determined by both its taste and aroma. The aromas that the human nose can perceive are numerous and their sensorial attributes can often be specifically described, e.g. earthy, pungent, fruity, cooked potato, etc. Taste attributes are generally limited to five modalities, i.e. sweetness, sourness, saltiness, bitterness and umami. Vegetables, including asparagus, often have rich aroma profiles which are also influenced by their processing history (e.g. fresh, canned, cooked, etc.). The aroma profile of *A. officinalis* has partly been studied in the past (Hoberg, Ulrich, & Wonneberger, 2008; Tressl, Bahri, et al., 1977; Ulrich et al., 2001) and these studies have indicated that cooked asparagus shows a complex aroma profile consisting of volatile compounds from diverse chemical classes, including aldehydes, pyrazines and sulfur compounds. A general overview of the biochemistry, health benefits and flavour profile of asparagus can be found in Pegiou et al. (2019).

White asparagus is strongly seasonal and is only harvested for a limited period between March until June in Western Europe. However, after harvest, around one-third of the total material has to be discarded (W. Zhang et al., 2014). This significant waste stream partially consists of sub-standard, crooked and broken spears, but the main waste comprises the stem bases which are cut off to produce spears with the same desired length for delivery to the supermarkets. This waste stream could become a valuable resource for food ingredients. Valorisation of these materials could reduce the amount of agricultural waste while generating aroma-rich natural food products. For example, asparagus waste could potentially be dried into powder for use as a natural flavour ingredient for soups, sauces etc.

Nevertheless, drying of asparagus waste into powders with retained characteristic aroma profile could be challenging because volatile compounds are known to be rendered or lost during the processing of vegetables (Bangs & Reineccius, 1982; Madene et al., 2006). For example, 2-Methoxy-3-isopropyl pyrazine is a key odorant of white asparagus (Hoberg et al., 2008; Ulrich et al., 2001), which appears to be lost during thermal processing. Therefore, it is important to retain this compound as much as possible in dried asparagus powder. On the other hand, some volatile compounds may be formed during drying through processes such

as thermal fragmentation, oxidative degradation of unsaturated fatty acids and initiation of Maillard reactions (Nijhuis et al., 1998; Tressl, Bahri, et al., 1977). These newly-formed compounds may have a positive or negative (off-flavour) effect on the dried product. Specifically, key odorants that can be formed upon thermal processing of asparagus are sulfur-containing compounds such as Dimethyl sulphide (DMS) and 3-Methylthiopropanal, whose indirect precursor is the sulfur-containing amino acid Methionine (Tressl, Bahri, et al., 1977; Tressl, Holzer, et al., 1977; Ulrich et al., 2001).The formation of such compounds should be suppressed during drying so that they are preferably formed / synthesized only upon food preparation just before consumption. Therefore, different properties of the aroma compounds and their impact on the typical asparagus aroma profile should be taken into consideration when optimizing any drying strategy to make asparagus powder.

Different drying strategies to retain important aroma compounds in asparagus powder have been described recently (Siccama et al., 2019). Spray drying is a method commonly used in the food industry to preserve fruit and vegetable juices in powder form (Shishir & Chen, 2017; Verma & Vir Singh, 2015). Spray drying allows for the encapsulation of volatile compounds thanks to the formation of a semipermeable skin during the dehydration process (Coumans et al., 1994). Additionally, during spray drying, the atomised droplets remain relatively low in temperature even though high inlet air temperatures are applied. This makes spray drying also suitable for the drying of materials containing heat-sensitive compounds (Madene et al., 2006). However, similar to other vegetable and fruit juices, spray drying of asparagus juice is challenging because of the presence of high levels of small sugars. This leads to stickiness issues resulting in fouling during spray drying and as the glass transition temperature (T_g) of the product is below ambient temperature, this makes it problematic to obtain a glassy powder. Therefore, carrier agents are often added to increase the T_g of the feed and to avoid fouling (Verma & Vir Singh, 2015). In particular, maltodextrins with low dextrose equivalents (DE) are of interest since they have a high T_g and form an elastic skin upon drying. Siccama et al. (2021) demonstrated that the addition of maltodextrin DE12 improved the physical properties and volatile profile of spray-dried asparagus powder.

The addition of carrier agents to a food matrix entails that such ingredients must be added to the label of the final product. Nowadays, the transition towards producing “clean-label” foods that contain only natural ingredients is gaining ever greater attention among consumers (Asioli et al., 2017; Ingredion, 2014). For example, potato fibre is a more acceptable

ingredient than maltodextrin (Ingredion, 2014). Spray-dried powder containing maltodextrin as a carrier agent does not meet the requirement of "clean-label" production. Therefore, it would be interesting to be able to at least partly replace maltodextrin with what are considered to be more authentic fibres, which are perceived as being more natural. Specifically, asparagus fibre might be used to (partially) replace maltodextrin as the carrier agent during the spray drying of asparagus juice, and so-doing, provide an extra opportunity to exploit the waste stream.

Here, various cellulose-based fibres have been tested for their suitability to replace maltodextrin. These were asparagus fibre (AF), citrus fibre (CF) and microcrystalline cellulose (MCC). Replacing maltodextrin by cellulose may be challenging due to their different physicochemical properties. Both maltodextrin and cellulose are carbohydrate polymers built up of glucose monomers, however, their conformation is different. The glucose-units in maltodextrin are coupled primarily through α-(1,4)-glucosidic linkages (Kennedy, Knill, & Taylor, 1995), whereas in cellulose through β-(1,4)-glucosidic linkages (BeMiller, 2019a). In addition, their degree of polymerization (DP) is significantly different. Maltodextrins are mixtures of polysaccharides derived from starch with DP values in the range of 2-20 and on average, have a DP > 5 (BeMiller, 2019b) and are soluble in water. Cellulose is a large polysaccharide with an average DP > 500 (BeMiller, 2019a), making it insoluble in water. The addition of insoluble cellulose-based material to the feed can lead to complications (e.g. increasing viscosity of the feed) for spray drying.

The objective of this research was to investigate the influence of partially replacing maltodextrin with cellulose-based carriers on the physical and aroma properties of obtained spray-dried asparagus powder. The hypothesis was that partial replacement would still provide a spray-dried asparagus powder of good quality. Specifically, it was expected that the addition of asparagus fibre may enrich the volatiles profile of the generated powders. For comparison, citrus and microcrystalline fibres were used as well to partly substitute maltodextrin. The quality of the spray-dried powders generated was evaluated on particle size distribution and particle morphology, as well as on the composition of the aroma compounds. The aroma profiles of the differently dried powders were compared by headspace solid-phase microextraction (HS-SPME), followed by gas chromatography-mass spectrometry (GC–MS).

3.2. Materials & Methods

3.2.1. Asparagus material and vegetable fibres

Raw, fresh asparagus cut-offs (*Asparagus officinalis*) were kindly provided by Teboza BV (Helden, The Netherlands). Concentrated asparagus juice was prepared from asparagus cut-offs by Wageningen Food & Biobased Research (Wageningen, the Netherlands). Specifically, asparagus juice was pressed out of the cut-offs and was then centrifuged to remove any solids. The juice was concentrated using reverse osmosis by a factor of 5.6 to produce an asparagus concentrate with a final dry matter content of 21.7 % w/w. This concentrated juice was aliquoted into 40 ml samples and stored in the freezer at -20 °C prior to experimentation. After pressing out the juice, the remaining asparagus fibre was dried in a hot air oven (Heraeus, Hanau, Germany) at 60 °C for 24 hours. Subsequently, the fibre was milled into fine powder in the multi mill with the ZPS configuration (Hosokawa Alpine AG, Augsburg, Germany), with an impact mill speed of 8000 rpm, the air flow at 45 m^3/h and the classifier wheel speed at 3000 rpm. The particle size distribution of the milled asparagus fibre is reported in the Supplementary data (Fig. A.3.1) where the average particle size (D_{50}) was 86 μm. The asparagus fibre had a moisture content of 4.4 ± 0.4 % w/w and contained 74.8 % total dietary fibre (i.e. 37.6 % cellulose, 18.2 % hemicellulose and 4.2 % lignin, all on dry basis). Citrus fibre (Herbacel® AQ® Plus Citrus) was kindly provided by Unilever (Unilever BV, Wageningen, The Netherlands). The moisture content of citrus fibre was 6.2 ± 0.2 % w/w and contained 85.6 % total dietary fibre (i.e. 63.9 % cellulose, 10.0 % hemicellulose and 1.5 % lignin, all on dry basis). The total dietary fibre was determined with the K-TDFR assay from Megazyme (Megazyme International Ireland, Wicklow, Ireland). The cellulose, hemicellulose and lignin contents were determined with the Neutral Detergent Fibre (NDF) method performed by Eurofins Agro (Eurofins Agro, Wageningen, The Netherlands). Microcrystalline cellulose (cellulose powder, 20 μm, 310697) was purchased from Sigma–Aldrich (St. Louis, MO, USA). Maltodextrin DE 12 was purchased from Roquette (Roquette Frères, Lestrem, France).

3.2.2. Analytical standards and chemicals

A series of n-Alkanes (C7-C21) was prepared from a set of stock solutions of the specific alkanes which had been purchased from Sigma-Aldrich (Milwaukee, WI, USA). The analytical standards (96-99 % purity) that were used for the metabolite identification were Dimethyl sulphide, 3-Methylthiopropanal, Hexanal, 1-Hexanol, 2,3-Pentanedione, 2-

Methylbutanol, 1-Octen-3-ol, 2-Pentylfuran, and 2-Methoxy-3-isopropyl pyrazine. All were purchased from Sigma-Aldrich. Methanol (Biosolve BV, The Netherlands) and was used for the preparation of the standard solutions. Calcium chloride ($CaCl_2$) and Ethylenediaminetetraacetic acid (EDTA) were also purchased from Sigma-Aldrich. Ultrapure water (Milli-Q™ Reference Ultrapure Water Purification System) was used for the preparation of the EDTA solution.

3.2.3. Sample preparation for spray drying

For every experiment, a new tube of the concentrated asparagus juice was first taken from the freezer and the concentrate was thawed in the fridge at 4 °C for 18-20 hours. Feed solutions for spray drying experiments were prepared according to Table 3.1. Specifically, feed solutions with an initial solids content of 30 % or 40 % w/w were prepared. In some samples, maltodextrin was partially replaced by cellulose-based materials, i.e. asparagus fibre (1 or 3 % w/w), citrus fibre (1 or 3 %) and MCC (3 or 10 % w/w). The replacement level was determined based on measured viscosity of the feed solutions (Supplementary data, Fig. A.3.2). The carrier materials were added to the asparagus concentrate and then stirred at room temperature at 400 rpm for 1 hour. All samples were prepared in duplicate.

3.2.4. Spray drying experiment

Spray drying was performed using a Büchi Mini Spray Dryer B-290 (Büchi Labortechnik AG, Flawil, Switzerland). The aspirator rate applied was 90 %, which corresponded to an air flow of 35 m^3/h. The speed of the peristaltic pump was adjusted to 3 – 10.5 ml feed/min to reach the desired outlet air temperature. The inlet temperature (T_{in}) was set to 180 °C, which is within the range recommended by Reineccius (2004). In all cases, it was aimed to adjust the pump to reach an outlet temperature (T_{out}) of 90 °C to provide sufficient drying capacity and to avoid fouling in the drying chamber. However, in some cases even at the maximal pump speed, the outlet temperature exceeded 90 °C (Table A.3.1). Moreover, for the samples with MD+MCC 30-10 %, we were not able to collect sufficient material from the collection vessel, instead, we collected the powder from the drying chamber.

Table 3.1 Preparation scheme of samples with maltodextrin (MD), asparagus fibre (AF), citrus fibre (CF) and microcrystalline cellulose (MCC) as carrier agents.

Sample name	Total solids (% w/w)	Asparagus solids from juice (% w/w)	MD (% w/w)	AF (% w/w)	CF (% w/w)	MCC (% w/w)
MD 30 %	30	19	11	-	-	-
MD 40 %	40	17	23	-	-	-
MD+AF 30-1 %	30	19	10	1	-	-
MD+AF 30-3 %	30	19	8	3	-	
MD+AF 40-1 %	40	17	22	1	-	
MD+AF 40-3 %	40	17	20	3	-	
MD+CF 30-1 %	30	19	10	-	1	-
MD+CF 30-3 %	30	19	8	-	3	-
MD+CF 40-1 %	40	17	22	-	1	-
MD+CF 40-3 %	40	17	20	-	3	-
MD+MCC 30-3 %	30	19	8	-	-	3
MD+MCC 30-10 %	30	19	1	-	-	10
MD+MCC 40-3 %	40	17	20	-	-	3
MD+MCC 40-10 %	40	17	13	-	-	10

3.2.5. Moisture content

Spray-dried powder (~ 0.5 g) was placed in a hot air oven (Heraeus, Hanau, Germany) to determine its moisture content. The powders were weighed before and after drying at 105 °C overnight, and the moisture content of the powder was calculated on a total weight basis (w/w). All measurements were carried out in triplicate.

3.2.6. Particle size distribution and morphology

The particle size distribution of the spray-dried samples was measured using a Mastersizer 3000 analyser (Malvern Inc, Worcestershire, UK). The laser diffraction measurement was performed using the dry powder disperser Aero S. The morphology of six powder samples, i.e. pure MCC, MD 40 %, MD+AF 40-3 %, MD+MCC 40-3 %, MD+MCC 40-10 % and CF+MD 40-3 %, was investigated with an FEI Magellan 400 FESEM (FEI, Thermo Fisher Scientific, Hillsboro, United States of America) at the Wageningen Electron Microscopy Centre (Wageningen University and Research, Wageningen, the Netherlands). The MD+MCC 40-10 % sample was first dried under vacuum at room temperature to remove the

excess water present. All samples were fixed on the sample holder by carbon adhesive tabs and sputter-coated with 12 nm of tungsten. SEM images were taken at 2 kV.

3.2.7. Sample preparation for volatiles analysis

Volatile compound analysis was performed on the pure carriers, four samples of concentrated asparagus concentrate, all spray-dried powders and quality control samples consisting of a mix of the 28 spray-dried powders. Samples were weighed based on equation 3.1, so that all the samples contained 30 mg of asparagus solids. The 10-ml GC glass vials containing the samples were subsequently stored at -80 °C until further analysis.

$$mass = \frac{30}{X_s\, X_{a(db)}} \tag{3.1}$$

Where X_s (kg solids / kg total) is the total solid content of the sample determined via moisture content analysis. $X_{a(db)}$ (kg asparagus solids / kg solids) is the fraction of asparagus solid in the solid content of the sample, which can be derived from the amount of asparagus solids from Table 3.1.

Prior to analysis, 0.73 g $CaCl_2$ was added to each sample. Next, a predefined volume of EDTA solution was added to all vials to obtain a total liquid volume of 1 ml per vial with a final concentration of 50 mM EDTA and 5 M $CaCl_2$ (saturated solution). The addition of $CaCl_2$ and EDTA was needed to deactivate any enzyme activity and to help drive the volatiles into the headspace (Verhoeven, Jonker, De Vos, & Hall, 2011). All samples were thoroughly mixed using a vortex, followed by 15 min in an ultrasound bath and kept subsequently on ice until analysis.

3.2.8. Analysis of volatile compounds

Volatile compounds in the headspace were measured using GC-MS and solid-phase microextraction (SPME) and were adsorbed onto a PDMS/DVB/CAR (Polydimethylsiloxane / Divinylbenzene / Carboxen) 50/30 µm diameter, 1 cm length (Supelco, PA, USA) fibre using an MPS2 sampling robot (Gerstel, Germany). Samples were pre-conditioned at 50 °C for 15 min under agitation (300 rpm). Volatiles were then trapped by exposing the fibre to the headspace of the vial for 15 min at 50 °C without agitation. Volatiles were thermally desorbed by inserting the fibre into the injector containing an empty glass liner (1 mm ID) (CIS4, Gerstel, Germany) at 250 °C for 2 min with a helium flow of 1 ml/min onto the GC column, in splitless mode. An Agilent GC7890A coupled to a 5975C quadrupole mass

spectrometer was used. A Zebron ZB-5MSplus (5 % phenyl and 95 % dimethylarylene siloxane) column (Phenomenex, the Netherlands) with dimensions 30 m x 0.25 mm id x 1 µm film thickness was used for chromatographic separation. The GC oven temperature was programmed to start at 45 °C for 2 min, then increased at a rate of 8 °C/min to 250 °C, then at a rate of 15 °C/min to 280 °C and then held at 280 °C for 3 min. The carrier gas was helium, at a constant flow rate of 1 ml/min. The column effluent was ionised by electron impact at 70 eV, in the scan range *m/z* 33–330. The MS interface temperature was set to 280 °C. For calculating retention indices (RIs), a series of n-alkanes (C7-C21) was injected and analysed using the same method as for the samples and as part of the same sample series. RIs were calculated using a third-degree equation.

GC-MS raw data were processed using an untargeted metabolomics workflow. MetAlign software was used for baseline correction (S/N >3) and alignment of the mass signals. The aligned mass signals were reconstructed to potential clusters (metabolites) using the MSClust tool. Metabolites were putatively identified by matching the obtained mass spectra and experimental RIs with those in commercial (e.g. NIST17) and in-house libraries. The given level of identification follows the Metabolomics Standards Initiative (Sumner et al., 2007). Prior to statistical analysis, zero values in the processed data were substituted with randomised values of ca. 10 % of the detection limit as this was determined in MetAlign during pre-processing.

3.2.9. Statistical analysis

All spray drying experiments were conducted at least in duplicate and results are presented as mean ± standard deviations. Significant differences in residual moisture contents of the powders were assessed by One-way analysis of variance (ANOVA) and Tukey's Honestly Significant Differences (HSD) post hoc test, with a $p \leq 0.05$ meaning the difference between groups was statistically significant. In the case of unequal variances, the Games-Howell post hoc test was used. The statistical analyses were performed using SPSS Statistics (SPSS 25; IBM, USA).

Processed GC-MS data were subjected to Principal Component Analysis (PCA) and Hierarchical Clustering Analysis (HCA), after log10 transformation and Pareto-scaling using SIMCA 15.0.2. software (Umetrics, Sartorius Stedim Data Analytics AB, Umeå, Sweden).

Additional uni- and multi-variate statistical analyses were performed using RStudio with R version 4.0.3 (2020-10-10). Graphs were also produced using Microsoft Office Excel.

3.3. Results and Discussion

We analysed the physical properties and volatile profiles of the spray-dried powders. While performing the spray drying experiments, we found that partial replacement of MD could occur up to a maximum of 3 % in the case of AF and CF or 10 % in the case of MCC. Higher replacement levels led to clogging of the spray drying nozzle due to insolubility of the fibres. In addition, the replacement of MD by AF or CF was limited by the increased viscosity of the feed solutions (Fig. A.3.2) while partial replacement with MCC did not increase the viscosity of the feed solutions. The MCC particles acted as inert particles and did not show swelling / water absorption compared to AF and CF, this may explain why more MCC could be added.

3.3.1. Moisture content

Residual moisture contents in spray-dried asparagus powders were measured (Table 3.2). It was found that the initial solids content largely influenced the residual moisture content in the powders. Solutions with an initial total solids content of 40 % w/w resulted in powders with lower moisture contents as compared to powders obtained from the 30 % w/w initial solids. This was, however, not a direct effect of the initial solids content, because we increased the feed flow rate of the 40 % w/w feed solutions to obtain the same water evaporation rate and thus equal outlet temperature (i.e. 90 °C) as the 30 % w/w solutions. We might explain the difference in moisture content by the difference in carrier formulations (Table 3.1). The powders prepared with 30 % w/w initial solids contained more asparagus solids on a dry weight basis (63 %) as compared to the powders prepared with 40 % w/w solids (43 %). Because asparagus solids contain a large amount of small sugars (± 67 % dry basis), the 30 % w/w samples have a more hygroscopic nature compared to the 40 % w/w samples. Drying of hygroscopic solutions, e.g. low molecular weight saccharides, is often hindered by a rapid decrease in drying rate at an intermediate moisture content. Consequently, these solutions remain wet even after prolonged drying (Matsuno & Adachi, 1993). Furthermore, the powders prepared using 30 % w/w solids may also have absorbed moisture from the environment after they were taken from the collection vessel due to their high hygroscopicity (King, Downton, & Flores-Luna, 1982; Li, Lin, Roos, & Miao, 2018).

The residual moisture content of asparagus powders slightly increased as the replacement level of MD by other cellulose-based carriers increased, when the initial total solids content of the feed is kept the same (Table 3.2). The partial replacement of MD may have influenced the drying behaviour of the feed solutions. It is hypothesized that the (partially) insoluble fibres, i.e. AF, CF and MCC, are encapsulated by maltodextrin. Therefore, it is suggested that maltodextrin and asparagus solids dominated the drying behaviour. Do et al. (2018) found that after spray drying mulberry juice with MD, gum arabic and MCC, the powder contained the extract and MCC as separate particles. The moisture contents in their final products were significantly reduced from 4.54 to 3.20 % after increasing the MCC concentrations from 0 % to 2 %. However, this positive effect of adding MCC to the feed solution on the residual moisture in mulberry powder was not observed in this study. This might be explained by the already high MCC concentration used in the current work. Moreover, the powder prepared from MD+MCC 30-10 % solution was collected from the drying chamber instead of the collection vessel, which explains the lower moisture content of this sample after being exposed to hot air for extended time.

Table 3.2 Effects of carrier formulations and initial solids content on the residual moisture content of spray-dried asparagus powders.

	Residual moisture content % w/w	
Sample name	Initial solids 30 % w/w	Initial solids 40 % w/w
MD	13.76 ± 0.01^{ab}	6.73 ± 0.03^{a}
MD+1 % AF	13.87 ± 0.13^{b}	8.51 ± 1.62^{ab}
MD+3 % AF	15.81 ± 0.79^{ab}	8.65 ± 1.38^{ab}
MD+1 % CF	15.41 ± 1.74^{ab}	7.39 ± 0.39^{ab}
MD+3 % CF	16.87 ± 1.61^{ab}	9.27 ± 1.78^{ab}
MD+3 % MCC	14.82 ± 1.40^{ab}	7.37 ± 0.64^{ab}
MD+10 % MCC	11.79 ± 0.18^{a}	8.32 ± 0.08^{b}

Note: Carrier agents: maltodextrin (MD), asparagus fibre (AF), citrus fibre (CF) and microcrystalline cellulose (MCC). Moisture content is expressed as average with standard deviations (n=2). The values followed by different lowercase letters (a–b) within a column are significantly different at $p \leq 0.05$. *The MD+10 % MCC with initial solids 30 % w/w samples were collected from the drying chamber instead of the collection vessel.

3.3.2. Particle size distribution

The particle size distributions of the spray-dried powders prepared with only MD, MD+3 % AF, MD+3 % CF and MD+10 % MCC are plotted in Fig. 3.1. All powders prepared with 40

% w/w initial solids content had one main peak located around 10 µm (Fig. 3.1A). For the powder obtained from MD+10 % MCC, this peak is shifted towards a larger particle size. The powders with 30 % w/w initial solids content have a broad size distribution (Fig. 3.1B). The peaks located at sizes above 100 µm indicate undesired particle agglomeration. This agglomeration could be explained by increasing stickiness due to the higher residual moisture content and lower glass transition temperature of these powders (Siccama, Pegiou, Zhang, et al., 2021). The first peak of MD 30 % has a smaller particle size compared to the peak of MD 40 %, 8.7 µm and 14.5 µm respectively. This increase in particle size for the higher initial solids content is probably related to the increase in viscosity of the feed resulting in larger droplets upon atomization (Santos et al., 2018).

For the 30 % w/w initial solids samples, we observe different results for MD+AF 30-3 % and MD+CF 30-3 % (Fig. 3.1B). Less agglomeration and overall smaller particle size were observed for CF samples compared to AF. It is worth noting that the particle size distribution of the pure carrier materials AF and CF cannot help to explain the different particle size distributions (Fig. A.3.1) as the peaks do not overlap with the spray-dried powders.

For the 30 % w/w initial solids, we observe a different size distribution for MD+MCC 30-3 % and MD+MCC 30-10 % (Fig. 3.1B). The distribution of MD+MCC 30-3 % contains two peaks, and is similar to MD+AF 30-3 %, whereas MD+MCC 30-10 % shows one peak around 60 µm. The particle size distribution was most likely affected by the collection process, as the MD+MCC 30-10 % powder was collected from the drying chamber instead of the collection vessel beneath the cyclone. Jedlińska et al. (2018) observed similar differences in particle size for powders collected from the drying chamber and the cyclone container. They suggested that the smaller particles are more easily blown out with the outlet air and thus could be mostly collected from the cyclone. The bigger particles, however, have larger inertia and therefore collide with the chamber wall and deposit there.

We can conclude that the physical properties of the powders prepared with 40 % w/w initial solids are of better quality compared to 30 % w/w. The 30 % w/w powders have a higher residual moisture content, which makes the powder sticky and this is also related to the undesired agglomeration that is observed.

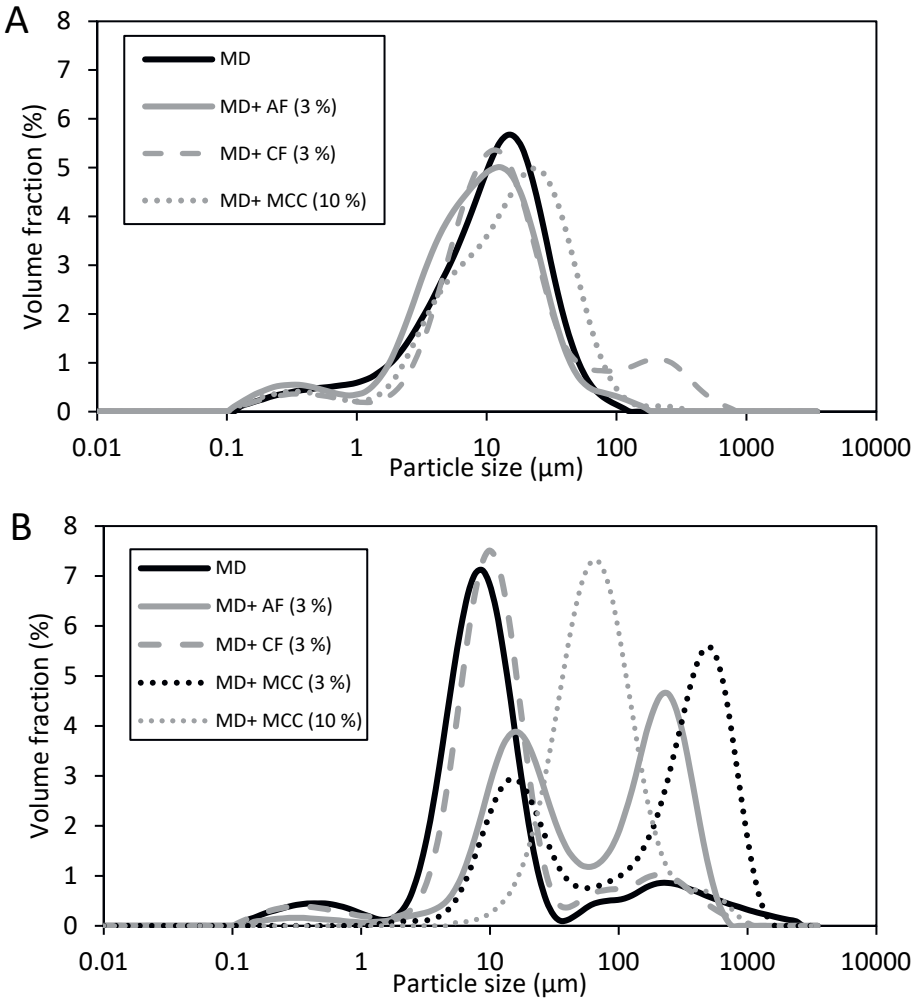

Figure 3.1 (A) Particle size distribution of spray-dried asparagus powders prepared with different carrier agents and initial total solids content of 40 % w/w. (B) Particle size distribution of spray-dried asparagus powders prepared with different carrier agents and initial total solids content of 30 % w/w. Carrier agents: maltodextrin (MD), asparagus fibre (AF), citrus fibre (CF) and microcrystalline cellulose (MCC).

3.3.3. Particle morphology

Scanning electron microscopy pictures of the spray-dried powders prepared with 40 % w/w initial solids are shown (Fig. 3.2) as these were not agglomerated compared to the 30 % w/w initial solids powders. The MD 40 % powder contained both dented (green box) and smooth (blue box) particles (Fig. 3.2A). The dented particles are characteristic for spray-dried

maltodextrin DE12 (Both, Karlina, Boom, & Schutyser, 2018; Siemons, Politiek, et al., 2020). The appearance of smooth particles may be linked to the feed composition but could also be explained by the drying process. Smooth particles have previously been observed by Siemons et al. (2020b) for drying of low molecular weight compounds xylose and trehalose. Besides, during spray drying, there is a broad droplet size distribution and each droplet experiences its own drying trajectory, which may influence the final particle morphology (Both, Boom, & Schutyser, 2020). The morphologies of MD+AF 40-3 % and MD+CF 40-3 % powders were very similar to that of the MD 40 % sample. For all three samples, individual particles with both smooth and wrinkled surfaces were observed. For MD+AF 40-3 % few elongated particles were detected (Fig. A.3.3B). For the powders that were prepared with MCC, next to the round-shaped particles, elongated particles were observed (Fig. 3.2D,E). The elongated particles were probably MCC as they had similar size and shape as the pure MCC particles before drying (Fig. 3.2F) and more of these particles are observed with an increase in MCC concentration. We assume these particles are inert fibres and were thus not altered by the spray drying process. However, the surface of the spray-dried MCC particles was smooth whereas pure MCC particles have a rough surface. It is therefore hypothesized that maltodextrin encapsulated the microcrystalline cellulose particles and therefore formed this smooth surface. Next to the elongated partciles and some dented particles, perfect small spheres are observed for MD+MCC 40-10 % (Fig. 3.2E). These small spheres may be related to the high concentration of small sugars in the soluble fraction. The addition of 10 % microcrystalline cellulose reduced the maltodextrin concentration in the feed solution from 23 to 13 % w/w (Table 3.1). Since microcrystalline cellulose is completely insoluble, the soluble solids fraction in the feed solution therefore became richer in asparagus solids, i.e. small sugars, compared to the reference MD 40 %. This large fraction of small sugars may have contributed to the formation of perfect small spheres and reduced the number of dented particles.

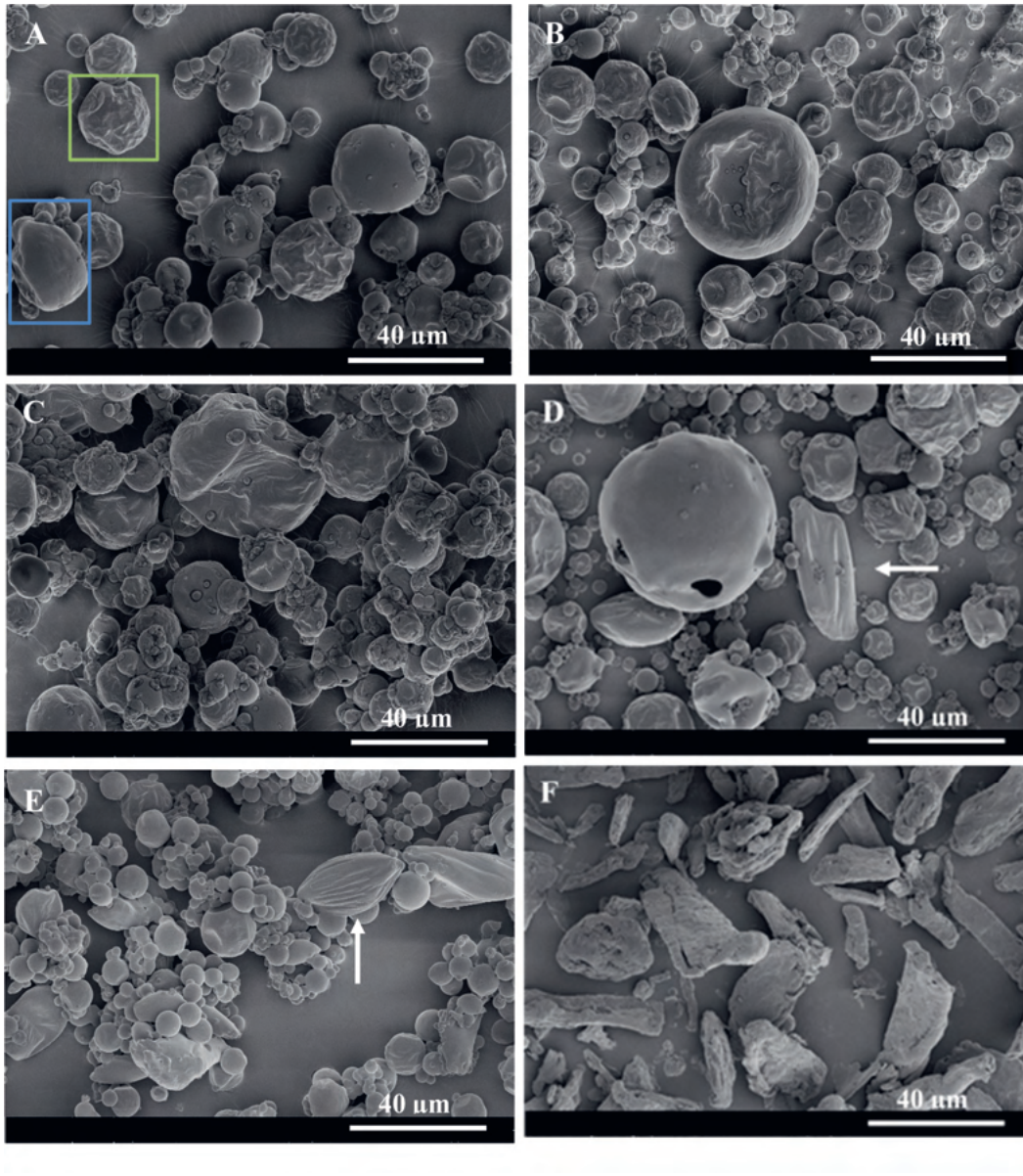

Figure 3.2 Scanning electron microscopy images of spray-dried powders at a magnification of 2000x with (A): MD 40 % (with the green box indicating a wrinkled particle, the blue box indicating a smooth particle), (B): MD+AF 40-3 %, (C): MD+CF 40-3 %, (D): MD+MCC 40-3 %, (E): MD+MCC 40-10 %, and (F): pure microcrystalline cellulose before spray drying. The arrows indicate the elongated particles. (For the list of abbreviations see Table 3.1.)

3.3.4. Untargeted analysis of volatiles and comparison of spray-dried powders

We aimed to inspect the influence of the total solids content used for the spray drying of asparagus concentrate on the volatiles profile of the obtained spray-dried powders. Moreover, the effect of partially replacing MD by cellulose-based carriers has also been investigated. HS–SPME was used for the extraction of the volatiles prior to GC-MS analysis as with a headspace extraction method, the volatiles profile should closely resemble the aroma profile that the potential consumer of the final product should experience. An untargeted metabolomics approach was followed to obtain a comprehensive overview of the similarities and variations between the volatile profiles of the different spray-dried asparagus powders. All spray-dried powder samples contained the same asparagus solids content to enable the direct comparison of the samples. The pure carriers were also analysed separately to verify potential unique compounds originating from the carriers themselves during spray drying.

A total of 244 compounds was detected. After filtering out all system artefacts, the remaining 221 volatile compounds were further studied as described in section 3.2.8 for untargeted data analysis. Identification of volatiles was restricted to those compounds that have been reported earlier in cooked asparagus materials and which have been highlighted as being key asparagus volatiles with significant sensory impact (Hoberg et al., 2008; Ulrich et al., 2001). Such compounds included e.g. hexanal, 3-methylthiopropanal, 2-methoxy-3-isopropyl pyrazine and 1-octen-3-ol. Moreover, some other compounds (e.g. the benzene derivative 1,2-dimethoxybenzene and the ester 2-butanol, 3-methyl, acetate) were further investigated as they could also be of particular relevance to the final flavour quality of the asparagus powder as proposed by Tressl et al. (1977a).

Initially, to investigate the influence of the various carriers on the overall volatiles profile, the structure of the dataset of the 221 volatiles in the 28 spray-dried powders was explored and analysed using unsupervised multivariate statistics. After performing hierarchical clustering using Ward's method (Ward & Joe, 1963), the effect of both the total solids content and the type of the cellulose-based carrier replacing MD was evident. In the dendrogram in Fig. 3.3A, the clustering of the analysed spray-dried powders is based on the carrier composition. Powders with CF form one cluster (yellow box), the AF-containing powders form a second cluster (green box) and the powders with MD and MD+MCC form a third cluster (black box). This implies that there is only a minor effect of partially substituting MD with MCC, as well as the potential contribution of unique compounds from CF and AF matrix

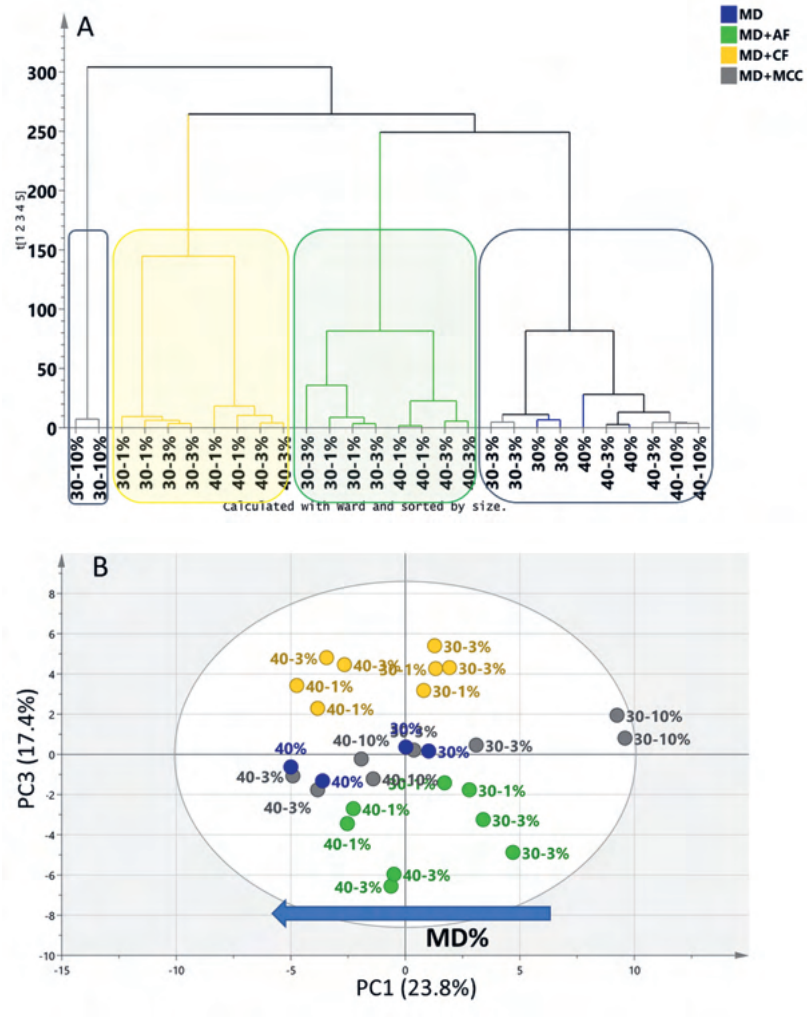

Figure 3.3 Unsupervised multivariate statistics on the 221 volatiles detected in 28 spray-dried asparagus powders with different carrier agents (MD, MD+AF, MD+CF and MD+MCC) and carrier concentrations (total solids content 30 % or 40 % w/w, in case of MD+AF, MD+CF and MD+MCC the percentage of the MD that was replaced by AF / CF / MCC is indicated: 1 / 3 / 10 %). Data have been log10-transformed and Pareto-scaled prior to analysis. (A): HCA Dendrogram showing the clustering of the spray-dried asparagus powders. HCA was calculated with Ward's method. Boxes indicate the formed clusters, based on the carrier type. (B): PCA score plot of the first and third PC with the % of explained variance given in the parenthesis. The ellipse represents the 95 % confidence interval from the Hotelling T2 function. (C): Loading plot from the PCA plot of (B). Asparagus key volatiles based on (Hoberg et al., 2008; Ulrich et al., 2001) that were detected are indicated in the plot. (For the list of abbreviations see Table 3.1.)

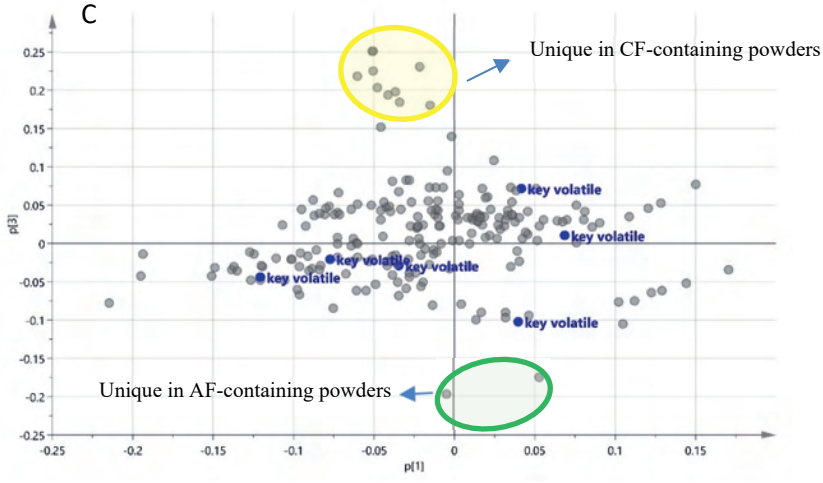

Figure 3.3 Continued

to the volatile profile. In the same dendrogram, within each cluster, the powders with the same total solids content also cluster close together, implying that their profiles are similar. The two powders with 30 % w/w total solids content, and 10 % MCC, are clustered separately and distant from all other samples. This highlights the effect of the higher concentrations of MD on the volatiles profile, as these two samples contain the least MD % (Table 3.1). This deviation of the volatile profiles between the powders with 10 % MCC and the rest can also be linked to the fact that the MD+MCC 30-10 % powders had to be collected from the drying chamber instead of the collection vessel. This might influence the volatiles profile, due to the extra heat load, but this requires further investigation.

As most information can be extracted by looking at variation, a PCA was also performed on the spray-dried powder samples (Fig. 3.3B). The first and third principal components (PCs) are plotted, as these summarized the most valuable information in the dataset. In this PCA score plot, there is a clear effect of the total solids content as all powders with a total solids content of 30 % w/w are located on the right side (positive PC1 values) and the powders with 40 % w/w total solids content are located on the left side of the plot (negative PC1 values). Furthermore, the variation summarized in the first PC can be also explained more specifically by the concentration of maltodextrin (MD %). The blue arrow in the plot indicates that the samples are distributed across PC1 (x-axis) based on the MD %. The samples on the right

had lower MD content, while those on the left of the plot had the higher MD %. In the same score plot, there is a trend along PC3 (y-axis), based on the type of the carrier replacing MD. Here, the samples containing AF locate in the lower part of the plot (negative PC3 values) while those with CF locate at the top of the PCA plot (positive PC3 values). This separation of the samples based on the type of the carrier, with the powders containing only MD or MD+MCC forming a group in the middle of the plot, implies that the asparagus and citrus fibres themselves may have contributed to the volatiles profile through their own aroma compounds. The pure carriers used for the spray drying of the asparagus concentrate were therefore also analysed. A subset of the raw total ion current (TIC) chromatograms is shown in Fig. A.3.4 and compared to the TIC chromatogram of the asparagus concentrate. Unique peaks correspond to compounds that originate from the AF and CF and were detected only in the AF- or CF- containing spray-dried powders, respectively. In the loading plot in Fig. 3.3C, the CF- and AF- specific compounds are indicated. The CF-specific compounds were seen to include a few monoterpenoids (e.g. p-mentha-1,3,8-triene) which could potentially impact the typical asparagus flavour profile. The AF-specific compounds were undecanenitrile and 5-methyl-2-phenyl-2-hexenal. None of these compounds have been previously reported in asparagus materials but they might have been formed here during the preparation process of the AF. The known key asparagus odorants (Ulrich et al., 2001) which are indicated in blue in the same plot (Fig. 3.3C: key volatile), were present in all spray-dried powders, but at different levels. In the future, sensory and olfactometry studies shall be used to evaluate whether these compounds have any impact on the sensory attributes of the powders. Both positive as well as negative (off flavour) attributes need to be evaluated. However, we anticipate that the latter is unlikely to be a major issue as such compounds are usually formed as a result of microbial deterioration, lipid oxidation, Maillard reactions and improper storage, all of which are unlikely in our process.

One- and two- way ANOVA showed that for most of the volatiles, the differences between the spray-dried powders were significant (p value < 0.05) both depending on the different type of carrier (Fig. A.3.5A) and different carrier concentrations (Fig. A.3.5B). The volcano plots in Fig. A.3.5C and A.3.5D show the volatiles that were present at significantly different levels in the powders where MD was partially replaced by AF or CF (Fig. A.3.5C) and AF or MCC (Fig. A.3.5D) with a fold-change cut-off of 1.5. In both cases, volatiles that were significantly more abundant in the powders containing AF comprised of a number of alcohols

(e.g. 1-pentanol and 3-methyl-1-butanol), some branched alkanes and compounds that could not be identified. Important asparagus odorants according to Hoberg et al. (2008) and Ulrich et al. (2001), such as 2-methoxy-3-isopropyl pyrazine, 3-methylthiopropanal and DMS were significantly more abundant in the powders containing AF compared to the ones containing CF (indicated with arrows in Fig. A.3.5C). Powders containing CF were characterized by especially higher amounts of some aldehydes and ketones (e.g. hexanal, heptanal, 2-butanone and 2-heptanone). In the case of powders containing MCC as carrier we found two aldehydes, one of which was pentanal, a few non-identified compounds and 2-methoxy-3-isopropyl pyrazine being more abundant compared to the AF – containing powders. Given the importance that the known asparagus odorants and the positive aroma attributes that the mentioned alcohols can have for the aroma profile of asparagus products, we suggest that using AF as a carrier for the spray drying of asparagus concentrate may have a positive impact on the aroma profile of the obtained powder.

The relative abundances of a number of identified volatiles are presented in Fig. A.3.6, and in most cases these are higher in the spray-dried powders with highest total solids content. In the case of compounds derived from asparagus but which are formed during processing due to applied high temperatures (e.g. 3-methylthiopropanal), peak intensities were significantly higher in the samples containing AF in the carrier, and specifically with the higher level of AF (3 %). This implies an extra contribution of AF as a carrier in the volatiles profile of the generated spray-dried powders, and eventually the aroma profile of the final product. Moreover, this verifies that indeed high temperatures can lead to the formation of these sulfur-containing asparagus key volatiles, given the drying method applied to the AF. Potential optimization of the processing of the raw asparagus fibre can lead to even richer aroma profile of the spray-dried powders with AF in the carrier.

3.3.5. Analysis and retention of selected volatiles in spray-dried powders

The influence of the spray drying on the volatiles and their retention in the powder is dependent on several variables including the drying conditions, the solids content and the relative volatility of the molecules (Bangs & Reineccius, 1982; Coumans et al., 1994; Jafari, Assadpoor, He, & Bhandari, 2008; Rosenberg, Kopelman, & Talmon, 1990). The drying conditions in the presented spray drying experiments here were similar. We calculated the retention of a selection of specific key volatiles under different spray drying conditions (solids content and carrier types). The asparagus concentrate mixed with the carriers were

analysed both before and after spray drying using the same HS-SPME GC-MS method. The samples with the same level of fibre supplement and those containing only MD were included in this analysis (Fig. 3.4). To estimate the retention of a detected volatile, the ratio of the peak intensity in the spray-dried powder to that in the mixture before spray drying was calculated. The level of retention was not the same for all volatiles analysed in the spray-dried powders but there is an apparent trend (Fig. 3.4). Retention of volatiles was higher in the samples with a total solids content of 40 % w/w, regardless of carrier type. A partial replacement of MD with the cellulose-based carriers led to lower retention of the volatiles, as compared to the powders containing only MD. However, the retention of important volatiles e.g. 2-methoxy-3-isopropyl pyrazine in the AF-containing powders was ca. 80 % and thus, acceptable (Fig. 3.4A).

Moreover, when comparing the retention and the abundance of important asparagus volatiles (e.g. 2-butanol, 3-methyl- acetate and 2-methoxy-3-isopropyl pyrazine) between the samples where MD was partially replaced with a vegetable fibre (CF or AF), those powders with AF performed slightly better (Fig. 3.4 and Fig. A.3.6). Few studies have addressed the role of cellulose-based carrier agents in the encapsulation of bioactive compounds. Chiou and Langrish (2007) evaluated the potential of CF as a carrier agent to fully replace MD. The obtained spray-dried powders had good physical properties and the bioactive compound (*Hibiscus sabdariffa* L.) has been detected within the fibre carriers, thus demonstrating the potential of CF to replace MD. On the other hand, Yousefi et al. (2015) found that high MCC concentration detrimentally affected the encapsulation of bioactive compounds in spray-dried black raspberry juice due to the structural changes of the powder particles. Do et al. (2018) also concluded that the bioactive compounds in spray-dried mulberry powder were less protected when MCC was added and explained this by the observed separation of the mulberry extract and MCC particles in the powder. We conclude that the partial replacements tested in this study led to acceptable retention of asparagus volatile compounds.

For several compounds, including 3-Methylthiopropanal, the retention was higher than 100 % (data not shown). This implies that the concentrations of these volatiles are higher in the spray-dried powder, implying that more of these volatiles have been formed during the spray drying process. This is likely due to e.g. thermal or oxidative degradation of the sulfur-containing amino acids or polyunsaturated fatty acids, or the initiation of temperature-induced Maillard reactions.

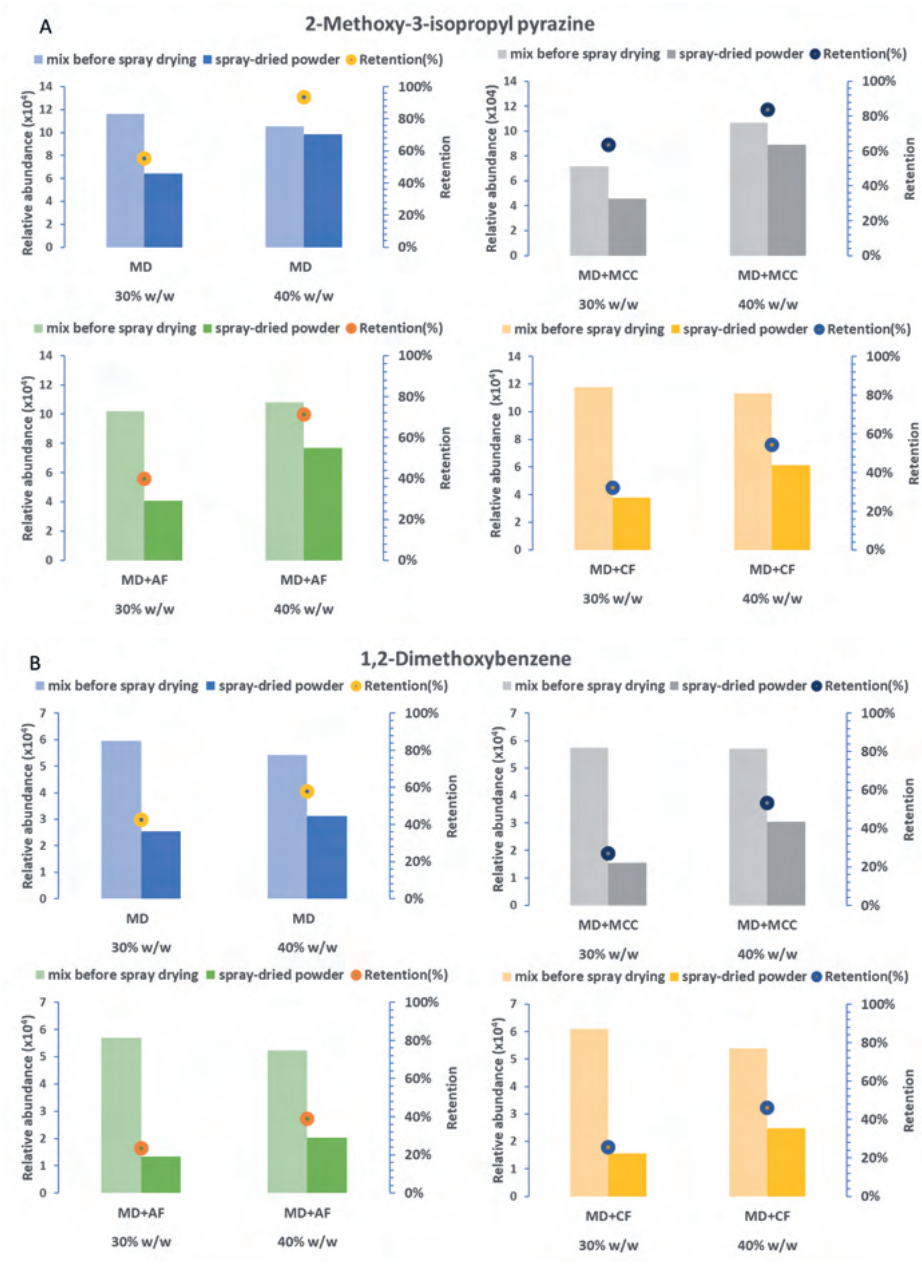

Figure 3.4 Relative abundance in the mix before and after spray drying, and the retention % in the samples with 30 % and 40 % w/w total solids content and MD (blue graphs), MD+MCC (grey graphs), MD+AF (green graphs), or MD+CF (yellow graphs) of selected volatiles (A): 2-Methoxy-3-isopropyl pyrazine, (B): 1,2-Dimethoxybenzene and (C): 2-Butanol, 3-methyl, acetate. (For the list of abbreviations see Table 3.1.)

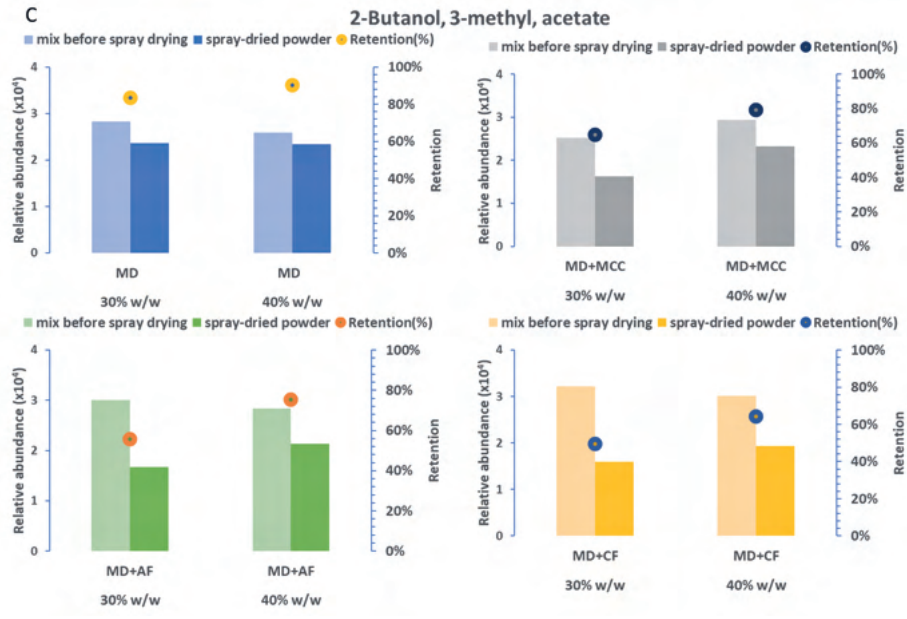

Figure 3.4 Continued

3.4. Conclusions

In this study, we demonstrated that partial replacement of MD by cellulose-based carriers is possible for successfully spray drying asparagus concentrate while retaining important asparagus volatile flavour compounds. Partial replacement of MD could be done up to a maximum of 3 % in the case of AF and CF or 10 % in the case of MCC. This limitation was due to the poor solubility of the vegetable fibres. Introducing an extra pre-treatment step for solubilising the asparagus fibre could overcome this disadvantage. Particle morphology and the levels of the detected volatile compounds differ in the prepared powders depending on the total solids content, as well as the type of the fibre used to replace MD. Spray-dried powders with a total solids content of 40 % w/w led to the formation of better-quality powders, compared to 30 % w/w total solids in terms of moisture content and particle morphology, as well as to better retention of many volatiles. Furthermore, powders where MD was replaced by AF, showed similar morphology to the powders with only MD but had a richer volatile profile because of a contribution of the AF carrier providing extra asparagus aroma compounds. These results suggest the further exploitation of vegetable fibres as a

potential (partial) replacement for MD. Further optimization of the processing technique used can contribute to effective exploitation of the extensive asparagus waste stream to produce high-quality natural food ingredients. Such natural flavour ingredients can then be used in soups, sauces, etc. to replace currently used artificial flavourings.

3.5. *Appendix*

Table A.3.1 Recorded outlet temperatures during spray drying of the samples

	Outlet temperature (°C)	
Sample name	Repeat 1	Repeat 2
MD 30 %	90	90
MD 40 %	97	90
MD+AF 30-1 %	90	90
MD+AF 30-3 %	90	90
MD+AF 40-1 %	96	90
MD+AF 40-3 %	90	90
MD+CF 30-1 %	90	90
MD+CF 30-3 %	90	90
MD+CF 40-1 %	90	90
MD+CF 40-3 %	100	117
MD+MCC 30-3 %	90	90
MD+MCC 30-10 %	90	90
MD+MCC 40-3 %	90	98
MD+MCC 40-10 %	90	90

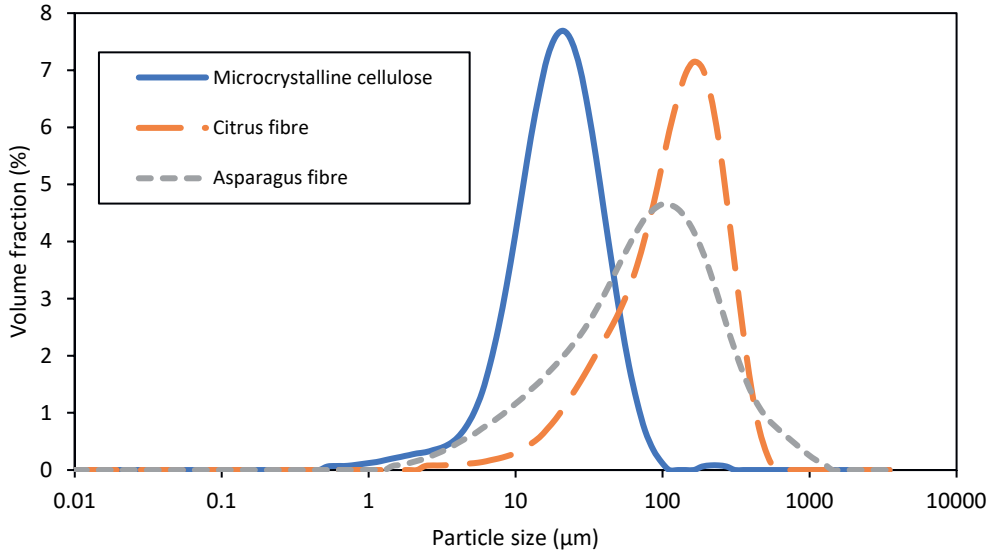

Figure A.3.1 Particle size distribution of the pure carrier materials.

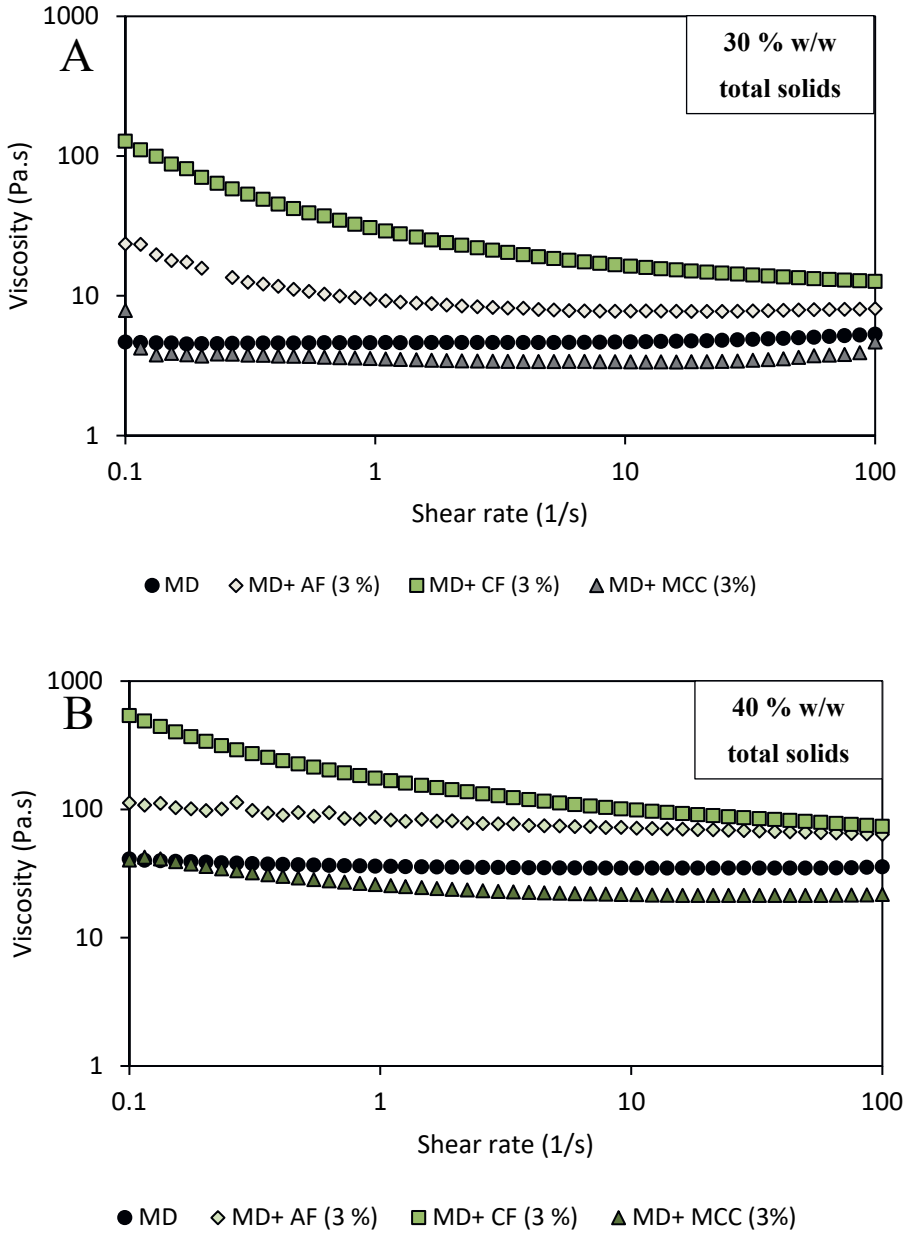

Figure A.3.2 (A) Viscosity as function of the shear rate of the feed solutions prepared with different carrier agents and total solids content of 30 % w/w. (B) Viscosity as function of the shear rate of the feed solutions prepared with different carrier agents and total solids content of 40 % w/w. Carrier agents: maltodextrin (MD), asparagus fibre (AF), citrus fibre (CF) and microcrystalline cellulose (MCC).

The viscosity of the feed solutions was determined using the Anton Paar rheometer (MCR301, Anton Paar GmbH, Graz, Austria) with a concentric cylinder geometry (CC-27). The carrier agents were mixed with asparagus concentrate according to Table 3.1 to achieve 40 or 30 % total solids. A shear rate sweep was performed at 25 °C with a logarithmic increasing shear rate. The range of the shear rate was set from 0.1 to 100 s^{-1}.

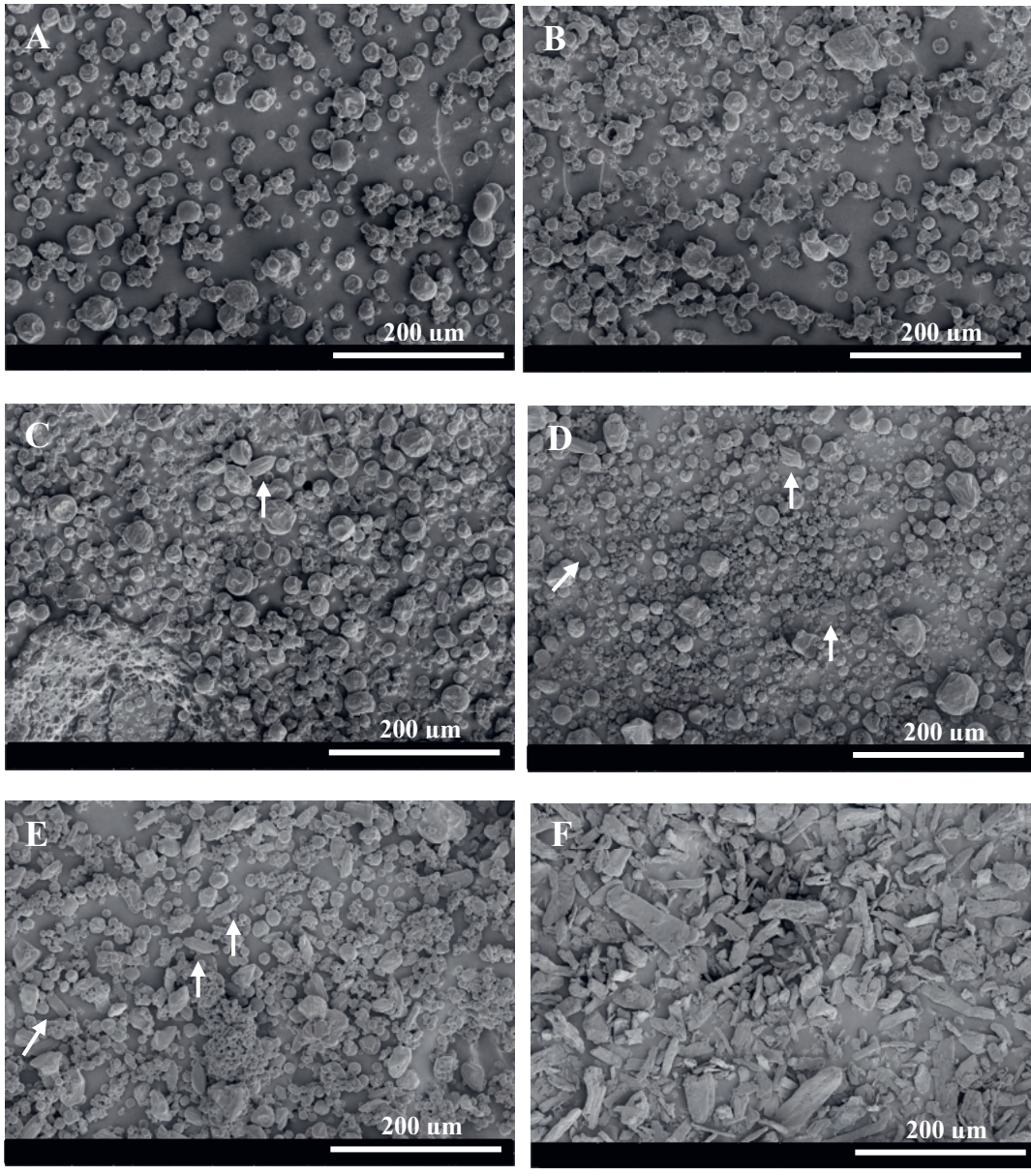

Figure A.3.3 Scanning electron microscopy images of spray-dried powders at a magnification of 500x with A: MD 40 %, B: MD+AF 40-3 %, C: MD+CF 40-3 %, D: MD+MCC 40-3 %, E: MD+MCC 40-10 %, and F: pure microcrystalline cellulose before spray drying. The arrows indicate the elongated particles. (For list of abbreviations, see Table 3.1.)

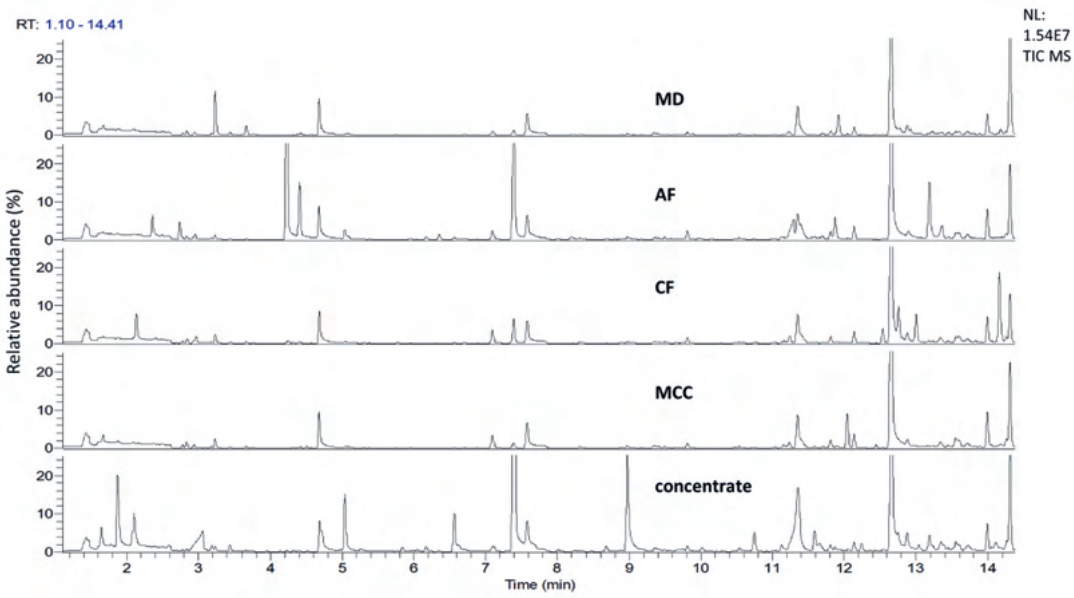

Figure A.3.4 GC-MS TIC chromatograms of pure carriers (MD, AF, CF, MCC) and asparagus concentrate juice, as analysed with the HS-SPME GC-MS described in Materials & Methods. (For list of abbreviations, see Table 3.1.)

ANOVA analysis

One- and two- way ANOVA were performed to investigate further the effects of the various carrier types and solids content on the levels of the volatiles. The obtained p-values were adjusted with Benjamini and Hochberg's False Discovery Rate (FDR) correction. Specific pairwise comparisons were performed with generalised linear hypothesis testing (glht function from multcomp R package and lmFit function from limma R package) applying a multiple testing correction with Tukey's Honestly Significant Differences (HSD).

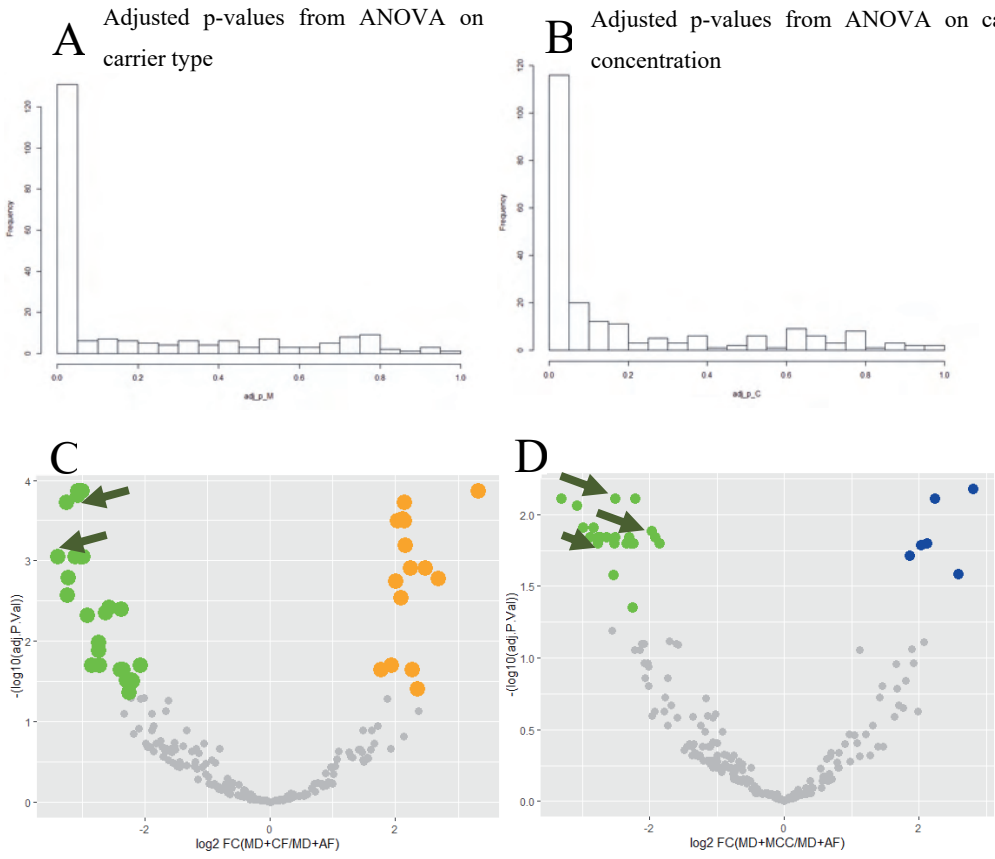

Figure A.3.5 ANOVA and Generalised Linear Hypothesis testing. (A): Histograms of adjusted p-values (with FDR) from ANOVA based on carrier type. (B): Histograms of adjusted p-values (with FDR) from ANOVA on carrier concentration. (C): Volcano plot showing volatiles that were present in significantly different levels in the powders where MD was partially replaced by AF or CF. with fold-change cut-off 1.5. (D): Volcano plot showing volatiles that were present in significantly different levels in the powders where MD was partially replaced by AF or MCC with fold-change cut-off 1.5. Colour coding corresponds to the carrier type used for the spray drying. Arrows indicate asparagus key odorants based on Hoberg et al. (2008) and Ulrich et al. (2001).

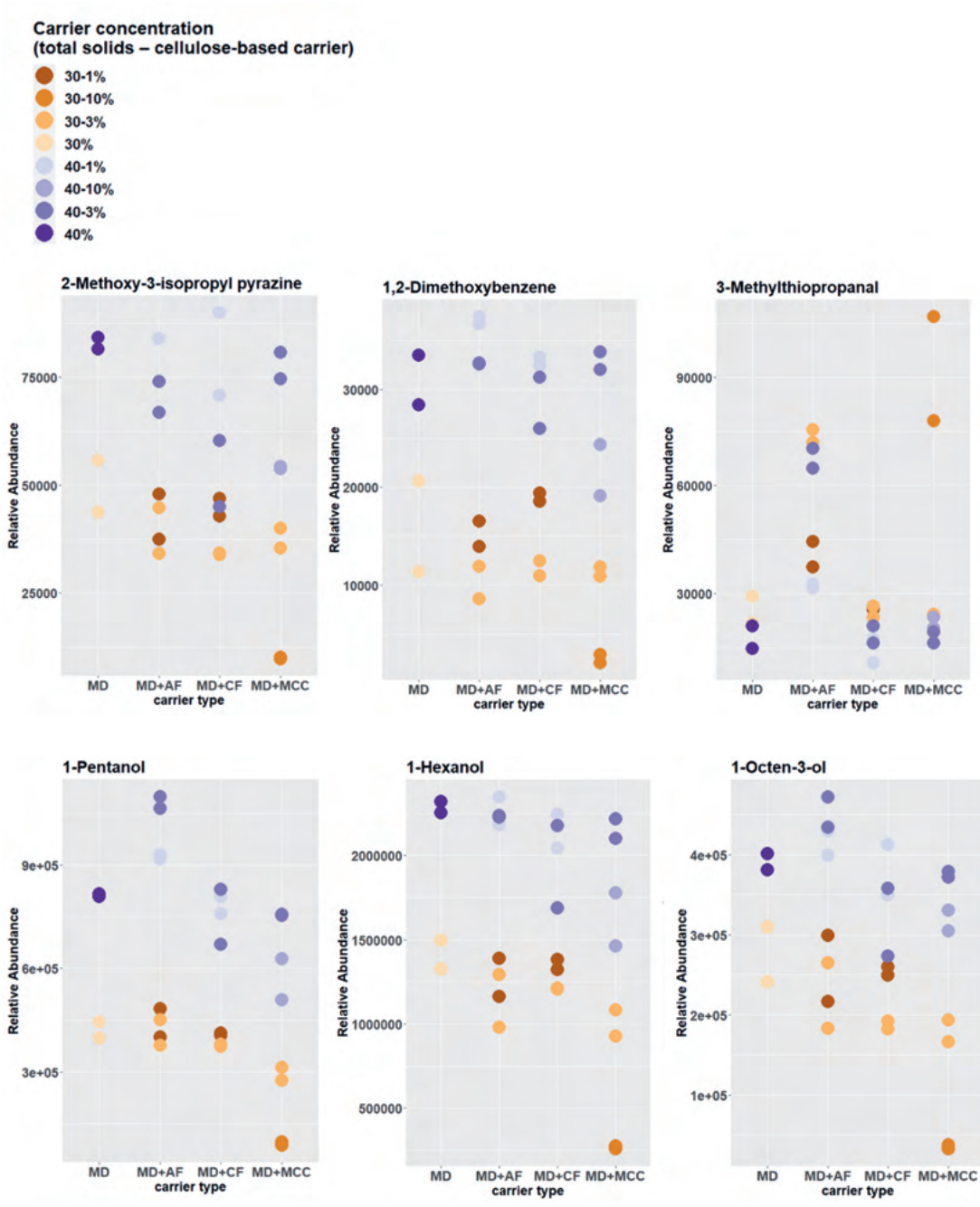

Figure A.3.6 Relative abundance of selected asparagus volatiles detected in the different spray-dried powders. Colour coding is based on the concentration of the carriers used during spray drying. (For list of abbreviations see Table 3.1).

Chapter 4

Steering the formation of cellobiose and oligosaccharides during enzymatic hydrolysis of asparagus fibre

4.1. Introduction

Agricultural waste streams consist mostly of polysaccharides and specifically contain high quantities of cellulose (~35-50 %) (Ragauskas et al., 2006). The conversion of cellulose-rich biomass into cello-oligosaccharides (COS) gained attention recently for emerging prebiotic applications such as functional foods (Ávila et al., 2021; Chen et al., 2021; Karnaouri et al., 2019a; Kluge et al., 2019). COS are oligomers with a degree of polymerization (DP) between 3-10 and consist of glucosyl units connected by β-(1→4)-glucosidic linkages. The disaccharide cellobiose, and COS with a DP ranging from 3 to 6, are water-soluble, but cannot be digested by humans (Ávila et al., 2021). The focus of this study is on the enzymatic conversion of cellulosic biomass into a mixture of cellobiose and COS to be employed as a natural carrier agent for spray drying.

Etzbach et al. (2020) recently suggested cellobiose as a potential carrier agent during spray drying of goldenberry juice. Compared to conventional carrier agents, e.g. maltodextrin and gum arabic, cellobiose showed similar or better results regarding physical properties of the spray-dried powders and carotenoid encapsulation efficiency. The good performance of cellobiose as a carrier agent in spray drying can be partly attributed to its relatively high glass transition temperature (T_g, 102 ºC), being higher than that of other disaccharides such as sucrose (62 ºC). To the best of our knowledge, no studies have reported the use of COS as carrier agent during spray drying. Nevertheless, based on the previous study of using cellobiose as a carrier, it is expected that COS will have good carrier properties and will increase the T_g of the spray drying feed since it has a higher molecular weight than cellobiose (hence higher T_g).

In the food industry, COS are not produced on a large scale yet. An interesting method is enzymatic hydrolysis since it is a mild and environmentally friendly approach to convert fibre components into soluble fibres and sugars. Similar hydrolysis methods have been studied for the production of biofuels (Bischof, Ramoni, & Seiboth, 2016). The use of enzymes is considered advantageous and more sustainable compared to e.g. acid hydrolysis processing, because of high product yield, substrate specificity, low processing temperatures and absence of toxic waste (Cuellar & Straathof, 2014; Vanderghem, Boquel, Blecker, & Paquot, 2010). For enzymatic hydrolysis of cellulose, a cocktail of cellulases is required, generally composed of endoglucanases (EGs), exo-active cellobiohydrolases (CBHs) and β-1,4-glucosidases (BGLs). The endoglucanases cleave the internal β-(1→4)-linkages between the

glucosyl units in the cellulose chains and prefer to bind to and act on the more amorphous regions of cellulose (Bischof et al., 2016; Lynd, Weimer, Zyl, & Isak, 2002; Reese, 1956). As a result, new chain ends are generated for CBHs to act on. CBHs cleave off cellobiose (DP2) from β-(1→4)-linked glucan chains from either the reducing (CBHI) or non-reducing (CBHII) ends (Bischof et al., 2016; Lynd et al., 2002; Reese, 1956). BGLs release glucose from soluble cellobiose and COS, acting from the non-reducing ends (Bischof et al., 2016; Lynd et al., 2002; Reese, 1956).

Prior to enzymatic hydrolysis, the cellulose-rich biomass is often subjected to a pre-treatment. The pre-treatment improves the enzyme accessibility by for example opening the cell wall structure and removal of inhibitory compounds. Different pre-treatments are available such as dilute acid, steam explosion and alkaline pre-treatment. Dilute acid pre-treatment is usually performed with H_2SO_4, HNO_3 or HCl, and temperatures between 140-200°C for minutes up to an hour. Dilute acid treatment mainly results in partial hydrolysis and solubilization of hemicelluloses (Galbe & Zacchi, 2007). Steam explosion involves rapid heating by high-pressure saturated steam typically at temperatures of 180-210°C for 1-10 min. After the rapid release of pressure, separation of individual fibres occurs and the cell wall structure disrupts (Jørgensen, Kristensen, & Felby, 2007). Both dilute acid and steam explosion significantly increase enzymatic digestibility of the fibres, but they only remove lignin to a small extent (Jørgensen et al., 2007). Moreover, these processes can degrade sugars into inhibitory compounds and operate at extreme processing conditions, e.g. high temperature and high pressure (Galbe & Zacchi, 2007; Kim, Lee, & Kim, 2016). Alkaline pre-treatment is the most widely used chemical method to enhance the enzymatic hydrolysis of various lignocellulosic biomasses (Singh, Suhag, & Dhaka, 2015). The pre-treatment is performed in dilute alkaline solutions, e.g. NaOH, KOH, $Ca(OH)_2$ and NH_4OH, and can be carried out under mild conditions (Kim et al., 2016; Singh et al., 2015). Alkaline pre-treatment increases the internal surface area, separates the structural linkages between lignin and carbohydrates and disrupts the lignin structure (Singh et al., 2015; Sun & Cheng, 2002). Alkaline pre-treatment is most effective on hardwood and agricultural residues with low lignin content (Singh et al., 2015). Alkaline pre-treatment was selected in this work as it is performed under less severe processing conditions than dilute acid and steam explosion treatments.

In this study, it was aimed to enzymatically release majorly cellobiose and COS from white asparagus fibres and, hereby, enhancing the T_g of the obtained mixture. Asparagus is a

seasonal crop and is only harvested between March and June in Western Europe. The worldwide consumption of asparagus has increased in recent years and asparagus is one of the world's top 20 vegetable crops in the USA and Europe (Pegiou et al., 2019). The global asparagus production (both white and green asparagus) increased from 1.23 million tonnes in 1971 to 8.45 million tonnes in 2020 growing at an average annual rate of 4.14 % (Knoema, 2021). Considering that after harvest one-third of the total length of each white asparagus spear is cut off and discarded (W. Zhang et al., 2014), a stream of by-products in the order of million tonnes is generated annually. These currently discarded by-products could potentially be used as food ingredients. Siccama et al. (2021b) proposed to extract the asparagus juice and produce spray-dried asparagus powder. The fibre-rich fraction that remains after extraction could also be considered as starting material for enzymatic hydrolysis. It contains 74.8 g/100 g (db) dietary fibre, which mainly consists of cellulose, i.e. 37.6 g/100 g db (Siccama et al., 2021a) making white asparagus waste a valuable feedstock for COS production. In addition, the lignin content (4.2 g/100 g db) of asparagus fibre is lower compared to several other biomass resources such as wood and herbaceous energy crops (Ragauskas et al., 2006). Lignin acts as an inhibitor on cellulase cocktails and therefore reduces the enzymatic conversion of cellulose (Sammond et al., 2014). It should be noted that while asparagus fibre is the model system in this study, the same principle may be applied to other fibre-rich waste streams as well.

This study reports on the novel combination of converting the asparagus fibre waste into cellobiose and COS and their application as natural carrier agent for spray drying. It was hypothesized that the formation of high amounts of cellobiose and COS, with limiting formation of monosaccharides will result in a high T_g and hence enhance spray drying. The formation of cellobiose/COS was investigated by using different doses of a commercial cellulase preparation. Furthermore, the effects of hydrolysis time and alkaline pre-treatment of the asparagus fibre on the yield of cellobiose and soluble oligosaccharides were investigated. A bench-scale experiment was conducted to produce cellobiose and soluble oligosaccharides in powder-form using subsequent enzymatic hydrolysis, concentration by evaporation and spray drying.

4.2. Materials & Methods

4.2.1. Materials

Fresh asparagus cut-offs (*Asparagus officinalis*) were kindly provided by Teboza BV (Helden, The Netherlands). The asparagus cut-offs were pressed with a twin gear juicer (Angel Juicer AG-140K, Angel Juicer, Busan, South Korea) to obtain asparagus juice and asparagus fibre by Wageningen Food & Biobased Research (Wageningen, The Netherlands). The wet asparagus fibre was stored at −20 °C prior to experimentation.

The commercial cellulase preparation Celluclast® (batch number: CCN03187) was kindly provided by Novozymes (Novozymes A/S, Bagsværd, Denmark). Celluclast is produced by *Trichoderma reesei* (filamentous fungus), which excretes mainly a variety of EGs, CBHs, and BGLs (Beldman, Voragen, Rombouts, Searle-Van Leeuwen, & Pilnik, 1988; Bischof et al., 2016). The enzyme activity of Celluclast was provided by Novozymes, i.e. 700 EGU/g (~ 840 EGU/mL). EGU (endoglucanase Units) refers to the amount of substrate converted in µmol/min. The enzyme activity was measured following the protocol "Cellulase activity, EGU – analysis by Konelab" as communicated by Novozymes. For this analysis, the substrate carboxymethyl cellulose (CMC) was hydrolysed at 50°C and pH 5. The reaction products were quantified via the reducing ends at 405 nm of the reducing carbohydrate-PAHBAH-bismuth complexes. The enzyme cocktail was used in this study without any further modification. EGU was converted to katal (mol/s), the SI unit of enzyme catalytic activity, i.e. the enzyme activity of Celluclast is 11.7 µkat/g and was used to calculate the enzyme loadings.

Standards used in this study were glucose, fructose, sucrose, cellobiose, kestose and nystose (Sigma-Aldrich, St. Louis, Missouri, US). All other chemicals used were of analytical grade.

4.2.2. Fibre preparation

The asparagus fibres were thawed at 4 °C for 10 h. Afterwards, the fibres were washed three times with lukewarm tap water and the excessive water was removed by using a Buchner vacuum filter (VWR, Amsterdam, The Netherlands). The washed fibres were dried in a TG 200 fluidized bed dryer (Retsch, Haan, Germany) at 70 °C for 2 h. The dried fibres were milled using a Pulverissette-14 RotorMill (Fritsch, Idar-Oberstein, Germany) with a 0.2 mm sieve and at 10,000 rpm. One batch of fibre was prepared and stored in plastic bags at ambient temperature until further use.

4.2.3. Moisture content

Asparagus fibre (~ 1 g) was placed in a hot air oven (Heraeus, Hanau, Germany) to determine its moisture content. The powders were weighed before and after drying at 105 °C overnight, and the moisture content of the powder was calculated on a total weight basis (g/100 g). Measurements were carried out at least in duplicate.

4.2.4. Composition analysis

The cellulose, hemicellulose and lignin contents of the asparagus fibres were determined based on Neutral Detergent Fibre (NDF) (AOAC Method 2002.04, 2002) and Fibre (Acid detergent) and lignin (H_2SO_4) (AOAC Method 973.18, 1973). The analysis was performed by Eurofins Agro (Eurofins Agro, Wageningen, The Netherlands). The protein content of the asparagus fibres was determined by using a Nitrogen Analyzer (Rapid N exceed, Dumas, Elementar, Langenselbold, Germany). A nitrogen-to-protein conversion factor of 5.98 was used (Urbat, Müller, Hildebrand, Wefers, & Bunzel, 2019). The ash content was determined by incineration of the fibre in an ashing furnace (Carbolite Gero, Sheffield, UK) at 525 °C for 5 h. The composition analysis was performed on one batch of processed fibre and the mean of the technical replicates was reported.

4.2.5. Particle size distribution and SEM Analysis

The particle size distribution of the asparagus fibre was measured using a Mastersizer 3000 analyser (Malvern Inc, Malvern, UK) with the dry powder disperser Aero S. The particle size distribution was determined with the Mastersizer 3000 software with the non-spherical analysis mode, which is applicable for particles which are irregular in shape such as fibres. The D_{50} values were reported, which represent the median particle size by volume. The microstructural properties of the asparagus fibres and spray-dried hydrolysate were examined using scanning electron microscopy (SEM). The material was attached to SEM stubs using carbon adhesive tabs, sputter-coated with gold under vacuum, and examined using a Neoscope JCM-7000 (JEOL, Tokyo, Japan). SEM was carried out at 10 kV.

4.2.6. Fibre pre-treatment

Alkaline pre-treatment was performed on asparagus fibre before enzymatic hydrolysis, to investigate the effect of this additional processing step on the production of cellobiose and soluble COS. Different studies performed the alkaline pre-treatment before enzymatic hydrolysis on dried and milled lignocellulosic biomass (Din, Lim, Maskat, & Zaini, 2021;

Vaz et al., 2021; Xu, Cheng, Sharma-Shivappa, & Burns, 2010). The drying and milling before pre-treatment allow good control of particle size and dosage. The pre-treatment was performed in a 1.25 mol/L NaOH solution with a fibre loading of 50 g/L. The fibre suspensions were incubated at ambient temperature for 45 min on a magnetic stirrer and pH values of 12-13 were measured at the end of the pre-treatment. The fibres were then washed with tap water using a Buchner vacuum filter (VWR, Amsterdam, The Netherlands). Lastly, the fibres were washed with 0.1 mol/L acetic acid solution to neutralize the pH followed by tap water until a pH between 4 and 5 was reached. The fibres were then dried in an oven at 80 °C for 24 h after the alkaline pre-treatment and milled once more in the Pulverisette-14 with a 0.2 mm sieve and at 10,000 rpm. The asparagus fibre samples with or without alkaline pre-treatment are referred to as *pre-treated* fibre and *untreated* fibre, respectively.

To reduce the number of processing steps, the alkaline pre-treatment was performed on wet asparagus fibre that was obtained after juice extraction. Those fibres had a moisture content of 85 g/100 g. The alkaline treatment was done at the same processing conditions as described above and the wet fibre weight was corrected to have the same fibre loading on dry basis. The treated fibres were then dried and milled according to the same procedure described in section 4.2.2. The obtained sample is referred to as *wet pre-treated* fibre. For each pre-treatment, one batch of fibre was prepared, and all pre-treated fibres were stored in plastic bags at ambient temperature until further use.

4.2.7. Fibre hydrolysis

Enzymatic hydrolysis experiments were performed in Eppendorf tubes with 0.0375 g fibre (i.e. untreated, pre-treated and wet pre-treated) and 1.5 mL 0.5 mol/L citrate buffer (pH 5.0) to obtain a solids loading of 25 g/L. The hydrolysis was done on a dried fibre sample for easy control of the dosage. Enzyme solutions were prepared by dilution of Celluclast in citrate buffer to obtain 420, 700 and 980 nkat/g substrate (see also section 4.2.1). After the addition of the enzyme solution to the fibre, the samples were incubated in an Eppendorf thermomixer (Thermo Fisher Scientific, Waltham, USA) at 50 °C and 900 rpm. The samples were incubated for 0, 0.5, 1, 2, 4, 7 and 16 h followed by inactivation of the enzymes at 100 °C and 900 rpm for 10 min. After inactivation, the samples were stored at 4 °C until analysis the next day. The fibre hydrolysis experiments were carried out in duplicate and fibres from the same processed batch were used.

4.2.8. HPLC analysis

The obtained hydrolysates after enzymatic conversion were analysed by using high-performance liquid chromatography (HPLC) (Thermo Ultimate 3000 HPLC, ThermoFisher Scientific, Waltham, USA) with a Shodex KS-802 8.0 × 300 (mm) column (Showa Denko K.K., Toyko, Japan). The column was operated at 50 °C and connected to a refractive index detector (Shodex RI-501, Showa Denko K.K., Toyko, Japan). Milli-Q water was used as eluent with a flow rate of 1 mL/min. Glucose and Cellobiose were detected and quantified using analytical standards as reference. Oligosaccharides were detected and quantified using analytical Fructo-oligosaccharides (FOS) as standards.

The conversion of cellulose into soluble compounds was defined as enzymatic hydrolysate yield (g/100 g cellulose) and calculated using equation 4.1 (Karnaouri et al., 2019b).

$$\frac{C1 + C2 \cdot 1.05 + C3 \cdot 1.07 + C4 \cdot 1.085}{C_{fibre} \cdot x_{cellulose} \cdot 1.111} \cdot 100 \quad (4.1)$$

C1 is the concentration (g/L) of glucose measured, C2 is the concentration of cellobiose, C3 is the concentration of Cellotetraose (DP3), C4 is the concentration of all oligosaccharides together with a DP equal and larger than 4. C_{fibre} is the initial concentration of asparagus fibre present in the sample and $x_{cellulose}$ is the fraction of cellulose in the asparagus fibre (-). Cellobiose and COS were expressed as 'free glucose', therefore the factors 1.05, 1.07 and 1.085 correct for the water molecules that are added during hydrolysis (Karnaouri et al., 2019b). Cellulose has an average DP > 500 (BeMiller, 2019a), therefore factor 1.111 was used. The maximum amount of cellulose conversion into glucose was considered as 100 g/100 g cellulose.

The conversion of cellulose into cellobiose and oligosaccharides, i.e. cellobiose and COS yield (g/100 g cellulose), was calculated using equation 4.2.

$$\frac{C2 \cdot 1.05 + C3 \cdot 1.07 + C4 \cdot 1.085}{C_{fibre} \cdot x_{cellulose} \cdot 1.111} \cdot 100 \quad (4.2)$$

4.2.9. Scale-up experiment

A scale-up experiment was performed to obtain sufficient hydrolysate for spray drying. Wet pre-treated fibres were used, which were prepared according to the treatment described in section 4.2.4. The hydrolysis was performed in a 1 L double-wall vessel with 900 mL 0.5 M

citrate buffer (pH 5), solid loading of 25 g/L and a Celluclast loading of 700 nkat/g substrate (see also section 4.2.1). The fibres were incubated at 50 °C and continuously stirred with a magnetic stirrer for 7 h. The asparagus hydrolysate was filtered with a vacuum filter with pore size 1 (i.e. 100-160 µm) (VitraPOR, VWR, Amsterdam, The Netherlands) and the enzymes in the filtrate were inactivated in a water bath at 100 °C for 10 min. The filtrate was concentrated with a rotary evaporator (RC-900, KNF, Vleuten, The Netherlands) to a Brix of 10°. The concentrated asparagus hydrolysate was stored at 4 °C until spray drying the next day. Two independent scale-up experiments were performed.

4.2.10. Spray drying

The concentrated asparagus hydrolysate mixtures were spray-dried separately with a Model B-290 mini spray dryer (Büchi Labortechnik AG, Flawil, Switzerland). The spray drying conditions were adapted from Etzbach et al. (2020), who used cellobiose amongst other carrier agents for the spray drying of goldenberry juice. The spray dryer aspirator rate was 100 %, which corresponded to approximately 35 m^3 air/h. The inlet air temperature was set to 140 °C and the speed of the peristaltic pump was adjusted to 10 mL feed/min. The corresponding outlet air temperature varied between 68-70 °C. The hydrolysate powders were collected at the outlet of the spray dryer for further analysis. The spray drying yield (%) was calculated based on the dry solids (DS) in the feed mixture and the powder obtained from the collection vessel using equation 4.3.

$$\frac{Powder\ (DS)}{Feed\ (DS)} \cdot 100 \tag{4.3}$$

4.2.11. Glass transition temperature (T_g) of the spray-dried hydrolysate

The T_g of the spray-dried hydrolysate was determined using differential scanning calorimetry (DSC) (DSC-250, TA Instruments, New Castle, UK). Samples of about 5 mg were weighed in aluminium Tzero pans and then sealed with a Tzero hermetic lid, which was punctured to let water vapour escape. A heat-cool-heat cycle was performed. Firstly, the samples were heated at a rate of 10 ºC/min from 0 to 140 °C to obtain anhydrous conditions. Then the samples were cooled back to 0 ºC at 10 ºC/min. Lastly, a second heat run was performed at 5 ºC/min to 140 ºC. The DSC thermograms were analysed using Trios software (TA Instruments, New Castle, UK). The second heat run was used for the analysis of the T_g. The

T_g was determined from the midpoint, which was based on the inflection of the endothermic shift due to glass transition, i.e. the peak of the derivative.

4.2.12. Statistical analysis

The composition analysis of untreated, pre-treated and wet pre-treated fibres was performed on one batch of processed fibres and experiments were performed at least in duplicate. The means of the technical replicates were presented and the analytical precision was reported using the pooled standard deviation. All hydrolysis experiments were conducted in duplicate and results were presented as mean ± standard deviations.

4.3. Results and Discussion

4.3.1. Composition of untreated and pre-treated fibres

The alkaline pre-treatment was performed to make the cellulose more accessible for enzymes and thereby increasing the hydrolysis yield (Kim et al., 2016). The alkaline pre-treatment was first performed on dried and milled fibre, this approach is also reported in several other studies (Din et al., 2021; Vaz et al., 2021; Xu et al., 2010). Secondly, the alkaline pre-treatment was also evaluated directly with wet asparagus fibres to possibly omit the energy intensive drying and milling steps.

The alkaline pre-treatment on dried and wet fibres removed a large part of the hemicellulose from the asparagus fibre (Table 4.1), consequently, the cellulose content on dry basis increased. Although dissolution of hemicellulose and lignin is one of the commonly observed results of alkaline pre-treatment reported in literature (Kim et al., 2016), the lignin content of our samples was not significantly affected by the alkaline treatment. The same pre-treatment was performed by Maepa et al. (2015) on maize tassels, there the lignin content decreased slightly from 18 to 15 g/100 g after the alkaline pre-treatment. The lignin content in the untreated asparagus fibres was only 4.6 g/100 g, which may explain why the alkaline pre-treatment did not lower the lignin content. The dried pre-treated and wet pre-treated fibres are similar in cellulose, hemicellulose and lignin content, although it was expected that the pre-treatment on the dried and milled fibres would be slightly more effective as the particle size of the dried and milled fibres (i.e. $D_{50} \sim 270$ µm) were smaller than of the wet asparagus fibre (i.e. $D_{50} > 0.5$ cm).

Table 4.1 Composition of untreated, dried pre-treated and wet pre-treated asparagus fibres. The compositional analysis was performed on the same batch of processed fibre and measurements were performed at least in duplicate. The analytical precision is presented via the pooled standard deviation.

	Cellulose (g/kg DS)	Hemicellulose (g/kg DS)	Lignin (g/kg DS)	Protein (g/kg DS)	Ash (g/kg DS)	Others[1] (g/kg DS)
Untreated	459	182	46	78	56	179
Dried pre-treated	606	13	56	43	123	159
Wet pre-treated	620	33	56	62	71	158
Pooled standard deviation	6	14	1	1	7	n.a.

[1] Calculated by the difference. DS: dry solids. n.a.: not applicable

When compared to the untreated fibre, the alkaline pre-treatment increased the ash content. Part of the salts from the sodium hydroxide solution and the neutralisation with acetic acid could have ended up in the asparagus fibre.

Furthermore, the microstructural surface properties of the fibres were examined by SEM and images are reported in the supplementary information (Fig. A.4.1). The surface of the untreated fibre was relatively smooth, whereas the surfaces for the pre-treated and wet pre-treated fibre appeared rougher. Similar effects of alkaline pre-treatment on fibre surface structures were observed by Din et al., 2021; Maepa et al., 2015; Taherdanak & Zilouei, 2014 and related to the removal of lignin and hemicellulose.

4.3.2. Effects of enzyme loadings and hydrolysis time on hydrolysis products of untreated and pre-treated fibres

The enzymatic hydrolysis was performed with milled asparagus fibre (untreated fibre) with an average particle size (D_{50}) of 270 µm. From preliminary experiments, it was found that fibre particle size did not significantly affect the hydrolysis rate of untreated fibres, as the conversion of cellulose into soluble compounds ranged between 17 and 19 g/100 g in 4 hours (data not shown). Particle sizes (D_{50}) tested were 40 µm, 180 µm and 480 µm.

Subsequently, the amounts of products formed were evaluated at various enzyme loadings to optimize the formation of these and eventually link to the T_g. Untreated and pre-treated fibres were incubated with different enzyme loadings, i.e. 420, 700 and 980 nkat/g substrate. The

enzymatic hydrolysate yield kept increasing during 16 hours of incubation (Fig. 4.1A) and a clear difference in hydrolysis yield between untreated and pre-treated fibres was observed. The yield after 16 h was much higher for pre-treated fibres compared to untreated fibres and is explained by improved substrate accessibility for the cellulases. Alkaline pre-treatments can improve substrate accessibility by different phenomena, e.g. dissolution of lignin and hemicellulose, increase of surface area, and reduction of the DP thereby increasing the reducing ends (Bali, Meng, Deneff, Sun, & Ragauskas, 2015; Kim et al., 2016). The occurrence of these phenomena depends on the severity of the alkaline treatment, i.e. temperature and pH. In this study, mild temperature conditions were used since the pre-treatment was performed at ambient temperature. A high pH was used and at the end of the alkaline pre-treatment of the fibres pH values of 12-13 were measured. Maepa et al. (2015) performed the alkaline pre-treatment on maize (tassel) plants with the same conditions, i.e. time, temperature, NaOH concentration, as in this study. They found that the hemicelluloses and lignin were removed from the maize tassel fibres during alkaline treatment. In addition, a higher crystallinity index was measured for the pre-treated maize tassel fibres compared to the untreated fibres due to the loss of amorphous hemicellulose. Furthermore, the alkaline pre-treatment appeared to have had a minimal effect on the cellulose structure (Maepa et al., 2015). Therefore, it is expected that in this study removal of hemicellulose was the main mechanism for the increase in enzyme accessibility.

Furthermore, higher enzyme loadings increased the enzymatic hydrolysate yield for both untreated and pre-treated fibres (Fig. 4.1A). Except for the conversion of the untreated fibres with 700 and 980 nkat/g substrate, which resulted in the same composition of formed soluble compounds (Fig. 4.1). This could be explained by the limited cellulose accessibility in the untreated fibre and therefore the hydrolysis was limited by the available substrate instead of enzyme concentration (Din et al., 2021).

The cellobiose and oligosaccharides yield (Fig. 4.1B) did not follow the exact same increasing trend as the enzymatic hydrolysate yield (Fig. 4.1A). During the first 7 hours of hydrolysis, the yield of cellobiose and oligosaccharides increased. Between 7 and 16 h, the conversion yield to cellobiose and oligosaccharides did not change significantly, while the conversion to monosaccharides continues, as indicated by the increasing enzymatic hydrolysate yield (Fig. 4.1A). For the following experiments, the enzyme loading of 700 nkat/g substrate was selected since its cellobiose and oligosaccharides yield was comparable

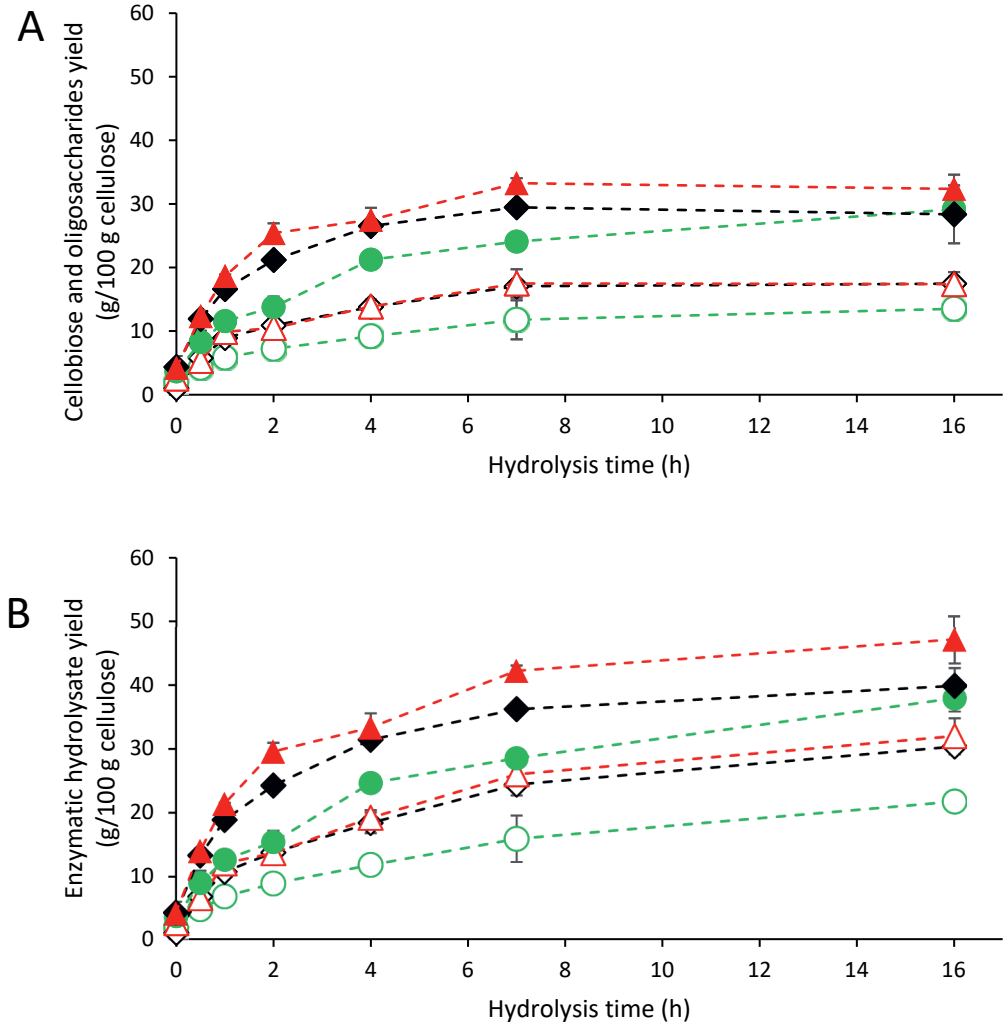

Figure 4.1 (A) Cellulose conversion to soluble compounds (g/100 g cellulose) with untreated asparagus fibre and alkaline pre-treated asparagus fibre as substrate with different enzyme loadings (EGU/g substrate). (B) Cellulose conversion to cellobiose and oligosaccharides (g/100 g cellulose) with untreated asparagus fibre and alkaline pre-treated asparagus fibre as substrate and different enzyme loadings (EGU/g substrate). Untreated fibre: 420 nkat/g substrate (○), 700 nkat/g substrate (◊) and 980 nkat/g substrate (△); Pre-treated fibre: 420 nkat/g substrate (●), 700 nkat/g substrate (♦) and 980 nkat/g substrate (▲). The error bars represent the standard deviation of the experimental data (n = 2). Dashed lines are drawn to guide the eyes.

with the 980 nkat/g, while the undesired formation of monosaccharides was lower for the 700 nkat/g.

The composition of hydrolysis products over time was analysed (Fig. 4.2) to select the most suitable hydrolysis time to maximize the yield of hydrolysates with cellobiose/COS. For both untreated and pre-treated fibre, cellobiose was the main compound formed during hydrolysis. The amount of formed COS was much lower compared to cellobiose, and most likely relates to cellobiose releasing CBH activity present in Celluclast (Beldman et al., 1988; Bischof et al., 2016; Lynd et al., 2002). Glucose amounts were also lower than those of cellobiose, which presumably relates to a relatively low BGL activity in Celluclast (Lynd et al., 2002), as has also been observed for the same cellulase cocktail by others (Karnaouri et al., 2019a). Cellobiose concentrations were highest for the pre-treated fibres compared to the untreated fibres (Fig. 4.2) and increased up to a hydrolysis time of 7h (Fig. 4.2). After 7h of hydrolysis, glucose increased further while cellobiose concentrations remained the same (Fig. 4.2). The increase in glucose is undesirable for the application of the enzymatic hydrolysate as carrier agent since glucose will decrease the T_g. Hence, the optimum seems to be around 7 h of hydrolysis for both untreated and pre-treated fibres.

4.3.3. Enzymatic hydrolysis after alkaline pre-treatment on dried and wet fibres

Enzymatic hydrolysis was performed using dried fibre powder to better control the dosage of substrates. However, for alkaline pre-treatment of the fibre, it would be more efficient to use the wet fibre fraction obtained after juice extraction to reduce the processing steps. Therefore, alkaline treated dried and wet asparagus fibre were compared.

The overall enzymatic hydrolysate yield of the dried pre-treated fibres was slightly higher compared to that of the wet pre-treated fibres in the first hours of hydrolysis (Fig. 4.3A). The slopes, i.e. hydrolysis rates, were comparable, but at time = 0 h more soluble compounds were measured in the dried pre-treated fibres than in the wet pre-treated fibres After the first hours of hydrolysis, the overall yields became identical. The same trend is observed for the cellobiose and oligosaccharides yields (Fig. 4.3B). Based on the results, there is no preference for dried or wet pre-treated fibres. Processing fibres by wet alkaline pre-treatment is less time- and energy-consuming than performing alkaline pre-treatment on dried fibres. Therefore, wet alkaline pre-treatment was selected for the bench-scale experiment.

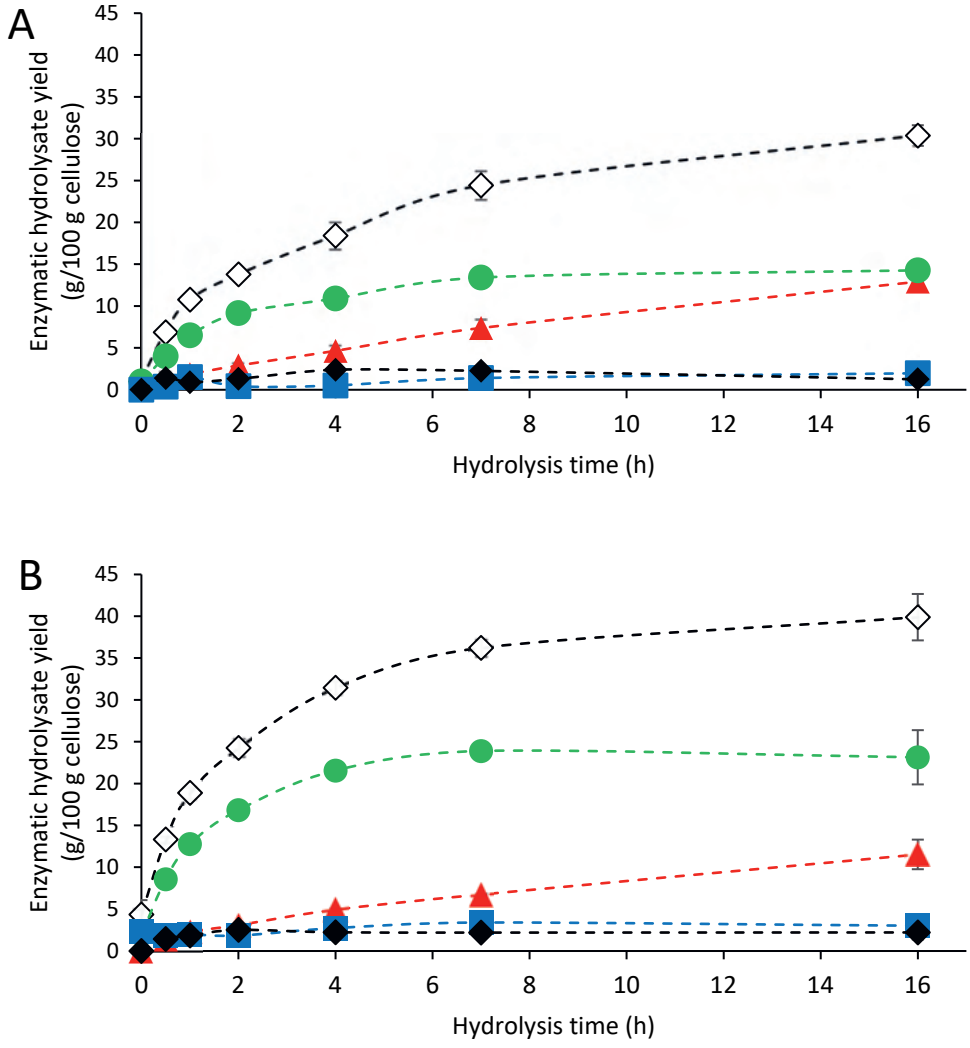

Figure 4.2 (A) Reaction products after hydrolysis of untreated asparagus fibre with an enzyme loading of 42 EGU/g substrate. (B) Reaction products after hydrolysis of alkaline pre-treated asparagus fibre with an enzyme loading of 700 nkat/g substrate. Total (◊), glucose (▲), cellobiose (●), DP3 (■) and >DP4 (♦). DP: degree of polymerisation. The error bars represent the standard deviation of the experimental data (n = 2). Dashed lines are drawn to guide the eyes.

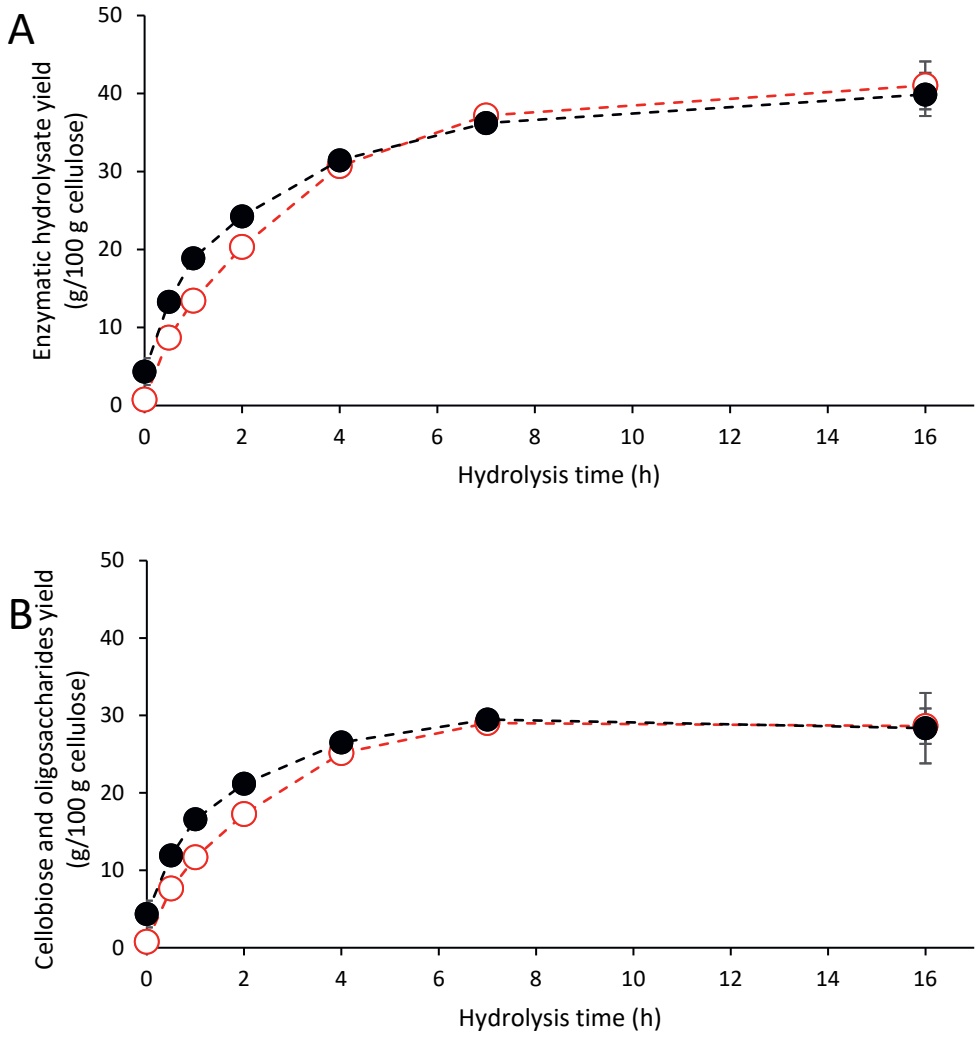

Figure 4.3 (A) Cellulose conversion to soluble compounds (g/100 g cellulose) with dried pre-treated and wet pre-treated asparagus fibre as substrate with an enzyme loading of 700 nkat/g substrate. (B) Cellulose conversion to cellobiose and oligosaccharides (g/100 g cellulose) with dried pre-treated and wet pre-treated asparagus fibre as substrate with an enzyme loading of 700 nkat/g substrate. Dried pre-treated fibres (●) and wet pre-treated fibres (○). *Dried pre-treated fibres* were first dried and milled before soaked into the sodium hydroxide solution. *Wet pre-treated fibres* were directly submerged in the sodium hydroxide solution. The error bars represent the standard deviation of the experimental data (n = 2). Dashed lines are drawn to guide the eyes.

4.3.4. Bench-scale experiment to evaluate the properties (T_g) of the spray-dried hydrolysate powder

A bench-scale experiment was conducted to produce cellobiose and soluble oligosaccharides in a powder form, by following three steps, i.e. enzymatic hydrolysis, evaporation concentration and spray drying. A bench-scale experiment was necessary to prepare at least 50 mL of feed solution (10º Brix) required for the spray dryer. The enzymatic hydrolysis conditions were selected based on results shown in previous sections, i.e. 700 nkat/g substrate, hydrolysis time of 7 h and wet pre-treated fibres as substrate. The reaction products from the small bench-scale enzymatic hydrolysis experiment were compared to the results from the Eppendorf tubes (Table 4.2). Performing the hydrolysis at a somewhat larger scale increased the total yield of soluble hydrolysates, which is explained by the active mixing of the asparagus fibre with enzyme solution inside the reaction vessel.

Table 4.2 Reaction products after hydrolysis of wet pre-treated fibres in the Eppendorf tubes and bench-scale with an enzyme loading of 700 nkat/g substrate for 7 h hydrolysis. The data is presented as mean ± standard deviations (n = 2).

	Total (g/100 g cellulose)	Glucose (g/100 g cellulose)	Cellobiose (g/100 g cellulose)	DP3 (g/100 g cellulose)	>DP4 (g/100 g cellulose)
Eppendorf tubes	37.2 ± 0.3	8.14 ± 0.05	25.3 ± 0.1	2.53 ± 0.06	1.2 ± 0.1
Bench-scale	44.6 ± 0.9	10.9 ± 0.6	30 ± 2	3.3 ± 0.2	1 ± 1

The obtained hydrolysis yield is determined by different factors, e.g. type of substrate, hydrolysis time, enzyme loadings and solids loadings. For example, higher solids loadings decrease the yield due to inhibition of enzyme adsorption by hydrolysis products at increasing substrate concentrations (Kristensen, Felby, & Jørgensen, 2009). Kristensen et al. (2009) performed hydrolysis of filter paper, using substrate concentrations in the range of 50-200 g/L and an enzyme loading of 10 FPU/g substrate, i.e. 10 µmol/min of glucose per g of substrate (~167 nkat/g substrate). A linear decrease was observed between conversion and initial substrate concentrations. In this study, solids loadings of 25 g/L were used and therefore it was assumed that there was limited inhibition by the formed hydrolysis products.

The cellulose conversions found in this study were compared to other studies. Karnaouri et al. (2019a) used Celluclast for the conversion of birch into COS and measured a cellulose

conversion of 23 g/100 g cellulose with 35 EGU/g (583 nkat/g) after 24 h of hydrolysis at 50°C and pH 5. The hydrolysis yield was similar to that of the untreated fibre with 420 nkat/g for 16 h, namely 22 g/100 g cellulose (Fig. 4.1A). In the work of La Peña-Armada et al. (2020), Celluclast was used for the release of COS from apple by-products and combined with a high hydrostatic pressure (HPP) treatment. The control sample (no HHP treatment) consisted of pre-hydrated apple by-product (100 g/L) with 92 EGU of Celluclast (~350 nkat/g substrate) and released 29 g soluble compounds/100 g dry material after 30 h of hydrolysis at 50°C. The result was somewhat higher than the conversion of untreated fibre with 420 nkat/g after 16 h in this study (Fig. 4.1A).

The bench-scale hydrolysates were concentrated and spray-dried to obtain a powder that can be used as an ingredient. During spray drying, minimal wall deposition in the drying chamber was observed, which indicates limited stickiness behaviour and a hydrolysate with sufficiently high T_g for spray drying (Shishir & Chen, 2017). The spray drying yield was 50 ± 4 %, which is similar to the yield of spray-dried cellobiose obtained by Etzbach et al. (2020). It should be noted that the yields obtained in small spray dryers like Büchi B-290 are much lower than in large-scale spray dryers (Islam, Edrisi, & Langrish, 2013). The T_g of the spray-dried powders was analysed with DSC and an anhydrous T_g of 108 ± 7 ºC was found. An example of the DSC thermogram is shown in Fig. 4.4 with the T_g expressed as the midpoint of the endothermic shift. The hydrolysate consisted of a combination of different monosaccharides, disaccharides and COS (Table 4.2), each contributing to the overall T_g. For example, glucose has a low T_g (31 ºC) and therefore suppresses the T_g, whereas the T_g of cellobiose (102 ºC) is closer to the overall T_g and cellobiose is the most abundant compound in the hydrolysate. The T_g of COS are not reported, but it is assumed that their T_g is higher than that of cellobiose based on molecular weight. Therefore, the presence of COS in the hydrolysates was likely to increase the T_g. It should be noted that the spray-dried powder also contains other impurities such as constituents of the citrate buffer (i.e. citric acid and sodium citrate), which might have influenced the T_g of the spray-dried powder. Furthermore, other reaction products could be formed during hydrolysis since Celluclast also contains some hemicellulose activity, e.g. xylanase and β-xylosidase (Y. Zhang et al., 2020). Some xylose was measured in the reaction products, roughly 0.25 g xylose for every gram of cellobiose formed (data not shown). The xylose was probably released from hydrolysed xyloglucans or

xylan, both hemicelluloses are found in white asparagus spears (Chitrakar et al., 2019; Rodríguez, Jiménez, Guillén, Heredia, & Fernández-Bolaños, 1999).

The morphology of the spray-dried hydrolysate particles was visualised (Fig. 4.5), the particles were round and had a smooth surface. Some of the larger particles had a few dents on the surface. In conclusion, the hydrolysate showed good spray drying behaviour and had a fairly high T_g.

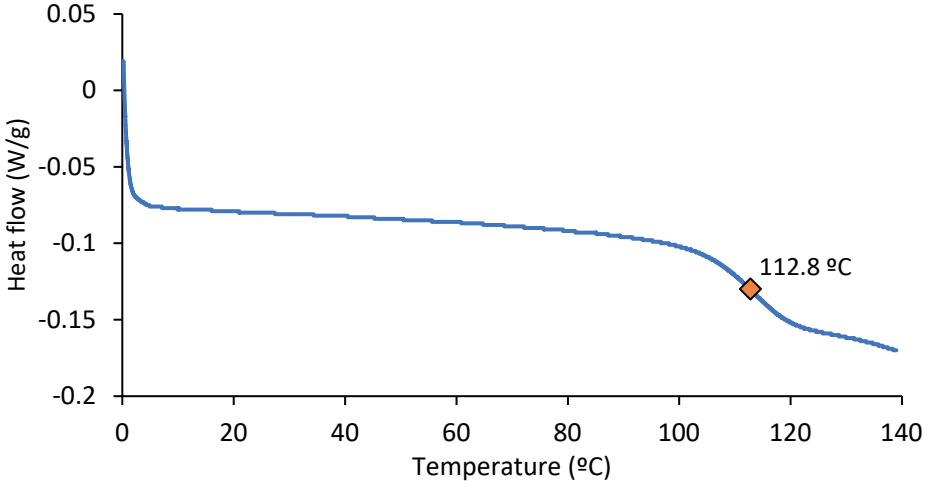

Figure 4.4 Example of the differential scanning calorimetry (DSC) thermogram of the spray-dried hydrolysate of the wet pre-treated asparagus fibre. Wet pre-treated fibres were directly submerged in the sodium hydroxide solution followed by enzymatic hydrolysis with an enzyme loading of 700 nkat/g substrate. The midpoint of the glass transition temperature (T_g) is located at 112.8 ºC.

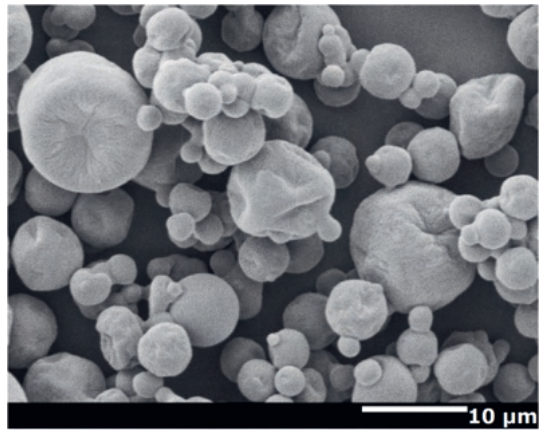

Figure 4.5 Scanning electron microscopy image of the spray-dried hydrolysate of the wet pre-treated asparagus fibre. Wet pre-treated fibres were directly submerged in the sodium hydroxide solution followed by enzymatic hydrolysis with an enzyme loading of 700 nkat/g substrate.

Purification of the hydrolysate might further increase its T_g and will enable easier application in food products. For example, asparagus hydrolysate can be used as a natural alternative for maltodextrin, which is commonly used for the encapsulation of aroma compounds (Siccama et al., 2021b).

4.4. Conclusions

An enzymatic treatment was performed to convert asparagus fibre waste into a cellobiose and COS powder having the potential to be used as a natural carrier agent. The formation of cellobiose and COS over monosaccharides during hydrolysis can be steered by choosing the suitable hydrolysis time and fibre pre-treatment. Alkaline pre-treatment on fibre increased cellulose concentration on dry basis and positively affected enzymatic hydrolysis as shown by the increased yield of cellobiose and COS from 17 to 30 g/100 g cellulose (7h), while glucose yield was similar to the untreated fibre (7 g/100 g cellulose). Furthermore, the feasibility of performing alkaline pre-treatment on wet asparagus fibre was proved. The hydrolysis of wet pre-treated fibres was successfully applied to make a spray-dried hydrolysate powder (with 45 g/100 g cellulose converted). The high T_g (108 ºC) of the spray-dried hydrolysate indicated its potential usage as carrier agent for spray drying. Furthermore, other studies (Karnaouri et al., 2019b; Sanz et al., 2005) proved that cellobiose and COS cannot be digested by humans, thus they are prebiotics and could promote gut health which will provide additional benefits compared to the use of conventional carrier agents such as maltodextrin.

This work demonstrates that enzymatic hydrolysis could be a method to produce ingredients that can function as carrier agent. We believe this work can serve as a useful reference for future studies on the valorisation of agro-fibre waste streams. However, to translate our findings into a viable production process a techno-economic assessment and further optimization of the process is required. For example, it is recommended to explore possibilities for neutralisation of the sodium hydroxide-rich waste stream that is generated after the alkaline pretreatment. Furthermore, it is worth to investigate if recycling of the unhydrolyzed substrates is feasible to limit waste generation during enzymatic hydrolysis. Alternatively, unhydrolyzed fibres may be further converted into compost and be used for fertilization. Furthermore, it would be of interest to investigate the recovery of the enzymes for example via ultrafiltration.

4.5. Appendix

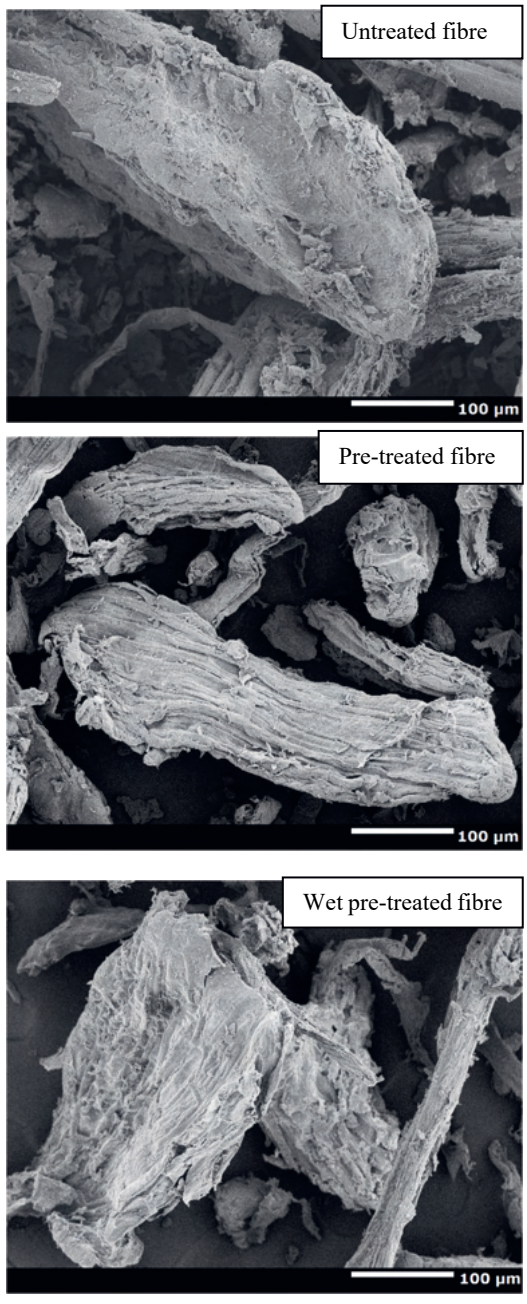

Figure A.4.1 Scanning electron microscopy images of untreated and pre-treated asparagus fibres. *Pre-treated fibres* were first dried and milled before soaked into the sodium hydroxide solution. *Wet pre-treated fibres* were directly submerged in the sodium hydroxide solution.

Chapter 5

Acetone release during thin film drying of maltodextrin solutions as model system for spray drying

This chapter has been submitted as Siccama, J.W., Wientjens, X., Zhang, L, Boom, R.M., Schutyser, M.A.I. Acetone release during thin film drying of maltodextrin solutions as model system for spray drying.

5.1. Introduction

Spray drying volatile organic compounds (VOCs) in a carrier matrix is an effective method for flavour encapsulation. The flavour molecules are encapsulated by the formation of a semi-permeable skin around the drying droplet, which is related to the drying kinetics. During spray drying, the atomised droplets are initially heated up to the wet-bulb temperature followed by moisture removal at a constant rate proportional to the surface area of the droplet (Santos et al., 2018). During this constant rate period, the droplet settles at the wet-bulb temperature where the convective heat transferred is equal to the removed heat due to water evaporation. Towards the end of the constant rate period, solutes accumulate close to the droplet surface and locally increase the viscosity and reduce the diffusivity, and a semi-permeable skin is formed (Anandharamakrishnan & Padma Ishwarya, 2015; Siemons, Politiek, et al., 2020). As soon as the skin is thick enough, the internal mass transfer will decrease, initiating the falling rate period. During this period, the evaporation of moisture is limited by internal diffusion. The droplet temperature increases and a concentration gradient develops within the droplet (Boel et al., 2020). The formation of the semi-permeable skin is the main encapsulation mechanism of volatile compounds since the skin is still sufficiently permeable to the small water molecules but hinders the release of larger molecules like most VOCs (Coumans et al., 1994).

For spray drying of VOCs, a matrix forming (carrier) material is required. A widely used carrier agent is maltodextrin, which is formed through controlled hydrolysis of starch. Maltodextrins provide a good balance between costs and effectiveness as they generally have a neutral flavour, a relatively low viscosity at high concentrations, a high glass transition temperature (T_g) which is an indication of their ability to form a diffusional barrier, and are available in a range of dextrose equivalents (Apintanapong & Noomhorm, 2003). The dextrose equivalent (DE) of maltodextrin is a measure of the extent of hydrolysis and is inversely related to the average molecular weight. Maltodextrins with different DE have different properties such as the viscosity of its aqueous solution (Avaltroni, Bouquerand, & Normand, 2004). Using maltodextrins with higher DE values as carrier agent are related to lower VOCs retention as studied by Bangs and Reineccius (1982) who analysed the average retention of twelve VOCs for different maltodextrin DEs. The aqueous solution of maltodextrins with lower DEs (i.e. larger average molecular weight) have a lower water diffusivity and thereby show faster semi-permeable skin formation, improved retention of

VOCs during drying because of the lower water diffusivity of maltodextrin molecules (Goubet, Le Quere, & Voilley, 1998). However, no significant difference in volatiles retention between the high molecular weight maltodextrins DE5 and DE10 was observed in previous studies (Bangs & Reineccius, 1982; Raja, Sankarikutty, Sreekumar, Jayalekshmy, & Narayanan, 1989), indicating that other factors are important. For low DEs, other phenomena such as interactions, insolubility and inclusions are suggested to also contribute to volatile retention (Goubet et al., 1998).

The role of maltodextrins for flavour encapsulation purposes in spray drying has been studied extensively (Reineccius, 2004; Rosenberg et al., 1990; Siccama, Pegiou, Zhang, et al., 2021). Most studies investigate the encapsulation mechanism by analysing remaining flavour compounds in the final spray-dried powder. However, this does not provide information about the kinetics of flavour encapsulation during drying. It is therefore of interest to study the volatile release kinetics during the spray drying process. The obtained knowledge could guide the design and optimization of volatile encapsulation systems and drying processes. Nevertheless, direct assessment of these kinetics within a spray dryer is challenging as volatile compound release and mass and temperature profiles are hard to monitor in-line. Therefore, a convective thin film dryer (TFD) was developed by Both, Tersteeg, Boom, & Schutyser (2019) to accurately assess the drying kinetics of complex matrices dried at relevant air temperatures and velocities.

To detect the release of VOCs in the drying air, we extend the TFD with a photo-ionisation detector (PID) in the current work. VOCs are ionised in the PID when their ionization energy is below that of the PID lamp. An electron and a positively charged ion are generated, which are subsequently detected by a cathode and anode creating a current that is transposed into a concentration-dependent signal (Ion Science, 2019). The conversion and detection occur within milliseconds, making the PID suitable to detect VOCs in-line (Haag & Wrenn, 2006).

In food applications, the use of PID has been limited for quality assessment in terms of microbial quality (Cagnasso et al., 2007) and sensory quality, i.e. overall volatile intensity (Vidrih, Hribar, & Zlatić, 2008). To the best of our knowledge, the use of a PID to study volatile release kinetics during thin film drying has never been attempted. The inline data obtained during thin film drying then help us better understand the mechanisms that determine the degree of volatile encapsulation that we can achieve.

Therefore, we here investigate the volatile release kinetics of acetone as influenced by the type (i.e. maltodextrin DE12 and DE21) and initial concentration of carrier agent (i.e. 20 % and 40 %) in the system. Acetone was selected as VOC since it is a water-soluble compound with high relative volatility and is frequently used as model compound for aroma encapsulation during spray drying (Coumans et al., 1994; Reineccius & Coulter, 1969; Rulkens & Thijssen, 1972). It was hypothesized that the volatile release kinetics of acetone are linked to the formation of the semi-permeable skin at the surface of the thin film: acetone release will occur mostly at the start of drying when no skin has yet been formed, and total acetone release will be lowest if the skin can be formed quickly. The acetone retention in the thin film can be calculated based on the initial acetone concentration and the release profile detected by the PID, which was then validated by analysing the remaining acetone in the thin films by high-performance liquid chromatography (HPLC) and 2,4-dinitrophenylhydrazine (2,4-DNPH) as a derivatizing reagent. In addition, spray drying experiments with a lab-scale spray dryer were done with the same matrices as used for the TFD. The retained acetone in the spray-dried powders was measured and compared with the thin films as validation of the use of the TFD to simulate spray drying.

A mechanistic model was developed to describe acetone retention as a function of carrier matrix and drying conditions. The model describes the aroma release by applying mass and heat transfer equations and the diffusion inside the matrix. The mutual diffusion coefficients of water and maltodextrin were taken from Siemons et al. (2019), while the acetone diffusion coefficient in maltodextrin solutions was taken from Menting et al. (1970).

5.2. Materials & methods

5.2.1. Materials

Maltodextrins with DE12 and 21 originating from corn starch were obtained from Roquette Frères (Levres, France). Acetone (Merck, Darmstadt, Germany), maltotriose (Merck, Darmstadt, Germany) 2,4-dinitrophenylhydrazine hydrochloride (DNPH) (TCI Chemical, Tokyo, Japan), acetonitrile (Actu-All Chemicals, Oss, The Netherlands) and methanol (Actu-All Chemicals, Oss, The Netherlands) were used in this study. Ultrapure water (Milli-Q™ Reference Ultrapure Water Purification System) was used throughout this study.

5.2.2. Characterization of maltodextrins

Molecular weight distributions of the different maltodextrins were determined by HPLC (Thermo Ultimate 3000 HPLC, ThermoFisher Scientific, Waltham, USA) using a Shodex KS-803 (300 × 8.0 mm) column (Showa Denko K.K., Toyko, Japan). The column was operated at 50 °C and connected to a refractive index (RI) detector (Shodex RI-501, Showa Denko K.K., Toyko, Japan). Milli-Q water was used as eluent with a flow rate of 1 mL/min.

The T_g of the maltodextrins was determined using differential scanning calorimetry (DSC) (DSC-250, TA Instruments, England). Maltodextrins were analysed directly as well as after desiccation under vacuum for 5 days. The dry matter content of all samples was determined by drying at 105 °C overnight. Samples of ± 10 mg were weighed in aluminium Tzero pans and sealed with a Tzero hermetic lid. A heat-cool-heat cycle was performed to remove the thermal history of the samples. After equilibration at 50 °C, temperature ramp measurements were carried out at a rate of 10 °C/min to a maximum temperature in the range of 130 to 200 °C. Then the samples were cooled to 50 °C at 10 °C/min. The second heat run was performed at 5 or 10 °C/min to 130-200 °C. The DSC thermograms were analysed using Trios software (TA Instruments, New Castle, UK). The T_g was determined from the second heating ramp as the midpoint of the endothermic shift at which a change in heat capacity was observed.

The anhydrous T_g of the maltodextrins ($T_{g,s}$) was calculated with the Couchman-Karasz equation:

$$T_g = \frac{y_w \Delta c_{p,w} T_{g,w} + y_s \Delta c_{p,s} T_{g,s}}{y_w \Delta c_{p,w} + y_s \Delta c_{p,s}} \tag{5.1}$$

Where y_w and y_s are the weight fractions of water and maltodextrin respectively, $\Delta c_{p,w}$ and $\Delta c_{p,s}$ represent the change in heat capacity at glass transition of pure water (1.91 kJ/kg·K) and maltodextrin (0.426 kJ/kg·K) respectively and $T_{g,w}$ and $T_{g,s}$ are the T_g of pure water (138 K) and the anhydrous maltodextrin (Siemons, Politiek, et al., 2020; Van Der Sman & Meinders, 2010).

5.2.3. Thin film drying

A TFD was previously developed (Both, Tersteeg, et al., 2019) and a PID sensor was inserted in the air outlet of the dryer (Fig. 5.1). The air tunnel was 50·14·2.6 cm (L·W·H), through which hot air was blown of 105 °C and 1 % relative humidity at a speed of 1 m/s. The sample

tray (4·9·0.05 cm L·W·H) was situated on a scale in the middle of the drying tunnel (Sartorius Cubis, Gottingen, Germany).

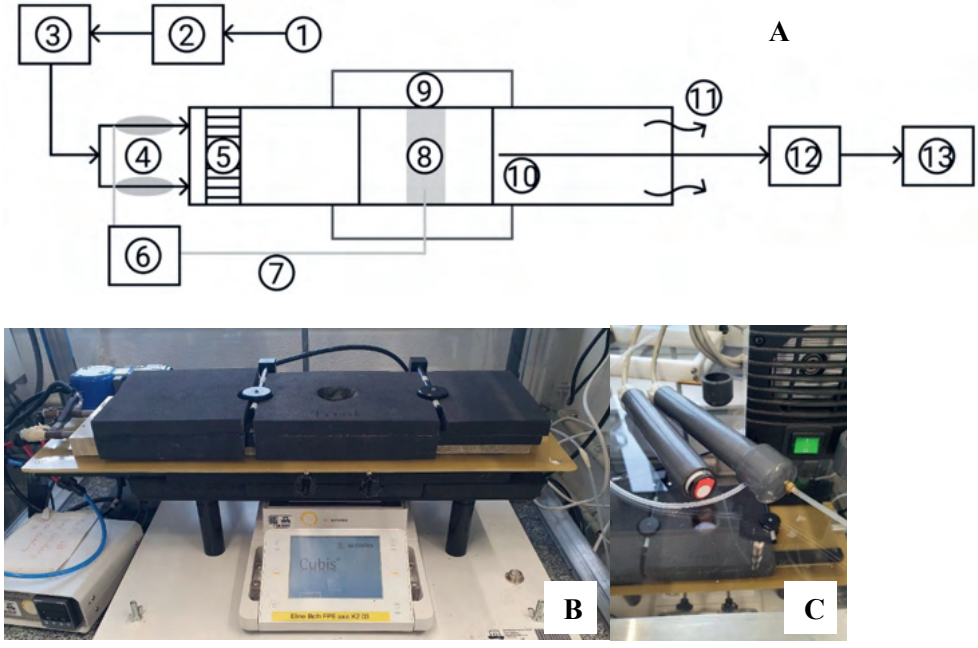

Figure 5.1 Thin film dryer (TFD) and photo-ionisation detector (PID) with (A) schematic top view, (B) TFD set-up, and (C) the PID sensor. With, (1) air inlet, (2) flow regulator, (3) dehumidifier and carbon filters, (4) heating element, (5) metal sieve for air distribution (6) temperature controller, (7) temperature sensor, (8) sample tray, (9) mass balance, (10) air inlet for PID, (11) air outlet TFD, (12) flow regulator PID and (13) PID.

For the preparation of different maltodextrin-acetone mixtures, the maltodextrins were first dissolved in water at concentrations ranging from 20 to 40 % (w/w) and stirred for at least 30 min at room temperature until a clear solution was obtained. Subsequently, acetone was added to the solution at 0.005 % (v/v) and the solution was gently agitated for approximately 30 s to dissolve the acetone. Acetone in water was used as reference material. The initial volume was 2 ml, resulting in an initial film thickness of 0.6 mm. Films were dried in the thin film dryer for 1 h. The weight of the film was recorded every 10 s, together with either the PID response or the temperature of the film during drying. The weight of the film during drying was used to calculate the water evaporation rate. The release of acetone was measured by sampling the outgoing air at 7 cm behind the thin film using a MiniPID 2 HS (Ion Science Ltd, Fowlmere, UK). During the first 5 min of drying, the acetone concentration was

measured every 3 s, followed by every 6 s for the remaining drying time. The acetone concentration (ppb) was plotted versus time and the total acetone release was determined from the area underneath the curve. The acetone release from water was used as reference for 100 % acetone release.

5.2.4. Spray drying

The same acetone-in-maltodextrin solutions were prepared as described in section 5.2.3 and were spray-dried using the Büchi B-290 mini spray dryer (Büchi Labortechnik AG, Flawil, Switzerland). The inlet temperature was 180 °C and the feed flow rate was 0.9 mL/min. The outlet temperature was controlled through the air flow rate to reach 105 °C, which was identical to the thin film drying temperature. The powders were collected at the outlet of the spray dryer and airtight packed and stored at -20 °C until further analysis.

5.2.5. Acetone content in thin films

The acetone retained in both the thin film- and spray-dried samples was quantified using DNPH as a derivatizing agent and detection with HPLC, based on methods described by Cardoso et al. (2003) and Kalkan et al. (2016). The initial acetone concentration (i.e. 0.005% (v/v)) was used as reference to calculate the acetone retention after drying. For every sample, 0.1 g of the thin films or spray-dried powders were dissolved in 0.4 mL water and added to 0.6 mL of 0.3 % (w/v) DNPH in 3 M HCl. The residual moisture contents of the dried films were considered neglectable based on the drying kinetics. The residual moisture contents of the spray-dried powders were analysed by overnight drying at 105 °C and the acetone content was corrected correspondingly. To prevent crystallisation of the acetone-DNPH derivatives, 0.4 mL acetonitrile was added. Acetone was quantified by HPLC (Thermo Ultimate 3000 HPLC, ThermoFisher Scientific, Waltham, USA) using a Gemini 3µm C18 (150 × 4.6 mm) column (Phenomenex, Torrance, USA). The column was operated at 30 °C and connected to a UV-Vis DAD detector that detected acetone-DNPH derivatives at 365 nm. A ratio of 3:7 water and methanol/acetonitrile (8:2) was used as eluent at a flow rate of 1 mL/min. A calibration curve was made by dissolving acetone in 0.4 mL water at concentrations from 0.0001 to 0.015 mL/L following the same sample preparation procedure.

5.2.6. Modelling

The water evaporation and acetone release during drying are described by a mechanistic model. We initially considered the system as a binary system of maltodextrin dissolved in

water since the acetone concentration is very low compared to the other components. The continuity equation of our system is:

$$\frac{\partial \phi_w}{\partial t} = -\frac{\partial \tilde{J}_w}{\partial z} \tag{5.2}$$

In which $\tilde{J}_w$ is the 'laboratory fixed frame of reference' flux of water: measured relative to the supporting platform. Since water is lost and we lose volume, the surface of the layer itself is moving inwards. We can define the velocity of the diffusing water relative to that of maltodextrin, u_w, via

$$u_w = \tilde{u}_w - u_s \tag{5.3}$$

In which u_i is the velocity of a component being either water or solid. Since the volume flux is equal to the velocity times the volume fraction ϕ_i, we can also define the volume flux of water relative to the volume flux of the maltodextrin,

$$\frac{J_w}{\phi_w} = \frac{\tilde{J}_w}{\phi_w} - \frac{J_s}{\phi_s} \rightarrow J_w = \tilde{J}_w - \left(\frac{\phi_w}{\phi_s}\right)\tilde{J}_s \tag{5.4}$$

Combination of equations 5.2 and 5.4 gives us:

$$\frac{\partial J_w}{\partial z} = -\phi_s \frac{\partial}{\partial t}\left(\frac{\phi_w}{\phi_s}\right) - \tilde{J}_s \frac{\partial}{\partial z}\left(\frac{\phi_w}{\phi_s}\right) \tag{5.5}$$

We can now find the flux of the water relative to the solids (which on the surface is equal to the motion of the surface) if we follow Hartley & Crank (1949) in converting z with the help of

$$m = \int_0^z \phi_s dz \;\; or \;\; \partial m = \phi_s \partial z \tag{5.6}$$

We then use the following conversions

$$\left(\frac{\partial J_w}{\partial z}\right)_t = \phi_s \left(\frac{\partial J_w}{\partial m}\right)_t$$

$$\phi_s \left(\frac{\partial}{\partial t}\left(\frac{\phi_w}{\phi_s}\right)\right)_m = \phi_s \left(\frac{\partial}{\partial t}\left(\frac{\phi_w}{\phi_s}\right)\right)_z + \phi_s \left(\frac{\partial}{\partial t}\left(\frac{\phi_w}{\phi_s}\right)\right)_t \left(\frac{\partial z}{\partial t}\right)_m \tag{5.7}$$

$$\tilde{J}_s = \phi_s \left(\frac{\partial z}{\partial t}\right)_m$$

in our equation (5.5), which results in a continuity equation that is now defined in a system with a fixed spatial coordinate, *m*:

$$\left(\frac{\partial J_w}{\partial m}\right)_t = -\left(\frac{\partial}{\partial t}\left(\frac{\phi_w}{\phi_s}\right)\right)_m \tag{5.8}$$

The flux equation can also be converted to the new spatial coordinate:

$$J_w = -D_{ws}\frac{\partial \phi_w}{\partial z} = -\phi_s D_{ws}\frac{\partial \phi_w}{\partial m} \tag{5.9}$$

Which, combined with the continuity equation (5.8) gives:

$$\frac{\partial}{\partial t}\left(\frac{\phi_w}{\phi_s}\right) = \frac{\partial}{\partial m}\left(\phi_s D_{ws}\frac{\partial \phi_w}{\partial m}\right) \tag{5.10}$$

This relation gives us the diffusion of water in the film and is invariant to the reduction in volume: a reduction of the volume at location *m* is accompanied by exactly the same increase in the concentration of the solids. Thus, m is invariant to shrinkage.

Since $\phi_s \approx 1 - \phi_w$, we can simplify the relation a bit further into

$$\frac{\partial \phi_w}{\partial t} = (1-\phi_w)^2\frac{\partial}{\partial m}\left(\phi_s D_{ws}\frac{\partial \phi_w}{\partial m}\right) \tag{5.11}$$

One boundary condition is set by the impermeability of the supporting platform:

$$J_{w,M} = -\phi_s D_{ws}(\phi_w, T)\left(\frac{\partial \phi_w}{\partial m}\right)_{m=M} = 0 \tag{5.12}$$

The other boundary condition arises at the interface with the air: diffusive mass transfer of water towards the interface should be matched with the convective evaporation of water from the interface at the gas phase side (v_w is the molecular volume of liquid water, $18 \cdot 10^{-6} m^3/mol$):

$$J_{w,m=0} = k_w v_w\left(\frac{p_w^{int}}{RT^{int}} - \frac{p_w^{\infty}}{RT^{\infty}}\right) \tag{5.13}$$

With k_w the mass transfer coefficient is given by a Sherwood relation. If we assume that the drying air has zero humidity, the equation changes to:

$$J_{w,m=0} = \frac{k_w v_w p_w^{int}}{RT^{int}} \tag{5.14}$$

Furthermore, we calculate the temperature of the film by the heat transfer coefficient. We assume that all heat is provided by the air and that the heat is quickly and homogeneously distributed over the whole film. The temperature changes because of the evaporation, but

also because of convective heating from the air with temperature T^{∞} and heat exchange with the supporting platform having temperature T_{sp}:

$$\rho Z c_{p,dr} \frac{dT}{dt} = h(T^{\infty} - T) + h_p\left(T_{sp} - T\right) + \Delta h_{ev} J_{w,0} \tag{5.15}$$

The release of the flavour (acetone, index *a*) involves true ternary diffusion, through a matrix that consists of water and maltodextrin. We assume a similar continuity equation as with water:

$$\frac{\partial}{\partial t}\left(\frac{\phi_a}{\phi_s}\right) = -\frac{\partial J_a}{\partial m} \tag{5.16}$$

Since $\phi_s \approx 1 - \phi_w$, we get after some rearrangement

$$\frac{\partial \phi_a}{\partial t} = -(1 - \phi_w)\frac{\partial J_a}{\partial m} - \frac{\phi_a}{(1 - \phi_w)}\frac{\partial \phi_w}{\partial t} \tag{5.17}$$

The first term on the right-hand side of the equation sign represents the normal diffusional flux term; the second term corrects for the increase in concentration that results from the shrinkage of the film due to the water evaporation.

The diffusion in this case is truly ternary. The acetone motion is slowed down by the maltodextrin that is retained but is dragged along with the evaporating water. The standard description of multicomponent mass transfer according to the Maxwell-Stefan framework is

$$\frac{d\mu_i}{dz} = -\sum_{j \neq i} R_{ij} c_j \left(\tilde{u}_i - \tilde{u}_j\right) \tag{5.18}$$

With μ_i the chemical potential of component *i*, c_i the concentration, R_{ij} the frictional coefficient between components *i* and *j*, and $\tilde{u}_i$ the absolute velocity of components *i*. For acetone (a) in a mixture of maltodextrin (s) and water (w), this translates to

$$\frac{d\mu_a}{dz} = -R_{as} c_s (\tilde{u}_a - \tilde{u}_s) - R_{aw} c_w (\tilde{u}_a - \tilde{u}_w) \tag{5.19}$$

In this, $\tilde{u}_i - \tilde{u}_s = u_i$, is the motion relative to the solids fixed frame of reference (see equation 5.3), so

$$\frac{d\mu_a}{dz} = -R_{as} c_s u_a - R_{aw} c_w (u_a - u_w) = -(R_{as} c_s + R_{aw} c_w) u_a + R_{aw} c_w u_w \tag{5.20}$$

As the volume fluxes are given by $J_i = \phi_i u_i$, we can convert this to

$$\phi_a \frac{d\mu_a}{dz} = -(R_{as}c_s + R_{aw}c_w)J_a + R_{aw}c_w \frac{\phi_a}{\phi_w} J_w \tag{5.21}$$

Expressing the driving force in volume fractions gives

$$\frac{d\mu_a}{dz} \approx \frac{RT}{\gamma_a x_a}\frac{d\gamma_a x_a}{dz} = \frac{RT}{n_a}\frac{dn_a}{dz} = \frac{RT}{\left(\frac{\bar{v}_a n_a}{V_T}\right)}\frac{d\left(\frac{\bar{v}_a n_a}{V_T}\right)}{dz} = \frac{RT}{\phi_a}\frac{d\phi_a}{dz} \tag{5.22}$$

We here assumed that the flavour is so dilute, that the activity coefficient γ_a is at least constant. And with $c_w = n_w/V_T = \bar{v}_w n_w/\bar{v}_w V_T = \phi_w/\bar{v}_w$,

$$\begin{aligned} \frac{d\phi_a}{dz} &= -\left(\frac{R_{as}}{RT}\frac{\phi_s}{\bar{v}_s} + \frac{R_{aw}}{RT}\frac{\phi_w}{\bar{v}_w}\right)J_a + \frac{R_{aw}}{RT}\frac{\phi_a}{\bar{v}_w}J_w \\ \rightarrow J_a &= -\left(\frac{R_{as}}{RT}\frac{\phi_s}{\bar{v}_s} + \frac{R_{aw}}{RT}\frac{\phi_w}{\bar{v}_w}\right)^{-1}\left(\left(\frac{d\phi_a}{dz}\right) - \frac{R_{aw}}{RT}\frac{\phi_a}{\bar{v}_w}J_w\right) \end{aligned} \tag{5.23}$$

The diffusion coefficient $D_{ij}$is defined as $v_j RT/R_{ij}$, so

$$J_a = -\left(\frac{\phi_s}{D_{as}} + \frac{\phi_w}{D_{aw}}\right)^{-1}\left(\phi_s\left(\frac{d\phi_a}{dm}\right) - \frac{\phi_a}{D_{aw}}J_w\right) \tag{5.24}$$

We now simplify the relation through

$$J_a = -\phi_s D_a\left(\frac{d\phi_a}{dm}\right) + \phi_a\frac{D_a}{D_{aw}}J_w \; with \; D_a = \left(\frac{\phi_s}{D_{as}} + \frac{\phi_w}{D_{aw}}\right)^{-1} \tag{5.25}$$

Should J_w be zero, then the equation collapses into the normal diffusion equation. Therefore, the second term is the drag resulting from the water that is diffusing out.

D_a is here in effect the diffusion coefficient of acetone in the mixture of water and maltodextrin. D_a is adapted from Menting et al. (1970) who experimentally determined the acetone diffusion coefficient in a maltodextrin-water system at 21.5 °C for different solute concentrations. The equation is extended with the temperature dependence based on the Arrhenius equation. It was not specified which DE of maltodextrin was used in this study.

$$D_a = \mathrm{A} \cdot \exp\left(\frac{-\mathrm{B}}{\sqrt{C_w}}\right) \cdot \exp\left(-\frac{E}{R} \cdot \left(\frac{1}{T} - \frac{1}{293}\right)\right) \tag{5.26}$$

With, A is $2.1 \cdot 10^{-5}$ m^2/s and B is 308 $(kg/m^3)^{1/2}$ as constants obtained through fitting and C_w is the moisture content in kg/m^3. The diffusion coefficient of acetone in just water, D_{aw} is found from the same equation, using $C_w = 1000$ kg/m^3.

The diffusion coefficient of water in a water-maltodextrin system was described by following the generalised Darken as proposed by Siemons et al. (2019), which combines the self-diffusion of maltodextrin and self-diffusion of water. The self-diffusion of carbohydrate molecules is predicted using the generalized Stokes-Einstein relation. The self-diffusion coefficient of water in a maltodextrin system is predicted using the free-volume theory. An extensive description of the equations used for the diffusion coefficients, and mass and heat transfer coefficients can be found in the appendix.

The total set of equations is solved using a simply forward-time centred solution strategy in MathCad Prime using 16 digits, with a time step that was small enough to not influence the results.

5.3. Results and discussion

5.3.1. Characterization of maltodextrins

The molecular weight distributions of the different DE maltodextrins used in this study were obtained using HPLC (Fig. 5.2). Maltodextrin DE12 contains more high molecular weight polymers than maltodextrin DE21 given the higher peak around an elution time of 6-6.5 min. Whereas, DE21 gives a higher response after 8.5 min, indicating that DE21 contains more low molecular weight polysaccharides. The molecular weight distributions of DE12 and DE21 are in line with previous research on maltodextrins (Avaltroni et al., 2004; Castro, Durrieu, Raynaud, & Rouilly, 2016; Siemons, Politiek, et al., 2020).

The T_g of the maltodextrins was determined at two different moisture contents (Fig. 5.3) and the Couchman-Karasz equation (5.1) was used to determine the anhydrous T_g of maltodextrin ($T_{g,s}$). The $T_{g,s}$ of DE12 (172 °C) and DE21 (140 °C) were somewhat higher in this study than in the work of Siemons et al. (2020). This could possibly be related to batch-to-batch variation.

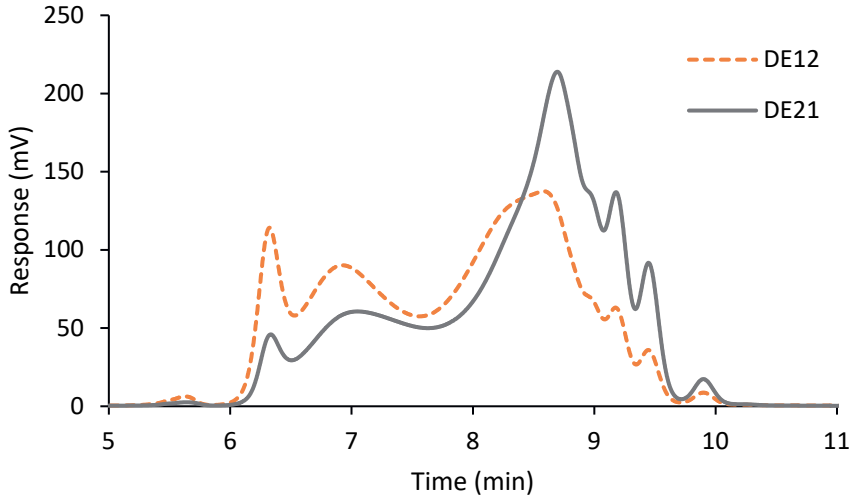

Figure 5.2 Molecular weight distribution of maltodextrins DE12 and DE21. Polymers with a higher molecular weight elute first, followed by low molecular weight polymers. Maltotriose (Merck, Darmstadt, Germany) was used as reference and had an elution time of 9.2 min.

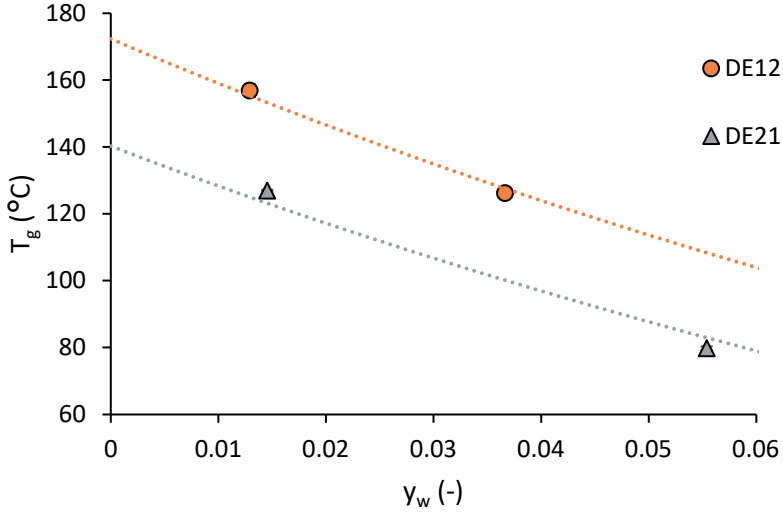

Figure 5.3 Glass transition temperature (T_g) of maltodextrins with different DEs as function of the moisture fraction of the samples. Dotted lines are the model predictions based on the Couchman-Karasz equation (orange: D12, grey: DE21). The error bars represent the standard deviation of the experimental data (n = 2).

5.3.2. Drying kinetics

The drying kinetics of water and maltodextrin solutions are shown in Fig. 5.4. The drying rate of DE21 is slightly higher than of DE12, which could be related to the lower viscosity of DE21 compared to DE12 (Siemons, Politiek, et al., 2020), thereby increasing water diffusion rates to the surface. From the water evaporation rates, no clear constant drying rate period can be detected as it continuously declines, although in the first 10 min for 20 % solids the decline is less strong. The absence of a clear constant rate period was also observed by Both et al. (2019) and was attributed to the spatial distribution of the drying behaviour along the film length, and due to equilibration of the temperature of the film.

The film temperature and mass were plotted over time for maltodextrin DE12 at 20 and 40 % initial solids (Fig. 5.5). During the first minutes of drying, the temperature of both films settles at a temperature a bit above the wet bulb temperature due to the conductive heat transfer from the supporting platform. For 40 % DE12, the temperature does not show a plateau thereby shwoing the absence of a clear constant rate period. For 20 % DE12, a constant temperature is visible between ~ 5 and 15 min showing that there is a constant rate period present even though this is only partially reflected in the evaporation rates. Based on the temperature profiles, the onset of skin formation, also referred to as the 'locking point', was determined and indicated by the dashed lines. The locking point at 40 % was much earlier than at 20 % for the DE12 thin films. Siemons, Vaessen, et al. (2020) also found that the locking points were earlier for higher initial solids contents during single droplet drying of different maltodextrin solutions. The skin formation is associated with the increase of viscosity at the surface of the film and the viscosity is positively correlated to the concentration. At the locking point of maltodextrin DE12 (Fig. 5.5), the corresponding solid contents were 55 and 51 % (w/w) at 20 and 40 % initial solids, respectively. These values are in line with the critical concentration of 50 % (w/w) for whey protein-maltodextrin (DE12) solutions as proposed by Both, Siemons, et al. (2019) during single droplet drying. We did not determine the locking points for DE21 thin films. Siemons, Politiek, et al. (2020) found that the locking point time during single droplet drying is longer for DE21 than DE12, which is related to the lower viscosity and higher solute diffusivity of DE21 solutions. Towards the end of drying, the temperature is around 75 °C, which is still far away from the drying air temperature of 105 °C. This may be due to heat losses in the TFD as it could not be perfectly insulated.

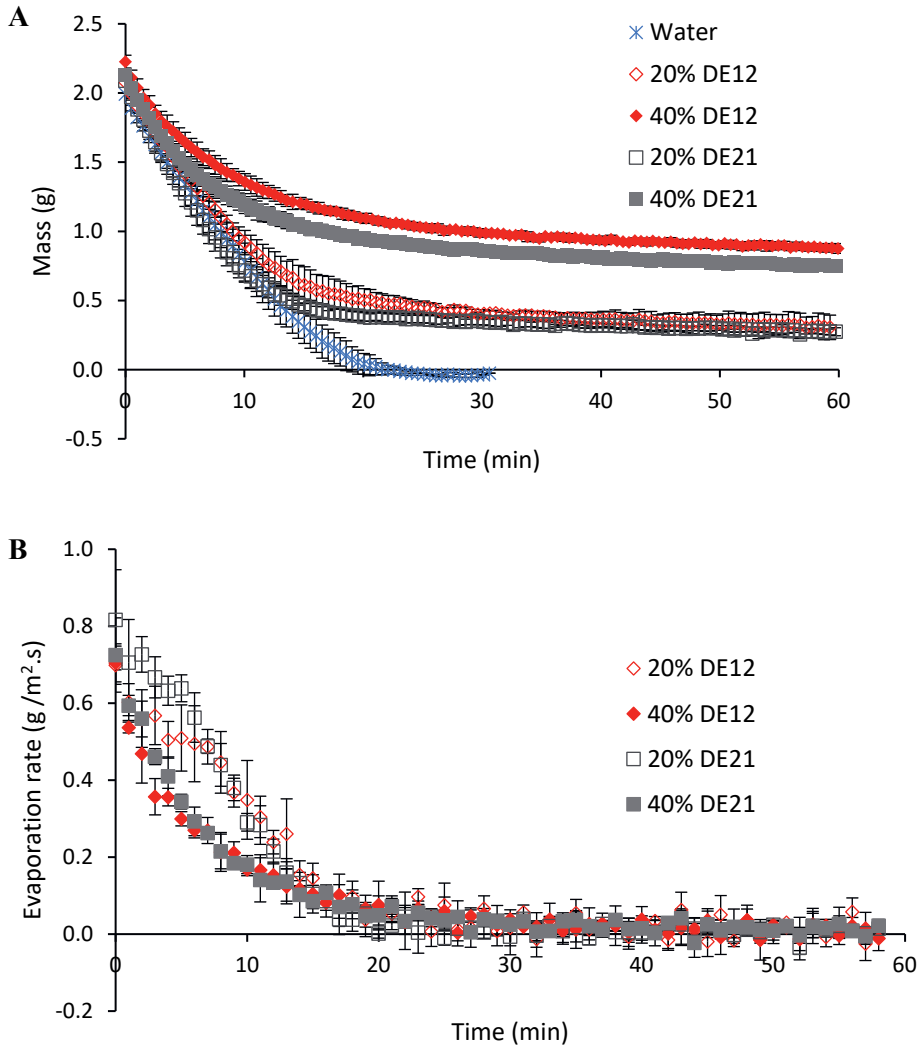

Figure 5.4 Drying kinetics of thin films prepared with maltodextrin with different DEs and 20 or 40 % initial solids content. The films had an initial thickness of 0.6 mm and were dried at 105 °C and 1 m/s air flow. (A) The mass decrease over time. (B) The evaporation rate (g/m^2·s) over time. A moving average is used over 6 data points. The error bars represent the standard deviation of the experimental data (n = 3).

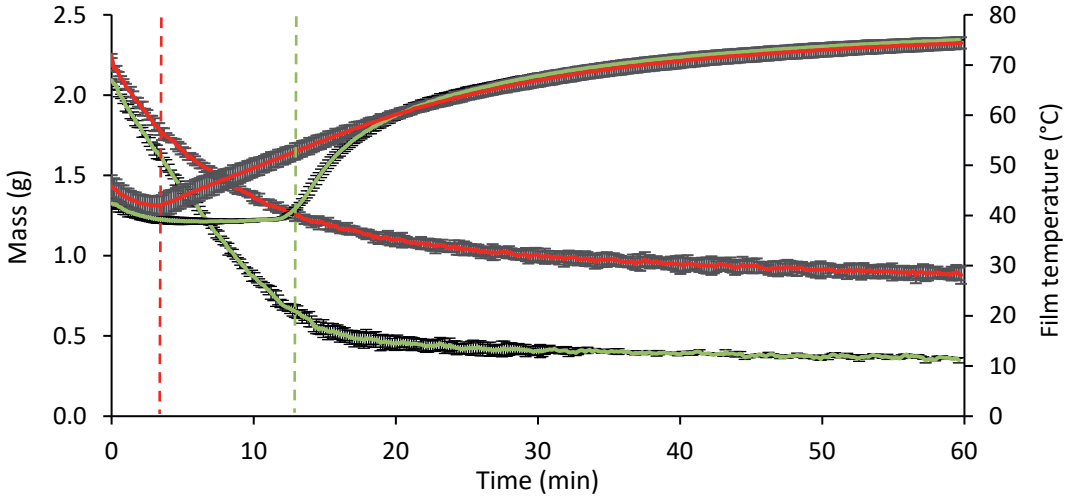

Figure 5.5 Drying kinetics of thin films, with mass decrease (left) and film temperature (right) over time. With 20% maltodextrin DE12 (green) and 40% maltodextrin DE12 (red) and the dashed lines indicate the locking points (i.e. skin formation) for both films. The films had an initial thickness of 0.6 mm and were dried at 105 °C and 1 m/s air flow. The error bars represent the standard deviation of the experimental data (n = 2).

5.3.3. Acetone release during drying

The acetone release during drying was measured by PID for 20 % (Fig. 5.6A) and 40 % (Fig. 5.6B) initial solids. Only the first 10 min are shown as no further acetone release was detected afterwards. For water, the acetone release approaches zero after 8 min of drying and it can be assumed that all acetone is released at this point. Surprisingly, the release from 20 % DE21 during the first minutes of drying is higher than from water (Fig. 5.6A), which cannot be explained directly. Later the response of DE21 drops below that of both water and DE12 as most acetone was probably already released. Furthermore, a second peak is visible for both DE12 and DE21, which is absent in the graph of water. We cannot explain the mechanism responsible for this second peak. The evaporation rate of DE12 is lower than that of DE21 (Fig. 5.4B), which could explain why less acetone is released in the first minutes of drying as acetone could be dragged along by the outgoing water flux. The acetone release from the 20 % films (Fig. 5.6A) approaches zero after 5-7 min, while according to the temperature profile (Fig. 5.5), the falling rate period commences after +/- 13 min. This suggests that the 20 % films could not form a skin quick enough to show a significant effect on acetone

retention, thus skin formation is not the mechanism responsible for encapsulation of acetone in the 20 % films.

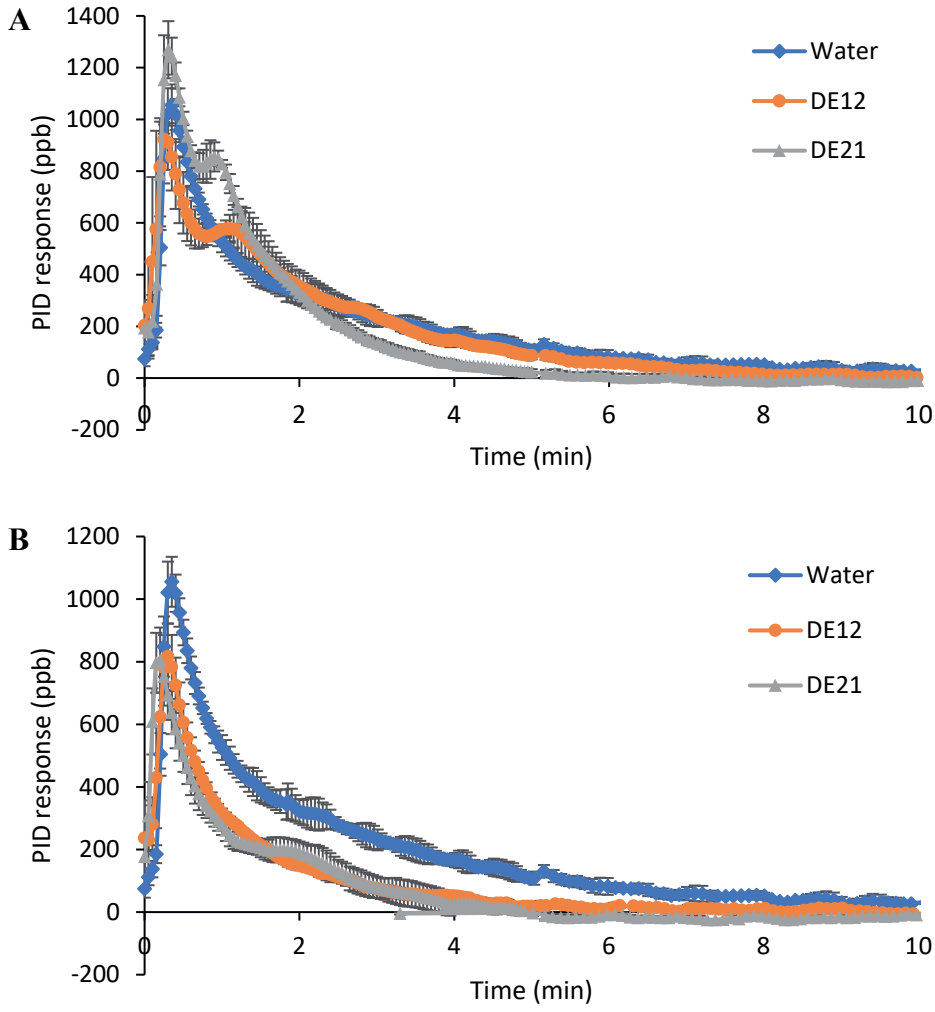

Figure 5.6 Acetone release during the first ten minutes of drying thin films containing 0.005 % acetone and maltodextrins with different DEs at an initial solids content of (A) 20 % and (B) 40 % as measured with a photo-ionisation detector. Acetone in water was used as reference. The films had an initial thickness of 0.6 mm and were dried at 105 °C and 1 m/s air flow. The error bars represent the standard deviation of the experimental data (n = 3).

Apart from concentration effects during drying, chemical interactions between maltodextrin and the VOC can affect the release profile as well. Siccama et al. (2021) found that the 1-octen-3-ol content in the headspace decreased with an increase in maltodextrin DE12 content in the liquid phase due to complexation. Acetone also interacts maltodextrin and, interestingly, the interactions decreased by lowering the DE from 61.5 to 20 (0.1 to 0.05 g/100 g db), whereas acetone interaction with glucose was much less than with starch, (0.1 and 4.4 g/100 g db, respectively) (Le Thanh, Thibeaudeau, Thibaut, & Voilley, 1992). The effect for the lower DE maltodextrins (e.g. DE10-12) was not investigated, thus we cannot translate this to the DE12 used in this study. The complexation of acetone by maltodextrin is likely attributed to two mechanisms. Firstly, the linear chains of maltodextrins can form helical complexes and thereby bind hydrophobic molecules (Madene et al., 2006; Wangsakan, Chinachoti, & McClements, 2003). Secondly, hydrogen bonds can be formed between the carbohydrate, water and acetone, as also suggested by Le Thanh et al. (1992). Acetone has a single proton-accepting carbonyl group that can form hydrogen bonds with proton-donating groups of carbohydrates and water (Chan, Chan, Tang, & Chang, 2018). It is plausible that both hydrophobic bonding and hydrogen bonds affect the acetone release during the constant rate period of drying.

For the 40 % films, the acetone release profiles of DE12 and DE21 are similar (Fig. 5.6B) and the PID response is much lower compared to the 20 % films (Fig. 5.6A). This can be related to the lower diffusion rates of acetone as it is dependent on the solute concentration, as illustrated in equation 5.26. The initial acetone diffusion coefficient for the 40 % films is already more than 5 times smaller than for 20 % based on this equation. In addition, interactions between acetone and maltodextrin are expected to increase at higher maltodextrin concentrations. The acetone release of samples with 40 % solids approaches zero after 4 min of drying (Fig. 5.6B). This can be related to the formation of the skin that is impenetrable for acetone and the residual acetone is thus retained. This is in line with the temperature profile of 40 % DE12 (Fig. 5.5), as the locking point is located at around 4 min. In addition, the area under the graph of the 40 % films is much smaller than that of water, hence acetone must be partly retained.

In Fig. 5.7, the acetone release for maltodextrin DE12 samples with different initial solid contents, i.e. 20, 25, 30 and 40 %, are plotted. The acetone release decreases with an increase in initial solids content. This is in line with the earlier statement that the acetone diffusion

rate is dependent on the solute concentration. Furthermore, the point where the release approaches zero comes earlier for higher initial solid contents, which can be linked to quicker skin formation (Siemons, Vaessen, et al., 2020).

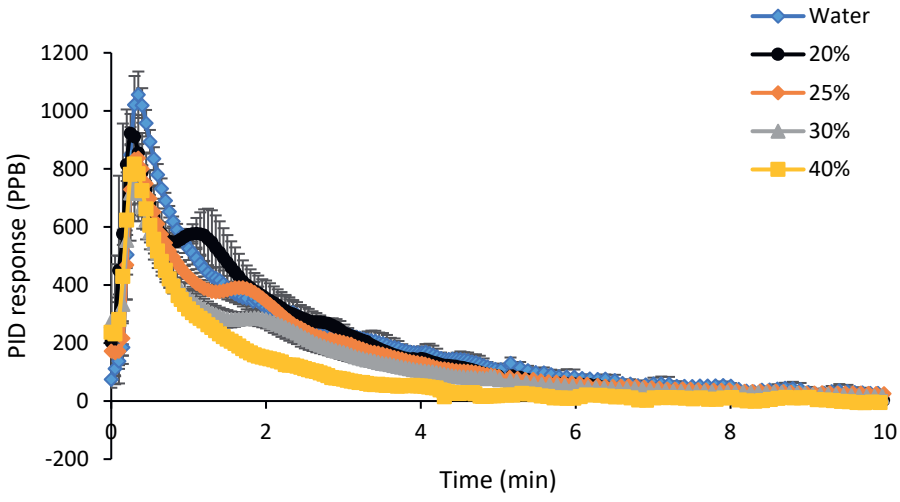

Figure 5.7 Acetone release during the first ten minutes of drying thin films containing 0.005 % acetone and maltodextrin DE12 with different initial solids content as measured with a photo-ionisation detector. The films had an initial thickness of 0.6 mm and were dried at 105 °C and 1 m/s air flow. The error bars represent the standard deviation of the experimental data (n = 3).

5.3.4. Acetone retention after drying

Two methods were applied to determine the overall acetone retention of the dried thin films. In the first method, we calculated the acetone content with the area underneath the PID response graphs based on the first 10 min of drying. The retention is calculated by comparison to the area under the PID response graph of water since it was assumed that no acetone was retained after drying the acetone-water solution, using the following equation:

$$Acetone\ retention\ (\%) = \left(1 - \frac{PID\ area\ MD}{PID\ area\ water}\right) \cdot 100 \tag{5.27}$$

In the second method, we determined acetone retention by quantifying the acetone content with HPLC (section 5.2.5). The initial solids content is positively correlated with the acetone retention for all samples (Fig. 5.8). For all 20 % films, no acetone was detected by HPLC. Furthermore, the acetone retention determined by the area under the graph is consistently

higher than with HPLC. Part of the acetone may already have evaporated before the drying process, which would lead to a slight underestimation of the acetone retention by HPLC, even though the films were dried as quickly as possible after acetone dissolution. For the HPLC results, the 40 % DE12 film is significantly higher in acetone compared to DE21. This is in agreement with others who found higher volatile retention for DE10-12 compared to DE20-22 (Bangs & Reineccius, 1982; Raja et al., 1989). However, the PID results indicate higher retention in DE21 films. The calculation of the area underneath the graph may be susceptible to small variations, given the standard deviations of the data points in Fig. 5.6. Therefore, the current PID results are more of qualitative nature. Increasing the acetone concentration is not feasible as we would quickly reach the upper detection limit of the device (2000 ppb). Alternatively, we could use a less sensitive PID sensor, which will also limit potential background noise. However, higher acetone concentrations will not be representative of the volatiles concentrations in food systems and may also change the interactions and activities in the systems (for example with water).

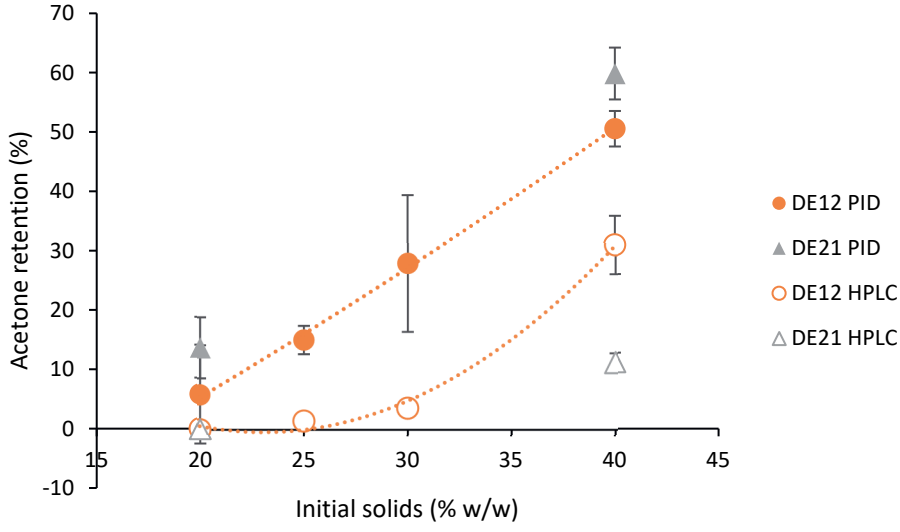

Figure 5.8 Acetone retention in maltodextrin thin films with DE12 and DE21 after 1 h of drying at 105 °C and 1 m/s air flow. Closed symbols indicate overall retention based on in-line PID measurements (n = 3) and open symbols indicate the retention of acetone quantified by HPLC (n = 2). The error bars represent the standard deviation of the experimental data. The dotted lines are drawn to guide the eye. For the samples with 20 % initial solids, no acetone was detected by HPLC for DE12 and DE21.

In addition to the TFD measurement, the same materials were dried in a lab-scale spray dryer and the overall acetone retentions were analysed with HPLC (Table 5.1). For both dryers, no acetone could be detected in the dried 20 % materials. Both TFD and spray drying resulted in higher retention for DE12 compared to DE21. However, the acetone retention measured in the TFD samples was consistently higher. The drying conditions were kept as similar as possible for both dryers, e.g. the outlet temperature of the spray dryer (105 °C) was the same as the drying temperature of the TFD. However, the film temperature never exceeded 75 °C, whereas for the spray dryer the product temperature usually approaches the outlet temperature at the exit. In addition, the spray drying feed was exposed to a high inlet air temperature of 180 °C leading to an initial higher acetone evaporation rate than during TFD. Furthermore, the surface-to-volume ratio in the lab-scale spray dryer is much larger since 2 mL results in 0.48 m^2 of total surface area (droplets of ~ 25 µm), whereas for the TFD this is only 0.0036 m^2. It should be noted that the droplet size in an industrial spray dryer is around 100 µm, reducing the droplet's surface-to-volume ratio by factor 4 (as surface area scales quadratically and volume scales to the power 3). Rulkens & Thijssen (1972) determined the acetone retention of spray-dried maltodextrin DE20 solutions and retained 21 and 30 % of acetone with 35 and 44 % initial solids at an inlet temperature of 235 °C (outlet temperature not reported). This retention is higher than found for spray-dried DE21 in this work. It should be noted that a bigger spray dryer was used in their study, i.e. drying chamber with 2 m inner diameter, which creates larger droplets (droplet size not reported) and hence volatile retention is higher (Rulkens & Thijssen, 1972).

Table 5.1 Acetone retention after thin film drying and spray drying of maltodextrin solutions prepared with DE12 and DE21. The data is presented as mean ± standard deviations (n = 2). The letters (a-b) indicate significant differences between the thin film-dried and spray-dried samples based on an independent T-Test (significant p-value < 0.05). For the 20 % w/w samples no acetone was detected for both DE12 and DE21.

Maltodextrin	Initial solids content (% w/w)	Thin film dryer Acetone retention (%)	Spray dryer Acetone retention (%)
DE12	40	30.98 ± 1.53 [a]	23.96 ± 3.71 [a]
DE21	40	11.28 ± 0.28 [a]	3.63 ± 0.24 [b]

We may conclude that the TFD predicted the proper qualitative trends in acetone retention during spray drying. The PID response graphs provide valuable information on the kinetics of volatile encapsulation that we cannot obtain easily in a spray dryer. The results illustrate that the length of the constant rate period is critical for acetone retention and as soon as the falling rate period commences, the residual acetone will be encapsulated. Furthermore, the release of VOCs during the constant rate period is also determined by the feed solution. Higher initial solids contents result in less release during the constant rate period. Furthermore, there were some differences observed between DE12 and DE21, specifically at lower initial solids concentrations. Less acetone was released from the DE12 solution compared to DE21, which was explained by the higher viscosity.

5.3.5. Modelling the acetone release during TFD

The acetone release during TFD was described with a mass transfer model and compared to the experimental observations. Because the model is a one-dimensional model and uses many parameters, it was not expected to provide accurate predictions but rather provide a qualitative trend. Although the acetone retention calculated with the model appears higher than the experimental data, it also shows an increasing trend in retention with increasing solids content (Fig. 5.9). We were not able to increase the initial solid content above 40 % (w/w) during the experiments as it complicates spreading the film evenly on the sample tray. At an initial solids content of 50 %, the predicted acetone retention is close to 100 %, which is in line with the solid concentration at the reported locking point of maltodextrin DE12 from the experimental data.

The difference in acetone retentions originates to considerable extent from the different drying kinetics since the start of the falling rate period is earlier in the model compared to the experimental data (Fig. 5.10) hence the dry skin is quicker formed. Once the skin is formed, there will be a rapid decrease in the acetone diffusion rate and the residual acetone will mostly be retained. For the model, we assumed that drying at the surface of the thin film is homogenous, while during experiments we observed that the film at the side of the air inlet dries somewhat quicker than at the outlet, which also made it more difficult to determine the constant rate period from the experimental data. The model indicates that the constant rate period ends after 6 min for 20 % and after 2 min for 40 %, whereas this took much longer during the experiments.

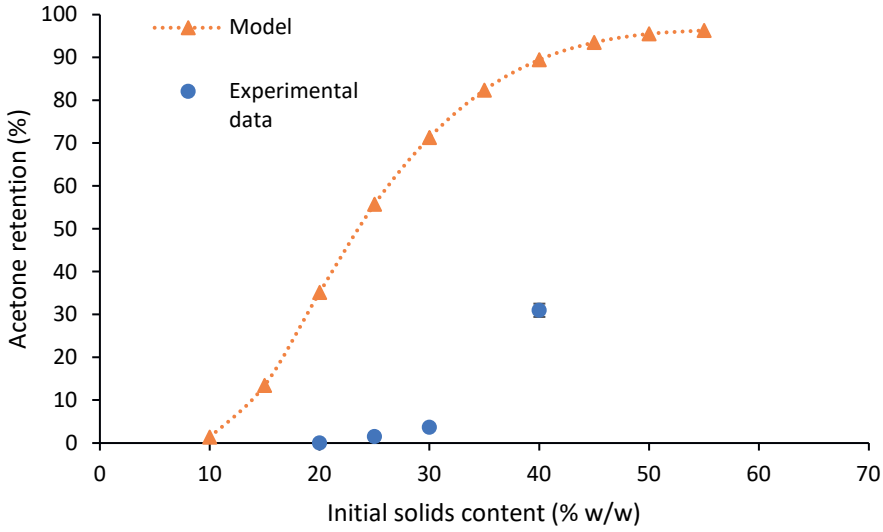

Figure 5.9 Acetone retention after thin film drying of maltodextrin DE12 solutions based on the experimental data (HPLC) and the model. The error bars represent the standard deviation of the experimental data (n = 2).

The acetone retention for 20 and 40 % maltodextrin solutions is plotted as a function of drying time (Fig. 5.11). Only the first 10 min are plotted as the acetone retention remained constant for the remaining drying time. In the beginning, acetone retention decreases rapidly, followed by a period where decrease is more gradual. Finally, the acetone retention remains constant. The rapid decrease in acetone retention only occurs during the first minute of drying. The second phase ends when the falling rate period starts and is therefore longer for the 20 % films compared to the 40 %. In the experimental data of the 20 % films, we found that all acetone is released before the constant rate period ended. When we run the model with 10 % initial solid content, we have a similar situation as most of the acetone is released during the constant rate period (data not shown) and only 1 % of acetone is finally retained. Most probably by further development of the model, the drying kinetics and acetone retention will be predicted more accurately. However, this effort was however considered beyond the scope of this study.

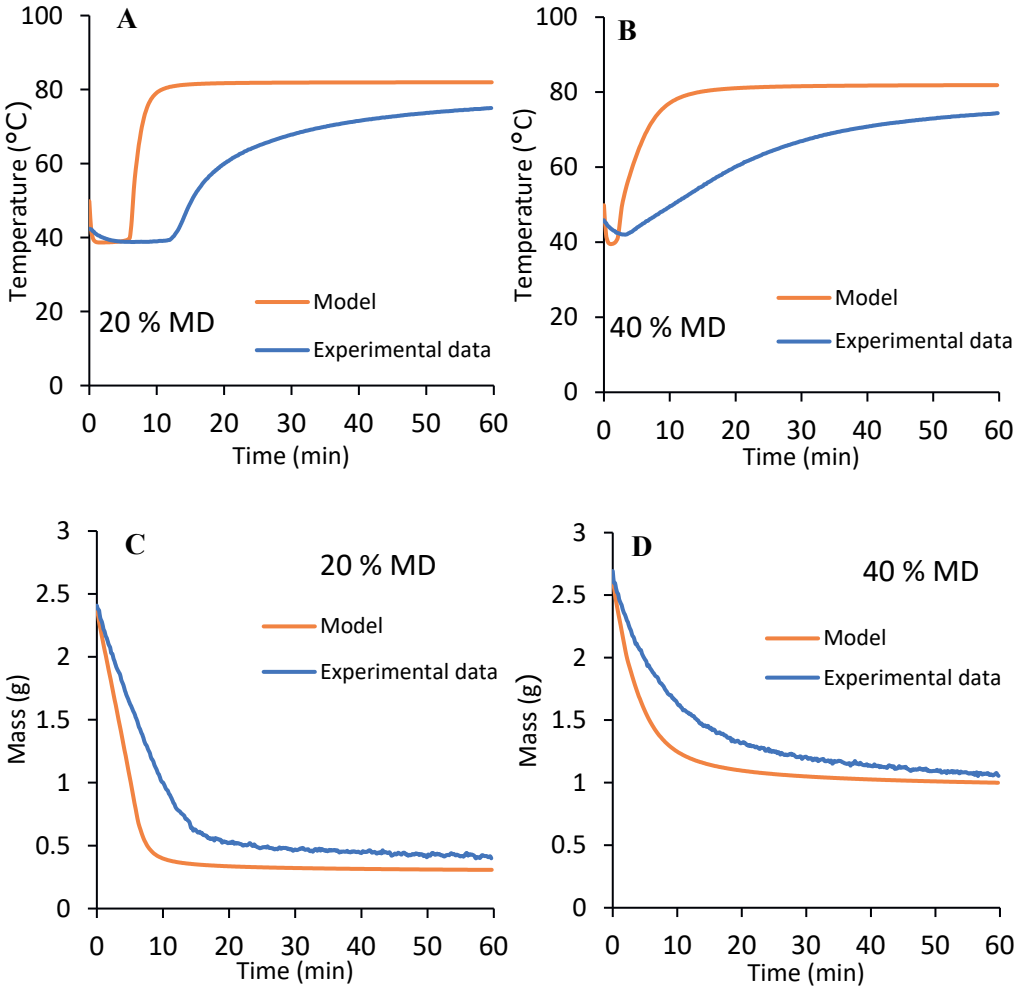

Figure 5.10 Drying kinetics of maltodextrin (MD) DE12 solutions during thin film drying based on the drying model and the experimental data. With film temperature of 20 % (A), film temperature of 40 % (B), mass decrease of 20 % (C) and mass decrease of 40 % (D).

We used this model to describe acetone release from maltodextrin DE12 solutions. However, it should be noted that DE12 might not have been the considered maltodextrin in the acetone diffusivity (equation 5.26). Hence this may have contributed to deviations between the model and experimental data. Further improvement of the model can be done by finetuning the parameters used, for example by determining the acetone diffusion in maltodextrin DE12 solutions.

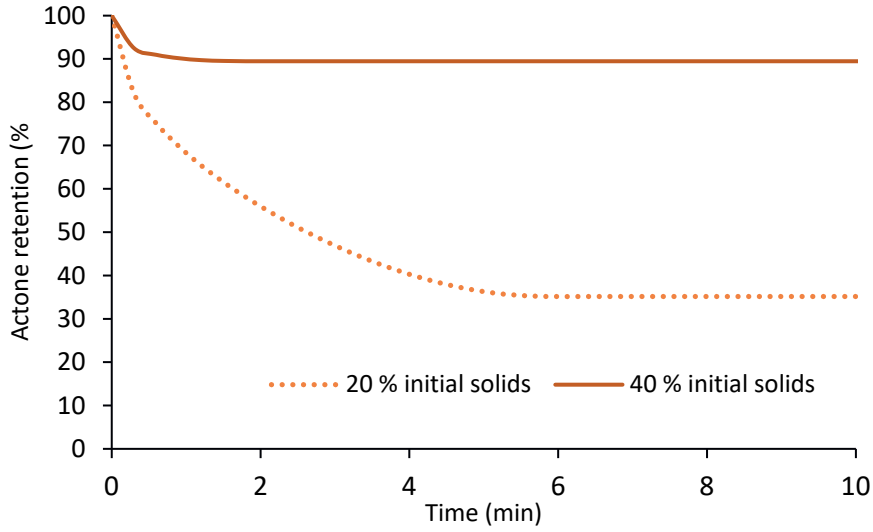

Figure 5.11 Acetone retention as function of drying time for 20 and 40 % (w/w) maltodextrin DE12 solutions obtained through modelling.

5.4. Conclusions

The influence of DE and initial solids content on drying kinetics and acetone release during thin film drying was studied. The results show that shortening the constant rate period (i.e. faster formation of the semi-permeable skin) led to higher retention of acetone in the films. Increasing the initial solid content of the film effectively reduced the release of acetone during the constant rate period (i.e. first 10 min of drying), which could be related to the lower acetone diffusivity and interactions between acetone and maltodextrin. Types of maltodextrin DE also influenced the kinetics of acetone release, but to a smaller extent. Maltodextrin DE12 resulted in less acetone release in the constant rate period compared to DE21, specifically at low initial solids content. This effect is attributed to the higher viscosity of the lower DE maltodextrin solutions. Interactions between acetone and maltodextrin may also influence the release.

Final acetone retentions calculated with the PID response were consistently higher than the HPLC data, although the overall trends were similar. We therefore suggest using the PID response to qualitatively describe the kinetics of VOC release. Acetone retention in thin films and in lab-scale spray-dried powders showed the same trend. The slightly lower acetone retention during spray drying was most likely due to the initial higher evaporation rate and

higher surface to volume ratio of the droplets. Lastly, a newly developed drying model including acetone transfer showed a strong correlation between acetone release and drying kinetics and could describe the experimental data in general terms.

This work demonstrates that the aroma release profile obtained from the PID sensor is strongly correlated to the formation of a semi-permeable low moisture skin on the surface of the thin film during drying. The TFD in combination with a PID can be used to help design formulations that facilitate aroma encapsulation and as a first screening method for spray drying.

5.5. Appendix

5.5.1. Water diffusivity in maltodextrin solutions

We assume that the concentration of flavour is so small, that it is not significant in the overall volume of the solution, and that it does not have any influence on the diffusion behaviour of water and maltodextrin (solids). The mutual diffusivity of water in maltodextrin solutions was described by following the generalised Darken relation (Darken, 1948; Krishna & Van Baten, 2005; Perdana, Van Der Sman, Fox, Boom, & Schutyser, 2013; Van Der Sman & Meinders, 2013).

$$D = \left(\phi_w D_{w,self} + (1-\phi_w) D_{s,self}\right) Q \tag{A.5.1}$$

In which D is the mutual diffusivity (m^2/s) of component w in a $w-s$ system, $D_{w,self}$ and $D_{s,self}$ (m^2/s) are the self-diffusivities of water and maltodextrin, respectively. ϕ is the volume fraction (m^3/m^3) and Q (-) is the thermodynamic factor, which is related to the derivative of the thermodynamic potential.

The thermodynamic factor can be written following the Flory-Huggins free energy function:

$$Q = (1 - 2\chi\phi_w(1-\phi_w)) \tag{A.5.2}$$

Where χ (-) is the Flory-Huggins interaction parameter between solvent and solute components, which is assumed to be composition dependent. The interaction parameter follows (Van Der Sman & Meinders, 2010):

$$\chi(\phi_w) = \chi_{sw} - (\chi_{sw} - \chi_{sw0}) \cdot \phi_w^2 \tag{A.5.3}$$

χ_{sw} is the interaction parameter of a nearly dry biopolymer ($\phi_s \approx 1$) and χ_{sw0} is the interaction parameter of a fully hydrated biopolymer ($\phi_s \approx 0$). For maltodextrins, $\chi_{sw} = 0.5$ and $\chi_{sw0} = 0.8$ as proposed by Siemons et al. (2019).

For a maltodextrin-water system, the self-diffusion of carbohydrate molecules is predicted using the generalized Stokes-Einstein relation:

$$D_{s,self} = \frac{kT}{6\pi r_H \eta_{eff}} \tag{A.5.4}$$

In which k is the Boltzmann constant, T (K) is the temperature, r_H (m) is the hydrodynamic radius of the molecules, and η_{eff} (Pa·s) is the effective viscosity. The hydrodynamic radius

is calculated from the degree of polymerization of maltodextrin DE12 following the Mark-Houwink relation (Scholte, Meijerink, Schoffeleers, & Brands, 1984):

$$r_H = \frac{a_u}{DP^{-0.49}} \tag{A.5.5}$$

DP is the degree of polymerization, $DP = 111.11/DE$ (Dokic, Jakovljevic, & Dokic-Baucal, 1998).The hard sphere radius of a monomeric subunit a_u (m) follows (Perdana et al., 2013):

$$a_u = \left(\frac{M_u}{4/3\pi N_a \rho_s}\right)^{1/3} \tag{A.5.6}$$

In which M_u is the molecular weight of the monomeric anhydroglucose unit, N_a the number of Avogadro and ρ_s the density of maltodextrin, fixed at 1550 kg/m^3.

The effective viscosity of the maltodextrin-water system is calculated by combining Spurlin-Martin-Tennent's (SMT) model and the Williams, Landel and Ferry free volume model (WLF) by using a smoothed step function (Both, Siemons, et al., 2019):

$$\eta_{eff,md} = \left(1 - \left(\frac{1}{1 + e^{-\frac{x_{md}-b}{t}}}\right)\right)\eta_{eff}^{SMT} + \left(\frac{1}{1 + e^{-\frac{x_{md}-b}{t}}}\right)\eta_{eff}^{WLF} \tag{A.5.7}$$

x_{md} is the mass fraction of maltodextrin (% w/w), b and t are fitting parameters, where b =0.45 represents the transition point from η_{eff}^{SMT} the effective viscosity as determined by SMT to η_{eff}^{WLF} the effective viscosity as determined by WLF. t is a measure of the abruptness of the transition, where t =0.03 was used as proposed by Both et al. (2019).

The self-diffusion coefficient of water in a maltodextrin system is predicted using the free-volume theory based on the work of Vrentas & Duda (1977):

$$D_{w,self} = D_0 exp\left(-\frac{E}{RT}\right) exp\left[\frac{-(m_w \tilde{V}_w^* + m_s \xi \tilde{V}_s^*)}{m_w\left(\frac{K_{1w}}{\gamma}\right)(K_{2w} - T_{g,w} + T) + m_s\left(\frac{K_{1s}}{\gamma}\right)(K_{2s} - T_{g,s} + T)}\right] \tag{A.5.8}$$

With D_0=1.48·10^{-7} is the pre-exponential factor (m^2/s), E the energy to overcome the attractive forces from neighbouring molecules, 2.34 (kJ/mol), R the gas constant (J/mol·K), T the temperature (K), $\tilde{V}_w^*$ the specific critical free volume of water, 9.1·10^{-4} (m^3/kg), $\tilde{V}_s^*$ the specific critical free volume of carbohydrates, 5.9·10^{-4} (m^3/kg), ξ the ratio of solvent and polymer jumping units, 0.79 (-). With K_{1w}, K_{2w}, K_{1s}, K_{2s} the free volume parameters, namely 1.945·10^{-6} (m^3/kg·K), -19.73 (K), 0.336·10^{-6} (m^3/kg·K) and 69.21 (K). $T_{g,w}$ is the glass transition temperature of water, 136 (K), $T_{g,s}$ is the glass transition temperature of

carbohydrates, 347 (K), and γ the overlap factor for shared free volume (between 0.5 and 1), set on 0.6 for maltodextrin. The same parameters were used as proposed by Siemons et al. (2019).

5.5.2. Mass and heat transfer coefficients

We determined relevant mass and heat transfer coefficients for the thin film dryer set-up, which were implemented in equations 5.14 and 5.15. The mass transfer coefficient is given by a Sherwood relation:

$$k_g = \frac{Sh \cdot D_{air}}{d_{tf}} \tag{A.5.9}$$

With d_{tf} the length of the sample tray, 0.04 (m), D_{air} the diffusion coefficient of water vapour in air at 100 ºC, $4 \cdot 10^{-2}$ (m^2/s), and Sh the Sherwood number for flow along a flat plate:

$$Sh = 0.664 \cdot Re^{0.5} \cdot Sc^{0.33} \tag{A.5.10}$$

With Re, the Reynolds number:

$$Re = \frac{\rho_{air} \cdot \nu_{air} \cdot d_{tf}}{\eta_{air}} \tag{A.5.11}$$

And ρ_{air} the density of air at 105 ºC, 0.934 (kg/m^3), ν_{air} the air flow rate, 1 (m/s), and η_{air} the viscosity of air at 105 ºC, $21.95 \cdot 10^{-6}$ (Pa·s).

Sc is the Schmidt number:

$$Sc = \frac{\eta_{air}}{\rho_{air} \cdot D_{air}} \tag{A.5.12}$$

The heat transfer coefficient in the thin film dryer is given by a Nusselt relation:

$$h = \frac{Nu \cdot \lambda_{air}}{d_{tf}} \tag{A.5.13}$$

With λ_{air} the heat conductivity of air at 105 ºC, 0.032 (W/m·K), and Nu the Nusselt number for heat transfer around a plate:

$$Nu = 0.664 Re^{0.5} \mathrm{Pr}^{0.33} \tag{A.5.14}$$

With Pr the Prandtl number:

$$Pr = \frac{\eta_{air} \cdot c_{p.air}}{\lambda_{air}} \quad \text{(A.5.16)}$$

With, $c_{p.air}$ the heat capacity of air at 105 ºC, 1012 (J/kg·K).

Furthermore, there is some heat exchange with the supporting platform as it is not perfectly insulated. At the beginning of the drying process, the preheated supporting platform will provide some additional heat to increase the temperature of the sample. Whereas, later in the drying process some heat will dissipate through the sample tray and lower the temperature.

$$h_p = \left(\frac{X_p}{\lambda_p} + \frac{X}{\lambda_{md}}\right)^{-1} \quad \text{(A.5.17)}$$

With, X_p the thickness of the platform, 0.005 (m), λ_p the heat conductivity of the polycarbonate layer at the platform, 0.19 (W/m·K), X the thickness of the film (m), λ_{md} the heat conductivity of the maltodextrin-water film, 0.562 (W/m·K).

Chapter 6

Metabolomics and sensory evaluation of asparagus ingredients in instant soups unveil important asparagus (off-)flavours

This chapter has been submitted as Pegiou. E. [1], Siccama, J.W. [1], Zhang, L, Mumm, R., Jacobs, D.M., Lauteslager, X.Y., Knoop, M.T., Schutyser, M.A.I, Hall, R.D. Metabolomics and sensory evaluation of asparagus ingredients in instant soups unveil important asparagus (off-flavours).

6.1. Introduction

When developing new food ingredients, an important aspect to consider is flavour. Flavour is the result of the interaction between aroma and taste and can be impacted by other attributes such as mouthfeel and visual signals. Within a metabolite profile that might consist of a few hundreds of volatile and non-volatile compounds, often only a small fraction of these is odour and flavour active. To evaluate the sensory profile of a product and to determine those compounds being relevant for sensory perception, it is necessary to combine information supplied by chemical analyses and sensory perception (e.g. odour and taste).

Instant vegetable soup is primarily composed of dried vegetable powders. Commercial vegetable powders are commonly made by oven-drying (i.e. hot-air drying) small vegetable pieces which are then milled into a fine powder (Kamiloglu et al., 2016; Karam et al., 2016). This drying process is known to irreversibly alter the flavour profile of the vegetable (Nijhuis et al., 1998; Sagar, Suresh Kumar, & Suresh Kumar, 2010). Consequently, supplementary flavour components often need to be added to the dried vegetable powders to obtain the desired sensory complexity of the final product (e.g. instant soups) and to ensure flavour stability. To produce products that are perceived as natural and healthy, the addition of these flavourings should ideally be avoided (Román et al., 2017).

A novel split-stream process has recently been developed to produce ingredients from vegetable waste streams generated during or after harvesting (Siccama, Pegiou, Zhang, et al., 2021). In this process, vegetable juice is separated from the fibre fraction and both streams are processed and dried separately, after which they can be recombined to yield vegetable powder. White asparagus (*Asparagus officinalis*) was selected as the model crop for two reasons. First, because the flavour of the commercial asparagus powders does not meet the standards of the industry and thus flavour supplements are required and second, due to the large waste volumes generated within a harvest season (ca. 30% of all harvested material). A significant part of this waste stream comprises the basal parts of each asparagus spear (ca. 5 cm) which are cut off and discarded (Pegiou et al., 2019). Within the scope of a more sustainable and circular food system, it is of interest to investigate the potential of exploiting these vegetable side-streams to generate dried powders for use as food ingredients in products such as instant soups (Siccama, Pegiou, Zhang, et al., 2021). The composition of volatile compounds of the obtained spray-dried asparagus powder has previously been investigated and it was suggested as a potential new natural food ingredient with high retention of volatile

flavour compounds (Siccama, Pegiou, Eijkelboom, et al., 2021), but yet its flavour profile still needs to be assessed concerning sensory attributes like aroma, taste and mouthfeel.

It is well-known that combining sensory evaluation and metabolomics may give a deeper insights into the flavour composition of food products (Jacobs, van den Berg, & Hall, 2021; Utpott, Rodrigues, Rios, Mercali, & Flôres, 2022). Recently, few studies have used the potential of both sensory evaluation and metabolomics for examining the flavour of food products, e.g., bell pepper (Eggink et al., 2012), apple (Aprea et al., 2012), strawberry (Buvé et al., 2018), beer (Bettenhausen et al., 2020), tomato soups (Davarzani et al., 2021) and soy sauce (Diez-Simon, Eichelsheim, Jacobs, Mumm, & Hall, 2021). There have been three studies combining sensory and metabolomics techniques to study cooked white asparagus (Dawid & Hofmann, 2012; Hoberg, Ulrich, Gottwald, & Rosen, 2003; Ulrich et al., 2001). It is thanks to these three studies that we can link specific steroidal saponins to the bitter asparagus notes (Dawid & Hofmann, 2012) and refer to several volatiles (e.g. dimethyl sulphide, 2-methoxy-3-isopropylpyrazine, hexanal) as being "key odorants" of cooked asparagus (Hoberg et al., 2003; Ulrich et al., 2001). Specifically, dimethyl sulphide (DMS), is considered to be the aroma compound giving the typical "cooked asparagus" flavour (Tressl, Bahri, et al., 1977; Tressl, Holzer, et al., 1977) and DMS is considered the aroma compound giving the typical "cooked asparagus" flavour (Ulrich et al., 2001). However, it is of relevance to confirm the contribution of the known asparagus flavour compounds to the sensory profile of the processed asparagus materials as it is likely that multiple compounds are required to give the true asparagus experience.

The main objective of the study described here was to compare the in-house processed asparagus ingredients (i.e. concentrate and spray-dried powder) to a commercial asparagus powder with and without a flavour supplement, by evaluating the flavour profile in an instant soup formulation. The soup formulations were prepared based on the composition of a commercial instant asparagus soup only differing in the asparagus ingredients. We hypothesized that the variation in the ingredient composition of the soups would be reflected by differences in both the metabolite composition and the sensory profiles. The spray-dried powder was hypothesized to have a richer flavour profile compared to the commercial powder which is oven-dried. Moreover, the asparagus fibre, which remains after the extraction of the juice from the asparagus pieces, was processed and added to some of the

soup prototypes. We hypothesized that the fibre would provide more structure and thickness to the soups, influencing the presumed mouthfeel sensation.

To investigate these hypotheses, the soup prototypes were assessed by a trained expert panel and were analysed using advanced metabolomics platforms. Solid phase microextraction gas chromatography mass spectrometry (SPME GC-MS) and liquid chromatography mass spectrometry (LC-MS) systems were employed to profile the volatile and non-volatile metabolites, respectively. Metabolite data were processed using an untargeted metabolomics approach. Random Forest techniques were used to link the sensory and metabolomics data. The odour-activity and aroma attributes of the highlighted volatile compounds were confirmed by GC Olfactometry MS (GC-O-MS). Physical properties (particle size distribution, viscosity and morphology) of the samples were also monitored in relation to the mouthfeel of the soups.

6.2. Materials & Methods

6.2.1. Chemicals and reagents

Maltodextrin DE12 (GLUCIDEX® 12, Roquette, Lestrem, France) was used as carrier for the spray drying. A mix of n-alkanes (C_6 – C_{21}) was prepared. All alkanes were purchased from Sigma-Aldrich (Zwijndrecht, The Netherlands). The analytical standards used for metabolite identification had a purity between 96-99 %. All standards were purchased from Sigma-Aldrich (the Netherlands) except for methanethiol, 1,3-diethylbenzene, styrene and 1,4-diethylebnzene which were purchased from Greyhound Chromatography (Wallasey, UK). All standards were dissolved in methanol (Biosolve BV, Valkenswaard, The Netherlands). Methanol, formic acid and acetonitrile (Sigma-Aldrich, Zwijndrecht, The Netherlands) were used for the extraction and analysis of semi-polar non-volatile metabolites present in the soup samples.

6.2.2. Production of asparagus ingredients

Raw fresh asparagus cut-offs were kindly provided by Teboza BV (Helden, The Netherlands). The concentrated asparagus juice (concentrate) and spray-dried powder were prepared under hygienic conditions and following the split-stream processing method as described previously (Siccama, Pegiou, Eijkelboom, et al., 2021). In brief, concentrated juice was prepared from asparagus cut-offs by pressing them, followed by centrifugation of the

juice to remove any solids. The juice was concentrated using reverse osmosis. The remaining asparagus fibre after pressing was dried with hot air and milled to fine powder.

Aliquots of the concentrate (21.7% w/w solids) were transferred to 1 L autoclaved glass bottles and stored at -20°C until further analyses. The remainder of the concentrate was used for spray drying after adding maltodextrin DE12 in a 1:2 mass ratio (asparagus solids : maltodextrin). A Mobile Minor spray dryer (GEA, Dusseldorf, Germany) was used for spray drying with inlet and outlet temperatures of 196±3°C and 85±1°C, respectively. The spray-dried powders were stored in sealed aluminium bags at ambient temperature.

The asparagus fibres were stored in sealed plastic bags at -20°C until further processing. After storage, the fibres were thawed in boiling water and washed at least three times at 70°C to remove traces of sand. Subsequently, they were blanched at 90°C for 3min and dried in a food dehydrator (Sedona, Tribest, USA) at 68°C for 20h. After drying, the fibres were milled using a Pulverissette-14 RotorMill (Fritsch, Idar-Oberstein, Germany) using a 0.2mm sieve and at 10,000rpm. The milled fibres were manually sieved using a 0.25mm sieve and the fine fraction was stored in sealed aluminium bags at ambient temperature for later use as one of the ingredients for two soup prototypes.

To ensure food safe processing of the asparagus ingredients, a risk assessment was performed. Hygiene indicators were tested by taking samples during different steps in the process. The analysed indicators were total viable count of *Enterobacteriaceae*, *Lactobacilli*, yeast, moulds, *Bacillus cereus* and *Staphylococcus aureus*. The results are reported in the Table A.6.1. Lastly, we ensured the elimination of microorganisms by heating the asparagus soups for at least 2 min at 70°C before consumption (Cebrián, Condón, & Mañas, 2017).

6.2.3. Preparation of asparagus soup prototypes

Six asparagus soup prototypes were prepared for evaluation of the sensory and metabolite profiles. Their composition was based on the recipe of a commercial asparagus instant soup. All prototypes included the same concentration of potato starch, salt, asparagus solids and final maltodextrin content. The six prototypes differed regarding the asparagus ingredients: the commercial dried asparagus powder with (CF) and without (C) asparagus flavour mix, the juice concentrate with (JA) and without (J) asparagus fibre and the spray-dried powder with (SA) and without (S) asparagus fibre (Table 6.1). The commercial powder and asparagus

flavour mix were kindly provided by Unilever (R&D Unilever BV, Wageningen, The Netherlands). Potato starch and sea salt were purchased from a local supermarket (Wageningen, The Netherlands).

Table 6.1 Recipe for the preparation of the six asparagus soup prototypes in 1 L water. The labels indicate the asparagus ingredients of the soups. The amount of the asparagus ingredient is on total weight basis, maintaining the same asparagus solids content per soup. The salt, starch and final maltodextrin content were the same for all prototypes and based on the composition of a commercial product. The volume mean particle diameter (D[4,3]) and the viscosity of the soups measured at 50 s^{-1} and 40 °C (n=2) are presented. The letters show the significant differences based on pairwise comparisons after one-way ANOVA with the Games-Howell post hoc test for unequal variances (significant p-value < 0.05).

Label	Asparagus ingredients	Primary asparagus component (powder or concentrate) (g)	Asparagus fibre (g)	Maltodextrin (g)	D[4,3] (µm)	Viscosity (mPa·s)
CF	Commercial powder and added flavour mix	7.15	0	41.54	214 ± 7 [a]	7.3 ± 4 [a]
C	Commercial powder	7.15	0	41.54	186 ± 48 [a]	8.4 ± 4 [a]
JA	Concentrate and asparagus fibre	14.31	3.58	41.54	227 ± 19 [a]	8.4 ± 0.5 [a]
J	Concentrate	28.62	0	41.54	184 ± 0 [a]	11.8 ± 6 [a]
SA	Spray-dried powder and asparagus fibre	10.84	3.58	35.55	223 ± 18 [a]	8.4 ±1 [a]
S	Spray-dried powder	21.68	0	29.43	199 ± 32 [a]	5.8 ± 0.7 [a]

Note: 23.08 g of potato starch and 5.85 g of salt were added to 1 L of all soups.

The dry ingredients, i.e. starch, maltodextrin, salt and asparagus powders, were weighed according to Table 6.1 and mixed four days before the first sensory evaluation training session and stored in sealed plastic opaque containers at room temperature. The concentrate (1L flask) was aliquoted into 50mL polypropylene screw cap test tubes (Sarstedt AG & Co, Germany) after thawing overnight at 4°C and aliquots were stored at -20°C until use. For each sensory evaluation, the required number of test tubes with concentrate were transferred to the fridge the day before and thawed to 4°C. Shortly before evaluation, 1L of boiling water per prototype was added to the dry ingredients. In the case of 'J' and 'JA', the aliquoted concentrate was added to the dry ingredients immediately before adding the water. All

samples were individually mixed using an electric hand-blender (Kenwood kMix Triblade Hand Blender, Kenwood Corporation, Tokyo, Japan) for 30 seconds. The samples were kept warm in Thermos flasks until the evaluation. When serving to the panellists, one additional sample (15ml) of each soup was taken and stored in a 50ml polypropylene screw cap test tube (Sarstedt AG & Co, Germany) at -20ºC for the metabolomics analysis.

6.2.4. Sensory evaluation

The sensory evaluation was carried out at the facilities of Essensor BV (Wageningen, The Netherlands). The expert sensory panel was selected from the top 10% of the population after screening on sensory abilities and sensitivities following the ISO 8586 criteria. Ten selected professional panellists were first trained to become acquainted with the six soup prototypes during four training sessions when similar prototype samples were used before the final descriptive evaluation. The sessions were carried out on separate days, and each started at 10:00 AM. A set of 24 attributes was determined for the soups during the four training sessions, which covered odour, taste, mouthfeel and aftertaste attributes (Table A.6.2). The panellists were pre-trained during the training sessions to be acquainted with the soup samples without knowing the composition of ingredients.

During the final descriptive sensory evaluation, the six soup prototypes were served to the panellists twice in randomized order. Each sample was labelled with a unique three-digit code. The serving temperature was 65-70 °C. The panellists first evaluated the soups on the odour attributes. Subsequently, each sample was tasted at 60 °C to evaluate the taste, mouthfeel and after-feel attributes. Each panel member used thermometers to confirm and monitor the temperature. Evaluation scores were within the range of 0-100.

6.2.5. Data processing and analysis

For the analysis of the sensory profiling data, the SenPAQ© software (QIStatistics, UK) was used. Principal component analysis (PCA) was performed to investigate the variation in the sensory profiles of the soup prototypes, after normalisation of the raw data (mean-centred and divided by the standard deviation). Two-way Analysis of variance (ANOVA) was performed per attribute and p-values were adjusted for multiple comparisons using the Benjamin-Hochberg approach. The Quality Index (QI) technique (Hyldig & Green-Petersen,

2004) was applied as a measurement of whether the panellists could reliably distinguish the soup prototypes regarding each sensory attribute.

6.2.6. Metabolomics

To profile the volatile and non-volatile chemical composition of the six soup prototypes, 15ml was taken from each soup on each training sensory session day as well as the final descriptive evaluation and stored at -20ºC. After the final descriptive evaluation was complete, all samples were transported to the lab on ice. Once fully defrosted, these were placed in a water-bath at 70ºC to mimic the temperature as served to the panellists. Afterwards, they were respectively aliquoted in glass vials and Eppendorf tubes for further analysis using SPME GC-MS and LC-MS as described below. All samples were analysed in a single sequence per metabolomics platform, in randomized order.

6.2.7. Analysis of volatile compounds

To profile the volatile compounds, 1mL per soup replicate was pipetted in a 10mL ND18 headspace screw glass vial (BGB®, Germany) and vials were closed with ND18 magnetic screw caps (8mm hole) with Silicone/PTFE septa (BGB®, Germany). Before extraction, each sample was preconditioned at 65ºC for 10min agitating at 350rpm, to release the volatiles to the headspace mimicking how the panellists smelled the samples. Volatiles in the headspace were extracted at 65ºC for 10min without agitation and absorbed onto a Polydimethylsiloxane/Divinylbenzene/Carboxen 50/30µm diameter, 1cm length fibre (Supelco, PA, USA). After extraction, SPME fibres were desorbed onto the GC-MS by heating the fibre at 250ºC for 2min. The GC-MS analysis settings were as previously described (Siccama, Pegiou, Eijkelboom, et al., 2021). A mixture of all samples was used for each quality control (QC) sample. QCs were analysed in the same way as all biological samples and were distributed along the analysis series. A range of n-alkanes (C_6 – C_{21}), prepared from a set of stock solutions of the individual, was analysed in the same way to calculate retention indices.

6.2.8. Analysis of non-volatile compounds

To profile the non-volatile compounds, ultra-performance LC-MS was performed. The semi-polar compounds were extracted by mixing 0.3mL of each soup replicate with 0.9mL 32.04M methanol and 0.035M formic acid followed by sonication and centrifugation, as described previously by De Vos et al. (2007). The LC-MS calibration and analysis settings were as

previously described (Pegiou et al., 2021) using both negative and positive ionization modes of the Q Exactive™ Plus Hybrid Quadrupole-Orbitrap™ Mass Spectrometer (Thermos Fisher Scientific™, Germany). A 0.3mL from the same mixture of all samples as prepared and mentioned in 6.2.6, was used for each QC sample and analysed in the same way as the biological samples.

6.2.9. Untargeted metabolomics data processing workflow

All GC-MS and LC-MS data were processed following the untargeted metabolomics workflow centred around the software packages MetAlign and MSClust as described before (Pegiou et al., 2021). The obtained relative abundances of the reconstructed metabolites in the processed data were log-transformed and a correction for signal drift was carried out, based on the QC samples (Wehrens et al., 2016).

6.2.10. Metabolite identification

Volatile metabolites were identified based on matching the reconstructed mass spectra and calculated RIs with authentic reference standards and those present in the NIST17 Mass Spectral Library and in-house databases. Non-volatile compounds were putatively identified based on matching their molecular ion mass and associated in-source fragments with the detected LC-MS asparagus compounds described by (Pegiou et al., 2021) and the online databases KnaPSAck (http://www.knapsackfamily.com/) and mzCloud (https://www.mzcloud.org/). The given level of identification (LOI) follows the guidelines of the Metabolomics Standards Initiative (Sumner et al., 2007).

6.2.11. Multivariate statistical analysis

The log-transformed metabolomics data were mean-centred, Pareto-scaled and variation between samples was initially explored by applying PCA. PCA analyses were performed using the R package ropls (Thevenot, Roux, Xu, Ezan, & Zunot, 2015). Random Forest was applied for the supervised analysis and variable selection, considering the composition of the data matrices obtained. The bootstrapping method, which is applied during random forest analyses, converges to the leave-one-out cross-validation method which is suitable for datasets with a limited number of observations, enabling a higher prediction performance. For the Random Forest analyses, log-transformed data were used and analyses were performed using the R package randomForest (Liaw & Wiener, 2002). The number of trees

(ntree) and the number of variables (mtry) for each decision rule were optimized for the minimum prediction error for each model. The Random Forest classification approach was followed to determine those GC-MS and LC-MS compounds indicating the ingredient composition of a specific soup prototype. Two classification analyses were performed per dataset; one based on the primary asparagus component (3 classes: commercial, concentrate, spray-dried) and one based on the presence of asparagus fibre (2 classes: yes, no) (Table 6.1). The commercial powder was classified as fibre-containing as it is produced from whole asparagus pieces, thus, including the fibres. The performance of each model was assessed by the out-of-bag (OOB) error rate which corresponds to the prediction error after leave-one-out cross-validation. Variable importance was estimated by the mean decreased accuracy which expresses how much accuracy the model loses by excluding each variable. Compounds with Mean Decrease Accuracy > 1 were considered relevant. Hierarchical clustering (HCA) of the soups was subsequently performed focusing on the selected variables after log-transforming and autoscaling their abundances, and this was visualised in a heatmap. The HCA analysis and visualisation were performed using the R packages pheatmap and ggplot2 in RStudio with R version 4.1.1 (2021-08-10). The Random Forest regression approach was followed to determine which individual compounds have a predicting relevance to sensory attributes having a QI > 0.65 and p-adjusted < 0.05 (Table A.6.2). The performance of each model was assessed by the mean square error (MSE). Variable importance was estimated by the increase in mean square error (%IncMSE) which expresses how much the percentage of prediction error increases by excluding each variable. Compounds with %IncMSE > 1.50 were considered relevant. Microsoft Excel and PowerPoint (version 2104, 2021) were used for additional data analysis and visualisation.

6.2.12. GC-Olfactometry-MS

The regression analyses highlighted 18 volatile compounds as being correlated to specific sensory attributes of which eight could be unambiguously identified (level 1). A mixture of the reference standards of these eight compounds was analysed with GC-O-MS, to determine whether these volatiles are odour-active within the concentration range detected in the soups without the extra addition of the flavour mix. A GC column splitter outlet was used to split 1:1 towards the MS and the olfactory detection port (ODP2, Gerstel, The Netherlands). The reference standards were dissolved in methanol and were used to prepare a solution in water comprising dimethyl sulphide (5µg/mL), pentanal (5µg/mL), 1-hexanol (5µg/mL), 1,3-

dimethylbenzene (0.2µg/mL), 1-octen-3-ol (0.5µg/mL), octanal (0.05µg/mL), *(E)*-2-heptenal (0.2µg/mL) and 2-methoxy-3-isopropyl pyrazine (0.2µg/mL). The same SPME GC-MS conditions as described in section 2.4.1 were used except that the GC oven temperature program was adjusted to shorten total run time to 24min by increasing the ramp to 20ºC/min after 15min. For sniffing and assigning the individual peaks to a specific aroma attribute (if any), three assessors were recruited within the laboratory. Each assessor smelled the GC-O profile of the prepared standard solution and noted down the perceived aroma per compound at the given retention times without knowing which compound corresponds to which peak.

6.2.13. Physical characteristics

Selective physical properties of the dry powders and soup prototypes were analysed. The particle size distributions of the commercial asparagus powder, spray-dried powder and asparagus fibre were measured using a Mastersizer 3000 analyser (Malvern Inc, Malvern, UK) with the dry powder disperser Aero S. The size distributions of the commercial asparagus powder and asparagus fibre were analysed in the non-spherical analysis mode using the refractive index (RI) of cellulose, i.e. 1.468, since cellulose was considered the most abundant compound. The spray-dried powders were analysed with the spherical analysis mode using the RI of maltodextrin, i.e. 1.670. Furthermore, the particle size distributions of the soup prototypes were analysed in the Hydro MV module and the Mastersizer 3000 with the non-spherical analysis mode. The RI of cellulose (1.468) was used for the dispersed phase and 1.330 for the continuous phase (water). In addition, the particle size distribution of pure starch dissolved in hot water was measured using the spherical analysis mode and the RI of starch (1.450).

The viscosity of the soups was determined with the Anton Paar rheometer (MCR301, Anton Paar GmbH, Graz, Austria) with a concentric cylinder geometry (CC-27). A shear rate sweep with a logarithmic increasing shear rate from 1 to 1000 s^{-1} was performed. The rheology measurements were performed at 40°C, which is assumed to be the relevant temperature inside the mouth before swallowing the soup (Deblais et al., 2021). The viscosities of the soups at 50 s^{-1} are reported (Table 6.1). This shear rate has been adopted as the oral shear rate standard by the National Dysphagia Diet task force and is considered a reasonable order of magnitude for swallowing liquids (Ong, Steele, & Duizer, 2018; Popa et al., 2013).

Microscopy images of the soups were taken using a light microscope (Carl Zeiss AxioScope, Jena, Germany) after the soup samples were vortexed to ensure homogeneity. A drop of the sample was placed on a microscopic slide under a coverslip. The images were captured (AxioCam MRc 5 camera) at a 20x magnification.

6.3. Results

6.3.1. The sensory profiles of the asparagus soups

Ten professional panellists evaluated the soup prototypes on 24 sensory attributes (Table A.6.2). PCA was performed on the sensory profiles and >79% of the overall variance was explained by the first two principal components (Fig. 6.1A). The soup containing the commercial powder (C) had a similar sensory profile as the soups containing the concentrate or the spray-dried powder with fibre (JA and SA), as these are located close to each other on the PCA plot. These three prototypes had a contrasting sensory profile to the soups with the concentrate or the spray-dried powder without fibre (J and S), as well as the one with the flavour-supplemented commercial powder (CF), which, along PC2, was separated from all the other soups (Fig. 6.1A). The loadings (sensory attributes) being close to each other were positively correlated while attributes being located at opposite directions in Fig. 6.1A were negatively correlated. Likewise, soups located close to specific attributes obtained a high score for those sensory characteristics. For instance, the 'CF' soups scored high on the asparagus odour (O_Asparagus), asparagus taste (T_Asparagus) and the overall aroma intensity (O_Intensity) (Fig. 6.1A). These scores were significantly higher (p adjusted < 0.05) compared to all soups except for the 'S' prototype (Fig. 6.1B). In contrast, the soups containing the commercial powder (C) or the in-house processed ingredients with asparagus fibre (SA, JA) had a significantly higher score on the cardboard taste (T_Cardboard) compared to the other soups (Fig. 6.1A,B). Significant differences between the soup prototypes were also observed regarding the thickness (M_Thickness), powdery mouthfeel and after-feel (M_Powdery, AF_Powdery) (Fig. 6.1B, Table A.6.2). The samples without asparagus fibre, i.e. 'J' and 'S', scored significantly lower on the powdery mouthfeel and after-feel compared to all the other soups. The 'J' prototype scored also significantly lower on thickness (Fig. 6.1B).

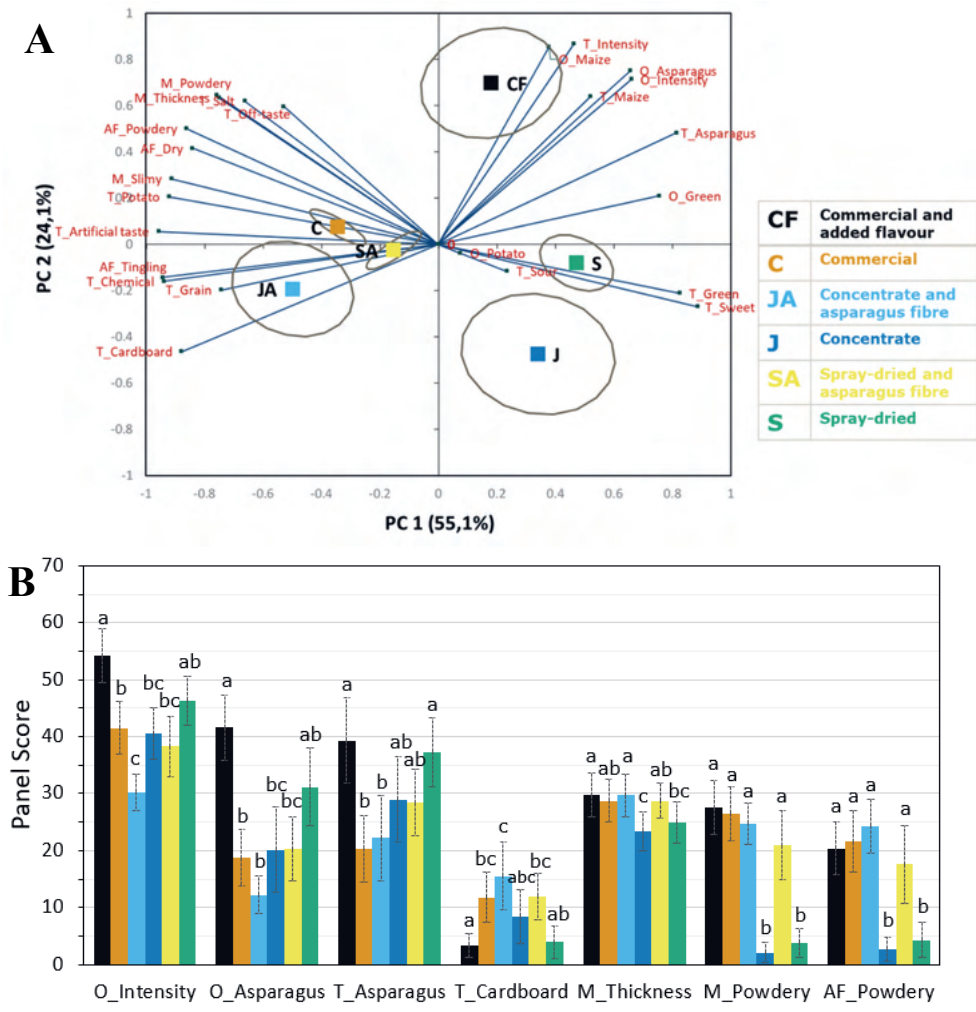

Figure 6.1 Statistical analysis of the sensory evaluation data of the six soup prototypes from ten trained professional panellists. Score range: 0 – 100 with min=0 and max=82.7. (A) PCA biplot of the six different soups and the 24 sensory attributes that were scored during the evaluation which are labelled as in Table A.6.2. Data points representing the soups are based on the average of all scores from all panellists and ellipses show the standard deviation. Data points are coloured based on the asparagus ingredients of the soups as presented in Table 6.1. The % of explained variance per PC is provided in parentheses on the x and y axes. (B) Bar graphs of the average score for seven selected sensory attributes that showed significant differences between the six soup prototypes related to odour (O), taste (T) mouthfeel (M) and after-feel (AF). The error bars show the 95% confidence intervals based on the scores of 10 panellists who evaluated each prototype twice (n=20). Bars are coloured based on the asparagus ingredients of the soups as in shown in (A). The letters indicate significant differences between the soup prototypes per attribute based on pairwise comparisons after two-way ANOVA. P-values were adjusted with the Benjamin Hochberg FDR procedure (significant p-value < 0.05).

The sensory attributes that had a significantly different score between any of the soup prototypes (p adjusted < 0.05 and QI > 0.65) (Table A.6.2) were further investigated by combining the sensory with the metabolomics results as indicated below.

6.3.2. The metabolite profiles of the asparagus soups

The chemical composition of the soups was studied regarding the secondary metabolites using SPME GC-MS (volatiles) and LC-MS (non-volatiles). Following an untargeted metabolomics workflow for processing the raw data the compounds retained for further examination were 85 volatiles and 951 non-volatiles (both ionisation modes). Sulfur-containing compounds, furans, pyrazines, aldehydes, alcohols, ketones, aromatics, hydrocarbons, flavonoid glucosides and saponins were among the main groups of annotated compounds (supplementary data). All compounds had a lower relative standard deviation (RSD) across the QCs than the biological samples and the mean RSD across the QCs was lower than 0.25, indicating good technical reproducibility.

The GC-MS and LC-MS profiles were studied separately by PCA to explore the variation between the soup prototypes (Fig. 6.2A,B). The main differentiation was detected along PC1, explaining 41% and 21% of the overall variation of the volatiles and non-volatiles, respectively, and was between the soups containing the commercial powder and those containing the in-house processed ingredients (Fig.6.2A,B). The metabolites with the highest contribution to the observed separation of the soups are depicted in Fig. 6.2C,D. These were one thiazole, acetoin, ethanol, one nitrogen-containing volatile compound (Fig. 6.2C) and three LC-MS compounds (pos_120, neg_334 and neg_309 in Fig. 6.2D) being detected at high levels in the in-house processed ingredients, and dimethyl disulphide (DMDS), *(E)*-2-heptenal, decanal, 2-butyl-2-octenal (Fig. 6.2C) and four LC-MS compounds (neg_71, neg_575, pos_521 and pos_727 in Fig. 6.2D) being detected at high levels in the commercial powder. The presence of asparagus fibre in the in-house ingredients appeared to influence the metabolite composition, which is most evident from the non-volatiles (Fig. 6.2B). The impact of adding the flavour mix to the commercial powder is only reflected by the volatiles (Fig. 6.2A). The three volatiles that were highly abundant in the flavour-supplemented soups were dimethyl sulphide (DMS), 2-methoxy-3-isopropylpyarzine and 2-methoxy-3-isobutylpyrazine (Fig. 6.2C).

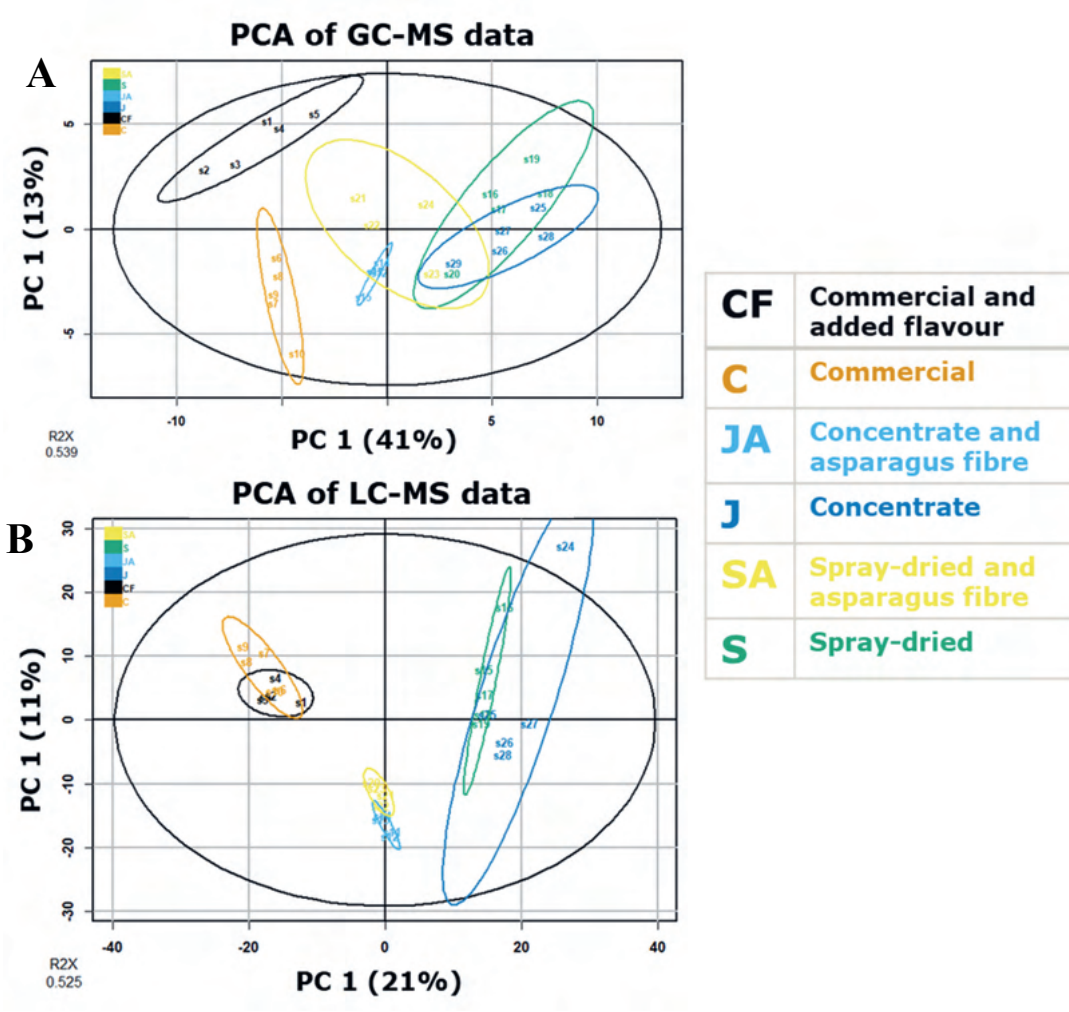

Figure 6.2 Principal component analyses (PCA) of the metabolite profiles of the six soup prototypes. PCA score plots based on (A) 85 volatiles and (B) 951 non-volatiles. The first two PCs are presented, and the explained variance is shown in parentheses on the axes. The black ellipses represent the 95 % confidence interval from the Hotelling T2 function. Data points are coloured based on the asparagus ingredients of each soup as presented in Table 6.1. The coloured ellipses show the confidence interval for each soup prototype based on the analysed replicates (n=4 or 5). (C): PCA loading plot of the GC-MS profile with the top12 variables highlighted. Annotation is given in case of LOI<3. (D): PCA loading plot of the LC-MS profiles with the variables having high contribution highlighted. Analyses and plots were made using the ropls R package.

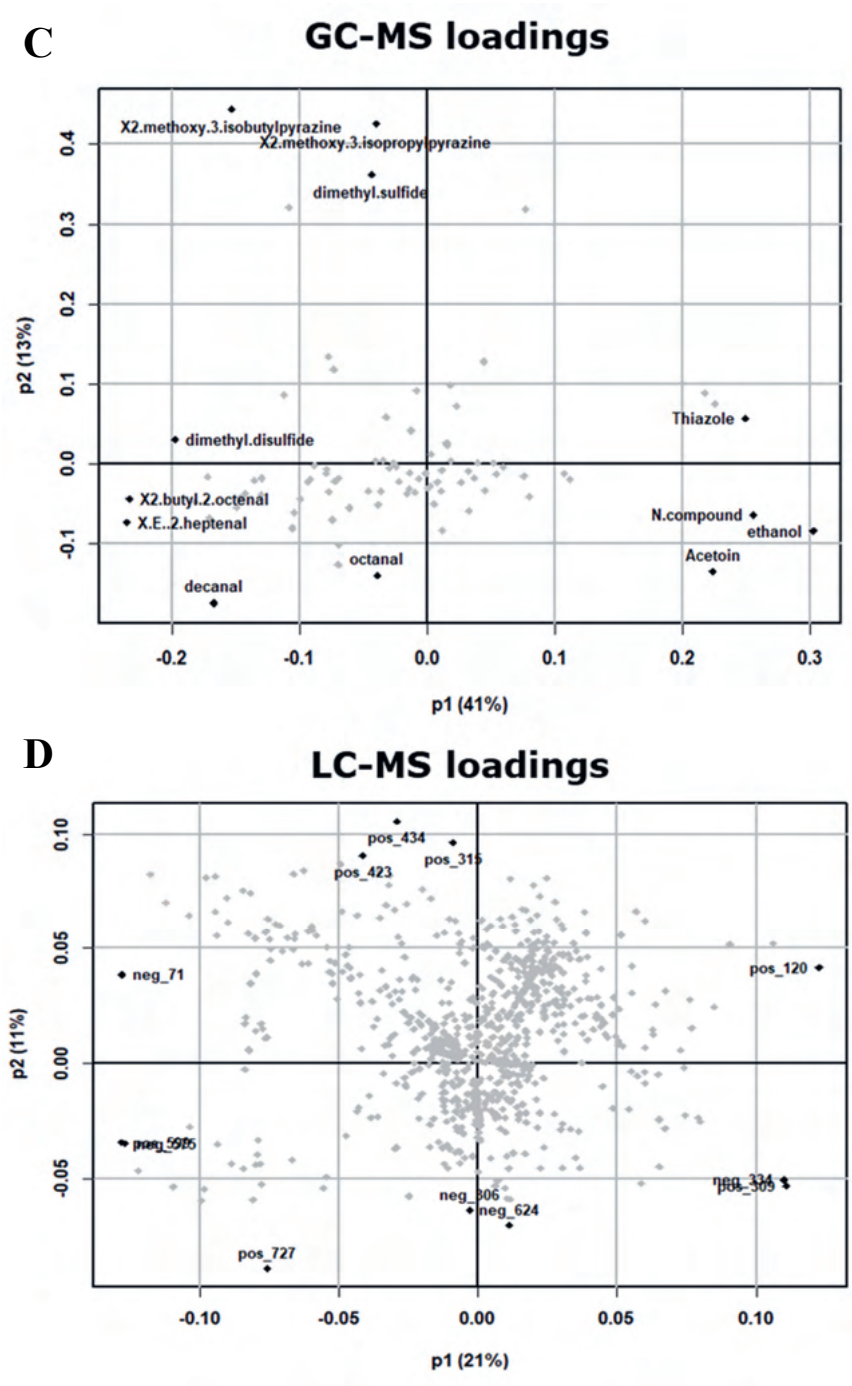

Figure 6.2 Continued

6.3.3. Compounds specific for the asparagus ingredients of the instant soups

The metabolite profiles of the soup prototypes varied based on the asparagus ingredients. The addition of asparagus fibre to the in-house prototypes appeared to have a dominant effect on their metabolite profiles (Fig. 6.2A,B). The composition of the soups was therefore, examined by performing two Random Forest classification analyses to highlight the discriminatory compounds. One analysis for classifying the soup prototypes based on the primary asparagus component (commercial, concentrate, spray-dried) and one based on the presence of asparagus fibre (CF, C, JA, SA contain fibre) (Table 6.1).

The Random Forest classification models highlighted eight compounds which were indicative for the primary asparagus component (mean OOB error rate from the two metabolomics datasets 26.7%) and 12 compounds indicating the presence (six compounds) or absence (six compounds) of asparagus fibre (mean OOB error rate from the two metabolomics datasets 3.6%). HCA of the soups based on the 20 discriminatory compounds demonstrated the grouping of the prototypes according to the asparagus ingredients (Fig. 6.3A). The soups without asparagus fibre are in cluster I and the soups with asparagus fibre are in cluster II (Fig. 6.3A). The 20 compounds were clustered in three main groups (Fig. 6.3A). The compounds in groups 1 and 2 are indicative of the absence or presence of asparagus fibre in the soups, respectively. The compounds in group 3 were highly abundant in the dried powders (spray-dried and commercial), except for DMS and 1-hexanol, which were specifically more abundant in the spray-dried and the flavour-supplemented commercial powder (Fig. 6.3A). The five sulfur-containing metabolites were examined in detail considering their reported high relevance to asparagus flavour notes. Asparagusic acid, S-methylmethionine and 1,2-dithiole followed similar patterns and were more abundant in the prototypes without fibre (Fig. 6.3B – 6.3D). DMS was detected at high levels in the ‘CF’, but also in the ‘S’ soups (Fig. 6.3E) and DMDS was highly abundant in the ‘C’ and ‘CF’ soups (Fig. 6.3F).

6.3.4. Compounds relevant for the perception of asparagus flavour notes

To retrieve compounds that are of specific relevance to certain sensory attributes, the outcomes of the descriptive sensory analysis and the metabolomics evaluation of the asparagus soups, were combined using advanced statistical tools. Of the 24 scored sensory attributes, 13 had significantly different scores between the soups (p adjusted < 0.05 and QI

> 0.65) (Table A.6.2). Random Forest regression analysis was performed to determine which metabolites potentially contribute to certain flavour characteristics. Five sensory attributes were reliably predicted by GC-MS profiles and three sensory attributes were reliably predicted by LC-MS profiles (MSE<25). In addition, the Pearson's correlation coefficient between each compound and the linked sensory attribute was calculated to help in the interpretation of their relationship (Table 6.2 and 6.3).

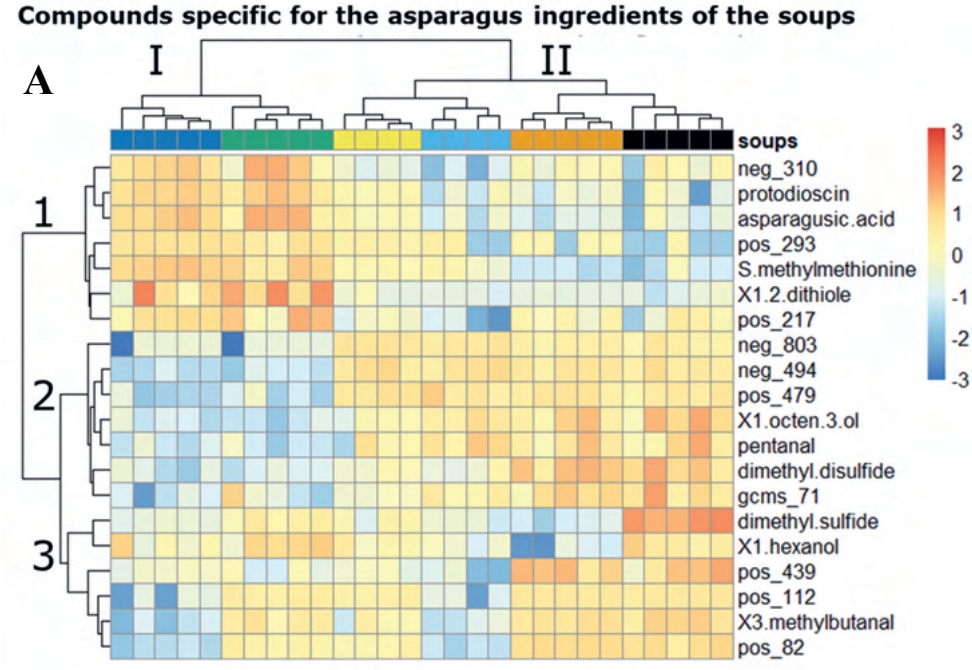

Figure 6.3 Visualisation and inspection of compounds found to be specific for the composition of the asparagus soups based on the Random Forest classification analyses. (A) Heatmap of the 20 highlighted compounds (Mean Decreased Accuracy > 1) and their abundances in the soup prototypes (Fibre-specific: protodioscin, pos_479, asparagusic acid, neg_494, neg_803, neg_310, S-methylmethionine, pos_217, gcms_71, dimethyl disulphide, 1,2-dithiole, pentanal. Ingredient-specific: pos_112, pos_439, pos_82, pos_293, 1-hexanol, 3-methylbutanal, 1-octen-3-ol, dimethyl sulphide). Data were log-transformed and scaled. Dendrograms correspond to the clustering of the soups or the compounds based on HCA using Ward's method. (B – F): The abundances of the five sulfur compounds shown in (A) in the six soup prototypes are presented as boxplots.

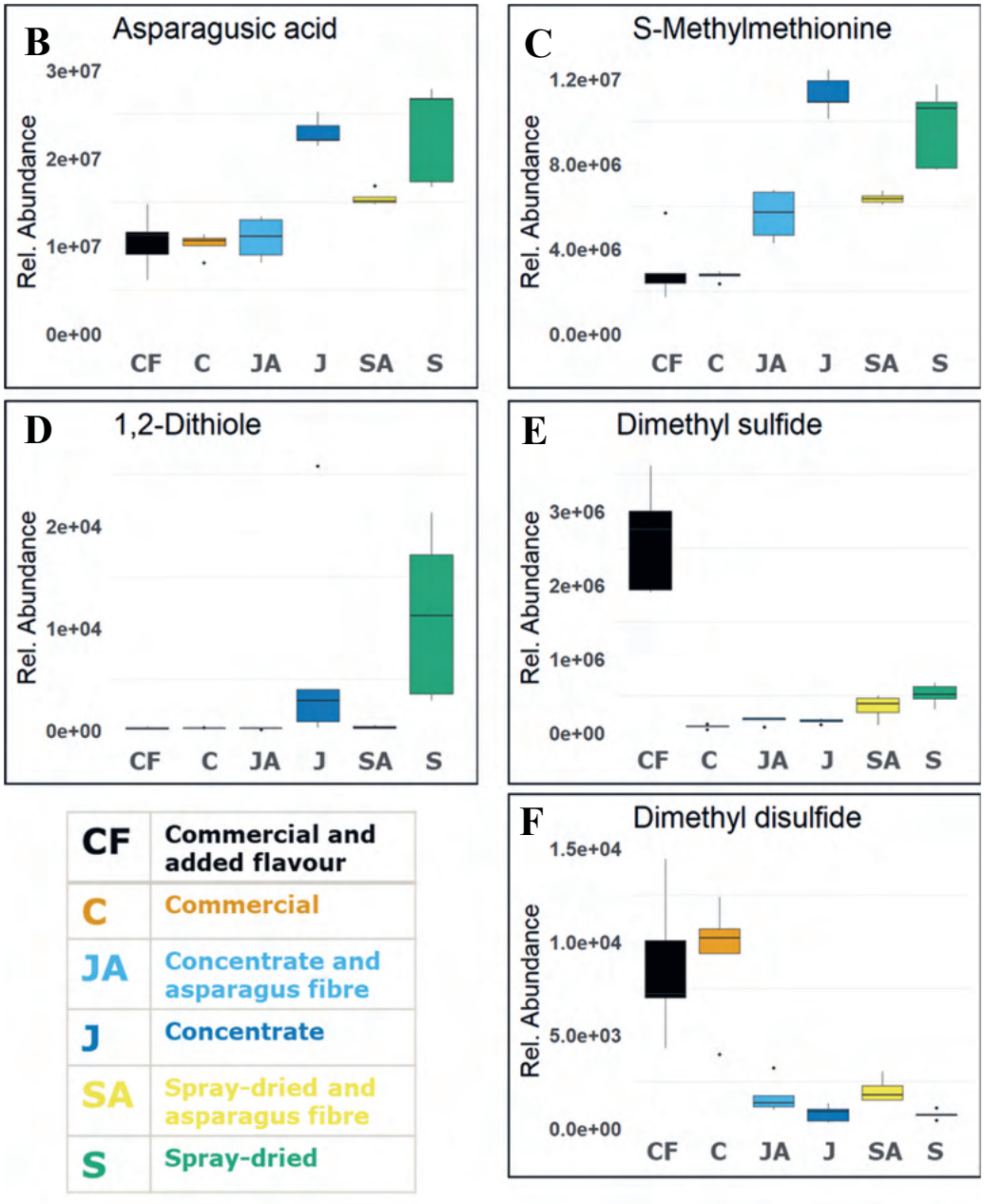

Figure 6.3 Continued.

Table 6.2 List of the volatile compounds that were linked to a sensory attribute based on Random Forest regression (%IncMSE>1.50). The Pearson's correlation coefficient of each compound with the related sensory attribute was calculated to interpret the relationship between them. The aroma characteristics per compound based on the Good Scents and FooDB databases are provided. In the final column, the aroma characteristics per compound as perceived by the assessors during the GC-O-MS analysis are listed.

Compound / ID	Sensory attribute(s)	Pearson's correlation coefficient	Aroma attribute based on databases[1]	Aroma attribute perceived at the ODP[2]
Dimethyl sulphide	O_Intensity O_Asparagus	0.55 0.59	onion, cabbage	earthy, asparagus, potato
2-Methoxy-3-isopropylpyrazine	O_Intensity O_Asparagus	0.49 0.52	earthy, bean, pea	earthy, vegetable, asparagus
gcms_112	O_Intensity	0.20		Na
1-Hexanol	O_Intensity	0.44	herbal, fruity	herbal, grassy
2-Methoxy-3-isobutylpyrazine	O_Intensity	0.36	bell pepper, earthy	Na
gcms_115	O_Asparagus	0.30		Na
3-Methyl-1-butanol	O_Asparagus	0.43	fruity, banana	Na
1,3-Dimethylbenzene	O_Asparagus	0.01	-	not detectable
gcms_105	T_Intensity	0.30		Na
Octanal	T_Intensity	0.20	waxy, orange peel	fruity, floral
gcms_66	T_Intensity	0.52		Na
Pentanal	M_powdery AF_Powdery	0.84 0.57	fermented, nutty	sweet, floral
1-Octen-3-ol	M_Powdery AF_Powdery	0.80 0.47	earthy, mushroom	earthy, mushroom
gcms_71 (alkane)	M_Powdery AF_Powdery	0.65 0.38		Na
gcms_43 (nitrogen-containing)	M_Powdery	-0.78		Na
(E)-2-Heptenal	M_Powdery	0.72	fatty, pungent	strong chemical
n-Caproic acid vinyl ester	M_Powdery	0.66	-	Na
gcms_76 (sulfur-containing)	M_Powdery	-0.77		Na

[1] aroma attribute based on The Good Scents (http://www.thegoodscentscompany.com/) and FooDB (https://foodb.ca/) databases. [2] aroma attribute perceived at the ODP by at least two of the three assessors. Na when no reference standard was analysed.

Concerning the GC-MS profiles, in total 18 volatiles were highlighted as significantly correlating to asparagus odour, overall odour and taste intensity and the two powdery attributes (Table 6.2). The highlighted relationships between volatiles and sensory attributes were mainly positively correlated. Specifically, the volatiles that were found to significantly correlate to high perception of asparagus odour and taste were DMS, 2-methoxy-3-isopropylpyrazine, 3-methyl-1-butanol, 1,3-dimethylbenzene and one unidentified compound (Table 6.2).

Table 6.3 List of the non-volatile compounds that were linked to a sensory attribute based on Random Forest regression (%IncMSE>1.50). The Pearson's correlation coefficient of each compound with the specific attribute was calculated to interpret the relationship between them. The calculated monoisotopic mass of each compound is provided. For the compound ID pos/neg refers to the mode of detection used.

Compound / ID	Sensory Attribute	Pearson's correlation coefficient	Calculated monoisotopic mass
neg_204	T_Cardboard	-0.45	312.0337
neg_411	T_Cardboard	-0.33	505.2473
neg_97	T_Cardboard	0.24	328.9810
pos_315	T_Cardboard	-0.52	355.0995
pos_479	T_Cardboard	0.51	168.0798
pos_490	T_Cardboard	-0.18	171.8606
Asparagusic acid	M_Powdery	-0.85	149.9806
S-Adenosylhomocysteine	M_Powdery	0.79	384.1209
neg_496	M_Powdery	-0.08	337.8662
neg_601	M_Powdery	0.62	312.2301
neg_629	M_Powdery	0.66	364.3021
neg_768	M_Powdery	0.78	998.5092
pos_371	M_Powdery	-0.83	1065.5092
neg_667	AF_Powdery	0.19	335.8705
Protodioscin	AF_Powdery	-0.66	1048.5468
pos_150	AF_Powdery	-0.61	304.0675
pos_283	AF_Powdery	-0.61	364.9045
pos_290	AF_Powdery	-0.57	422.1227

Concerning the LC-MS profiles, six compounds were found to be highly associated with cardboard taste and 12 compounds were linked to the two powdery attributes (Table 6.3). For each compound, the provided monoisotopic mass was calculated based on the base peak and the Pearson's correlation coefficient indicates whether the presence (positively correlated) or absence (negatively correlated) of these specific compounds can predict the perception of the linked flavour attribute. For example, S-adenosylhomocysteine was positively correlated with the powdery mouthfeel while protodioscin was negatively correlated with the same attribute (Table 6.3).

6.3.5. GC-Olfactory-MS confirms the sensory-activity of asparagus volatiles.

To test whether the volatile compounds that were associated with specific flavour attributes are odour-active a series of GC-O-MS analyses were executed. A mix of eight identified volatile compounds that were purchased as pure standards was prepared. The mix was then analysed with GC-O-MS and smelled by three assessors in independent runs. Retention times of the eight compounds were such that each peak could be readily evaluated separately. Results showed that 2-methoxy-3-isopropyl pyrazine, 1-octen-3-ol and *(E)*-2-heptenal were odour-active based on all three assessors who also recorded similar aromas (Table 6.2). DMS, pentanal, 1-hexanol and octanal were also odour-active and could be detected by two of the three assessors, while 1,3-dimethylbenzene was not perceived by any of the assessors (Table 6.2). Interestingly, when the three assessors were finally asked to smell the mixture of the standards from the GC vial, two directly described this as being like asparagus.

6.3.6. Physical properties and mouthfeel of the soup prototypes

The particle size distributions of the dry asparagus ingredients (i.e. commercial, spray-dried powder and asparagus fibre) were analysed using the dry powder dispenser and different size distributions were observed (Fig. A.6.1A). Despite the fine milling and sieving, the asparagus fibre preparation consisted of the largest particles, with a volume mean particle diameter (D[4,3]) of 236µm, whereas the commercial and the spray-dried powders were characterised with a D[4,3] of 160 and 155 µm, respectively. Therefore, it was anticipated that the presence of fibre might negatively influence the sensory perception of the soups, giving a sandy and thicker mouthfeel. Hence, physical properties of the soup samples were measured and then related to the perceived mouthfeel. Despite the differences in perceived sensorial properties (i.e. powdery mouthfeel) (Fig. 6.1B), the D[4,3] values indicated no significant differences

among the soup prototypes (Table 6.1). The particle size distributions of the soups were almost the same despite the different asparagus ingredients used, which were also identical to the particle size distribution of pure starch suspended in hot water (Fig. A.6.1B). The small quantity of asparagus fibre present did not yield changes in the particle size distribution of the soups. In addition, the viscosity of soups measured at $50s^{-1}$ shear rate and 40°C did not differ significantly, and all soup samples showed similar shear-thinning behaviour (data not shown).

The soup prototypes containing spray-dried powder with or without asparagus fibre were also observed under the light microscope (Fig. 6.4). As expected, the presence of asparagus fibre was clearly visible in the 'SA' soup as a dense and elongated particle. The other particles that were visualised in both 'S' and 'SA' soups were starch granules given their morphology of swollen and round particles. Other soup prototypes were also analysed and the images of the samples with fibre (CF, C and JA) were similar to the 'SA' soup, while the sample without fibre (J) was similar to the image of 'S' (data not shown).

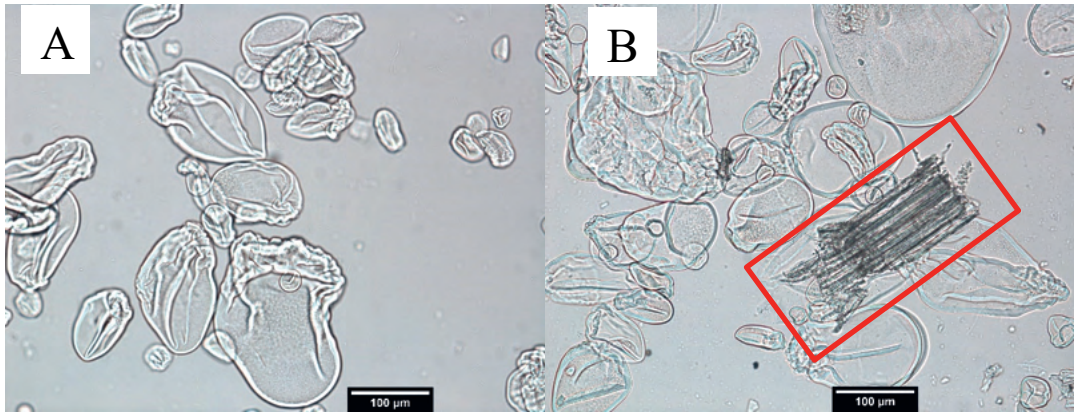

Figure 6.4 Microscopy images of the soup prototypes prepared with spray-dried powder (A) and spray-dried powder with asparagus fibre added (B). The red rectangle highlights an asparagus fibre particle.

6.4. Discussion

6.4.1. A positive impact of spray drying on the flavour profile of instant asparagus soups

The flavour-supplemented commercial powder scored significantly higher than the commercial powder on its own with regards to asparagus flavour and flavour intensity (Fig.

6.1A,B), indicating the effectivity of the added flavour mix on the overall sensory perception. However, the ultimate goal for industry would be to design a product which can avoid this required addition of flavour supplements in food products (Román et al., 2017). This would result in a more natural and sustainable solution.

The sensory and the metabolomics results indicate that the soup prototypes with split-stream processed asparagus ingredients but without asparagus fibre had similarities with the flavour-supplemented commercial powder (Fig. 6.1A, 6.2A,B). Specifically, the soups containing the spray-dried powder were awarded higher scores on the key attributes asparagus odour and taste than the soups containing the commercial powder without the supplementary flavour mix (Fig. 6.1B). This indicated that the sensory profile of the spray-dried powder was richer in asparagus flavours compared to the hot-air dried commercial powder. The soups containing the spray-dried powder had slightly higher scores on the asparagus odour and taste attributes than those containing the concentrate (Fig. 6.1B), highlighting a positive impact of spray drying on the flavour profile. This confirms the richer flavour of the spray-dried powder compared to the concentrate as was also suggested based on the chemical composition of the processed asparagus ingredients (Siccama, Pegiou, Zhang, et al., 2021).

Known asparagus aroma compounds, such as DMS and 2-methoxy-3-isopropylpyrazine (Hoberg et al., 2003; Tressl, Bahri, et al., 1977; Ulrich et al., 2001) were seen to be highly abundant in the flavour-supplemented commercial powder (Fig. 6.2C) and were also positively correlated with the asparagus flavour attributes (Table 6.2). However, when comparing the spray-dried to the commercial powder, these key odorants were more abundant in the spray-dried powder and hardly detected in the commercial one (Fig. 6.3E and supplementary data). This confirms the successful retention of key aroma compounds upon spray-drying, as was predicted previously (Siccama, Pegiou, Zhang, et al., 2021).

With respect to the sulfur-containing flavour compounds, which have been previously investigated in cooked asparagus spears highlighting their sensory-relevance (Tressl, Bahri, et al., 1977; Ulrich et al., 2001), we detected and monitored two non-volatile precursors (S-methylmethionine and asparagusic acid) and the volatiles DMS, DMDS and 1,2-dithiole (Fig. 6.3B-F). The non-volatile precursors which can be converted on heating to DMS and DMDS were more abundant in the spray-dried powder compared to the commercial one (Fig. 6.3B,C). This explains the higher levels of DMS in the spray-dried powder compared to the

pure commercial powder (Fig. 6.3E). Therefore, spray drying which we predict leads to the encapsulation of aroma compounds (Siccama, Pegiou, Zhang, et al., 2021) may also have a positive impact on retaining key flavour precursors. The fact that DMDS is equally high in both prototypes with the commercial powder indicates that it was already present in the actual commercial powder (and not in the flavour mix). Given that DMDS is also formed during heat treatment (Belitz, Grosch, & Schieberle, 2008; Parry, Mizusawa, Chiu, Naidu, & Ricciardone, 1985; Tressl, Holzer, et al., 1977), the much higher abundance in the commercial powders compared to the others can be explained by the fact that the commercial powder has undergone a longer heat treatment than the in-house produced powders.

6.4.2. The negative impact of asparagus fibre on the flavour profile and mouthfeel of instant asparagus soups

During the split-stream processing of asparagus waste streams, as a first step, the fibres are separated from the juice (Siccama, Pegiou, Eijkelboom, et al., 2021). To fully exploit the generated asparagus "waste" in a sustainable and circular manner, it was considered that the asparagus fibre could potentially be reintroduced into the production process to make powders. It was hypothesized, that the addition of the processed fibre in the final soup formulation could (positively) affect the mouthfeel sensation by providing more structure and thickness to the soups, thereby having a higher sensory impact. Lyly *et al*. (2004) evaluated the sensory characteristics and rheological properties of vegetable soups enriched with soluble fibres in the form of oat and barley β-glucans. They found that the concentration of β-glucan positively correlated to the viscosity and perceived thickness of the soups. Alqahtani *et al.* (2014) investigated the addition of insoluble fibre (i.e. orange, wheat and oat fibre) to beverages and demonstrated that the fibre-enriched beverages are perceived favourably by the panellists. Furthermore, the oat fibre samples received the highest score on overall acceptability, even higher than the commercial prototype. In the study presented here, samples with added asparagus fibres scored higher on cardboard taste, artificial taste, off-taste and powdery mouthfeel (Fig. 6.1A), which may suggest that the addition of fibres negatively impacts the overall sensory perception.

Interestingly, despite these differences in mouthfeel as perceived by the panellists (Fig. 6.1B), the volume mean particle diameter (D[4,3]) and viscosity of the soups were not significantly different (Table 6.1). While examining the morphology of the soup prototypes under a light

microscope, we saw clear differences between samples with and without fibre. The asparagus fibre was different in shape compared to the starch granules (Fig. 6.4). The textural perception of particles is strongly influenced by the size, shape and deformability of the particles (Appelqvist, Cochet-Broch, Poelman, & Day, 2015; Tyle, 1993). Although the starch granules and asparagus fibres were found to be in the same size range, the asparagus fibres were rigid insoluble particles that were less deformable compared to starch granules. In addition, asparagus fibres were more irregular in shape, due to the milling process. Tyle (1993) demonstrated that hard and angular particles result in more perceived grittiness than soft and round particles. Therefore, in this study, the perceived thicker and powdery mouthfeel of the soups containing asparagus fibre was possibly caused by the presence of these rigid and angular fibre particles.

The metabolite profiles of the asparagus instant soups which were affected by the presence of fibre (Fig. 6.2A,B, 6.3A) were also linked to the sensory data. Some of the fibre-specific metabolites (Fig. 6.3A) were also found to correlate with specific flavour attributes (Table 6.2 and 6.3). The compound pos_479 which was highly abundant in all the fibre-containing prototypes (Fig. 6.3A), was also highly positively correlated with the cardboard taste of the soups (Table 6.3), suggesting that this non-volatile compound should be further investigated as an off-flavour in the asparagus soups (Whitson, Miracle, & Drake, 2010). The volatile compounds, pentanal, 1-octen-3-ol and gcms_71 which were highly abundant in the fibre-containing prototypes (Fig. 6.3A), were positively correlated with the powdery mouthfeel (Table 6.2). The powdery sensation for an instant soup is likely undesirable (Ssepuuya, Katongole, & Tumuhimbise, 2018), as it was also indicated by the sensory evaluation of the soups where the powdery attributes were positively correlated with the off-taste and artificial attributes (Fig. 6.1A,B). The fibre-containing soups scored higher on powdery mouthfeel compared to the other soups (Fig. 6.1A,B), suggesting a negative impact of the asparagus fibre on the flavour sensation. Thus, the fibre-specific metabolites may potentially be related to off-flavours if they were sensory-active.

6.4.3. Proposal of new asparagus odorants and off-flavours

The previously reported key asparagus odorants DMS, 2-methoxy-3-isopropylpyrazine and 2-methoxy-3-isobutylpyrazine (Ulrich et al., 2001) were in this study strongly correlated with important asparagus flavour attributes of the soups (Table 6.2) and moreover DMS and 2-methoxy-3-isopropyl pyrazine were also perceived to have an earthy and asparagus smell by

at least two of the three assessors during the GC-O-MS study (Table 6.2). Additionally, 3-methyl-1-butanol, 1-hexanol, octanal and four unidentified compounds (gcms_66, gcms_105, gcms_112 and gcms_115) were also highly associated with sensory attributes, specifically with asparagus odour, overall odour and taste intensity. The three annotated compounds have fruity and herbal aroma attributes (Table 6.2) that resemble fresh asparagus. The aromatic compound 1,3-dimethylbenzene was linked to asparagus odour, but in the GC-O-MS analysis, it was not detected by any of the assessors (Table 6.2). This is in agreement with the Good Scents database (http://www.thegoodscentscompany.com/) which does not associate it with a detectable aroma. It may be that this compound acts as an aroma enhancer when present in a matrix, but this would require additional studies using an aroma matrix dilution series.

The powdery sensation which was evaluated regarding the mouthfeel and after-feel (Table A.6.2) is not a preferred feature for soup products (Ssepuuya et al., 2018) and this was confirmed as the powdery attributes were positively correlated with off-taste (Fig. 6.1A), although potential causality should be further investigated for their contribution to off-flavours. Asparagusic acid, two saponins (protodioscin and pos_371) (Table 6.3) and two volatiles (one nitrogen-containing and one sulfur-containing compound) (Table 6.2) were negatively correlated with the powdery mouthfeel implying their contribution to "positive" asparagus flavours. The essential role of asparagusic acid in the formation of important sulfur-containing asparagus odorants is known (Parry et al., 1985; Tressl, Bahri, et al., 1977). Further investigation of the two volatiles (gcms_76 and gcms_43), which were highly abundant in the prototype soups without fibre (supplementary data) might lead to the discovery of two new asparagus odorants. In contrast, pentanal, *(E)*-2-heptenal, 1-octen-3-ol and n-caproic acid vinyl ester which were highly positively correlated with the powdery sensation of the soups are potential off-flavours worthy of attention. Blanda *et al.* (2010) investigated the volatile composition of boiled potatoes and the influence of additives on the flavour. They showed that increased levels of medium-chained aldehydes (e.g. pentanal, 2-heptenal) led to the formation of off-flavours as perceived by the panellists. Pentanal, *(E)*-2-heptenal and 1-octen-3-ol have been previously reported as key odorants in cooked white asparagus (Ulrich et al., 2001) but here are suggested as causal off-flavours. This contradiction is likely related to the different matrix of the asparagus materials used (cooked spear versus instant soup) as well as the concentration of the specific compounds and the rest

of the profile. Regarding the non-volatile profile of the asparagus soups, six compounds were positively correlated with the cardboard taste attribute (Table 6.3), suggesting that these compounds are also potentially causal off-flavours. Table 6.4 summarizes the outcomes of our study and our proposal with respect to the asparagus flavours and off-flavours.

Table 6.4 Summarizing list of the confirmed asparagus sensory-relevant compounds which are known from the literature and the compounds that are proposed as new (off-)flavours based on this study. For the unidentified non-volatiles pos/neg refers to the mode of detection used.

Volatiles	Non-volatiles
Known flavour compounds (confirmed)	
Dimethyl sulphide	Asparagusic acid
2-Methoxy-3-isopropyl pyrazine	Protodioscin
New flavour compounds (suggested)	
3-Methyl-1-butanol	
1-Hexanol	
Octanal	
gcms_112 (alkane)	
gcms_115 (ether)	
gcms_43 (N-containing compound)	
gcms_76 (S-containing compound)	
Causal off-flavours (suggested)	
Pentanal	neg_204
(E)-2-Heptenal	neg_411
1-Octen-3-ol	neg_97
n-Caproic acid vinyl ester	pos_315
	pos_479
	pos_490

6.5. Conclusion

This sensory descriptive analysis showed that soup prototypes prepared with spray-dried asparagus powder made from concentrated asparagus juice had similar flavour notes to those prepared from a flavour-supplemented commercial powder. Adding asparagus fibre negatively affected the flavour and mouthfeel of the soup prototypes. Using advanced metabolomics tools, a chemical characterization of the soups was performed and the datasets of the two analyses (sensory and metabolomics) were fused and examined following Random Forest approaches. Not only key known asparagus odorants were highlighted and confirmed, but we also suggest new compounds with potential relevance for the sensory profile of the asparagus ingredients. In conclusion, this study has revealed that spray drying of asparagus concentrate is a promising processing method to produce flavour-rich asparagus powder, as

compared to the conventional oven-drying process. A similar process may be tested to upcycle other vegetable waste streams to produce flavour-rich food ingredients, in turn contributing to the sustainability of food systems. Ultimately, this could reduce the usage of supplemental flavourings in food products to make them more natural.

6.6. Appendix

Table A.6.1 Microbiological analysis of hygiene indicators after different processing steps of the asparagus juice (J) and asparagus fibre (F). ND: not determined.

Label	Processing step	Total viable count (kve/g)	*Entero bacteriacea* (kve/g)	*Lacto bacilli* (kve/g)	Yeast (kve/g)	Moulds (kve/g)	*B. cereus* (kve/g)	*S. aureus* (kve/g)
J-01	Asparagus juice (after pressing)	> $3.0 \cdot 10^5$	>$1.5 \cdot 10^5$	> $3.0 \cdot 10^5$	$1.0 \cdot 10^4$	$3.3 \cdot 10^4$	<10	<10
J-02	Microbial decontaminated juice	20	<10	<10	<10	<10	<10	<10
J-03	Concentrated juice	150	10	<10	<10	<10	<10	<10
J-04	Spray drying feed	230	10	<10	<10	<10	<10	<10
J-05	Spray-dried powder	$3.6 \cdot 10^3$	60	<10	<10	<10	<10	<10
F-01	Asparagus fibre (after pressing)	$6.4 \cdot 10^4$	95	$4.9 \cdot 10^4$	575	<10	<10	<10
F-02	Thawed and washed asparagus fibre	1100	<10	<10	<10	<10	<10	<10
F-03	Blanched asparagus fibre	100	<10	<10	<10	<10	<10	<10
F-04	Dried asparagus fibre	1300	450	<10	<10	<10	<10	ND
F-05	Milled asparagus fibre	$1.4 \cdot 10^4$	<10	<10	<10	<10	<10	<10

Table A.6.2 List of the 24 sensory attributes concerning the odour, taste, mouthfeel and after-feel sensation which were scored by the professionally trained panellists during the descriptive analysis of the six soup prototypes. A description is provided per attribute. The p-values are adjusted for false discovery rate for multiple comparisons after two-way ANOVA comparing the six soup prototypes (significant p-value < 0.05). The Quality Index (QI) is a measurement of the agreement between panellists concerning the differentiation between soups based on each attribute (QI>0.65 reliable data).

LABEL	ASPECT	ATTRIBUTE	ATTRIBUTE DESCRIPTION	*p*-Value	QI
O_Intensity	Odour	Intensity	Total odour intensity	<0,01	0,88
O_Asparagus	Odour	Asparagus	Total asparagus odour	<0,01	0,93
O_Potato	Odour	Potato	Total intensity of potato (all kinds of potato)	0,61	0,02
O_Maize	Odour	Maize	Total maize odour	<0,01	0,84
O_Green	Odour	Green	Total green odour (e.g. green beans)	0,09	0,48
T_Intensity	Taste	Intensity	Total taste intensity	<0,01	0,69
T_Asparagus	Taste	Asparagus	Total asparagus taste	<0,01	0,87
T_Artificial taste	Taste	Artificial	Total artificial taste	<0,01	0,76
T_Potato	Taste	Potato	Total potato taste (all kinds of potato)	0,06	0,60
T_Sweet	Taste	Sweet	Total sweet taste	0,04	0,65
T_Sour	Taste	Sour	Total sour taste	0,60	0,00
T_Salt	Taste	Salt	Total salty taste	0,05	0,56
T_Green	Taste	Green	Total green taste (e.g. green beans)	0,11	0,49
T_Grain	Taste	Wheat/grain	Total taste of Brinta, wheat, grain, bread	0,06	0,62
T_Maize	Taste	Maize	Total maize taste	0,21	0,43
T_Cardboard	Taste	Cardboard	Total taste of cardboard	<0,01	0,85
T_Chemical	Taste	Chemical	Total chemical taste (e.g. glue, chlorine)	0,02	0,69
T_Off-taste	Taste	Offtaste	Total off taste (e.g. liquorice, woody/earthy, old garlic)	0,12	0,55
M_Thickness	Mouthfeel	Viscosity	The degree to which the product feels viscous	<0,01	0,85
M_Slimy	Mouthfeel	Slimy	The degree to which the product feels (s)limy	<0,01	0,63

Table A.6.2 Continued.

LABEL	ASPECT	ATTRIBUTE	ATTRIBUTE DESCRIPTION	*p*-Value	QI
M_Powdery	Mouthfeel	Powdery	The degree to which the product feels powdery	<0,01	0,95
AF_Powdery	After-feel	Powdery	The degree to which the product gives a powdery aftertaste	<0,01	0,88
AF_Dry	After-feel	Dry	The degree to which the product gives a dry aftertaste	<0,01	0,82
AF_Tingling	After-feel	Tingling/stinging sensation	The degree to which the product gives a tingling/stinging sensation	0,04	0,64

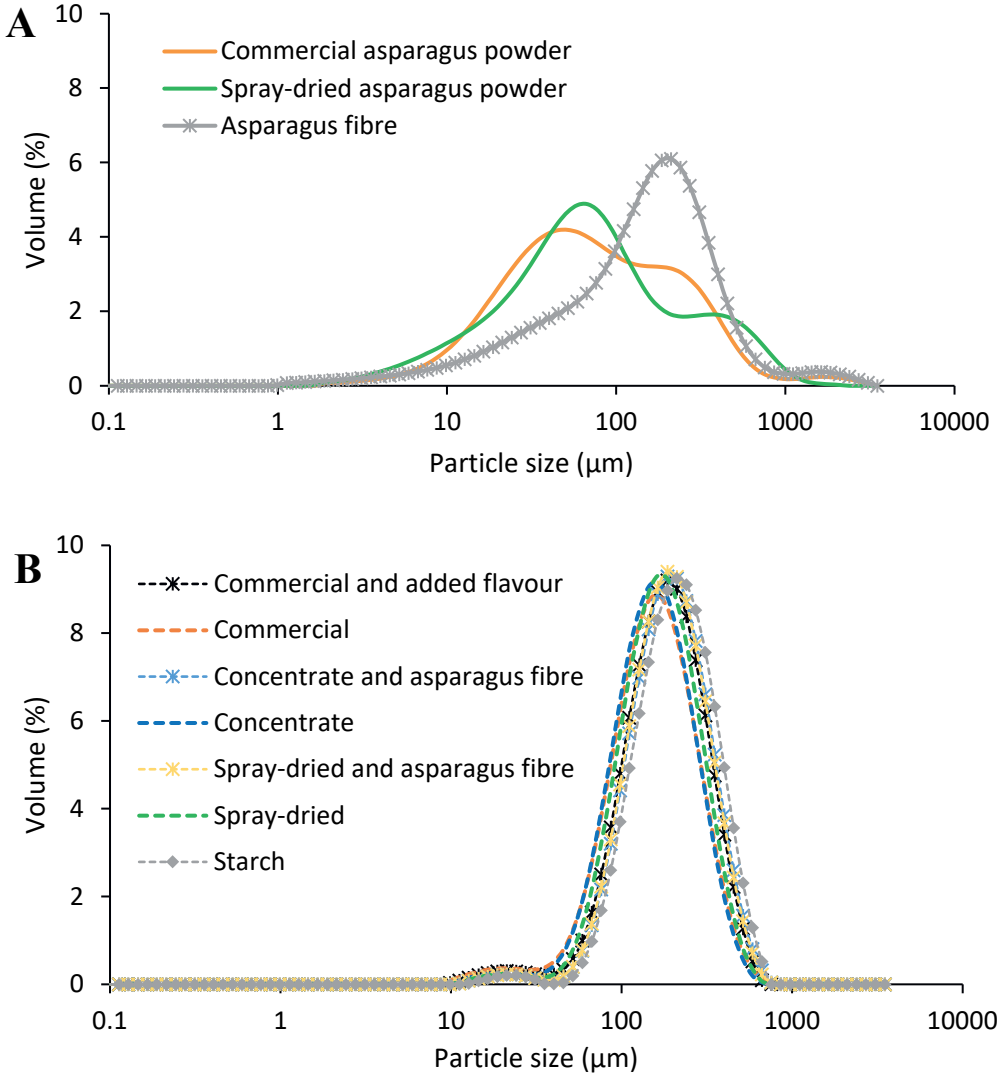

Figure A.6.1 Analysis of the physical properties of the asparagus ingredients used in the six soup prototypes. (A) Particle size distribution of the dried asparagus ingredients measured in the dry powder disperser Aero S (Mastersizer 3000, Malvern Inc, Malvern, UK). (B) Particle size distribution of the six soup prototypes formulated with different asparagus ingredients and only starch dissolved in hot water. The soups were analysed in the Hydro MV module (Mastersizer 3000, Malvern Inc, Malvern, UK) using water as the continuous phase.

6.7. Supplementary data

Supplementary data will be made available online after publication. If needed it can be made available upon request by email to joanne.siccama@wur.nl/joanne.siccama@outlook.com.

Chapter 7

General discussion

7.1. Introduction

The aim of this project was to develop a novel processing route using spray drying for conversion of vegetable waste streams into flavour-rich powder ingredients with specific focus on the waste streams of white asparagus. The project covered the entire process chain of the asparagus waste stream into asparagus powders including a sensory study and a more fundamental study on flavour release during drying amongst others. A split-stream processing method is proposed to separate the asparagus waste stream into juice and fibre fractions. Subsequently, the juice fraction is spray dried with a carrier to obtain a flavour-rich asparagus ingredient.

In this general discussion, the main findings of the thesis are presented, the processing approach for asparagus is translated to other vegetables, the potential of asparagus fibre hydrolysed is further explored, and the chapter is concluded with an outlook towards future research.

7.2. Main findings

The main findings of this thesis are schematically summarised in Fig. 7.1. The role of carrier agents and spray drying conditions was investigated for volatile compound retention and other properties of spray-dried asparagus powders. In **chapter 2**, we report about concentration of asparagus juice into asparagus concentrate (21.7 % w/w) and subsequent spray drying with maltodextrin DE12 (MD12) as carrier agent. We performed headspace GC-MS with untargeted metabolomics to assess the overall metabolite profile of the spray-dried asparagus powders and identified 70 volatile compounds. The maltodextrin content appeared positively correlated to the retention of an asparagus key odorant 1-octen-3-ol, as well as other alcohols and aldehydes. In addition, a higher concentration of maltodextrin in the feed led to powders with better physical properties. The Gordon-Taylor equation was fitted to the measured glass transition temperatures (T_g) of all samples, and we found a minimum weight fraction of 0.67 (w/dw) maltodextrin to obtain glassy asparagus powder for storing at ambient conditions.

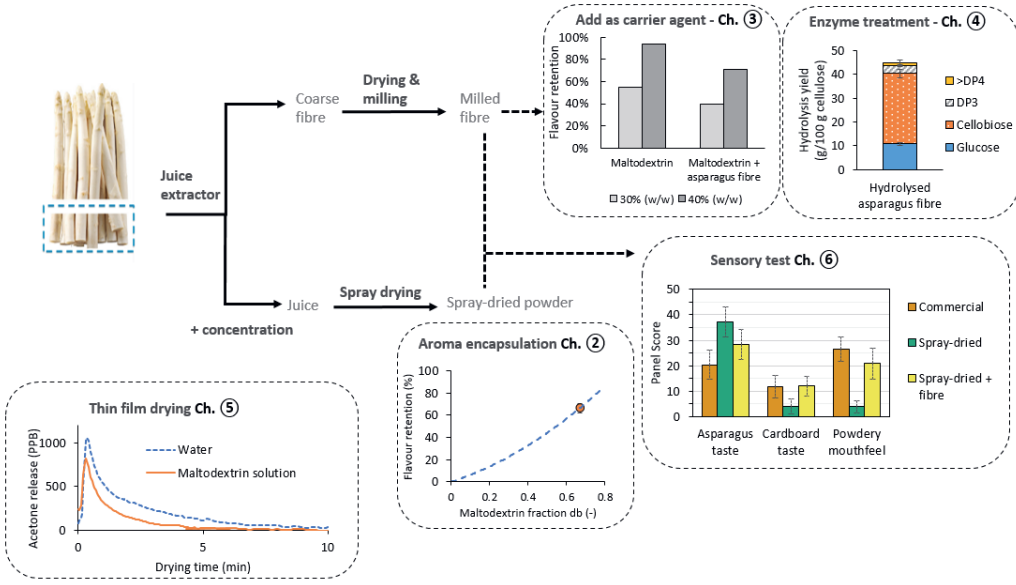

Figure 7.1 Schematic overview of the main findings in the thesis.

Ideally, the spray-dried powders consist fully of asparagus and do not require other additives such as maltodextrin. Furthermore, maltodextrin is high in calories therefore replacing it by vegetable fibres would be preferred. Therefore, in **chapter 3** different cellulose-based food materials were tested, i.e. asparagus fibre, citrus fibre or microcrystalline cellulose, to partially replace maltodextrin as carrier agent during spray drying. Asparagus concentrate was spray-dried with different carrier formulations varying the amount of cellulose-based carrier and MD12 at initial solid contents of 30 and 40 % w/w. Microcrystalline cellulose could replace up to 94 % of MD12. Asparagus fibre and citrus fibre could only replace MD12 up to 29 % due to fibre insolubility and increased viscosity of the feed. Partial replacement of maltodextrin by asparagus fibre and citrus fibre resulted in powders with similar physical properties as the control and did not detrimentally influence the aroma profiles as analysed by headspace solid-phase microextraction and gas chromatography-mass spectrometry. Powders obtained from feed solutions with an initial solids content of 40 % w/w showed in general better physical properties and aroma retention than 30 % w/w. It was thus demonstrated that fibre obtained from asparagus waste streams could potentially be used as a carrier up to 29 % of MD12 to produce spray-dried asparagus powder with retained key asparagus volatiles such as 2-methoxy-3-isopropyl pyrazine.

To improve the functionality of asparagus fibre as carrier agent an enzymatic treatment was proposed in **chapter 4** to convert the cellulose-rich asparagus fibre into cellobiose and cello-oligosaccharides (COS). The enzyme cocktail 'Celluclast' was used to steer towards maximum conversion and minimum formation of monosaccharides to obtain an enzymatic hydrolysate with a high T_g. Different enzyme loadings and hydrolysis times were tested in combination with a sodium hydroxide pre-treatment of the asparagus fibre. An enzyme loading of 700 nkat/g substrate and 7 h of hydrolysis time resulted in the best yield/purity combination, namely conversion of 36 g/ 100 g cellulose with 81 % celllobiose/COS. The same hydrolysis conditions were tested in a larger bench-scale experiment (conversion of 45 g/100 g cellulose) and the soluble hydrolysates were concentrated and spray-dried. The high T_g (108 ºC) of the spray-dried hydrolysates of asparagus fibre indicated its potential usage as a carrier agent for spray drying.

To better understand the mechanism of volatile release during spray drying and the role played by the encapsulates, we employed a thin-film dryer equipped with an electric nose to study volatile release in detail in **chapter 5**. Specifically, the effects of the initial solid content and dextrose equivalent (DE) of maltodextrin on the acetone release were investigated. A photo-ionisation detector monitored the release of acetone for 1 hour drying of thin films with initial solid contents of 20 to 40 % of maltodextrin (DE 12 or DE 21). Higher initial solid contents decreased the acetone release and could be correlated to a lower drying rate and quicker formation of a semi-permeable skin. The effect of DE on the acetone release was smaller with a lower DE resulting in slightly lower release. The experimental data obtained from the inline results were used to validate a drying model that describes the acetone release using the diffusion coefficients of water and acetone in maltodextrin solutions and the heat and mass transfer coefficients of the drying air.

In **chapter 6**, the newly developed asparagus ingredients following the split-stream processing approach and a commercial convectively dried asparagus powder were compared by evaluating their flavour profile in a soup formulation. The flavour profile was analysed using a trained sensory panel and metabolomics to provide information about important sensory-relevant compounds. The essential role of previously reported key asparagus odorants was confirmed. Seven new compounds were proposed to also contribute to key asparagus flavour notes and most of them were more abundant in the spray-dried powder. The spray-dried powder scored significantly higher on asparagus odour and taste compared

to the commercial powder. The fibre had a negative impact on the taste (e.g. cardboard and off-taste) and mouthfeel of the soups, which was also related to differentiations in the metabolite profile. The findings in this chapter indicate the feasibility of upcycling asparagus by-streams into flavour-rich ingredients with good sensorial properties for food applications.

7.3. Translation to other vegetables

The split-stream process proposed can effectively valorise asparagus waste stream into aroma-rich food ingredients. The learnings from asparagus could potentially be translated to other vegetables such as bell pepper which also contains a waste stream during its production. Bell pepper juice concentrate was prepared in a similar way as asparagus juice concentrate using membrane processing (Fig. 7.2), followed by spray drying with maltodextrin DE12 as carrier agent. The bell pepper juice samples and spray-dried bell pepper powders were analysed with solid-phase microextraction gas chromatography-mass spectrometry (SPME-GC-MS) for the profiling of the volatile composition of the different materials.

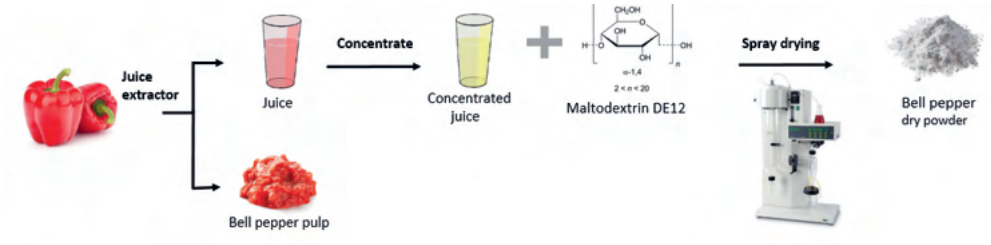

Figure 7.2 Schematic overview of the split-stream processing of red bell peppers. Red bell peppers are pressed and separated into juice (top) and bell pepper pulp (bottom). The juice is concentrated through membrane processing during which the red colour got lost. The concentrated juice is mixed with maltodextrin DE12. This mixture is dried into a fine bell pepper powder using the Büchi B-290 spray dryer.

7.3.1. Bell pepper concentrate

First, pressing of 60 kg fresh red bell peppers (seeds and stems removed, wet weight) yielded in a juice fraction of 50 kg and a fibre fraction of 10 kg. During subsequent juice processing, two waste streams were generated, namely a centrifugate and an ultrafiltration retentate. Together, these two waste streams represent 14 % of the juice fraction, the other 86 % was concentrated by reversed osmosis to yield the final concentrated juice. The concentrate contained 21 % w/w solids, resulting in a concentration factor of 3 compared to the juice (6.4

% w/w solids). During processing of the red bell pepper, the colour disappeared from the bell pepper concentrate (Fig. 7.3). The disappearance of colour might have led to the loss of flavour compounds as well. Therefore, the volatile profiles of the fresh bell pepper (starting material), the fibres, juice and residues of the various processing steps (Fig. 7.3) were analysed with SPME-GC-MS and their volatile profiles were compared via the raw chromatograms. Since the juice was concentrated, the peak areas of the volatile compounds should increase accordingly.

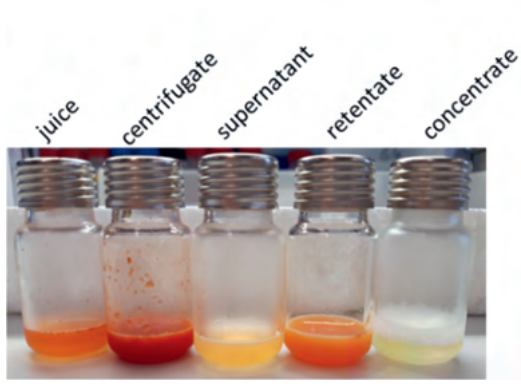

Figure 7.3 Glass vials containing the liquid samples from bell pepper processing that were analysed with SPME-GC-MS for profiling of the volatiles. *Juice* is the liquid obtained after pressing the bell peppers (Fig. 7.2), the *supernatant* is an intermediate product and *concentrate* is the final product, which was later spray-dried. *Centrifugate* and *retentate* are the residues generated during centrifugation and ultrafiltration, both leading to colour loss of the product.

Comparing the raw GC-MS chromatograms it can be derived that the volatile profile of the concentrate is richer compared to those of the juice, the fibre, and the starting material (fresh bell pepper) (Fig. 7.4). The volatile profile of the concentrated juice is also richer than those of the residue samples (centrifugate and retentate) (Fig. 7.5). By comparing the peak areas of individual peaks/compounds detected in the juice, retentate and concentrate, we could conclude that the concentration of volatile terpenes was successful (concentration factor based on peak areas ca. 3). It was not the same for other volatiles such as medium-chain aldehydes (concentration factor based on peak areas ca. 1.5-2) or the ‘bell pepper’ pyrazine (concentration factor based on peak areas ca. 1). Such compounds were, however, not more abundant in the retentate. Therefore, they are not lost with the red colour, but it might be that they are generally more labile.

The solid composition of the bell pepper juice concentrate was analysed and compared to that of asparagus juice concentrate (Table 7.1). The composition of both vegetable concentrates was similar and indicates that both concentrates are rich in monosaccharides (i.e. glucose and fructose) and also contain a significant fraction of soluble protein. It is therefore hypothesized that the physical properties of the spray-dried bell pepper and asparagus powder will be similar.

Table 7.1 Composition of asparagus juice concentrate and bell pepper juice concentrate.

Composition (g/100 g)	Asparagus concentrate	Bell pepper concentrate
Total solids	21.7	21.8
Protein	7.2	9.6
Sugars	14.5	15.4
Sucrose	*0.7*	*0.0*
Glucose	*6.6*	*7.3*
Fructose	*7.2*	*8.0*

7.3.2. Spray-dried bell pepper powder

Bell pepper concentrate was spray-dried using maltodextrin DE12 as carrier agent in a 1:2 ratio (bell pepper solids : maltodextrin) and 40 % (w/w) initial solids content. The bell pepper concentrate was dried at an inlet temperature (T_{in}) of 160 ºC and a feed flow rate of 0.54 L/h, which resulted in an outlet temperature (T_{out}) around 82 ºC. We compared the results to the spray-dried asparagus powder from **chapter 2**, which was also prepared with a 1:2 ratio of juice solids to maltodextrin. The asparagus juice concentrate was dried at the same T_{in} (160 ºC). It should be noted that the initial solids content of the asparagus feed solution was 45 % (w/w) since this solution was not diluted before drying. Furthermore, the T_{out} was somewhat higher, i.e. 90 ºC.

We hypothesized that the physical properties of the spray-dried bell pepper and asparagus powder will be similar due to the similarity in the composition of both juice concentrates (Table 7.1). Experimental results showed that the T_g of the obtained bell pepper powder (43.7 ºC) was indeed similar to that of asparagus powder (44.5 ºC).

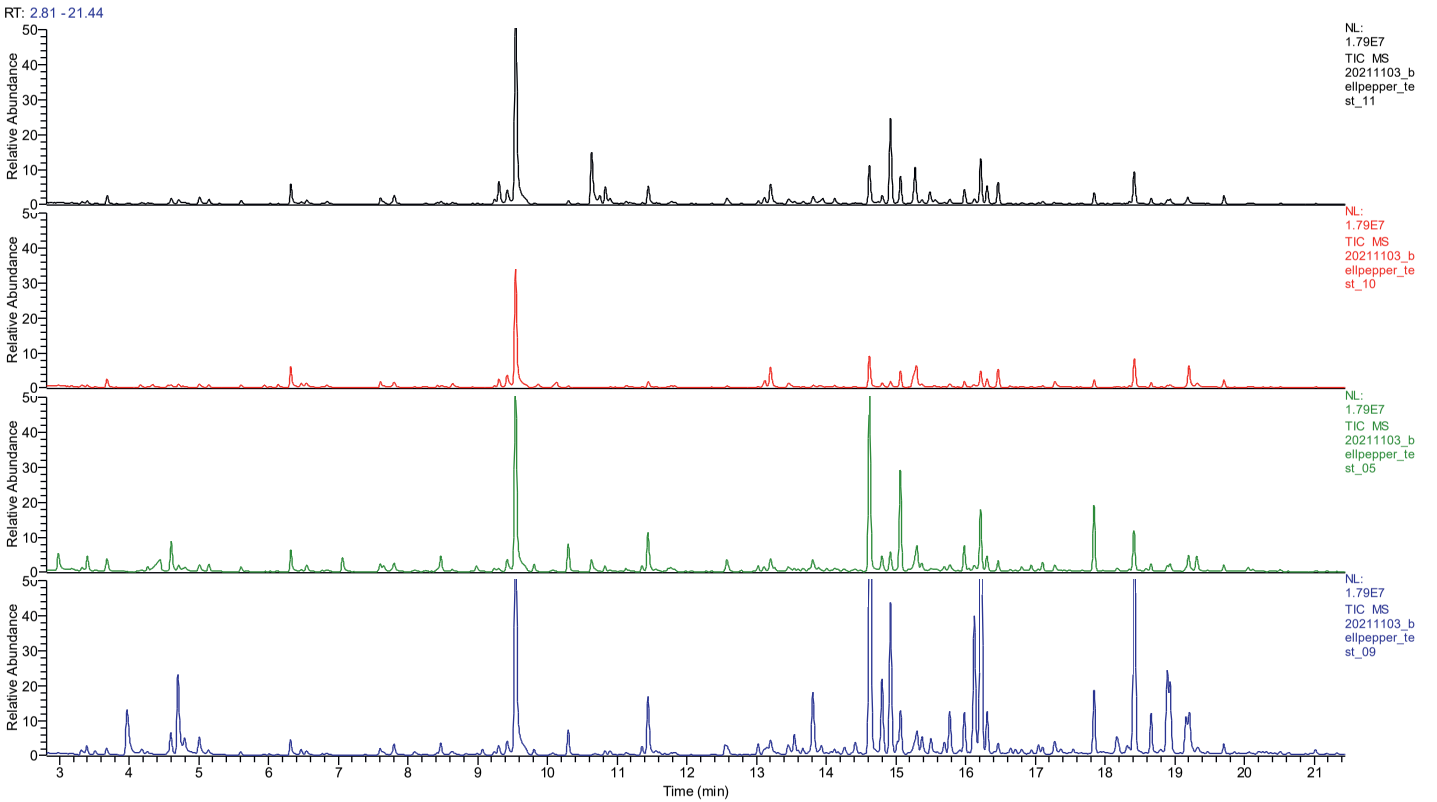

Figure 7.4 GC-MS chromatograms of the bell pepper samples showing their volatile profiles after extracted in the headspace using SPME; black: fresh bell pepper, red: fibre, green: juice, blue: concentrated juice. Chromatograms are presented in the same scale of the y axis (relative abundance). In the x axis is the retention time (min) of each compound (peak) during separation with GC and after detection in the MS.

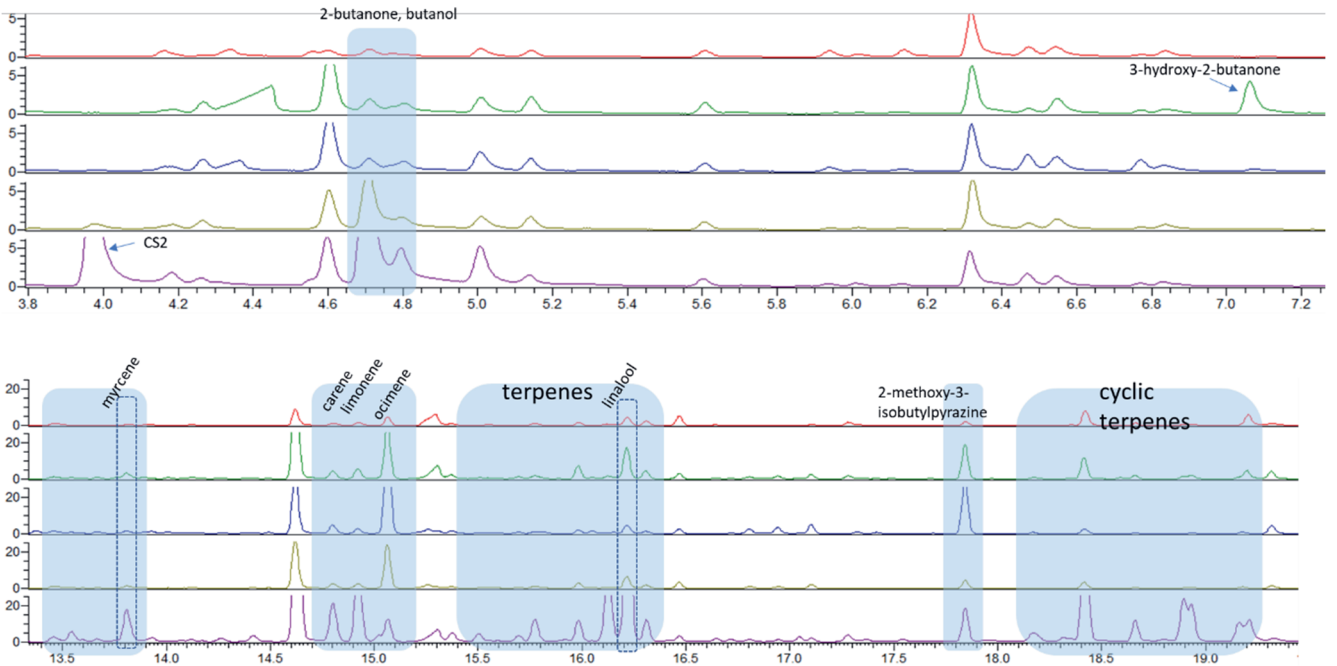

Figure 7.5 GC-MS chromatograms of the bell pepper samples showing their volatile profiles after being extracted in the headspace using SPME; red: fibre, green: juice, blue: centrifugate, yellow: retentate, purple: concentrated juice. Chromatograms are presented on the same scale of the y axis (relative abundance). In the x-axis is the retention time (min) of each compound (peak) during separation with GC and after detection in the MS. The blue boxes indicate peaks of known bell pepper aroma (group of) compound

Furthermore, the volatile profile of the spray-dried bell pepper powder was analysed. Direct comparison between flavour profiles of spray-dried bell pepper and asparagus powders is less relevant as the vegetables differ in composition of volatile compounds and their intensities. Nevertheless, several volatile compounds can be found in both vegetables and contribute to their characteristic flavour profile. These compounds include amongst others 2-methylbutanal, 3-methylbutanal, hexanal, dimethyl-sulphide and 2-methoxy-3-isopropyl pyrazine (Luning, De Rijk, Wichers, & Roozen, 1994; Luning, Yuksel, Vries, & Roozen, 1995; Wampler & Barringer, 2012). In particular, the latter is of importance for the characteristic bell pepper aroma (Buttery, Seifert, Guadagni, & Ling, 1969), although this compound also contributes to the earthy notes in asparagus (Pegiou et al., 2019). The compounds 2-methylbutanal, 3-methylbutanal and dimethyl sulphide are generally related to dried vegetables, as the formation of these compounds is heat-induced (Tressl, Bahri, et al., 1977).

We compared the volatile profile of the spray-dried bell pepper powder with that of a commercial bell pepper powder produced with hot air drying. It was found that the commercial powder had overall a richer volatile profile compared to the spray-dried bell pepper powder. Selected compounds known as bell pepper odorants were specifically analysed (Table 7.2). Compounds known to be formed under long exposure to high temperatures (e.g. dimethyl sulphide, 3-methylbutanal) were more abundant in the spray-dried powder than in the feed solution, but even more abundant in the commercial powder. It was hypothesized that the level of these flavours could still increase when the reconstituted spray-dried bell pepper powder is heated. This was checked by dissolving the powders in hot water (90 °C) for 15 min to mimic the instant soup preparation (Table 7.2). Indeed, it was observed that the level of heat-induced compounds increased for both the reference powder as well as the spray-dried powder although the final levels are far from similar for both powders. 2-Methoxy-3-isopropyl pyrazine reduced in abundance after spray drying, which is in line with Luning, Yuksel, Vries, & Roozen (1995) who also found that this pyrazine is more abundant in fresh bell peppers and will reduce after drying. The abundance of 2-methoxy-3-isopropyl pyrazine was higher in the spray-dried powder than in the commercial reference, which suggests that its encapsulation was more successful during spray drying. Furthermore, the abundance of this pyrazine was reduced during the soup preparation. Lastly, it should be noted that the bell peppers used for the commercial powder are most likely from

a different variety than the bell peppers that were spray-dried. Therefore, it is suggested that not only the drying process but also the bell pepper varieties could contribute to the differences observed in the relative abundance of the flavour compounds.

Table 7.2 Selected volatile compounds which are known bell pepper odorants and detected in the bell pepper samples analysed with SPME-GC-MS. Relative abundances of dimethyl sulphide, 2-methylbutanal, 3-methylbutanal, hexanal and 2-methoxy-3-isobutylpyrazine in the feed solution before spray drying, spray-dried bell pepper powder and commercial reference bell pepper powder are reported. The samples were analysed directly after dissolution in a CaCl2 – EDTA solution or the samples were first heated at 90 ºC for 15 min in the same solution to mimic the instant soup preparation, these samples are referred to as *in soup*.

Flavour compound (x 10^5)	Feed solution	Spray-dried	Spray-dried in soup	Reference	Reference in soup
Dimethyl sulphide	$2.0 \cdot 10^4$	$5.2 \cdot 10^5$	$1.2 \cdot 10^6$	$3.4 \cdot 10^6$	$2.2 \cdot 10^6$
2-Methylbutanal	$4.3 \cdot 10^5$	$1.5 \cdot 10^6$	$1.8 \cdot 10^6$	$7.0 \cdot 10^6$	$7.9 \cdot 10^6$
3-Methylbutanal	$6.3 \cdot 10^5$	$2.3 \cdot 10^6$	$2.9 \cdot 10^6$	$1.2 \cdot 10^7$	$1.6 \cdot 10^7$
Hexanal	$6.4 \cdot 10^5$	$9.0 \cdot 10^5$	$1.5 \cdot 10^6$	$4.1 \cdot 10^6$	$6.8 \cdot 10^6$
2-Methoxy-3-isobutyl pyrazine	$1.1 \cdot 10^6$	$9.1 \cdot 10^5$	$7.5 \cdot 10^5$	$1.7 \cdot 10^5$	$1.7 \cdot 10^5$

7.3.3. Conclusions

During membrane concentration, the bell pepper concentrate lost its red colour. However, the volatile profile of the concentrate was found richer compared to those of the juice, the fibre and the starting material (fresh bell pepper). The spray-dried powder was found to have a less rich volatile profile compared to the commercial reference bell pepper powder prepared from hot air-dried and milled bell pepper. However, flavours in the reference powder are most probably formed upon long exposure to heat. Reconstitution of the spray-dried bell pepper powder in hot water increased the formation of heat-induced compounds. The results imply that there is potential for adopting a similar approach for bell pepper as for asparagus for making a spray-dried vegetable powder, although the colour of bell pepper is lost. Future studies should indicate if the colourless spray-dried bell pepper powder is of commercial interest and sensory testing with the spray-dried bell pepper should be done including a cooking step after reconstitution.

7.4. Application of asparagus fibre as carrier agent

In **chapter 4**, enzymatic hydrolysis of asparagus fibre following an alkaline pre-treatment yielded in hydrolysates mainly contain cellobiose and COS. The potential of the hydrolysed asparagus fibre as carrier agent was indicated given its high T_g (108 ºC). However, other important aspects should be considered for the future application of hydrolysed asparagus and the upscaling of the process, including the flavour profile of the hydrolysates, the economic aspects of the enzymatic processing and the overall scale of asparagus fibre waste in the Netherlands.

7.4.1. Flavour profile of the hydrolysed fibre

The volatile flavour profile of the asparagus hydrolysate was analysed with GC-MS and compared to that of fresh asparagus fibre (unprocessed, see Fig. 7.6). Each sample was weighed to a total solid content of 90 mg and all samples were analysed in duplicate. We specifically focussed on the volatile compounds that are considered key odorants for asparagus that were previously described by Pegiou et al. (2019) and in **chapter 6**.

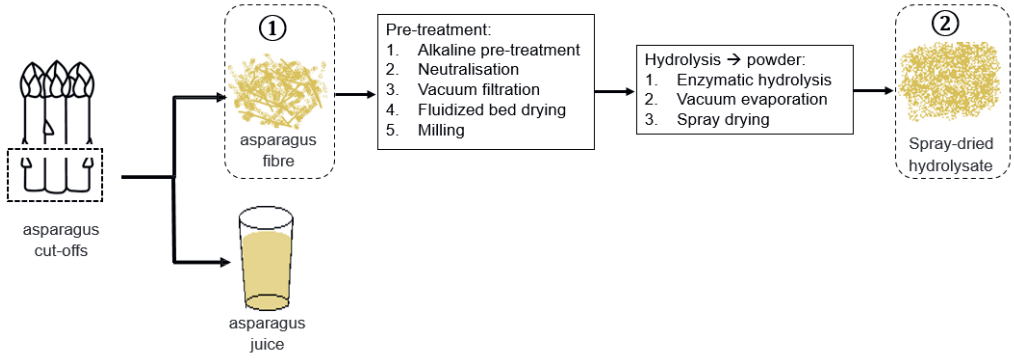

Figure 7.6 Processing of asparagus fibre (1) into spray-dried asparagus hydrolysate powder (2) following the same processing steps as described in Chapter 4. The volatile flavour profiles of the asparagus fibre and hydrolysate were analysed with GC-MS.

The volatile profile of the asparagus hydrolysate was different from the fresh asparagus fibre and most of the compounds decreased in abundance (Fig. 7.7). The lack of asparagus key odorants in the spray-dried asparagus fibre hydrolysates was likely to be caused by some processing steps that were used to produce the powder, e.g. vacuum evaporation.

Nevertheless, the lack of aromatic compounds could be an advantage when applying the fibre hydrolysates as encapsulates during spray drying or as additives in food products (e.g. as prebiotics). In addition, several medium chain aldehydes, e.g. e-2-hexenal, 2-heptenal and pentanal, are linked to potential cardboard off-flavours (Blanda et al., n.d.), which was also suggested in **chapter 6**. Lowering the intensity of these compounds could be beneficial to reduce off-flavours.

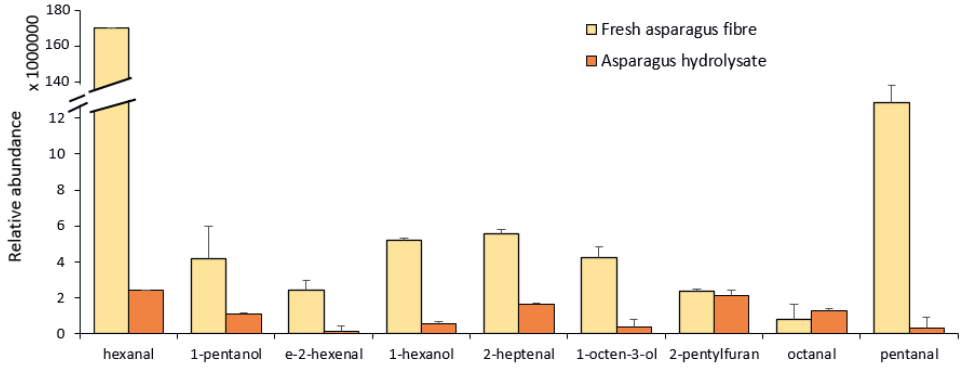

Figure 7.7 Selected volatile compounds which are known as asparagus odorants and detected in the fresh asparagus fibre and asparagus hydrolysate analysed with SPME-GC-MS.

7.4.2. Mass balance of the process

To evaluate the potential of large-scale enzymatic hydrolysis of asparagus fibre, we considered the availability of asparagus waste generated in the Netherlands and the conversion efficiency. Fig. 7.8 gives an overview of the mass balances (dry basis) of the entire process. The largest fraction after juice extraction ends up in the juice stream and relatively few losses occur until spray drying of the juice concentrate. Some losses occurred during centrifugation and membrane filtration of the juice. Processing the fibre fraction into soluble compounds by hydrolysis leads to higher losses. Firstly, 21 kg of the fibres consist of non-cellulose compounds (e.g. hemicellulose, lignin, sugars) and this fraction cannot be hydrolysed using the cellulase cocktail described in **chapter 4**. Secondly, the enzymatic conversion of cellulose has a yield of ± 45 % based on the experimental conditions tested, thus an additional fraction of unreacted cellulose remains. It would be of interest to explore opportunities to reintroduce the unhydrolyzed cellulose into the process to increase the overall conversion yield. Furthermore, hydrolysis of hemicellulose could potentially increase the conversion of fibre into reaction products. However, this requires an in-depth study of

the type of hemicelluloses present in the asparagus fibre first. Consequently, it needs to be evaluated if potential reaction products of hemicellulose hydrolysis would be of interest.

In the mass balance, maltodextrin is used as carrier agent for spray drying of the asparagus juice concentrate using a 1:2 ratio of juice concentrate to maltodextrin, which was found as the best ratio based on **chapter 2**. Ideally, we want to use the hydrolysed cellulose stream as carrier agent for spray drying the juice concentrate. Based on the sizes of the streams, only a small fraction of juice concentrate could be spray-dried using hydrolysed cellulose. Therefore, an additional carrier agent would remain necessary when it is desired to spray dry all juice concentrate.

In the Netherlands roughly ~ 3000 tons of collectable asparagus waste with 7 % dry matter is available (**chapter 1**). This would translate to 17 tonnes of hydrolysed cellulose and 342 tonnes of spray-dried powder with maltodextrin as carrier agent.

7.4.3. Techno-economic assessment

A techno-economic assessment of the asparagus hydrolysis process is made based on the proposed process (Fig. 7.6). Before the assessment, some remarks need to be made. First, the processing of asparagus fibre included a drying step after pre-treatment in the experimental set-up, which was performed to control the dosage of the substrate for hydrolysis. For industrial applications, this drying step will be omitted, as the enzymatic hydrolysis could directly be performed after the neutralisation of the pre-treated fibres. Furthermore, the experiments in **chapter 4** were designed for Eppendorf tubes and relatively low solid loadings were used (25 g/L) as mixing was difficult. Consequently, the concentration of reaction products was low and to obtain a spray-dried hydrolysate a significant amount of water would need to be removed. Larger reaction vessels likely could facilitate higher solid loadings due to better mixing. The higher concentration of reaction products will reduce the amount of water to be removed making the overall process less energy-intensive.

The costs of the enzymatic conversion are estimated based on the bioethanol production costs from lignocellulosic biomass. Bioethanol production involves a series of steps to convert the biomass. First, the biomass is pre-treated (physical and/or chemical treatment) to improve enzyme accessibility. Also, the lignin fraction is removed as this is a nonfermentable fraction that otherwise interferes with subsequent processing steps.

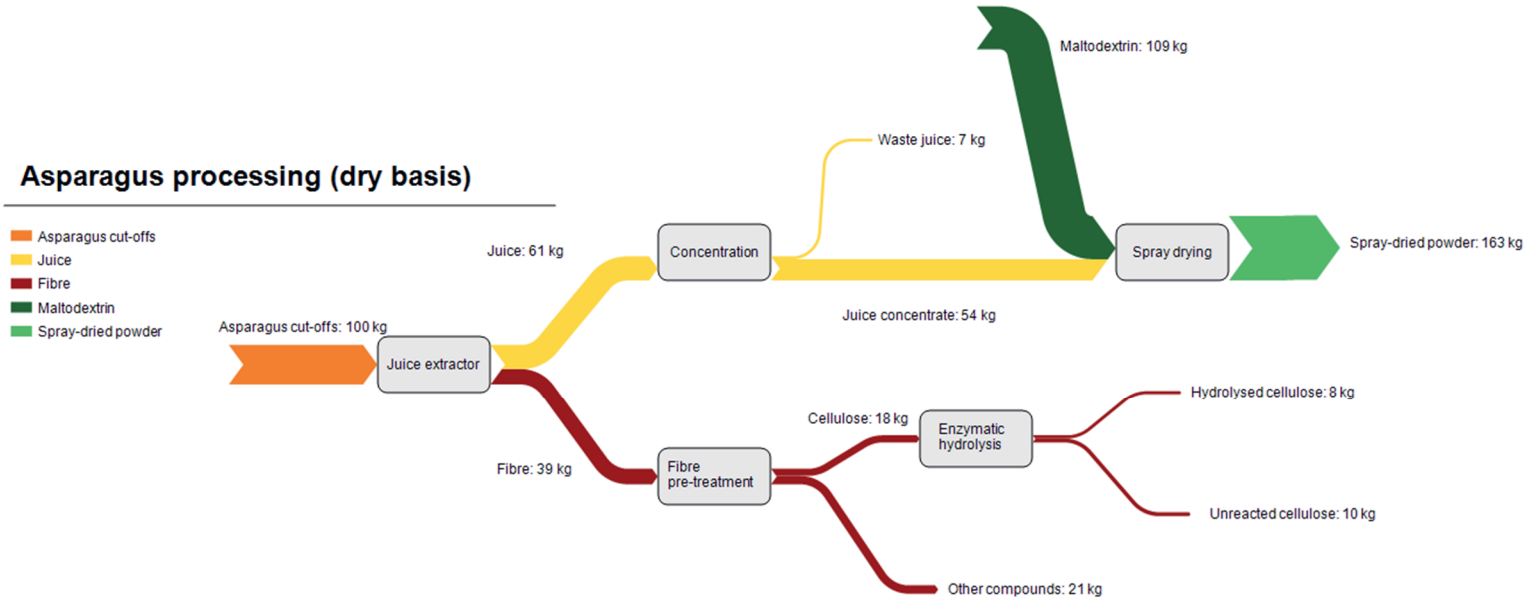

Figure 7.8 Mass balance on dry basis of processing 100 kg asparagus cut-offs following the split-stream processing approach in combination with enzymatic hydrolysis of the asparagus fibre.

Next, the cellulose and/or hemicellulose are hydrolysed into soluble fermentable hexose and pentose sugars by using cellulases and hemicellulases. Finally, the sugars are fermented into ethanol, which is frequently done using the yeast *Saccharomyces cerevisiae* (Cuellar & Straathof, 2014). The fermentation step is not part of the enzymatic conversion of asparagus into soluble compounds and should therefore be excluded from the cost estimation.

The costs of bioethanol production depend for a significant part on the feedstock used. A differentiation is made between so-called "first generation" and "second generation" feedstocks. First-generation feedstocks (1G) often comprise sugar- and starch-containing materials and therefore compete with their conventional use as food or feed. Second generation (2G) feedstocks involve lignocellulosic biomass, such as straw, agricultural waste, and crop and wood residues. These feedstocks are not competitive with food and feed crops (Bušić et al., 2018). The advantage of 1G feedstocks is that they are often easily fermented. The disadvantage is that they compete with food and feed production and are considered therefore less sustainable, and their price is higher than of 2G feedstocks. The asparagus fibre by-streams are classified as 2G feedstock since they consist of lignocellulose and are not used for consumption.

Macrelli et al. (2012) performed a techno-economic evaluation of 2G bioethanol production from 'bagasse' (dry pulp residue after the extraction of juice from sugar cane) and sugar cane leaves. Different scenarios were investigated. The scenarios differed in the integration of processing sugar cane (1G feedstock) in the 2G process through the exchange of heat and streams, the addition of leaves to the 2G feedstock, the enzyme dosage for hydrolysis (low/high) and the hydrolysis time (48/72 h). We selected "scenario E" for in-depth analysis, this scenario did not integrate heat and streams from the 1G process, no leaves, high enzyme loading and 48 h of hydrolysis. The minimum ethanol selling price for scenario E is 1.15 €/L (Table 7.3). The enzymes, energy, and capital costs contributed significantly to the selling price. It should be noted that part of the energy supply of the plant was provided by energy generated from the pentose-rich liquid fraction obtained after filtration of the pre-treated material and from the solid residues after hydrolysis. Therefore, energy costs without these processes would be higher. The costs for chemicals used in the pre-treatment (acid and bases) contributed to 6 % of the selling price. Based on these numbers, it can be concluded that enzymes largely determine the total costs of bioethanol production and the same will likely be the case for asparagus fibre hydrolysis. Fortunately, cellulase enzyme prices have been

reduced more than 10 times in the last decades and continue to decrease (Bušić et al., 2018). Nevertheless, it is worth exploring possibilities for recovery of the enzymes as cellulases remain active after hydrolysis.

Table 7.3 Cost overview of 2G bioethanol production, adapted from (Macrelli et al., 2012) using an exchange rate of 0.92 €/US$.

Cost item	€/L	%
Enzymes	0.43	37.6
Acid	0.06	4.8
Base	0.01	0.8
Water consumption	0.03	2.4
Labour, maintenance, insurance	0.07	6.4
Electricity export/opportunity cost	0.25	21.6
Capital cost	0.30	26.4
Minimum ethanol selling price	1.15	100

To estimate the costs for asparagus hydrolysis based on the bioethanol costs, there are a few things to consider. First, although, the fermentation step is not part of the asparagus fibre hydrolysis, the effect on the total costs will be relatively small as the yeast for fermentation is recovered and enzymatic hydrolysis requires higher temperatures than fermentation (Cuellar & Straathof, 2014; Macrelli et al., 2012). Furthermore, bioethanol is recovered through the distillation of the ferment. We obtained the hydrolysate in powder-form through vacuum evaporation and spray drying. The specific heat of vaporization of ethanol (879 kJ/kg) is about three times lower than that of water (2257 kJ/kg), therefore evaporation of water is more energy-intensive than ethanol. Furthermore, the ratio of ethanol and water is high since the substrate for hydrolysis (water-insoluble solids) is 7 % in the study by Macrelli et al. (2012). The substrate will not be fully converted into ethanol, thus the ethanol concentration will be less than 7 %. The substrate concentration used in our study was even lower (2.5 %) but could probably be increased to 7 % as well when using larger reaction vessels. Nevertheless, still, more than 93 % of water needs to be removed after hydrolysis to obtain the hydrolysate in powder form.

The costs for processing up until the enzymatic hydrolysis step were estimated based on the 1.15 €/L for bioethanol, which converts to 1.46 €/kg bioethanol. As the fermentation step is not part of the asparagus fibre processing, we compare the wet asparagus hydrolysate to the intermediate product *glucose* that is formed in the bioethanol case. Based on conversion losses during fermentation of glucose into ethanol (e.g. formation of CO_2), the estimated costs for the asparagus hydrolysate are 0.75 €/kg on dry basis. However, these costs are excluding the drying step.

To estimate the drying costs of the hydrolysate, the energy and economic evaluation of spray drying described by Qiu (2019) was used. The assumptions in Table 7.4 were made to determine the capital expenditures (CAPEX) and operating expenditures (OPEX). We used a relatively small spray dryer (dewatering capacity of 50 kg/h) as for the yearly production of 17 tons of hydrolysate roughly 340 tons of water (95 % w/w) needs to be removed. The CAPEX costs for the spray dryer (€ 610,000) were obtained from (Qiu, 2019), who plotted the spray dryer investment costs as function of the dewatering capacity.

Table 7.4 Assumptions used for OPEX calculations spray dryer, adapted from (Qiu, 2019).

Category	Assumptions
Gas price	0.025 €/kWh
Electricity price	0.06 €/kWh
Operating hours	7000 h/year
Dewatering capacity	50 kg/h
CAPEX	610,000 €
Maintenance costs	3 % of CAPEX
Contingency costs	15 % of CAPEX
Produced hydrolysate	17 ton/year
Water removal	340 ton/year
Depreciation	10 years

Based on the CAPEX and OPEX, the yearly costs for operation (excluding personnel) are €101,000. This translates into 0.30 €/kg of water removed and 5.96 €/kg hydrolysate. The production costs of hydrolysis and dewatering together will be 6.71 €/kg hydrolysate.

Compared to the costs for enzymatic hydrolysis, the drying costs are very large. It is therefore recommended to apply a more efficient concentration step such as evaporation before spray drying to reduce costs.

This business case provides a rough estimation of the costs needed for the production of the asparagus hydrolysate. There is not a comparable product in the market that we could use as a direct reference. The asparagus fibre hydrolysate is a more high-end product than the maltodextrin that we want to replace. The asparagus hydrolysate provides health benefits as cellobiose and oligosaccharides are prebiotics (Karnaouri, Matsakas, Krikigianni, et al., 2019; Sanz et al., 2005). It is evident that it will be more expensive than maltodextrin. We compared the estimated price of the asparagus hydrolysis with that of commercially available citrus fibre. Citrus fibre is obtained from side streams of the orange juice industry and has prebiotic properties. The selling price of food-grade citrus fibre from the company CitrusStar is ~ 13.80 €/kg (15 US$/kg). If the selling price of asparagus hydrolysate will be similar, the process could be profitable.

7.5. Future directions for research

This thesis investigated a promising route to process asparagus waste into a flavour-rich food ingredient. Spray drying of asparagus juice concentrate with a carrier agent proved to be an effective strategy to encapsulate volatile flavour compounds. The research methodologies developed in this thesis could also be used to investigate spray drying of other matrices with volatiles, for example, essential oils. Essential oil comprises volatile and semi-volatile organic compounds determining its specific flavour attributes. Spray drying of oil-in-water emulsions is a suitable encapsulation technique to protect the flavour of essential oils. Spray drying emulsions will, however, add complexity compared to the matrices used in this thesis as the oil phase is immiscible in water and therefore will act as a separate phase. Research directions could involve the evaluation of drying kinetics and volatile release during thin film drying of emulsions. Furthermore, the role of carrier materials, e.g. maltodextrin, on the encapsulation efficiency of volatile aroma compounds in emulsions should be evaluated.

The sensory study indicated that the addition of asparagus fibre negatively influenced the flavour profile and mouthfeel of the soup prototypes. Enzymatic hydrolysis of the asparagus fibre already proved that the functionality of the fibre could be increased. It would be of interest to explore other processes and/or applications to valorise the asparagus fibre. For

example, the addition of asparagus fibre in traditional foods could increase dietary fibre intake among consumers and thereby improve their health. For the sensory study, the asparagus fibre was oven-dried, milled and sieved to obtain a fine powder. The asparagus fibre powder could alternatively be used for fortification of dietary fibre in bread, which is considered a suitable carrier for fibre-fortification (L. Zhang et al., 2019). Furthermore, asparagus fibre could be added as an ingredient in functional beverages. Beverages are interesting as functional foods as they are excellent delivery systems for nutrients and bioactive compounds. Furthermore, beverages provide convenience and the possibility to meet consumer demands for container contents, size, shape, and appearance (Corbo, Bevilacqua, Petruzzi, Casanova, & Sinigaglia, 2014). The insolubility of the asparagus fibre could, however, lead to phase separation of the beverage because of sedimentation. Homogenisation could stabilise asparagus fibre dispersions and thereby improve their functionality. Valoppi et al. (2021) demonstrated that the insoluble fractions of oat side streams were able to form stable suspensions and emulsions after mechanical treatment (i.e. high-pressure homogenization).

Finally, the combination of food process engineering and plant metabolomics in this project generated valuable insights. This combination could be applied to other projects as well to understand the effect of food processing on volatile and non-volatile flavour compounds.

7.6. Conclusions

The work reported in this thesis has provided insights on the retention of flavour compounds during spray drying of asparagus following a split-stream processing approach. The split-stream process enabled the production of flavour-rich spray-dried powder and facilitated complete valorisation of the asparagus waste stream. The same approach can be used for other vegetables as well, as indicated with the red bell pepper study. Next to spray drying of asparagus juice concentrate, asparagus fibre was converted into soluble cellobiose and cello-oligosaccharides by enzymatic hydrolysis, but other strategies were proposed as well. In addition to lab-scale spray drying experiments, the thin film drying experiments provided information on flavour release during the drying process. Novel insights on spray drying of asparagus are obtained and conclusions are drawn on directions for future research to develop high-quality products which are functional and have excellent sensorial properties.

R

References

Alqahtani, N. K., Ashton, J., Katopo, L., Haque, E., Jones, O. A. H., & Kasapis, S. (2014). Consistency of UHT beverages enriched with insoluble fibre during storage. *Bioactive Carbohydrates and Dietary Fibre*, *4*(1), 84–92. https://doi.org/10.1016/J.BCDF.2014.06.005

Anandharamakrishnan, C., & Padma Ishwarya, S. (2015). Encapsulation of flavors and specialty oils. In *Spray Drying Techniques for Food Ingredient Encapsulation* (pp. 126–155). John Wiley & Sons, Ltd. https://doi.org/https://doi.org/10.1002/9781118863985.ch6

AOAC Method 2002.04. (2002). Amylase-treated neutral detergent fiber in feeds. *Official Method of Analysis of the Association of Official Analytical Chemists*.

AOAC Method 973.18. (1973). Fiber (acid detergent) and lignin in animal feed. *Official Method of Analysis of the Association of Official Analytical Chemists*.

Apintanapong, M., & Noomhorm, A. (2003). The use of spray drying to microencapsulate 2-acetyl-1-pyrroline, a major flavour component of aromatic rice. *International Journal of Food Science & Technology*, *38*(2), 95–102. Retrieved from https://www.academia.edu/8592821/The_use_of_spray_drying_to_microencapsulate_2_acetyl_1_pyrroline_a_major_flavour_component_of_aromatic_rice

Appelqvist, I. A. M., Cochet-Broch, M., Poelman, A. A. M., & Day, L. (2015). Morphologies, volume fraction and viscosity of cell wall particle dispersions particle related to sensory perception. *Food Hydrocolloids*, *44*, 198–207. https://doi.org/10.1016/J.FOODHYD.2014.09.012

Aprea, E., Corollaro, M. L., Betta, E., Endrizzi, I., Demattè, M. L., Biasioli, F., & Gasperi, F. (2012). Sensory and instrumental profiling of 18 apple cultivars to investigate the relation between perceived quality and odour and flavour. *Food Research International*, *49*(2), 677–686. https://doi.org/10.1016/j.foodres.2012.09.023

Asioli, D., Aschemann-Witzel, J., Caputo, V., Vecchio, R., Annunziata, A., Næs, T., & Varela, P. (2017). Making sense of the “clean label” trends: A review of consumer food choice behavior and discussion of industry implications. *Food Research International*, *99*, 58–71. https://doi.org/10.1016/j.foodres.2017.07.022

Assaf, S., Hadar, Y., & Dosoretz, C. G. (1997). 1-Octen-3-ol and 13-hydroperoxylinoleate are products of distinct pathways in the oxidative breakdown of linoleic acid by Pleurotus pulmonarius. *Enzyme and Microbial Technology*, *21*(7), 484–490. https://doi.org/10.1016/S0141-0229(97)00019-7

Avaltroni, F., Bouquerand, P. E. E., & Normand, V. (2004). Maltodextrin molecular weight distribution influence on the glass transition temperature and viscosity in aqueous solutions. *Carbohydrate Polymers*, *58*(3), 323–334. https://doi.org/10.1016/J.CARBPOL.2004.08.001

Ávila, P. F., Silva, M. F., Martins, M., & Goldbeck, R. (2021). Cello-oligosaccharides production from lignocellulosic biomass and their emerging prebiotic applications. *World Journal of Microbiology and Biotechnology*, *37*(5), 1–11. https://doi.org/10.1007/s11274-021-03041-2

Bali, G., Meng, X., Deneff, J. I., Sun, Q., & Ragauskas, A. J. (2015). The effect of alkaline pretreatment methods on cellulose structure and accessibility. *ChemSusChem*, *8*(2), 275–279. https://doi.org/10.1002/cssc.201402752

Bangs, W. E., & Reineccius, G. A. (1982). Influence of dryer infeed matrices on the retention of volatile flavor compounds during spray drying. *Journal of Food Science*, *47*(1), 254–259. https://doi.org/10.1111/j.1365-2621.1982.tb11072.x

Bearth, A., Cousin, M.-E., & Siegrist, M. (2014). The consumer's perception of artificial food additives: Influences on acceptance, risk and benefit perceptions. *Food Quality and Preference*, *38*, 14–23. https://doi.org/10.1016/J.FOODQUAL.2014.05.008

Beldman, G., Voragen, A. G. J., Rombouts, F. M., Searle-Van Leeuwen, M. F., & Pilnik, W. (1988). Specific and nonspecific glucanases from *Trichoderma viride*. *Biotechnology and Bioengineering*, *31*(2), 160–167. https://doi.org/10.1002/bit.260310209

Belitz, H. D., Grosch, W., & Schieberle, P. (2008). *Food Chemistry*. Springer Science & Business Media.

BeMiller, J. N. (2019a). Cellulose and cellulose-based hydrocolloids. In *Carbohydrate Chemistry for Food Scientists* (pp. 223–240). Elsevier. https://doi.org/10.1016/b978-0-12-812069-9.00008-x

BeMiller, J. N. (2019b). Starches: Conversions, modifications, and uses. In *Carbohydrate Chemistry for Food Scientists* (pp. 191–221). AACC International Press. https://doi.org/10.1016/B978-0-12-812069-9.00007-8

Bettenhausen, H. M., Benson, A., Fisk, S., Herb, D., Hernandez, J., Lim, J., … Hayes, P. M. (2020). Variation in sensory attributes and volatile compounds in beers brewed from genetically distinct malts: An integrated sensory and non-targeted metabolomics approach. *Journal of the American Society of Brewing Chemists*, *78*(2), 136–152. https://doi.org/10.1080/03610470.2019.1706037

Bhandari, B. . R., & Howes, T. (1999). Implication of glass transition for the drying and stability of dried foods. *Journal of Food Engineering*, *40*(1–2), 71–79. https://doi.org/10.1016/S0260-8774(99)00039-4

Bischof, R. H., Ramoni, J., & Seiboth, B. (2016, June 10). Cellulases and beyond: The first 70 years of the enzyme producer *Trichoderma reesei* . *Microbial Cell Factories*. BioMed Central Ltd. https://doi.org/10.1186/s12934-016-0507-6

Blanda, G., Cerretani, L., Comandini, P., Gallina Toschi, T., & Lercker, G. (n.d.). Investigation of off-odour and off-flavour development in boiled potatoes. *2010*, *118*. https://doi.org/10.1016/j.foodchem.2009.04.135

Boel, E., Koekoekx, R., Dedroog, S., Babkin, I., Vetrano, M. R., Clasen, C., & Van den Mooter, G. (2020). Unraveling particle formation: From single droplet drying to spray drying and electrospraying. *Pharmaceutics*, *12*(7), 1–58. https://doi.org/10.3390/pharmaceutics12070625

Bonazzi, C., & Dumoulin, E. (2011). Quality changes in food materials as influenced by drying processes. In *Modern Drying Technology: Product Quality and Formulation* (pp. 1–20). Retrieved from https://pdfs.semanticscholar.org/b2ec/b64b13f1eb2ecb24a1217fea477474de4c30.pdf

Both, E. M., Boom, R. M., & Schutyser, M. A. I. (2020). Particle morphology and powder properties during spray drying of maltodextrin and whey protein mixtures. *Powder Technology*, *363*, 519–524. https://doi.org/10.1016/j.powtec.2020.01.001

Both, E. M., Karlina, A. M., Boom, R. M., & Schutyser, M. A. I. (2018). Morphology development during sessile single droplet drying of mixed maltodextrin and whey protein solutions. *Food Hydrocolloids*, *75*, 202–210. https://doi.org/10.1016/j.foodhyd.2017.08.022

Both, E. M., Nuzzo, M., Millqvist-Fureby, A., Boom, R. M., & Schutyser, M. A. I. (2018). Morphology development during single droplet drying of mixed component formulations and milk. *Food Research International*, *109*, 448–454. https://doi.org/10.1016/j.foodres.2018.04.043

Both, E. M., Siemons, I., Boom, R. M., & Schutyser, M. A. I. (2019). The role of viscosity in morphology development during single droplet drying. *Food Hydrocolloids*, *94*, 510–518. https://doi.org/10.1016/j.foodhyd.2019.03.023

Both, E. M., Tersteeg, S. M. B., Boom, R. M., & Schutyser, M. A. I. (2019). Drying kinetics and viscoelastic properties of concentrated thin films as a model system for spray drying. *Colloids and Surfaces A: Physicochemical and Engineering Aspects*, 124075. https://doi.org/10.1016/j.colsurfa.2019.124075

Bušić, A., Mardetko, N., Kundas, S., Morzak, G., Belskaya, H., Šantek, M. I., … Šantek, B. (2018). Bioethanol production from renewable raw materials and its separation and purification: A review. *Food Technology and Biotechnology*, *56*(3), 289. https://doi.org/10.17113/FTB.56.03.18.5546

Buttery, R. G., Seifert, R. M., Guadagni, D. G., & Ling, L. C. (1969). Characterization of some volatile constituents of bell peppers. *Journal of Agricultural and Food Chemistry*, *17*(6), 1322–1327. Retrieved from https://pubs.acs.org/sharingguidelines

Buvé, C., Neckebroeck, B., Haenen, A., Kebede, B., Hendrickx, M., Grauwet, T., & Van Loey, A. (2018). Combining untargeted, targeted and sensory data to investigate the impact of storage on food volatiles: A case study on strawberry juice. *Food Research International*, *113*(July), 382–391. https://doi.org/10.1016/j.foodres.2018.07.022

Cagnasso, S., Dalcanale, E., Bolzoni, L., Berni, E., Cocconi, E., & Vittadini, E. (2007). Early detection of fungal growth in pear nectars: use of photoionization detector (PID) and comparison with EOS 835. Pt.2. *FAO Agris*, *81*(4), 343–351.

Cardoso, D. R., Bettin, S. M., Reche, R. V., Lima-Neto, B. S., & Franco, D. W. (2003). HPLC-DAD analysis of ketones as their 2,4-dinitrophenylhydrazones in Brazilian sugar-cane spirits and rum. *Journal of Food Composition and Analysis*, *16*(5), 563–573. https://doi.org/10.1016/S0889-1575(03)00061-9

Castro, N., Durrieu, V., Raynaud, C., & Rouilly, A. (2016). Influence of DE-value on the physicochemical properties of maltodextrin for melt extrusion processes. *Carbohydrate Polymers*, *144*, 464–473. https://doi.org/10.1016/j.carbpol.2016.03.004

Cebrián, G., Condón, S., & Mañas, P. (2017). Physiology of the inactivation of vegetative bacteria by thermal treatments: Mode of action, influence of environmental factors and inactivation kinetics. *Foods*, *6*(12), 1–21. https://doi.org/10.3390/foods6120107

Chan, T. C., Chan, C. H. C., Tang, W. Y., & Chang, N. W. (2018). Effects of hydrogen bonding on diffusion of aromatic compounds in acetone: An experimental investigation from 268.2 to 328.2 K. *The Journal of Physical Chemistry B*. https://doi.org/10.1021/acs.jpcb.8b08539

Chen, P., Shrotri, A., & Fukuoka, A. (2021). Synthesis of cello-oligosaccharides by depolymerization of cellulose: A review. *Applied Catalysis A: General*, *621*(April), 118177. https://doi.org/10.1016/j.apcata.2021.118177

Chen, X., Qin, W., Ma, L., Xu, F., Jin, P., & Zheng, Y. (2015). Effect of high pressure processing and thermal treatment on physicochemical parameters, antioxidant activity and volatile compounds of green asparagus juice. *LWT - Food Science and Technology*, *62*(1), 927–933. https://doi.org/10.1016/j.lwt.2014.10.068

Chiou, D., & Langrish, T. A. G. (2007). Development and characterisation of novel nutraceuticals with spray drying technology. *Journal of Food Engineering*, *82*(1), 84–91. https://doi.org/10.1016/j.jfoodeng.2007.01.021

Chitrakar, B., Zhang, M., & Adhikari, B. (2019, November 1). Asparagus (*Asparagus officinalis*): Processing effect on nutritional and phytochemical composition of spear and hard-stem byproducts. *Trends in Food Science and Technology*. Elsevier Ltd.

https://doi.org/10.1016/j.tifs.2019.08.020

Chung, S., & Villota, R. (1990). Changes in partition coefficients of alcohols as affected by the presence of various food solids. *Journal of Food Process Engineering*, *13*(2), 169–189. https://doi.org/10.1111/j.1745-4530.1990.tb00066.x

Cialiè Rosso, M., Liberto, E., Spigolon, N., Fontana, M., Somenzi, M., Bicchi, C., & Cordero, C. (2018). Evolution of potent odorants within the volatile metabolome of high-quality hazelnuts (*Corylus avellana* L.): evaluation by comprehensive two-dimensional gas chromatography coupled with mass spectrometry. *Analytical and Bioanalytical Chemistry*, *410*(15), 3491–3506. https://doi.org/10.1007/s00216-017-0832-6

Corbo, M. R., Bevilacqua, A., Petruzzi, L., Casanova, F. P., & Sinigaglia, M. (2014). Functional beverages: The emerging side of functional foods: Commercial trends, research, and health implications. *Comprehensive Reviews in Food Science and Food Safety*, *13*(6), 1192–1206. https://doi.org/10.1111/1541-4337.12109

Couchman, P. R., & Karasz, F. E. (1978). A classical thermodynamic discussion of the effect of composition on glass-transition temperatures. *Macromolecules*, *11*(1). https://doi.org/10.1021/ma60061a021

Coumans, W. J., Kerkhof, P. J. A. M., & Ruin, S. (1994). Theoretical and practical aspects of aroma retention in spray drying and freeze drying. *Drying Technology*, *12*(1–2), 99–149. https://doi.org/10.1080/07373939408959951

Cuellar, M. C., & Straathof, A. J. J. (2014). Biochemical conversion: Biofuels by industrial fermentation. In *Biomass as a Sustainable Energy Source for the Future: Fundamentals of Conversion Processes* (Vol. 9781118304, pp. 403–440). https://doi.org/10.1002/9781118916643.ch13

Darken, L. S. (1948). Diffusion, mobility and their interrelaton through free energy in binary metallic systems. *Transactions of the American Institute of Mining, Metallurgical and Petroleum Engineers*, *175*, 184–201.

Davarzani, N., Diez-Simon, C., Großmann, J. L., Jacobs, D. M., van Doorn, R., van den Berg, M. A., … Westerhuis, J. A. (2021). Systematic selection of competing metabolomics methods in a metabolite-sensory relationship study. *Metabolomics*, *17*(9), 1–12. https://doi.org/10.1007/s11306-021-01821-3

Dawid, C., & Hofmann, T. (2012). Identification of sensory-active phytochemicals in asparagus (*Asparagus officinalis L.*). *Journal of Agricultural and Food Chemistry*, *60*(48), 11877–11888. https://doi.org/10.1021/jf3040868

De Laurentiis, V., Corrado, S., & Sala, S. (2018). Quantifying household waste of fresh fruit and vegetables in the EU. *Waste Management*, *77*, 238–251. https://doi.org/10.1016/J.WASMAN.2018.04.001

De Vos, R. C. H., Moco, S., Lommen, A., Keurentjes, J. J. B., Bino, R. J., & Hall, R. D. (2007). Untargeted large-scale plant metabolomics using liquid chromatography coupled to mass spectrometry. *Nature Protocols*, *2*(4), 778–791. https://doi.org/10.1038/nprot.2007.95

Deblais, A., Hollander, E. den, Boucon, C., Blok, A. E., Veltkamp, B., Voudouris, P., … Velikov, K. P. (2021). Predicting thickness perception of liquid food products from their non-Newtonian rheology. *Nature Communications*, *12*(1), 1–7. https://doi.org/10.1038/s41467-021-26687-w

Diez-Simon, C., Eichelsheim, C., Jacobs, D. M., Mumm, R., & Hall, R. D. (2021). Stir bar sorptive extraction of aroma compounds in soy sauce: Revealing the chemical diversity. *Food Research International*, *144*(February), 110348. https://doi.org/10.1016/j.foodres.2021.110348

Diez-Simon, C., Mumm, R., & Hall, R. D. (2019). Mass spectrometry-based metabolomics of volatiles as a new tool for understanding aroma and flavour chemistry in processed food products. *Metabolomics*, *1*, 41. https://doi.org/10.1007/s11306-019-1493-6

Din, N. A. S., Lim, S. J., Maskat, M. Y., & Zaini, N. A. M. (2021). Bioconversion of coconut husk fibre through biorefinery process of alkaline pretreatment and enzymatic hydrolysis. *Biomass Conversion and Biorefinery*, *11*(3), 815–826. https://doi.org/10.1007/s13399-020-00895-8

Do, H. T. T., & Nguyen, H. V. H. (2018). Effects of spray-drying temperatures and ratios of gum arabic to microcrystalline cellulose on antioxidant and physical properties of mulberry juice powder. *Beverages*, *4*(4), 101. https://doi.org/10.3390/beverages4040101

Dokic, P., Jakovljevic, J., & Dokic-Baucal, L. (1998). Molecular characteristics of maltodextrins and rheological behaviour of diluted and concentrated solutions. *Colloids and Surfaces A: Physicochemical and Engineering Aspects*, *141*(3), 435–440. https://doi.org/10.1016/S0927-7757(97)00118-0

Eggink, P. M., Maliepaard, C., Tikunov, Y., Haanstra, J. P. W., Bovy, A. G., & Visser, R. G. F. (2012). A taste of sweet pepper: Volatile and non-volatile chemical composition of fresh sweet pepper (*Capsicum annuum*) in relation to sensory evaluation of taste. *Food Chemistry*, *132*(1), 301–310. https://doi.org/10.1016/j.foodchem.2011.10.081

Eiser, J. R., Coulson, N. S., & Eiser, C. (2002). Adolescents' perceptions of the costs and benefits of food additives and their presence in different foods. *Journal of Risk Research*, *5*(2), 167–176. https://doi.org/10.1080/13669870010004979

Etzbach, L., Meinert, M., Faber, T., Klein, C., Schieber, A., & Weber, F. (2020). Effects of carrier agents on powder properties, stability of carotenoids, and encapsulation efficiency of goldenberry (*Physalis peruviana L.*) powder produced by co-current spray drying. *Current Research in Food Science*, *3*(November 2019), 73–81. https://doi.org/10.1016/j.crfs.2020.03.002

Eurostat. (2022). Asparagus crop production in EU standard humidity. Retrieved April 25, 2022, from https://ec.europa.eu/eurostat/databrowser/view/APRO_CPSH1__custom_2570637/default/table?lang=en

FAO. (2014). *Global initiative on food loss and waste reduction*.

Farag, M. A., Ali, S. E., Hodaya, R. H., El-Seedi, H. R., Sultani, H. N., Laub, A., … Wessjohann, L. A. (2017). Phytochemical profiles and antimicrobial activities of *Allium cepa* red cv. and *A. sativum* subjected to different drying methods: A comparative MS-based metabolomics. *Molecules*, *22*(5), 761. https://doi.org/10.3390/molecules22050761

Fortune Business Insights. (2021). *Market research report: spray-dried vegetable powder*. Retrieved from https://www.fortunebusinessinsights.com/spray-dried-vegetable-powder-market-103181

Fuentes-Alventosa, J. M. M., Rodríguez-Gutiérrez, G., Jaramillo-Carmona, S., Espejo-Calvo, J. A. A., Rodríguez-Arcos, R., Fernández-Bolaños, J., … Jiménez-Araujo, A. (2009). Effect of extraction method on chemical composition and functional characteristics of high dietary fibre powders obtained from asparagus by-products. *Food Chemistry*, *113*(2), 665–671. https://doi.org/10.1016/j.foodchem.2008.07.075

Galbe, M., & Zacchi, G. (2007). Pretreatment of lignocellulosic materials for efficient bioethanol production. In L. Olsson (Ed.), *Biofuels* (pp. 41–65). Berlin, Heidelberg: Springer Berlin Heidelberg. https://doi.org/10.1007/10_2007_070

Goubet, I., Le Quere, J.-L., & Voilley, A. J. (1998). Retention of aroma compounds by carbohydrates: Influence of their physicochemical characteristics and of their physical state. A review. *J. Agric. Food Chem*, *46*, 1981–1990. https://doi.org/https://doi.org/10.1021/jf970709y

Grabowski, J. A., Truong, V.-D. D., & Daubert, C. R. (2006). Spray-drying of amylase hydrolyzed sweetpotato puree and physicochemical properties of powder. *Journal of Food Science*, *71*(5), E209–E217. https://doi.org/10.1111/j.1750-3841.2006.00036.x

Guiné, R. P. F. (2018). The drying of foods and its effect on the physical-chemical, sensorial and nutritional properties. *International Journal of Food Engineering*. https://doi.org/10.18178/ijfe.4.2.93-100

Gustavsson, J., Cederberg, C., Sonesson, U., Van Otterdijk, R., Meybeck, A., & Rome, F. (2011). *Global food losses and food waste*. Retrieved from http://www.fao.org/docrep/014/mb060e/mb060e00.pdf

Haag, W., & Wrenn, C. (2006). *The PID Handbook - Theory and Applications of Direct-Reading Photoionization*. San Jose: RAE Systems Inc.

Hartley, G. ., & Crank, J. (1949). Some fundamental definitions and concepts in diffusion processes. *System*, *29*, 801–817.

Hoberg, E., Ulrich, D., Gottwald, J., & Rosen, A. (2003). Environmental influences on the sensory quality of *Asparagus officinalis L.* . *Acta Horticulturae*, *604*, 395–401. https://doi.org/10.17660/ActaHortic.2003.604.42

Hoberg, E., Ulrich, D., & Wonneberger, C. (2008). Proposal for a flavour standard - Sensory profiles of European white Asparagus officinalis L. cultivars. *Acta Horticulturae*, *776*, 239–245.

Hyldig, G., & Green-Petersen, D. M. B. (2004). Quality index method-an objective tool for determination of sensory quality. *Journal of Aquatic Food Product Technology*, *13*(4), 71–80. https://doi.org/10.1300/J030v13n04_06

Ingredion. (2014). The Clean Label Guide to Europe. Retrieved May 12, 2020, from https://emea.ingredion.com/Campaign/Clean-Label-Guide.html

IonScience. (2019). MiniPID 2 (3PIN).

Islam, M. I. U., Edrisi, M., & Langrish, T. (2013). Improving process yield by adding WPI to lactose during crystallization and spray drying under high-humidity conditions. *Drying Technology*, *31*(4), 393–404. https://doi.org/10.1080/07373937.2012.737396

Jacobs, D. M., van den Berg, M. A., & Hall, R. D. (2021). Towards superior plant-based foods using metabolomics. *Current Opinion in Biotechnology*, *70*, 23–28. https://doi.org/10.1016/j.copbio.2020.08.010

Jafari, S. M., Assadpoor, E., He, Y., & Bhandari, B. (2008). Encapsulation efficiency of food flavours and oils during spray drying. *Drying Technology*, *26*(7), 816–835. https://doi.org/10.1080/07373930802135972

Jedlińska, A., Samborska, K., Janiszewska-Turak, E., Witrowa-Rajchert, D., Seuvre, A.-M., & Voilley, A. (2018). Physicochemical properties of vanilla and raspberry aromas microencapsulated in the industrial conditions by spray drying. *Journal of Food Process Engineering*, *41*(7), e12872. https://doi.org/10.1111/jfpe.12872

Jørgensen, H., Kristensen, J. B., & Felby, C. (2007). Enzymatic conversion of lignocellulose into fermentable sugars: Challenges and opportunities. *Biofuels, Bioproducts and Biorefining*, *1*(2), 119–134. https://doi.org/10.1002/BBB.4

Jouquand, C., Ducruet, V., & Giampaoli, P. (2004). Partition coefficients of aroma compounds in polysaccharide solutions by the phase ratio variation method. *Food Chemistry*, *85*(3), 467–474. https://doi.org/10.1016/j.foodchem.2003.07.023

Kalkan, E. A., Sahiner, M., Cakir, D. U., Alpaslan, D., & Yilmaz, S. (2016). Quantitative clinical diagnostic analysis of acetone in human blood by HPLC: A metabolomic search for acetone as indicator. *Journal of Analytical Methods in Chemistry*, *2016*. https://doi.org/10.1155/2016/5176320

Kamiloglu, S., Toydemir, G., Boyacioglu, D., Beekwilder, J., Hall, R. D., & Capanoglu, E. (2016). A review on the effect of drying on antioxidant potential of fruits and vegetables. *Critical Reviews in Food Science and Nutrition*, *56*. https://doi.org/10.1080/10408398.2015.1045969

Karam, M. C., Petit, J., Zimmer, D., Baudelaire Djantou, E., & Scher, J. (2016). Effects of drying and grinding in production of fruit and vegetable powders: A review. *Journal of Food Engineering*, *188*, 32–49. https://doi.org/10.1016/j.jfoodeng.2016.05.001

Karnaouri, A., Matsakas, L., Bühler, S., Muraleedharan, M. N., Christakopoulos, P., & Rova, U. (2019). Tailoring celluclast® cocktail's performance towards the production of prebiotic cello-oligosaccharides from waste forest biomass. *Catalysts*, *9*(11). https://doi.org/10.3390/catal9110897

Karnaouri, A., Matsakas, L., Krikigianni, E., Rova, U., & Christakopoulos, P. (2019). Valorization of waste forest biomass toward the production of cello-oligosaccharides with potential prebiotic activity by utilizing customized enzyme cocktails. *Biotechnology for Biofuels*, *12*(1), 1–19. https://doi.org/10.1186/s13068-019-1628-z

Kennedy, J. F., Knill, C. J., & Taylor, D. W. (1995). Maltodextrins. In *Handbook of Starch Hydrolysis Products and their Derivatives* (pp. 65–82). Boston, MA: Springer US. https://doi.org/10.1007/978-1-4615-2159-4_3

Kim, J. S., Lee, Y. Y., & Kim, T. H. (2016). A review on alkaline pretreatment technology for bioconversion of lignocellulosic biomass. *Bioresource Technology*, *199*, 42–48. https://doi.org/10.1016/j.biortech.2015.08.085

King, C. J. (1995). Spray drying: Retention of volatile compounds revisited. *Drying Technology*, *13*(5–7), 1221–1240. https://doi.org/10.1080/07373939508917018

King, C. J., Downton, G. E., & Flores-Luna, J. L. (1982). Mechanism of stickiness in hygroscopic, amorphous powders. *Industrial and Engineering Chemistry Fundamentals*, *21*(4), 447–451. https://doi.org/10.1021/i100008a023

Kluge, S., Bonhage, B., Viell, J., Granström, M., Kindler, A., & Spiess, A. C. (2019). Enzymatic production of cello-oligomers with endoglucanases. *Cellulose*, *4*, 4279–4290. https://doi.org/10.1007/s10570-019-02390-4

Knoema. (2021). Production statistics - crops, crops processed. Retrieved June 8, 2020, from https://knoema.com/FAOPRDSC2020/production-statistics-crops-crops-processed?item=1000090-asparagus

Krishna, R., & Van Baten, J. M. (2005). The darken relation for multicomponent diffusion in liquid mixtures of linear alkanes: An investigation using Molecular Dynamics (MD) simulations. *Industrial and Engineering Chemistry Research*, *44*(17), 6939–6947. https://doi.org/10.1021/ie050146c

Kristensen, J. B., Felby, C., & Jørgensen, H. (2009). Yield-determining factors in high-solids enzymatic hydrolysis of lignocellulose. *Biotechnology for Biofuels*, *2*, 1–10. https://doi.org/10.1186/1754-6834-2-11

Kubota, S., Konno, I., & Kanno, A. (2012). Molecular phylogeny of the genus *Asparagus* (Asparagaceae) explains interspecific crossability between the garden asparagus (*A. officinalis*) and other Asparagus species. *Theoretical and Applied Genetics*, *124*(2), 345–354. https://doi.org/10.1007/S00122-011-1709-2/FIGURES/3

La Peña-Armada, R. De, Villanueva-Suárez, M. J., Rupérez, P., & Mateos-Aparicio, I. (2020). High hydrostatic pressure assisted by celluclast® releases oligosaccharides from apple by-product. *Foods*, *9*(8), 1–13. https://doi.org/10.3390/foods9081058

Le Thanh, M., Thibeaudeau, P., Thibaut, M. A., & Voilley, A. (1992). Interactions between volatile and non-volatile compounds in the presence of water. *Food Chemistry*, *43*(2), 129–135. https://doi.org/10.1016/0308-8146(92)90226-R

Li, R., Lin, D., Roos, Y. H., & Miao, S. (2018). Glass transition, structural relaxation and stability of spray-dried amorphous food solids: A review. *Drying Technology*, *37*(3), 287–300. https://doi.org/10.1080/07373937.2018.1459680

Liaw, A., & Wiener, M. (2002). Classification and regression by RandomForest. *R News*, *2*(3), 18–22.

Lommen, A. (2009). MetAlign: Interface-driven, versatile metabolomics tool for hyphenated full-scan mass spectrometry data preprocessing. *Analytical Chemistry*, *81*(8), 3079–3086.

https://doi.org/10.1021/ac900036d

Luning, P. A., De Rijk, T., Wichers, H. J., & Roozen, J. P. (1994). Gas chromatography, mass spectrometry, and sniffing port analyses of volatile compounds of fresh bell peppers (*Capsicum annuum*) at different ripening stages. *J. Agric. Food Chem*, *42*, 977–983. Retrieved from https://pubs.acs.org/sharingguidelines

Luning, P. A., Yuksel, D., Vries, R., & Roozen, J. P. (1995). Aroma changes in fresh bell peppers (*Capsicum annuum*) after hot-air drying. *Journal of Food Science*, *60*(6), 1269–1276. https://doi.org/10.1111/j.1365-2621.1995.tb04571.x

Lyly, M., Salmenkallio-Marttila, M., Suortti, T., Autio, K., Poutanen, K., & Lähteenmäki, L. (2004). The sensory characteristics and rheological properties of soups containing oat and barley β-glucan before and after freezing. *LWT - Food Science and Technology*, *37*(7), 749–761. https://doi.org/10.1016/J.LWT.2004.02.009

Lynd, L. R., Weimer, P. J., Zyl, W. H. Van, & Isak, S. (2002). Microbial cellulose utilization: Fundamentals and biotechnology. *Microbiology and Molecular Biology Reviews*, *66*(3), 506–577. https://doi.org/10.1128/MMBR.66.3.506

Macrelli, S., Mogensen, J., & Zacchi, G. (2012). Techno-economic evaluation of 2nd generation bioethanol production from sugar cane bagasse and leaves integrated with the sugar-based ethanol process. *Biotechnology for Biofuels*, *5*(22). https://doi.org/10.1186/1754-6834-5-22

Madene, A., Jacquot, M., Scher, J., & Desobry, S. (2006). Flavour encapsulation and controlled release - a review. *International Journal of Food Science and Technology*, *41*(1), 1–21. https://doi.org/10.1111/j.1365-2621.2005.00980.x

Maepa, C. E., Jayaramudu, J., Okonkwo, J. O., Ray, S. S., Sadiku, E. R., & Ramontja, J. (2015). Extraction and characterization of natural cellulose fibers from maize tassel. *International Journal of Polymer Analysis and Characterization*, *20*(2), 99–109. https://doi.org/10.1080/1023666X.2014.961118

Matsuno, R., & Adachi, S. (1993). Lipid encapsulation technology - techniques and applications to food. *Trends in Food Science and Technology*, *4*(8), 256–261. https://doi.org/10.1016/0924-2244(93)90141-V

Menting, L. G. ., Hoogstad, B., & Thijssen, H. A. C. (1970). Diffusion coefficients of water and organic volatiles in carbohydrate-water systems. *International Journal of Food Science & Technology*, *5*(2), 111–126. https://doi.org/10.1111/J.1365-2621.1970.TB01549.X

Nijhuis, H. ., Torringa, H. ., Muresan, S., Yuksel, D., Leguijt, C., & Kloek, W. (1998). Approaches to

improving the quality of dried fruit and vegetables. *Trends in Food Science & Technology*, *9*(1), 13–20. https://doi.org/10.1016/S0924-2244(97)00007-1

Nindo, C. I., Sun, T., Wang, S. W., Tang, J., & Powers, J. R. (2003). Evaluation of drying technologies for retention of physical quality and antioxidants in asparagus (*Asparagus officinalis, L.*). *LWT - Food Science and Technology*, *36*(5), 507–516. https://doi.org/10.1016/S0023-6438(03)00046-X

Ong, J. J. X., Steele, C. M., & Duizer, L. M. (2018). Challenges to assumptions regarding oral shear rate during oral processing and swallowing based on sensory testing with thickened liquids. *Food Hydrocolloids*, *84*, 173–180. https://doi.org/10.1016/J.FOODHYD.2018.05.043

Paramita, V., Iida, K., Yoshii, H., & Furuta, T. (2010). Effect of additives on the morphology of spray-dried powder. *Drying Technology*, *28*(3), 323–329. https://doi.org/10.1080/07373931003627098

Parry, R. J., Mizusawa, A. E., Chiu, I. C., Naidu, M. V., & Ricciardone, M. (1985). Biosynthesis of sulfur compounds. Investigations of the biosynthesis of asparagusic acid. *Journal of the American Chemical Society*, *107*(8), 2512–2521. https://doi.org/10.1021/ja00294a051

Pegiou, E., Mumm, R., Acharya, P., de Vos, R. C. H., & Hall, R. D. (2019). Green and white asparagus (*Asparagus officinalis*): A source of developmental, chemical and urinary intrigue. *Metabolites*, *10*(1), 17. https://doi.org/10.3390/metabo10010017

Pegiou, E., Zhu, Q., Pegios, P., De Vos, R. C. H., Mumm, R., & Hall, R. D. (2021). Metabolomics reveals heterogeneity in the chemical composition of green and white spears of asparagus (*A. officinalis*). *Metabolites*, *11*(10), 708. https://doi.org/10.3390/metabo11100708

Perdana, J., Van Der Sman, R. G. M., Fox, M. B., Boom, R. M., & Schutyser, M. A. I. (2013). Measuring and modelling of diffusivities in carbohydrate-rich matrices during thin film drying. *Journal of Food Engineering*, *122*(1), 38–47. https://doi.org/10.1016/j.jfoodeng.2013.08.033

Popa, S., Murith, N. • M., Chisholm, • H, Engmann, • J, Popa Nita, S., Murith, M., … Engmann, J. (2013). Matching the rheological properties of videofluoroscopic contrast agents and thickened liquid prescriptions. *Dysphagia*, *28*(2), 245–252. https://doi.org/10.1007/s00455-012-9441-x

Qiu, J. (2019). *Mild conductive drying of foods*.

Ragauskas, A. J., Williams, C. K., Davison, B. H., Britovsek, G., Cairney, J., Eckert, C. A., … Tschaplinski, T. (2006). The path forward for biofuels and biomaterials. *Science*, *311*(5760), 484–489. https://doi.org/10.1126/science.1114736

Raja, K. C. M., Sankarikutty, B., Sreekumar, M., Jayalekshmy, A., & Narayanan, C. S. (1989). Material

characterization studies of maltodextrin samples for the use of wall material. *Starch - Stärke*, *41*(8), 298–303. https://doi.org/10.1002/STAR.19890410805

Reese, E. T. (1956). A microbiological process report; enzymatic hydrolysis of cellulose. *Applied Microbiology*, *4*(1), 39–45. https://doi.org/10.1128/aem.4.1.39-45.1956

Reineccius, G. A. (2004). The spray drying of food flavors. *Drying Technology*, *22*(6), 1289–1324. https://doi.org/10.1081/DRT-120038731

Reineccius, G. A., & Coulter, S. T. (1969). Flavor retention during drying. *Journal of Dairy Science*, *52*(8), 1219–1223. https://doi.org/10.3168/jds.S0022-0302(69)86728-7

Rodríguez, R., Jiménez, A., Guillén, R., Heredia, A., & Fernández-Bolaños, J. (1999). Turnover of white asparagus cell wall polysaccharides during postharvest storage. *Journal of Agricultural and Food Chemistry*, *47*(11), 4525–4531. https://doi.org/10.1021/jf981392k

Roos, Y. (1993). Melting and glass transitions of low molecular weight carbohydrates. *Carbohydrate Research*, *238*(C), 39–48. https://doi.org/10.1016/0008-6215(93)87004-C

Roos, Y. H. (2010). Glass transition temperature and its relevance in food processing. *Annu. Rev. Food Sci. Technol*, *1*, 469–496. https://doi.org/10.1146/annurev.food.102308.124139

Rosenberg, M., Kopelman, I. J., & Talmon, Y. (1990). Factors affecting retention in spray-drying microencapsulation of volatile materials. *J. Agric. Food Chem*, *38*(5), 1288–1294. https://doi.org/10.1021/jf00095a030

Rulkens, W. H., & Thijssen, H. A. C. (1972). The retention of organic volatiles in spray-drying aqueous carbohydrate solutions. *International Journal of Food Science & Technology*, *7*(1), 95–105. https://doi.org/10.1111/j.1365-2621.1972.tb01644.x

Sablani, S. S. (2007). Drying of fruits and vegetables: Retention of nutritional/functional quality. *Drying Technology*. https://doi.org/10.1080/07373930600558904

Sagar, V. R., Suresh Kumar, P., & Suresh Kumar, S. V. R. (2010). *Recent advances in drying and dehydration of fruits and vegetables: a review*. *Mysore J Food Sci Technol* (Vol. 47). Springer-Verlag. https://doi.org/10.1007/s13197-010-0010-8

Sammond, D. W., Yarbrough, J. M., Mansfield, E., Bomble, Y. J., Hobdey, S. E., Decker, S. R., … Crowley, M. F. (2014). Predicting enzyme adsorption to lignin films by calculating enzyme surface hydrophobicity. *Journal of Biological Chemistry*, *289*(30), 20960–20969. https://doi.org/10.1074/jbc.M114.573642

Santos, D., Maurício, A. C., Sencadas, V., Santos, J. D., Fernandes, M. H., & Gomes, P. S. (2018). Spray drying: An overview. In *Biomaterials - Physics and Chemistry - New Edition*. InTech.

https://doi.org/10.5772/intechopen.72247

Sanz, M. L., Gibson, G. R., & Rastall, R. A. (2005). Influence of disaccharide structure on prebiotic selectivity in vitro. *Journal of Agricultural and Food Chemistry*, *53*, 5192–5199. https://doi.org/10.1021/jf050276w

Scholte, T. G., Meijerink, N. L. J., Schoffeleers, H. M., & Brands, A. M. G. (1984). Mark–Houwink equation and GPC calibration for linear short-chain branched polyolefines, including polypropylene and ethylene–propylene copolymers. *Journal of Applied Polymer Science*, *29*(12), 3763–3782. https://doi.org/10.1002/app.1984.070291211

Searchinger, T., Hanson, C., Ranganathan, J., Lipinski, B., Waite, R., Winterbottom, R., … Ben, T. (2014). *Creating a sustainable food future. A menu of solutions to sustainably feed more than 9 billion people by 2050. World resources report 2013-14: interim findings*. *World Resources Institute*.

Shim, S.-M., Seo, S. H., Lee, Y., Moon, G.-I., Kim, M.-S., & Park, J.-H. (2011). Consumers' knowledge and safety perceptions of food additives: Evaluation on the effectiveness of transmitting information on preservatives. *Food Control*, *22*(7), 1054–1060. https://doi.org/10.1016/J.FOODCONT.2011.01.001

Shishir, M. R. I., & Chen, W. (2017). Trends of spray drying: A critical review on drying of fruit and vegetable juices. *Trends in Food Science & Technology*, *65*, 49–67. https://doi.org/10.1016/J.TIFS.2017.05.006

Siccama, J. W., Pegiou, E., Eijkelboom, N. M., Zhang, L., Mumm, R., Hall, R. D., & Schutyser, M. A. I. (2021). The effect of partial replacement of maltodextrin with vegetable fibres in spray-dried white asparagus powder on its physical and aroma properties. *Food Chemistry*, *356*, 129567. https://doi.org/10.1016/j.foodchem.2021.129567

Siccama, J. W., Pegiou, E., Zhang, L., Mumm, R., Hall, R. D., Boom, R. M. M., & Schutyser, M. A. I. (2021). Maltodextrin improves physical properties and volatile compound retention of spray-dried asparagus concentrate. *LWT - Food Science and Technology*, *142*(February), 111058. https://doi.org/10.1016/j.lwt.2021.111058

Siccama, J. W., Zhang, L., & Schutyser, M. A. I. (2019). Strategies to retain volatile compounds during convective drying. In *7th European Drying Conference*.

Siemons, I., Boom, R. M., van der Sman, R. G. M., & Schutyser, M. A. I. (2019). Moisture diffusivity in concentrated and dry protein-carbohydrate films. *Food Hydrocolloids*, *97*(July), 105219. https://doi.org/10.1016/j.foodhyd.2019.105219

Siemons, I., Politiek, R. G. A., Boom, R. M., van der Sman, R. G. M., & Schutyser, M. A. I. (2020). Dextrose equivalence of maltodextrins determines particle morphology development during single sessile droplet drying. *Food Research International*, *131*, 108988. https://doi.org/10.1016/j.foodres.2020.108988

Siemons, I., Vaessen, E. M. J., Oosterbaan van Peski, S. E., Boom, R. M., & Schutyser, M. A. I. (2020). Protective effect of carrier matrices on survival of *Lactobacillus plantarum* WCFS1 during single droplet drying explained by particle morphology development. *Journal of Food Engineering*, *292*, 110263. https://doi.org/10.1016/j.jfoodeng.2020.110263

Singh, J., Suhag, M., & Dhaka, A. (2015). Augmented digestion of lignocellulose by steam explosion, acid and alkaline pretreatment methods: A review. *Carbohydrate Polymers*, *117*, 624–631. https://doi.org/10.1016/j.carbpol.2014.10.012

Srikiatden, J., & Roberts, J. S. (2007). Moisture transfer in solid Food materials: A review of mechanisms, models, and measurements. *International Journal of Food Properties*, *10*(4), 739–777. https://doi.org/10.1080/10942910601161672

Ssepuuya, G., Katongole, J., & Tumuhimbise, G. A. (2018). Contribution of instant amaranth (*Amaranthus hypochondriacus* L.)-based vegetable soup to nourishment of boarding school adolescents. *Food Science and Nutrition*, *6*(6), 1402–1409. https://doi.org/10.1002/fsn3.664

Sumner, L. W., Amberg, A., Barrett, D., Beale, M. H., Beger, R., Daykin, C. A., … Viant, M. R. (2007). Proposed minimum reporting standards for chemical analysis: Chemical Analysis Working Group (CAWG) Metabolomics Standards Initiative (MSI). *Metabolomics*, *3*(3), 211–221. https://doi.org/10.1007/s11306-007-0082-2

Sun, Y., & Cheng, J. (2002). Hydrolysis of lignocellulosic materials for ethanol production: A review. *Bioresource Technology*, *83*(1), 1–11. https://doi.org/10.1016/S0960-8524(01)00212-7

Taherdanak, M., & Zilouei, H. (2014). Improving biogas production from wheat plant using alkaline pretreatment. *Fuel*, *115*, 714–719. https://doi.org/10.1016/j.fuel.2013.07.094

Thevenot, E. A., Roux, A., Xu, Y., Ezan, E., & Zunot, C. (2015). Analysis of the human adult urinary metabolome variations with age, body mass index, and gender by implementing a comprehensive workflow for univariate and OPLS statistical analyses. *Journal of Proteome Research*, *14*(8), 3322–3335. https://doi.org/https://doi.org/10.1021/acs.jproteome.5b00354

Thijssen, H. A. C. (1971). Flavour retention in drying preconcentrated food liquids. *Journal of Applied Chemistry and Biotechnology*, *21*(12), 372–377. https://doi.org/10.1002/jctb.5020211208

Tikunov, Y. M., Laptenok, S., Hall, R. D., Bovy, A., & de Vos, R. C. H. (2012). MSClust: A tool for

unsupervised mass spectra extraction of chromatography-mass spectrometry ion-wise aligned data. *Metabolomics*, *8*(4), 714–718. https://doi.org/10.1007/s11306-011-0368-2

Too Good To Go. (2022). What food is wasted? Retrieved July 7, 2022, from https://toogoodtogo.com/en-us/movement/knowledge/what-food-is-wasted

Tressl, R., Bahri, D., Holzer, M., & Kossa, T. (1977). Formation of flavor components in asparagus. 2. Formation of flavor components in cooked asparagus. *Journal of Agricultural and Food Chemistry*, *25*(3), 455–459. https://doi.org/10.1021/jf60211a025

Tressl, R., Holzer, M., & Apetz, M. (1977). Flavor components in Asparagus. 1. Biosynthesis of sulfur-containing acids in asparagus. *Journal of Agricultural and Food Chemistry*, *40*(3), 509. Retrieved from https://pubs.acs.org/sharingguidelines

Tyle, P. (1993). Effect of size, shape and hardness of particles in suspension on oral texture and palatability. *Acta Psychologica*, *84*(1), 111–118. https://doi.org/10.1016/0001-6918(93)90077-5

Ulrich, D., Hoberg, E., Bittner, T., Engewald, W., & Meilchen, K. (2001). Contribution of volatile compounds to the flavor of cooked asparagus. *European Food Research and Technology*, *213*(3), 200–204. https://doi.org/10.1007/s002170100349

Urbat, F., Müller, P., Hildebrand, A., Wefers, D., & Bunzel, M. (2019). Comparison and optimization of different protein nitrogen quantitation and residual protein characterization methods in dietary fiber preparations. *Frontiers in Nutrition*, *6*(August), 1–8. https://doi.org/10.3389/fnut.2019.00127

Utpott, M., Rodrigues, E., Rios, A. de O., Mercali, G. D., & Flôres, S. H. (2022). Metabolomics: An analytical technique for food processing evaluation. *Food Chemistry*, *366*(February 2021). https://doi.org/10.1016/j.foodchem.2021.130685

Valoppi, F., Wang, Y. J., Alt, G., Peltonen, L. J., & Mikkonen, K. S. (2021). Valorization of native soluble and insoluble oat side streams for stable suspensions and emulsions. *Food and Bioprocess Technology*, *14*(4), 751–764. https://doi.org/10.1007/S11947-021-02602-5/TABLES/3

Van Der Sman, R. G. M., & Meinders, M. B. J. (2010). Prediction of the state diagram of starch water mixtures using the Flory-Huggins free volume theory. *Soft Matter*. https://doi.org/10.1039/c0sm00280a

Van Der Sman, R. G. M., & Meinders, M. B. J. (2013). Moisture diffusivity in food materials. *Food Chemistry*, *138*(2–3), 1265–1274. https://doi.org/10.1016/J.FOODCHEM.2012.10.062

Vanderghem, C., Boquel, P., Blecker, C., & Paquot, M. (2010). A multistage process to enhance

cellobiose production from cellulosic materials. *Applied Biochemistry and Biotechnology*, *160*(8), 2300–2307. https://doi.org/10.1007/s12010-009-8724-7

Vaz, F. L., da Rocha Lins, J., Alves Alencar, B. R., Silva de Abreu, Í. B., Vidal, E. E., Ribeiro, E., … Dutra, E. D. (2021). Chemical pretreatment of sugarcane bagasse with liquid fraction recycling. *Renewable Energy*, *174*, 666–673. https://doi.org/10.1016/j.renene.2021.04.087

Verhoeven, H. A., Jonker, H., De Vos, R. C., & Hall, R. D. (2011). Solid phase micro-extraction GC–MS analysis of natural volatile components in melon and rice. In *Plant Metabolomics. Methods in Molecular Biology (Methods and Protocols)* (pp. 85–99). Humana Press. https://doi.org/https://doi.org/10.1007/978-1-61779-594-7_6

Verma, A., & Vir Singh, S. (2015). Spray drying of fruit and vegetable juices-A review. *Food Science and Nutrition*. https://doi.org/10.1080/10408398.2012.672939

Vidrih, R., Hribar, J., & Zlatić, E. (2008). Photo ionisation detector as a tool for apple quality determination. *Acta Horticulturae*, (796), 205–210. https://doi.org/10.17660/ActaHortic.2008.796.27

Vrentas, J. S., & Duda, J. L. (1977). Diffusion in polymer—solvent systems. I. Reexamination of the free-volume theory. *Journal of Polymer Science: Polymer Physics Edition*, *15*(3), 403–416. Retrieved from https://onlinelibrary.wiley.com/doi/full/10.1002/pol.1977.180150302

Wampler, B., & Barringer, S. A. (2012). Volatile generation in bell peppers during frozen storage and thawing using Selected Ion Flow Tube Mass Spectrometry (SIFT-MS). *Journal of Food Science*, *77*(6). https://doi.org/10.1111/J.1750-3841.2012.02727.X

Wangsakan, A., Chinachoti, P., & McClements, D. J. (2003). Effect of different dextrose equivalent of maltodextrin on the interactions with anionic surfactant in an isothermal titration calorimetry study. *Journal of Agricultural and Food Chemistry*, *51*(26), 7810–7814. https://doi.org/10.1021/jf034052u

Ward, J., & Joe, H. (1963). Hierarchical Grouping to optimize an objective function. *Journal of The Americal Statistical Association*, *58*(301), 236–244.

Wehrens, R., Hageman, J. A., van Eeuwijk, F., Kooke, R., Flood, P. J., Wijnker, E., … de Vos, R. C. H. (2016). Improved batch correction in untargeted MS-based metabolomics. *Metabolomics*, *12*(5). https://doi.org/10.1007/s11306-016-1015-8

Whitson, M. E., Miracle, R. E., & Drake, M. A. (2010). Sensory characterization of chemical components responsible for cardboard flavor in whey protein. *Journal of Sensory Studies*, *25*(4), 616–636. https://doi.org/10.1111/j.1745-459X.2010.00289.x

Wishart, D. S. (2008). Metabolomics: applications to food science and nutrition research. *Trends in Food Science and Technology*, *19*(9), 482–493. https://doi.org/10.1016/J.TIFS.2008.03.003

Xia, J., Guo, Z., Fang, S., Gu, J., & Liang, X. (2021). Effect of drying methods on volatile compounds of burdock (*Arctium lappa L.*) root tea as revealed by Gas Chromatography Mass Spectrometry-Based Metabolomics. *Foods 2021, Vol. 10, Page 868*, *10*(4), 868. https://doi.org/10.3390/FOODS10040868

Xu, J., Cheng, J. J., Sharma-Shivappa, R. R., & Burns, J. C. (2010). Sodium hydroxide pretreatment of switchgrass for ethanol production. *Energy and Fuels*, *24*(3), 2113–2119. https://doi.org/10.1021/ef9014718

Yousefi, S., Emam-Djomeh, Z., Mousavi, M., Kobarfard, F., & Zbicinski, I. (2015). Developing spray-dried powders containing anthocyanins of black raspberry juice encapsulated based on fenugreek gum. *Advanced Powder Technology*, *26*(2), 462–469. https://doi.org/10.1016/j.apt.2014.11.019

Zhang, A., Sun, H., Wang, P., Han, Y., & Wang, X. (2012). Modern analytical techniques in metabolomics analysis †. *Analyst*, *137*(293). https://doi.org/10.1039/c1an15605e

Zhang, L., van Boven, A., Mulder, J., Grandia, J., Chen, X. D., Boom, R. M., & Schutyser, M. A. I. (2019). Arabinoxylans-enriched fractions: From dry fractionation of wheat bran to the investigation on bread baking performance. *Journal of Cereal Science*, *87*, 1–8. https://doi.org/10.1016/j.jcs.2019.02.005

Zhang, W., Wu, W., Wang, Q., Chen, Y., & Yue, G. (2014). The juice of asparagus by-product exerts hypoglycemic activity in streptozotocin-induced diabetic rats. *Journal of Food Biochemistry*, *38*(5), 509–517. https://doi.org/10.1111/jfbc.12084

Zhang, Y., Yang, J., Luo, L., Wang, E., Wang, R., Liu, L., … Yuan, H. (2020). Low-cost cellulase-hemicellulase mixture secreted by *Trichoderma harzianum* EM0925 with complete saccharification efficacy of lignocellulose. *International Journal of Molecular Sciences*, *21*(2). https://doi.org/10.3390/ijms21020371

Zuidam, N. J., & Heinrich, E. (2010). Encapsulation of aroma. In *Encapsulation Technologies for Active Food Ingredients and Food Processing* (pp. 127–160). New York, NY: Springer New York. https://doi.org/10.1007/978-1-4419-1008-0_5

S

Summary

Samenvatting

Summary

Significant food waste and loss are common in the production chain of many agro-materials. This research focused on the conversion of vegetable by-streams into food ingredients with retained flavour profile. White asparagus was chosen as a model vegetable crop knowing that during its production about 15 % of the stem and due to peeling even more material is wasted. Moreover, the asparagus powders available in the market suffer from poor aroma profiles which is often compensated by undesired addition of artificial flavours in food formulations that use such powders. A split-stream processing method was proposed to process wasted asparagus stems, thereby separating the juice from the fibre fraction. The asparagus juice was mildly concentrated and spray-dried into powder with encapsulated volatile flavour compounds. The mechanism of flavour encapsulation during spray drying was investigated as it was hypothesized to provide more flavour retention than traditional hot air drying. For valorisation of the asparagus fibre, different processing methods such as hot air drying, milling, and enzymatic hydrolysis were evaluated to reintroduce the fibre in the final asparagus ingredient.

In **chapter 2**, we investigated the role of carrier agents for encapsulation of volatile compounds during spray drying as well as the effect on physical properties of the spray-dried powder. Maltodextrin was used as carrier agent in this work as it is already used on a large scale for the manufacturing of spray-dried products thanks to amongst others its high glass transition temperature. We systematically varied the spray drying conditions and feed formulations and analysed the spray-dried powders in terms of physical properties and volatile compounds profile. Increasing maltodextrin concentration resulted in spray-dried powders with better physical properties and increased retention of asparagus key-odorant 1-octen-3-ol, other alcohols and an aldehyde. The drying conditions tested in this study did not significantly affect the physical properties of asparagus powder nor the volatile retention. Whereas an increased amount of several asparagus volatile compounds that are known to be formed upon heat treatment was detected in powders that were dried at higher outlet air temperatures.

In **chapter 3**, various vegetable fibres were explored as an alternative carrier agent to (partially) replace maltodextrin during spray drying, which may in the end lead to a more natural final product and reduced caloric content. Among these vegetable fibres, asparagus fibre was tested, thereby facilitating the complete use of the asparagus waste stream. We

successfully replaced up to 29 % of the maltodextrin in the feed formulation. Adding more vegetable fibres did, however, pose some challenges as the fibres were mostly insoluble and increased the viscosity of the feed solution significantly. Both aspects hampered the spray drying process. Spray drying feed with an initial solids content of 40 % w/w led to the formation of better-quality powders, compared to 30 % w/w initial solids in terms of moisture content, particle morphology and volatile retention. Furthermore, replacement by asparagus fibre resulted in powders with a richer volatile profile because asparagus fibre carrier contributed extra asparagus aroma compounds.

As only up to 29 % of maltodextrin could be replaced, alternative strategies to treat the asparagus fibres were explored and an enzymatic treatment was suggested in **chapter 4**. First, the asparagus fibre was pre-treated with sodium hydroxide to improve enzyme accessibility. The pre-treatment was followed by enzymatic hydrolysis with a cellulases cocktail that contained a low β-glucosidase activity. The low β-glucosidase activity helped us to steer the conversion of asparagus fibre into soluble cello-oligosaccharides compounds, i.e. mainly cellobiose and some oligo-saccharides, while limiting the formation of glucose. The obtained hydrolysate was then concentrated and spray dried. The hydrolysed product had a high T_g (108 ºC) and could thus potentially be used as carrier agent for spray drying. In addition, cellobiose and COS are prebiotics and could promote gut health, which will provide additional benefits compared to the use of conventional carrier agents such as maltodextrin.

In **chapter 5**, we studied the volatile release during drying in detail to better understand the mechanism during spray drying and the role played by the encapsulates. We employed a thin-film dryer equipped with a photoionization detector, which mimics the spray dryer and allows for on-line volatile release measurements. Acetone was dissolved in maltodextrin solutions of dextrose equivalent (DE)12 and 21 at different initial solids contents. Thin films of the solutions were dried and the acetone release during drying was monitored. Acetone release decreased with an increase in initial solids content, which was correlated to the quicker formation of the skin. Maltodextrin solutions prepared with 20 % initial solids did not retain any acetone. For higher solid contents maltodextrin DE12 was more effective in acetone encapsulation than maltodextrin DE21. A mechanistic model was developed to describe acetone release during thin film drying. For this drying model, we implemented water and acetone diffusivity equations as a function of the maltodextrin concentration and performed calculations of the heat and mass transfer in the film exposed to the drying air. Although there

were some deviations with the experimental data, the model confirmed the correlations between acetone release and drying kinetics as observed by the experiments.

In **chapter 6**, the ingredients produced via the split-stream process, i.e. asparagus juice concentrate, dried and milled fibre and spray-dried powder, were compared to the commercial hot air-dried asparagus powder. The asparagus ingredients were formulated in soup prototypes and tested in a sensory study. Furthermore, the soup prototypes were evaluated on chemical composition and physical properties. Sensory evaluation indicated that the spray-dried asparagus ingredients outperformed the commercial powder in terms of asparagus odour and taste intensity. Relevant sensory attributes were linked to metabolomics using GC-MS and LC-MS. The sensory experiment provided an outlook on the potential application of the newly processed ingredients in food products.

Finally, in **chapter 7** we placed our findings into a broader context by translating the learnings from asparagus to other vegetables. We performed the split-stream process on red bell pepper. During the preparation of the bell pepper juice concentrate, the red colour was lost. Despite the colour loss, most flavour compounds were retained. Similar to asparagus, spray drying with maltodextrin proved to be effective for encapsulation of volatile flavour compounds in bell pepper concentrate. In particular, the key volatile compound 2-methoxy-3-isobutyl-pyrazine was well retained during drying and was more than 5 times higher in intensity than in a commercial bell pepper powder. Moreover, in this chapter, we discuss the application of asparagus fibre as carrier agent via analysis of the flavour profile, techno-economic assessment of the hydrolysis process and the potential production scale for the Netherlands. Compared to the unprocessed asparagus fibre, the asparagus fibre hydrolysate was much lower in volatile compound intensity. The decrease in intensity is related to the harsh processing conditions and could be advantageous for the application of the hydrolysate in (non-)asparagus products. It was estimated that about 17 tonnes of asparagus hydrolysate powder can be produced annually from 3 kilotons of collectable asparagus waste (wet weight) available in the Netherlands. Insights obtained in this work indicate the feasibility of upcycling asparagus waste streams into flavour-rich ingredients for food applications by following a split-stream processing approach.

Samenvatting

Aanzienlijke hoeveelheden grondstoffen worden verspild in onze voedselproductieketen. Dit onderzoek richtte zich op de verwerking van groenteresteströmen tot hoogwaardige ingrediënten van levensmiddelen, waarbij vooral vluchtige smaakstoffen behouden blijven. Witte asperge werd als groente gekozen in deze studie vanwege het relatief hoge percentage van de aspergespeer (15%) die aan de onderkant wordt afgesneden en samen met eventuele schillen weggegooid. Daarnaast bevatten traditionele aspergepoeders die gemaakt worden met behulp van heteluchtdroging weinig natuurlijke aroma's, wat gecompenseerd wordt door toevoeging van kunstmatige aroma's. In dit onderzoek stellen we een nieuw proces voor om de onderkanten van asperges te verwerken, waarbij het aspergesap wordt gescheiden van de vezelfractie. Het aspergesap wordt op milde wijze geconcentreerd en vervolgens gesproeidroogd met een drager zoals maltodextrine, tot een poeder waarbij de vluchtige aroma's worden behouden. In het onderzoek is het mechanisme bestudeerd dat zorgt voor behoud van aroma's tijdens sproeidrogen. De hypothese was dat meer aroma kan worden behouden tijdens sproeidrogen dan tijdens het traditionele heteluchtdrogen. Om ook de afgescheiden aspergevezel te gebruiken als nuttige grondstof, zijn verschillende methoden onderzocht om de vezel weer te herintroduceren in het asperge-eindproduct. Dit wordt gedaan via twee manieren, ofwel via heteluchtdroging, waarna de vezels worden vermalen en vervolgens toegevoegd aan het gesproeidroogde aspergepoeder, ofwel via enzymatische hydrolyse, waarbij de vezels worden omgezet tot een mengsel met voornamelijk cellobiose, om deze te gebruiken als drager voor het maken van aspergepoeder.

In **hoofdstuk 2** hebben we beschreven wat de rol van een drager is op het behoud van aroma's tijdens het sproeidrogen van geconcentreerd aspergesap en wat voor invloed dit heeft op de fysieke eigenschappen van de gesproeidroogde poeders. In dit onderzoek hebben we maltodextrine gebruikt als drager, omdat maltodextrine al op grote schaal wordt gebruikt voor het maken van gesproeidroogde producten vanwege vooral de hoge glastransitietemperatuur. We hebben hiervoor de sproeidroogcondities en de productformulering gevarieerd. Vervolgens hebben we de fysieke eigenschappen en het aromaprofiel van de gesproeidroogde poeders geanalyseerd. Door het maltodextrinegehalte te verhogen, werden de fysieke eigenschappen van de gesproeidroogde poeders verbeterd en bleven er meer 1-octen-3-ol (een belangrijke aspergegeurstof), verschillende andere alcoholen en een aldehydecomponent behouden. De verschillende onderzochte

droogcondities hadden geen merkbaar effect op de fysieke eigenschappen en het behoud van aroma's. Daarentegen nam de hoeveelheid aspergearoma's waarvan bekend is dat deze gevormd worden onder invloed van temperatuur toe, bij hogere uitgaande luchttemperatuur in de sproeidroger.

In **hoofdstuk 3** hebben we verschillende plantaardige vezels als drager onderzocht om daarmee (gedeeltelijk) maltodextrine te vervangen tijdens het sproeidrogen. Het doel was om een natuurlijker product te maken met bovendien een gereduceerde hoeveelheid calorieën. De aspergevezel was een van de onderzochte vezels en was gekozen om daarmee de aspergereststroom volledig te benutten. Als referentie werd het geconcentreerde aspergesap gesproeidroogd met toevoeging van maltodextrine tot een drogestofgehalte van 30 of 40 % (w/w) in de voeding. Vervolgens werd de maltodextrine gedeeltelijk vervangen door vezels. Uit de experimenten bleek dat tot maximaal 29 % van de maltodextrine kon worden vervangen in de formulering van het aspergepoeder. Het toevoegen van meer vezels zorgde voor problemen aangezien de vezels onoplosbaar zijn, waardoor de viscositeit van de formulering te hoog werd om nog te kunnen vernevelen. Wanneer de voeding van de sproeidroger een drogestofgehalte van 40 % (w/w) had, leidde dit tot een betere poederkwaliteit op basis van vochtgehalte, deeltjes morfologie en aromabehoud, dan bij een drogestofgehalte van 30 % (w/w). Daarnaast leidde het vervangen van maltodextrine door aspergevezel tot een rijker aromaprofiel, omdat deze vezel ook aspergearomacomponenten bevat.

Aangezien slechts maximaal 29 % van de maltodextrine vervangen kon worden, hebben we alternatieve methodes bestudeerd om aspergevezels beter toepasbaar te maken. Als alternatief stellen we in **hoofdstuk 4** enzymatische hydrolyse voor, waarbij de aspergevezel eerst voorbehandeld wordt met een natronloogoplossing om de toegankelijkheid voor de enzymen te vergroten. Vervolgens vindt enzymatische hydrolyse plaats met een cocktail van cellulases met een lage β-glucosidase-activiteit. De conversie van aspergevezel tot oplosbare cello-oligosachariden (voornamelijk cellobiose) kan beter gestuurd worden met deze lage β-glucosidase-activiteit en daarmee ongewenste glucosevorming voorkomen. Het verkregen hydrolysaat werd vervolgens geconcentreerd en gesproeidroogd. Dit hydrolysaat heeft een hoge glastransitietemperatuur (108 ºC) en kan daardoor in principe worden gebruikt als drager voor sproeidrogen. Een bijkomend voordeel is dat cello-oligosachariden prebiotica zijn en daardoor de darmgezondheid mogelijk kunnen bevorderen.

In **hoofdstuk 5** hebben we in detail onderzocht hoe aroma's vrijkomen tijdens het drogen om zo beter te begrijpen hoe het sproeidroog-mechanisme werkt en wat de rol van een drager hierbij is. Hiervoor hebben we een dunne- filmdroger met een foto-ionisatiedetector gebruikt. Met deze opstelling wordt een sproeidroger nagebootst, waarbij het wel mogelijk is om online het vrijkomen van aroma's te meten. Aceton was opgelost in een maltodextrineoplossing met dextrose-equivalent (DE) 12 of 21 en verschillende drogestofgehaltes. De oplossingen werden verspreid in dunne films die we vervolgens hebben gedroogd, waarbij tijdens dit proces het vrijkomen van aceton werd gemeten. Zo ontdekten we dat het vrijkomen van aceton afnam als het drogestofgehalte in de oplossingen werd verhoogd, wat waarschijnlijk gerelateerd is aan het sneller vormen van een droog oppervlak aan de bovenkant van de film. Maltodextrineoplossingen bereid met 20 % drogestof hielden geen aceton vast tijdens het drogen. Voor de hogere drogestofgehaltes bleek maltodextrine DE12 effectiever in het behouden van aceton dan maltodextrine DE21. Naast de experimenten hebben we een mechanistisch model ontwikkeld om het vrijkomen van aceton in de dunne-filmdroger te beschrijven. Voor dit model hebben we aceton- en waterdiffusievergelijkingen opgezet als functie van de maltodextrineconcentratie en hebben we berekeningen uitgevoerd met betrekking tot de warmte- en massaoverdracht in de film die blootgesteld wordt aan de drogende lucht. Ondanks dat er wat afwijkingen waren met de experimentele data, kon het model wel dezelfde verbanden leggen tussen het vrijkomen van aceton en de droogkinetiek zoals we die ook zagen in de experimenten.

In **hoofdstuk 6** hebben we op basis van het eerder beschreven proces verschillende ingrediënten geproduceerd (geconcentreerd aspergesap, gedroogde en gemalen vezel, en gesproeidroogd poeder) en deze vergeleken met een commercieel heteluchtgedroogd aspergepoeder. Deze asperge-ingrediënten zijn gebruikt als bestanddeel in instantaspergesoepen, die vervolgens getest zijn in een sensorische studie. Daarnaast zijn dezelfde soepen geanalyseerd op de chemische samenstelling en fysieke eigenschappen. De sensorische test liet zien dat de gesproeidroogde asperge-ingrediënten beter presteerden dan het commerciële aspergepoeder op het gebied van aspergegeur en -smaak. Relevante sensorische eigenschappen werden gerelateerd aan metabolomics data, gegenereerd met GC-MS en LC-MS. Op basis van de resultaten kunnen we concluderen dat de gesproeidroogde asperge-ingrediënten potentie hebben om toegepast te worden in de voedselindustrie.

Tot slot hebben we in **hoofdstuk 7** onze bevindingen in een bredere context geplaatst, waarbij we onder andere onze inzichten voor asperges hebben vertaald naar andere groenten. Zo hebben we hetzelfde proces uitgevoerd met rode paprika. Tijdens de bereiding van het paprikasapconcentraat verdween echter de rode kleur. Ondanks het verlies in kleur bleven de meeste aromacomponenten behouden. Net als bij asperges, bleek sproeidrogen met maltodextrine effectief voor het behouden van vluchtige aromacomponenten in het paprikaconcentraat. In het bijzonder bleef het belangrijke paprika-aroma 2-methoxy-3-isobutyl-pyrazine goed behouden tijdens het drogen en was de intensiteit van dit aroma 5 keer hoger vergeleken met een commercieel paprikapoeder. Daarnaast hebben we in dit hoofdstuk de toepassing van aspergevezel als drager verder bediscussieerd aan de hand van het bestuderen van het aromaprofiel, het maken van een technisch-economische analyse van het hydrolyseproces en het in kaart brengen van de mogelijke productieschaal binnen Nederland. Vergeleken met de niet-verwerkte (rauwe) aspergevezel had het aspergevezelhydrolysaat een veel lagere intensiteit in aromacomponenten. Deze afname in intensiteit is gelinkt aan de intensieve processtappen om het hydrolysaat te verkrijgen. De afname kan echter een voordeel zijn voor de toepassing in (non-)aspergeproducten. De inschatting is dat ongeveer 17 ton aspergehydrolysaatpoeder kan worden geproduceerd van de 3 kiloton aspergeafval (nat gewicht) beschikbaar in Nederland. De inzichten verkregen in dit onderzoek laten zien dat het mogelijk is om aspergereststromen op te waarderen tot aromarijke ingrediënten, die geschikt zijn voor de voedselindustrie.

Appendices

Acknowledgements – Dankwoord

About the author

Publications

Overview of completed training activities

Acknowledgements

Writing the acknowledgements section makes me realize that my PhD is really coming to an end. The last four years were full of trips, courses, and conferences, but also involved working from home and many Teams calls. Thankfully, most of the time I was surrounded by my like-minded, ambitious and enthusiast colleagues. I would like to take the opportunity to thank those who have helped me during this PhD journey.

First, I would like to thank my supervisors *Maarten* and *Lu* who guided me throughout the four years of my PhD project. *Maarten*, thanks that I could always drop by your office for a question or quick chat. I have learned a lot from your interesting talks about spray drying. I will never forget the obligated isolation after we both tested positive for COVID during the IDS conference in the US. *Lu* thank you for your enthusiasm and constructive feedback. You always came up with good ideas for the experimental design and your on-point comments improved my presentations and manuscripts a lot. I also really appreciated that both of you always very quickly reviewed my manuscripts and thesis, you spared me a lot of stress! Furthermore, I want to thank you *Remko* for your input, your 'idea generator' was always working during our meetings and without you the Mathcad model (chapter 5) would not have been able to describe the acetone release.

Eirini – as the other PhD student in the Waste2Taste project we worked a lot together, which also resulted in several shared publications! 'Dankjewel' for sharing your enthusiasm and passion for flavours and the fun talks we had! I wish you a lot of success with finalizing your PhD! I would also like to thank all project partners of the Waste2Taste project (ISPT, Unilever, Teboza, Growers United and WFBR). I really enjoyed our partner meetings with the valuable discussions and the tours at your facilities.

A large part of the project was carried out in the lab, which would not have been able without the help of the FPE technicians. Bedankt *Maurice* voor al je hulp met de DSC, HPLC en SEM en het uitzoeken van allerlei dingen als we een nieuwe methode wilden uittesten. *Jos*, ik stond regelmatig in de deuropening van je kantoor met allerlei vragen van het bedienen van de Rheometer tot aan het bestellen van computeraccessoires, dankjewel voor het altijd enthousiast beantwoorden van mijn vragen. *Martin*, bedankt voor de gezellige gesprekken en uiteraard je hulp bij het invullen van declaraties en urenschrijven. *Wouter*, dankjewel voor je hulp met de mastersizer en ultrasizer en je gezelligheid in de coffee corner! *Jarno*, bedankt

voor het delen van je passie voor het beschermen van onze planeet en ik probeer ook mijn CO_2 footprint te beperken.

Thanks to the FPE secretary for managing all organisational things regarding my PhD. *Marjan, Ilona* en *Evelyn* hartelijk dank!

I would also like to thank all the thesis students that worked together with me on this project: *Qadry, Solange, Aniek, Nienke, Kim, Judith, Derk, Tasha, Tessa, Rianne, Xanthe* and *Stijn*. Thank you all for your enthusiasm and hard work! I really enjoyed supervising you. *Nienke, Rianne,* and *Xanthe* thank you for your significant contribution to my publications.

I would also like to thank my office mates *Sirinan, Yu, Sicong, Koen, Somayeh, Lina* and *Jiarui. Sirinan*, you have been my office mate from the beginning till the end of my PhD. It was always great to hear and experience your passion for cooking Thai dishes and other foods! Thank you for being my paranymph! Thanks, *Yu*, for being a great office mate and probably the one I talked most to ;). Although it is more difficult to stay in touch now that you're in China I hope we still will! *Sicong*, I really enjoyed our talks and could always appreciate your directness. I hope to visit you in Sweden one day! *Koen*, het was erg gezellig om met jou het kantoor te delen! We delen allebei een passie voor sport en was jij net zo gek als ik om in de hitte en hoge luchtvochtigheid tijdens de PhD trip in Singapore meerdere keren te gaan hardlopen. Heel fijn dat jij mijn paranimf bent! *Somayeh, Lina* and *Jiarui* thanks for our fun talks in the office!

Also, thanks to the Dry Food Processing people from FPE I worked with: *Aaditiya, Ana, Anneloes, Eline, Evelien, Isabel, Jan-Eise, Julia, Koen, Lyneth, Martin, Nienke, Patrick, Qinhui, Quinten, Raquel, Regina, Ruihao, Sicong, Yifeng* and *Yizhou*. I enjoyed our DryFoodProcess meetings, talks in the coffee corner or drying lab, and the yearly pizza dinners at Maarten's place. *Evelien*, het was erg leuk om samen met jou mee te doen aan de 'drying contest' tijdens Eurodrying in Turijn en bedankt dat ik je telefoon mocht lenen toen ik die van mij in NL had laten liggen ;). *Nienke*, bedankt voor je gezelligheid tijdens IDS en vervolgens voor je support toen ik daar COVID kreeg ;). *Yifeng*, I really enjoyed our collaboration and I'm very happy you will continue to work with asparagus!

Thanks also to all other colleagues of FPE for the fun time during our coffee and lunch breaks! Thanks to the FPE colleagues who joined the Veluweloop and thank you *Sten* for the co-organization. Thanks to *Jarno* for setting up the FPE team for the WE-day, both editions

I joined were a lot of fun! My fellow F1-fans (*Martin*, *Jan-Eise* and *Laurens*), thanks for the fun talks about the GPs. Also, thanks to the borrel-committee for organising the borrels!

Natuurlijk wil ik ook mijn lieve vrienden en familie bedanken. Lieve meiden van *BC Leilani*, m'n *Thymosbestuur,* en de *MiLa meiden*, bedankt voor het aanhoren van m'n PhD verhalen, maar vooral bedankt voor jullie gezelligheid! Lieve *Tove*, dankjewel voor de prachtige cover die je hebt gemaakt! *Carolien* bedankt voor je hulp met het doorlezen en verbeteren. *Pap*, *mam* en *Frederiek*, bedankt voor jullie support! Lieve *Tom*, tegelijk met de start van mijn PhD zijn we ook een ander groot avontuur begonnen namelijk de aankoop van ons huis waar we de afgelopen jaren flink aan hebben geklust. Beide projecten (vooral de laatste) waren zonder jou niks geworden. Dankjewel dat ik m'n PhD ervaringen met jou kan delen en voor het meedenken, voor mij het verschil te leren tussen een waterpomptang en een bahco en natuurlijk voor de superfijne tijd samen!

About the author

Joanne Siccama was born on the 2nd of September 1992 in Ede, The Netherlands. She attended Marnix College in Ede, where she obtained her VWO diploma in 2010, with majors in Natuur & Techniek (Nature & Engineering) and Natuur & Gezondheid (Nature & Health).

In 2010, Joanne started the study Food Technology at Wageningen University & Research. In 2012, she did a minor in Food Business and Marketing at University College Cork in Ireland. She finished her bacherlor studies with a thesis at the Laboratoy of Food Process Engineering in 2013 about the effects of pH, salt and enzyme treatment on water holding capacity in hydrated and blanched mushrooms.

In the academic year 2013-2014, Joanne was a full-time board member of the Wageningen sports foundation SWU Thymos. In 2014, Joanne continued with her master studies in Food Technology, with a specialization in Sustainable Food Process Engineering, and her master studies in Sustainable Energy Technology at TU Delft, The Netherlands. During her master thesis/internship, she investigated the physical (rheological) properties of sewage sludge and digestate in the context of their processing in supercritical water gasification. This research was performed at the start-up company Gensos and the WaterLab at the Civil Engineering and Geosciences faculty, TU Delft. For her second master thesis, Joanne worked on the use of double emulsions for iron encapsulation with focus on the physical stability in the gastrointenstinal tract at the Laboratory of Food Process Engineering. She obtained her master's degrees in 2018.

Joanne started as a PhD candidate at the Laboratory of Food Process Engineering in 2018. She investigated spray drying of asparagus waste streams for the encapsulation of volatile flavour compounds, and results of this research are described in this thesis.

Contact: joanne.siccama@outlook.com

Publications

E. Paudel, R.M. Boom, E. van Haaren, **J.W. Siccama**, R.G.M. van der Sman, Effects of cellular structure and cell wall components on water holding capacity of mushrooms. *Journal of Food Engineering, 187, (2016).* https://doi.org/10.1016/j.jfoodeng.2016.04.009.

J.W. Siccama, E. Pegiou, L. Zhang, R. Mumm, R.D. Hall, R.M. Boom, M.A.I. Schutyser, Maltodextrin improves physical properties and volatile compound retention of spray-dried asparagus concentrate. *LWT*, *142, (2021)*. https://doi.org/10.1016/j.lwt.2021.111058.

J.W. Siccama[1], E. Pegiou[1], N.M. Eijkelboom, L. Zhang, R. Mumm, R.D. Hall, M.A.I. Schutyser, The effect of partial replacement of maltodextrin with vegetable fibres in spray-dried white asparagus powder on its physical and aroma properties. *Food Chemistry, 356, (2021)*. https://doi.org/10.1016/j.foodchem.2021.129567.

J.W. Siccama, R. Oudejans, L. Zhang, M.A. Kabel, M.A.I. Schutyser, Steering the formation of cellobiose and oligosaccharides during enzymatic hydrolysis of asparagus fibre. *LWT, 160 (2022).* https://doi.org/10.1016/j.lwt.2022.113273

E. Pegiou[1], **J.W. Siccama**[1], L. Zhang, R. Mumm, D.M. Jacobs, X.Y. Lauteslager, M.T. Knoop, M.A.I. Schutyser, R.D. Hall, Metabolomics and sensory evaluation of asparagus ingredients in instant soups unveil important asparagus (off-flavours). *Submitted for publication.*

J.W. Siccama, X. Wientjens, L. Zhang, R.M. Boom, M.A.I. Schutyser, Acetone release during thin film drying of maltodextrin solutions as model system for spray drying. *Submitted for publication.*

Overview of completed training activities

Discipline specific activities

Courses

Summer school Zelcor, Wageningen, The Netherlands [a]	2018
Star CCM+ course, Den Bosch, The Netherlands	2018
Basiscursus Kleurtheorie, Nieuwegein, The Netherlands	2018
Advanced Food Analysis, Wageningen, The Netherlands	2019
Microscopy and Spectroscopy in Food and Plant Science, Wageningen	2019
Chemometrics, Wageningen, The Netherlands	2020
Summer Course Glycosciences, Wageningen, The Netherlands	2021
Sensory Perception & Food Preference, Wageningen, The Netherlands	2021

Conferences

NWGD symposium, Wageningen, The Netherlands	2018
Eurodrying symposium, Turin, Italy [a]	2019
Wageningen PhD symposium, Wageningen, The Netherlands [a]	2019
Wageningen Food Science symposium, Wageningen, The Netherlands	2020
Online NWGD event - Unilever, Online [b]	2020
Spotlight talk EFCE, Online [b]	2020
NWGD symposium, Online	2021
NWGD mini-symposium processing vegetables, Wageningen [b]	2022
International Drying Symposium, Worchester, United States [b]	2022

General courses

VLAG PhD week, Baarlo, The Netherlands	2018
Introduction to R, Wageningen, The Netherlands	2019
PhD Workshop Carousel, Wageningen, The Netherlands	2019
Applied Statistics, Wageningen, The Netherlands	2019
Scientific Writing, Wageningen, The Netherlands	2019
DSC and MDSC course, Stockholm, Sweden	2019
Supervising BSc & MSc students, Wageningen, The Netherlands	2020

Other activities

Preparation of research proposal	2018
FPE weekly group meetings	2018-2022
PhD study tour to Canada	2018
PhD study tour to Singapore	2022

[a] *Poster presentation,* [b] *Oral presentation*

The work described in this thesis was carried out in the framework of the Institute of Sustainable Process Technology (ISPT) under the project 'TKITOEDR-20-11': Waste2Taste. Partners in this project are Growers United, ISPT, Teboza BV, Unilever BV, and Wageningen University & Research.

This project was co-funded by TKI-E&I with the supplementary grant 'TKI- Toeslag' for Topconsortia for Knowledge and Innovation (TKI's) of the Ministry of Economic Affairs and Climate Policy and the project number is TKITOEDR-20-11.

Cover design by Tove Hofstede

Printed by Proefschriftmaken || www.proefschriftmaken.nl